UNIVERSITÄTSKLINIKUM HAMBURG-EPPENDORF

Zentrum für Geburtshilfe, Kinder- und Jugendmedizin

Prof. Dr. med. Kurt Hecher

CD8+ T cells in pregnancy: Characterization and function of uterine CD8+ T cells

Dissertation

zur Erlangung des Doktorgrades Dr. rer. biol. hum.
an der Medizinischen Fakultät der Universität Hamburg.

vorgelegt von:

Lilja Harðardóttir
aus Reykjavík

Hamburg 2023

(wird von der Medizinischen Fakultät ausgefüllt)

Angenommen von der
Medizinischen Fakultät der Universität Hamburg am: 27.02.2023

Veröffentlicht mit Genehmigung der
Medizinischen Fakultät der Universität Hamburg.

Prüfungsausschuss, der/die Vorsitzende: Prof. Dr. Maria Emilia Solano

Prüfungsausschuss, zweite/r Gutachter/in: Prof. Dr. Hans-Willi Miittrücker

Table of Contents

List of figures

List of tables

1 Introduction

1.1 The feto-maternal interface

The feto-maternal interface is located in the uterus, where the semi-allogenic fetus and the placenta which is of fetal origin gain close contact with the endometrium. The feto-maternal interface is first established when an embryo attaches to the surface of the endometrium, termed embryo implantation (Abrahamsohn & Zorn, 1993; Carson et al., 2000). In mice, this takes place on gestation day (GD) 4.5, when vaginal copulation plug, indicating that mating has taken place, is detected the following morning as GD 0.5. Mouse pregnancy contains multiple implantations, where each implantation unit contains a fetus, a placenta and the part of the uterus surrounding that fetus and placenta **(Figure 1A)**, while human pregnancies generally contain one fetus and one placenta surrounded by the whole uterus **(Figure 1B)**.

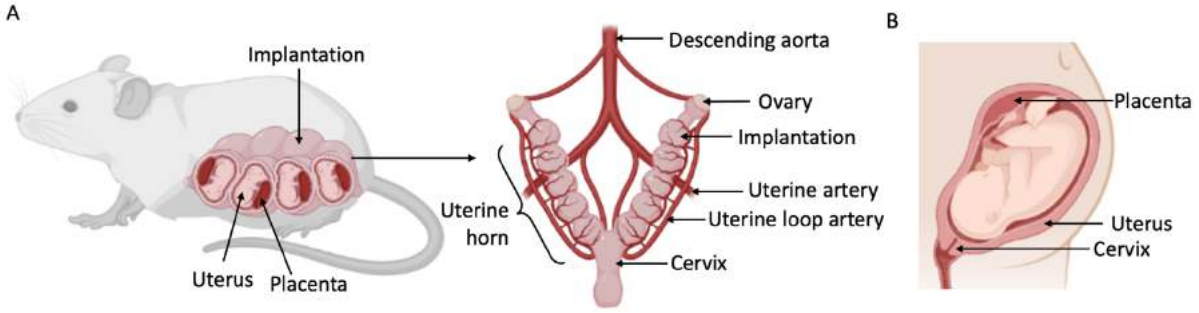

Figure 1. Schematic overview of implantations in mouse and human pregnancies.
A) *Pregnant multiparous mouse with multiple implantations where each implantation consists of a fetus, placenta, fetal membranes, and surrounding uterus. Mouse uterus contains two uterine horns, each connected to an ovary and the uterine arteries connected/irrigating to the mesometrial side of the uterus.* ***B)*** *Pregnant uniparous woman containing a single fetus and a placenta encapsulated by the whole uterus.*

1.1.1 Uterine remodelling

The uterus is an essential organ for reproduction. Its main role is to accommodate the fetus and to allow for its development and growth, followed by actively promoting fetal delivery. These processes involve vast changes to the uterine tissue including cellular differentiation, enlargement of the uterine tissue and peristaltic contraction (Gee & Frey, 2020; Kagami et al., 2020; Ono & Maruyama, 2015). The uterus is a dynamic organ, both during the reproductive cycle and in the context of pregnancy, where uterine growth, remodelling and involution takes place, orchestrated by the hormones estrogens and progesterone (Das et al., 2009). The uterus is a complex and heterogeneous tissue **(Figure 2)**. It can be divided into two main anatomical compartments, the mesometrial side and the anti-mesometrial side. Furthermore, the uterus is

made of several layers. The outermost layer is the myometrium which is subdivided into the outer longitudinal and inner circular layers, and a recently identified mesh-like middle myometrial layer. The myometrium layers serve to co-ordinate uterine adaptations to the growing fetus and labour contraction (Kagami et al., 2020). In mid pregnancy (GD 8.5) a transient tissue, the so called mesometrial lymphoid aggregate of pregnancy (MLAp) forms between the two myometrial layers of which role is yet unknown, but it is known to contain uterine NK cells (Elia & Georgiades, 2021). With formation of the MLAp, the inner layer of the myometrium at the mesometrial side disappears. The mesometrial myometrium and MLAp are often termed together as the mesometrium and the subsequent undelaying layer is called endometrium. Endometrial remodelling during pregnancy is crucial for the formation and maintenance of the feto-maternal interface (Croy et al., 2015). The blastocyst (the fertilised egg) implants into the anti-mesometrial uterus, which triggers fibroblasts of the endometrium to undergo decidualisation, resulting in an epithelial-like decidual cell, on the anti-mesometrial side which later spreads to the mesometrial side (Abrahamsohn & Zorn, 1993; Croy et al., 2015). Decidualisation is accompanied by a remodelling of the extracellular matrix by the stromal cells within the endometrium. Furthermore, decidual cells support pregnancy by various ways, by controlling oxidative stress and local estrogen levels (Das et al., 2009; Hirota et al., 2010), and by production of various molecules necessary for feto-maternal crosstalk and adaptation to pregnancy, including immunomodulatory molecules, and for angiogenesis. As the mesometrial uterine lumen starts to surround the embryo, the cells forming the outer layer of the embryo, called trophoblast cells, invade into the uterine epithelial layer and phagocyte the epithelial cells, resulting in disappearance of the basement membrane and a direct contact with the decidualized endometrium (Bevilacqua & Abrahamsohn, 1988, 1989; Parr et al., 1987). This is the start of a fascinating and intimate cellular relationship between trophoblast cells and the endometrial cells, allowing for a permissive parasitic-like phenomenon.

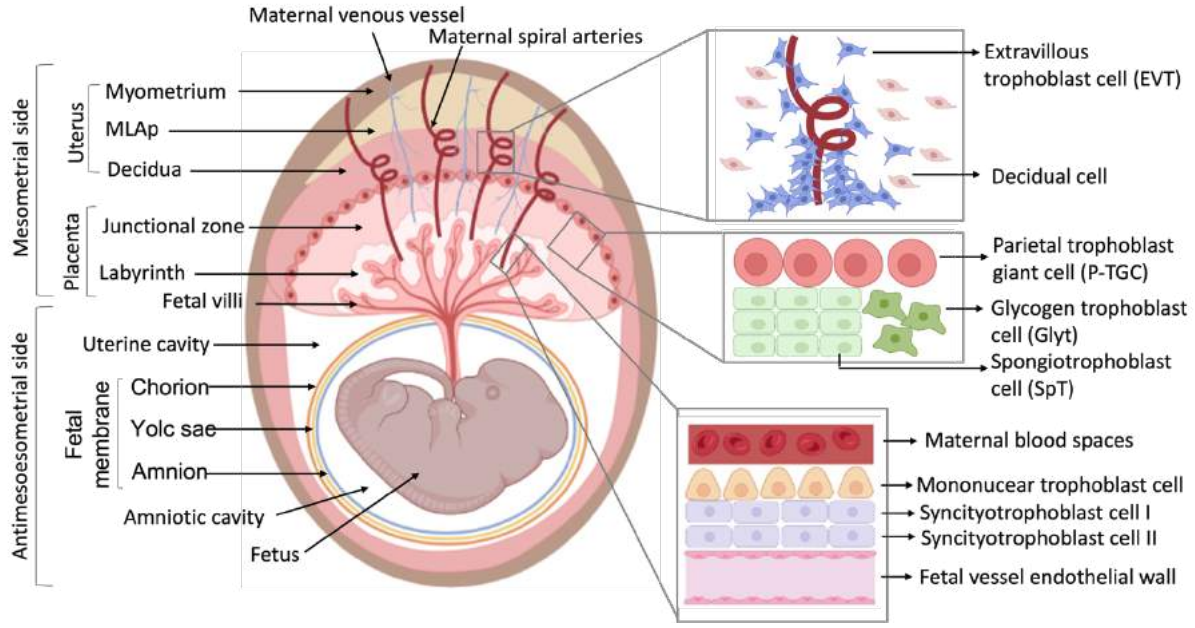

Figure 2. A schematic overview of the mouse feto-maternal interface.
The figure demonstrates the mesometrial and anti-mesometrial uterine compartments, the uterine layers, placental zones including cell types, fetal membranes, and the location of the fetus. Figure was created with Biorender.

1.1.2 Placentation

In mice, before formation of the placenta, a primitive „early placenta“ is formed, called choriovitelline placenta, supported by the anti-mesometrial decidua, providing the embryo with nutrients from approximately GD 6-10, hereinafter the fully formed definitive chorioallontoic placenta, supported by the mesometrial decidua, takes over for fetal nourishment. Trophoblast cells further phagocyte decidual cells allowing for embryo growth, and with progress of the pregnancy, the anti-mesometrial decidua regresses while the mesometrial decidua remains as the maternal contribution of the placenta (Croy et al., 2015). The chorioallontoic placenta is a unique temporary organ, that consists of various cell types and compartments. Its role is to mediate an exchange of nutrient, wastes, and gases. Furthermore, it has a crucial endocrine function and it is an important component of a proper adaptation of the maternal immune system towards the fetus (Croy et al., 2015). The chorioallontoic placenta is a complex organ and can be divided into several zones **(Figure 2)**. The part furthest from the fetus is the above-mentioned maternal decidua which contains maternal vessels, called spiral arteries and venous sinuses. Invasive extravillous trophoblast cells (EVT) migrate into the decidual layer, and some invade and line the spiral arteries. The underlying placental layer is called junctional zone, composed of a thin layer of parietal trophoblast cells, spongiotrophoblast cells and glycogen trophoblast cells. The main function of these cells is endocrine activity. Underneath the junctional zone lies the labyrinth, which contains a vascular network of fetal capillaries and maternal blood

spaces/canals where the exchange of nutrients, waste and gas takes place (Erlebacher, 2013). Here, a perforated interhemal membrane separates the fetal blood from maternal blood, consisting of one layer of mononuclear trophoblast giant cells, two synciticotrophoblast layers and an endothelial cell lining of fetal capillaries. After complete placentation and perforation of maternal vessels (GD 12.5), the labyrinth part of the placenta further expands, both in size and complexity until birth (Croy et al., 2015). The placenta is the most probable sources of fetal antigens, with highest levels of shedding of trophoblast cells, microparticles and exosomes into the circulation, due to the direct contact with the trophoblast cells as the anti-mesometrial uterus as the fetal membranes are impermeable (Croy et al., 2015; Erlebacher, 2013).

Mice are a good mouse model for investigating pregnancy due to similarities between the mouse and human feto-maternal interface. For instance, both species have hemochorial placentas, referring to the direct contact between trophoblasts and maternal cells and circulation. Differences include a deeper invasion of EVT into the decidua and deeper invasion of decidual arteries in humans (Croy et al., 2015; Redline & Lu, 1989). Another difference is the timing of organ development of mouse and human fetuses as human fetus can survive outside of the mother‘s womb in the third trimester, while mouse fetuses are not mature enough to survive until the last days of pregnancy. **Figure 3** shows the timeline of pregnancy milestones in mice and humans.

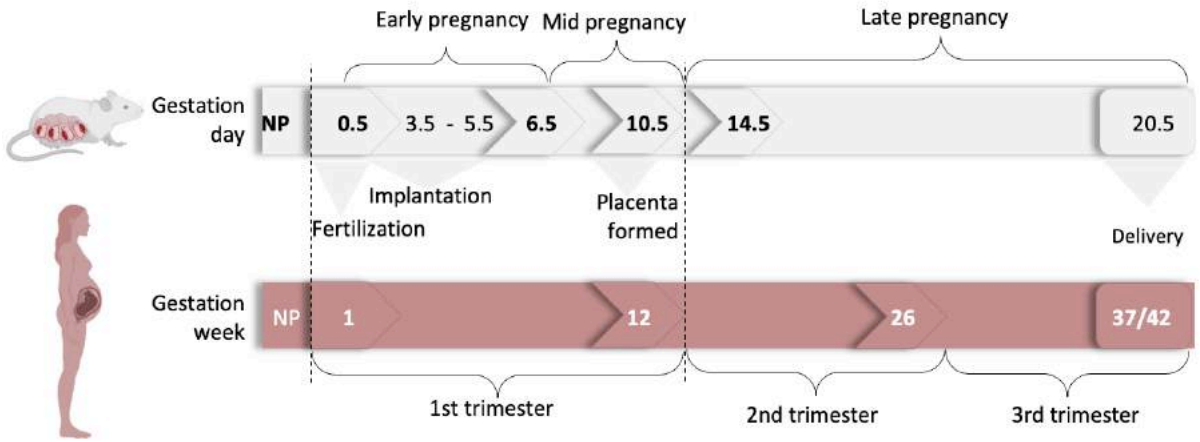

Figure 3. A schematic overview of the timeline of pregnancy milestones in mouse and human pregnancies.
The figure demonstrates the timeline of mouse pregnancy (top) and in humans (bottom) and the pregnancy milestones: fertilization, implantation, placental formation, and delivery. In mice, pregnancy periods are usually referred to as early, mid and late pregnancy, while they are referred to as first, second and third trimesters in humans. Gestation days in bold refer to the main gestation days investigated in this dissertation. NP: not pregnant. Figure was created with Biorender.

1.2 The immunological paradox of pregnancy.

Peter Medawar developed the concept of allogenic organ transplantation rejection which led him to identify the immune paradox of pregnancy. The semi-allogenic pregnancy holds some resemblance to organ transplantation as both contain immunologically foreign grafts from the host, thus raising the question of how pregnancy is possible (Rendell et al., 2020). Sixty years ago, Peter Medawar formulated the research question "how does the pregnant mother contrive to nourish within itself, for many weeks or months, a foetus that is an antigenically foreign body?'' and with that he set the ground for the field of reproductive immunology. His hypotheses to solve this paradox included the anatomical separation between the mother and the fetus, fetal antigenic immaturity, and the immunological indolence of the mother (Billingham et al., 1953; Billington, 2003; Male, 2021). These hypotheses have been refuted as now it is known that the physical barrier between the mother and the fetus is permeable with a direct contact at the feto-maternal interface and fetal cells are detected in the peripheral maternal circulation (Rendell et al., 2020). Also, fetal antigens are not completely immature as they play an important role in feto-maternal crosstalk and although unspecific maternal immune tolerance leads to a higher susceptibility of particular infections, it still contains robust immune response towards pathogens (Head & Billingham, 1986; Rendell et al., 2020). Although the hypotheses have been largely proven incorrect, Sir Peter Medawar's question is still not completely answered, however scientists are continually expanding and filling in gaps in the knowledge of this complex paradox.

An important aspect in the immunological paradox of pregnancy is the Major Histocompatibility complex (MHC) system, which is a highly polymorphic genomic region that encodes the polymorphic glycoprotein on the cell membrane of all nucleated cells. They can be either MHC class I or MHC class II. Their role is to present peptide fragments derived from proteins of foreign objects to CD8+ T cells (MHC class I) or to CD4+ T cells (MHC class II). In humans, MHC class I are known as human leucocyte antigen (HLA). They contain the classical MHC: HLA-A, HLA-B and HLA-C, and the non- classical MHC including HLA-E, HLA-F and HLA-G. In mice, MHC are called H-2 complex, which contains the classical MHC-I $H2\text{-}D^{b}$ and $H\text{-}2K^{b}$ in Bl6 mice (C57BL/6 strain) and non-classical (MHC class Ib) $Qa1^{b}$ and $Qa2^{a}$ (Affymetrix eBioscience, n.d.; Levy et al., 2013).

Clearly, immune tolerance towards the fetus must be achieved for a successful pregnancy and several tolerance mechanisms at the feto-maternal interface have been identified (Arck &

Hecher, 2013). Examples of some of these tolerance mechanisms include the expansion of the CD4+ regulatory T cell (CD4+ Treg) pool. Furthermore, elevated progesterone levels, dampening of the pro-inflammatory Th1 and Th17 responses, suppression of CD4+ T cell activity and entrapment of antigen precenting cells (APC) such as dendritic cells within the decidual tissue facilitate an anti-inflammatory environment for fetal growth (Alivuhare et al., 2004; Collins et al., 2009; Engler et al., 2017; Hughes et al., 2013; Muñoz-Cruz et al., 2011). Furthermore, a research group suggested that effector CD8+ T cells have limited capacity to enter the feto-maternal interface due to chemokine gene silencing (Nancy et al., 2012). The regulation of the immune system during pregnancy seems to be a fine-tuned regulation as global immune suppression would render the mother and fetus at risk from pathogen infection. The establishment of immune tolerance is pivotal for proper fetal and placental development and failures to establish it has been related to fetal loss and pregnancy complications such as intrauterine growth restriction (IUGR).

1.3 CD8+ T cells

1.3.1 General characteristics and function

The immune system serves to protect the organism from foreign substances, such as pathogens. It consists of multitude of different cell types orchestrating a complex immune response against these foreign substances (Arck & Hecher, 2013). In addition to the innate immune system, which are the first line of defence, the adaptive immune system contains highly sophisticated defence mechanisms. The adaptive immune system contains T cells, generally divided into CD8+ and CD4+ T cells, and B cells. CD8+ T cells are commonly known as the attackers of the immune system (Zhang & Bevan, 2011). Their primary role is to scan the body for intracellular pathogens including viruses and bacteria, as well as for tumours and to eradicate the thread. Another key role is to form a lasting immunological memory in order to mount a rapid response upon re-encounter with the same threat (Gerritsen & Pandit, 2016). They achieve this by recognizing and binding antigens via highly variable antigen-specific receptors, called T cells receptors (TCR), which are membrane-bound glycoproteins.

The TCR receptor contains heterodimer, typically the T cell receptor alpha (TCRα) chain and the T cell receptor beta chain (TCRβ) chain, each chain composing of a constant and a variable domain (Arnaud et al., 1997). Somatic rearrangement of variable (V), diversity (D) and joining (J) gene segments forms the chains by a random insertion or removal of nucleotides (Bassing et al., 2002), yielding enormous variety of the T cell receptor (Chiffelle et al., 2020; Davis &

Boyd, 2019). The diverse antigen specificity comes from a variable gene arrangement of the highly polymorphic genes, where each CD8+ T cell clone expresses a particular antigen receptor resulting in a multitude of distinct clones with unique antigen specificity. CD8+ T cells mainly recognise peptide antigen, bound to MHC-I molecule, thus the ligand for CD8+ T cells is the peptide antigen/MHC-I complex (Croy et al., 2015; Zhang & Bevan, 2011).

A distinct population of T cells contain the gamma (γ) and delta (δ) chains instead of α and β chains, called γδ T cells. Although αβ and γδ T cells are similar in structure, they possess different function. Compared to αβ T cells, γδ T cells antigen recognition is not dependent on MHC-peptide antigen complex. Less is known about the γδ T cells but they tend to share properties with innate lymphocytes, particularly natural killer (NK) cells. The T cell co-receptors CD8 and CD4, determine whether the T cell is an often-termed cytotoxic cell (CD8+ T cell) or a helper T cell (CD4+ T cell). The CD8 molecule binds to a distinct side of the MHC-I than TCR, necessary for CD8 specific antigen recognition and function. Typically, the CD8 molecule on T cells consists of one α and one β chain (CD8 αβ T cells), while some contain two alpha chains (CD8 αα T cells). While CD8 αβ T cells can be regarded as conventional T cells, CD8 αα T cells are often atypical T cells, found in particular tissues, such as in intestinal intraepithelium, and often possess distinct characteristics and function (Konno et al., 2002; Ruscher et al., 2017).

Upon TCR/antigen presenting cell interaction, in addition with CD8 co-stimulation, naive/quiescent CD8+ T cells becomes activated where extensive proliferation and differentiation takes place. They contain three main killing mechanisms. The first involves secretion of inflammatory cytokines such as TNFα (Tumor necrosis factor alpha) and IFNγ (Interferon gamma). The second killing mechanism involves production and release of cytotoxic granules containing the cytotoxic proteins perforin and granzymes where perforin first creates pores in the target's cell membrane, allowing the cytotoxic proteins to enter the target cell, damaging protein production which results in apoptosis (Janeway Jr et al., 2001). Importantly, CD8+ T cells act specifically to the target cells via the immune synapse, leaving innocent neighbouring cells undisturbed. The third killing mechanism is via the Fas ligand (FasL) expressed on CD8+ T cells which binds to the Fas receptor on target cell, leading to a signalling cascade within the target cell and eventually to apoptosis (Janeway Jr et al., 2001).

1.3.2 CD8+ T cell heterogeneity

1.3.2.1 Differentiation trajectories

CD8+ T cells represent a highly heterogeneous cell populations with multiple differentiation trajectories resulting in distinct roles and functions within different subtypes. CD8+ T cell differentiation trajectory is a complex phenomenon. In general, a widely accepted view is that naive CD8+ T cells survey the body for their specific foreign molecule and upon an encounter with that foreign molecule, they differentiate into effector cells. Upon resolution of the threat, most effector cells die off while some remain to become the long-living memory cells, that undergo a gradual transition into an effector T cell upon re-encounter with the antigen (Gerritsen & Pandit, 2016). This theologically appealing, textbook view, sometimes called "the circular" model or "effector first" model has however been challenged and the lineage relationship between effectors and memory cells, their timing and differentiation, is one of the most debated topics in the field of T cell immunology. An alternative model includes the "linear model" sometimes called the "developmental model" or "memory first model", proposes that naive cells develop directly into memory cells without an effector intermediate stage, admittedly planting the effector cell as an intermediate stage in T cell development, thus suggesting memory cells represent a separate population with the key determinants of T cell differentiation being the strength and duration of antigenic and inflammatory signals. Recent experimental data favour the latter model. Rosato et al. (2020), recently proposed yet another model, the terrace model, which recognizes the issue of the scientists attempting to create ambiguous definition of effectors and memory cells based on diverging criteria (Rosato et al., 2020). One convenient and popular criteria being cell surface markers or transcription factors which can falsely represent the actual function such as migration patterns, proliferation capacity and developmental plasticity. Thus, they remove effector T cells out of the model as the word "effector" is ambiguous and does not provide information about future differentiation potential. This model thus highlights developmental potential and plasticity and migrational heterogeneity. With current classification of the lineage hierarchy and developmental relationship of CD8+ T cell subpopulations, placing newly defined subsets is a hard task, adding yet another level of complexity to the ongoing debate (Rosato et al., 2020).

CD8+ T cells are often divided into subpopulations based on expression of CD44 and CD62L. Generally, CD44 is a marker for T cell activation and distinguishes effectors and memory cells from naive T cells (Schumann et al., 2015), while CD62L is a marker for trafficking of T

lymphocytes to and from peripheral lymph nodes, which sheds from the cell membrane following T cell activation (Yang et al., 2011). CD8+ T cell phenotypes considered in this dissertation are based on a more extensive antibody panel, including further markers for naive, effector and memory phenotypes, allowing for identification of various CD8+ T subpopulations. Those include CD44-CD62L+ CD8+ T cells which contain naive cells, early activated cells (EA), and stem cell memory (SCM), CD44+CD62L- CD8+ T cells, containing early effector cells (EEC), short-lived effector cells (SLEC), memory precursor cells (MPEC), effector memory (EM) and tissue resident memory cells (TRM), and CD44+CD62L+ CD8+ T cells, containing central memory cells (CM).

Essentially, a memory CD8+ T cell is a cell that has responded to its respective antigen and has persisted long-term. They can populate peripheral organs and can quickly respond to re-stimulation by vigorous proliferation, perform cytotoxic functions and secrete effector cytokines (Martin & Badovinac, 2018). Memory CD8+ T cells represent yet another heterogeneous population of cells that consist of variety of phenotypes and functions (and protective capacity). The stem cell memory subset is a naive-like memory cell with high capability to self-renew. They are mainly found in lymphoid organs where they give rise to other memory cell subsets (Lugli et al., 2021). Central memory cells are mainly found in secondary lymphoid organs. Due to the expression of lymphoid homing receptors, they mainly circulate in the blood and lymph. Effector memory cells, mainly circulate in non-lymphoid tissues, their expression of particular receptors allows them to enter inflammation sites. They contain high cytolytic potential compared to other memory cells. Tissue resident memory cells are a relatively newly identified cell population that infiltrate non-lymphoid tissues where they undergo a differentiation program into a tissue resident cell. Tissue resident memory cells govern the tissue and can re-encounter with their antigen locally, making them the first line of defence with rapid inflammatory response (Fonseca et al., 2020). Tissue resident memory cells are one of the cells that have been difficult to place in the current lineage hierarchy, they share properties with other CD8+ T cell effector and memory populations, and whether they are terminally differentiated is under debate (Fonseca et al., 2020; Jameson & Masopust, 2019; Rosato et al., 2020). The ability of tissue resident memory cells to re-enter the peripheral circulation has also been debated, but evidence of a re-circulation has been published (Fonseca et al., 2020). Recently, a distinct memory population within non-lymphoid tissue has been identified, termed peripheral memory T cells (TPM), which can traffic the blood, lymph nodes and peripheral non-lymphoid tissues. Here, high, intermediate, and low levels of CX3CR1

expression have been suggested to separate effector memory, peripheral memory, and central memory cells, respectively (Gerlach et al., 2016; Martin & Badovinac, 2018).

CD8+ T cell populations in humans are not consistently identified with the same markers as used in mice. For instance, instead of CD44 and CD62L, CD45RA and CD27/CCR7 are commonly used to identify human naive (CD45RA+, CCR7/CD27-), effector memory (CD45RA-CCR7/CD27-), central memory (CD45RA-CCR7/CD27+), and the so-called effector memory re-expressing CD45RA (CD45RA+CCR7/CD27+) associated with enhanced cytotoxicity. Other markers such as CD127, KLRG1, CD69 and CD103 are typically used for further identification as in mice.

Table 1. Markers used for identification of mouse CD8+ T cell subsets considered in this dissertation. *EA: early activated, EEC: early effector cell, SCM: stem cell memory, SLEC: short-lived effector cell, MPEC: memory precursor effector cell, TRM: tissue resident memory cell, CM: central memory, CML: central memory like. N/A: not available.*

	Naive	EA	SCM	EEC	SLEC	MPEC	EM	TRM	CM
CD44	-	-	-	+	+	+	+	-	+
CD62L	+	+	+	-	-	-	-	-	+
CD69	-	+/-	N/A	-	+/-	-	-	+	+/-
CD127	+/-	+/-	+	-	-	+	+	+	+
KLRG1	-	+/-	-	-	+	-	+	-	-
CD122	-	N/A	+	N/A	N/A	N/A	N/A	N/A	+/-

1.3.2.2 Cellular functional states

CD8+ T cells develop in the thymus where they undergo a strict selection of cells allowed to enter the circulation. This involves a negative selection of self-reactive T cells resulting in central tolerance. However, a deletion of self-reactive T cells is an imperfect process, thus additional peripheral tolerance mechanisms are crucial (Bouneaud et al., 2000). Those involve the establishment of variable responsiveness of a stimulus, which can be viewed as „responsive states“ of a CD8+ T cell or its functional state, generating immune tolerance to the stimulus. These states include quiescence, ignorance, anergy, exhaustion, dysfunction, senescence and deletional tolerance (Hardardottir et al., 2021). In this dissertation, CD8+ T cell fate is considered to enter two parallel and overlapping developmental trajectories where the first is the above-mentioned activation of a naive cell followed by differentiation into diverse effector and memory populations, the second being the cell‘s functional state (Hardardottir et al., 2021). Chronic antigen stimulation can lead to a CD8+ T cell to acquire an exhausted state, however exhausted cells have been reported early in infection suggesting there are additional means of

acquiring the exhausted state beside chronic antigen exposure (Speiser et al., 2014). Exhausted cells exhibit specific features, which are likely related to microenvironment-specific cues, for instance, exhausted cells have been detected at infection sides and in a tumour microenvironment. The general view is that their existence prevents immunopathology within the host by reducing inflammatory responses (Alfei et al., 2019; Blank et al., 2019; Frebel et al., 2012). A misconception is that exhausted cells completely lack effector function, which would more accurately describe a dysfunctional state, more commonly found in tumours (Philip & Schietinger, 2019). Of note, exhausted CD8+ T cells can be dysfunctional but not all dysfunctional CD8+ T cells are exhausted (Blank et al., 2019). Exhausted cells have been associated with expression of inhibitory checkpoint receptors, such as PD1 (Programmed cell death protein 1), Tim3 (T cell immunoglobulin and mucin domain-containing protein 3), Lag3 (Lymphocyte activation gene 3), Tigit (T-cell immunoglobulin and ITIM domain) and CTLA4 (cytotoxic T-lymphocyte-associated antigen 4) (Blank et al., 2019), partly accounting for the reduced or modulated immune response. However, these inhibitory receptors have likewise been associated with other CD8+ T cell states, such as dysfunction and various CD8+ T cell trajectories. Therefore, the use of those inhibitory markers for identification of exhaustion is troublesome and to some extent inaccurate. Recent work has identified a few transcription factors allowing for more accurate identification of exhausted cells, those are TOX (Thymocyte selection-associated HMG bOX) and TCF1 (Transcription factor 1), with TOX+TCF1+ cells being stem cell-like progenitors which self-renew and generate the TOX+TCF1- population containing terminally differentiated exhausted T cells (Jeannet et al., 2010). Yet, no definitive marker is accepted to accurately distinguish exhausted cells from other CD8+ T cell subsets (Blank et al., 2019).

1.4 CD8+ regulatory T cells

T cells with a regulatory function have been identified in humans and mice. Those are commonly referred to as CD4+ regulatory T cells, which express the transcription factor FoxP3, often termed Treg cells (Herndon et al., 2005). CD4+ Treg cells maintain homeostasis and self-tolerance, by limiting T cell proliferation and cytokine production, thereby suppressing the immune system and their dysregulation often leads to immunopathology disorders (Kondělková et al., 2010).

Although CD4+ Treg cell are typically considered as „The Treg cells“, subset of CD8+ T cells with a suppressive/regulatory potential was discovered decades before CD4+ Treg cells (Xu &

Larbi, 2017). The reason the research on CD8+ Treg cells did not take off, was the dilemma of phenotypically distinguishing them from other CD8+ T cell subsets, while research on CD4+ Treg cells progressed massively. Although research on regulatory CD8+ T cells is still to this day hindered by the lack of definite markers and mechanisms, the field has progressed with identification of several candidate markers and interesting findings on their role in various biological context and pathologies, such as in autoimmune diseases, organ transplantations, infections and in tumour tolerance (Bézie et al., 2018; Cyktor et al., 2013; Endharti et al., 2011; Gershon & Kondo, 1970; Jiang et al., 2010; Li et al., 2022; Saligrama et al., 2019; Smith & Kumar, 2008).

1.4.1 Identification and origin of CD8+ regulatory T cells

Multiple markers and co-expressed sets of markers for CD8+ regulatory T cells have been reported in mice and humans. CD8+ T cells expressing the surface molecule CD122, which is the beta chain of the Interleukin 2 receptor (IL-2Rβ), is of particular interest as they have been shown to contain regulatory function in mice. As CD8+CD122+ T cells can also be memory cells, CD122 alone is not sufficient for identification of CD8+CD122+ regulatory T cells. In humans, CD8+ regulatory T cells cannot be distinguished by CD122 expression. The molecule CXCR3 has been hypothesized to be the human equivalent of mouse CD122 in CD8+ regulatory T cells (Shi et al., 2009), but these findings are debated. Scientists have attempted to discover additional markers for their identification in mice and humans. One finding is the expression of previously mentioned inhibitory checkpoint molecule PD1 (Cagnoni et al., 2021; Dai et al., 2010; Dai et al., 2014; Elizondo et al., 2019; Li et al., 2014; Liu et al., 2017). Another recent finding of CD8+ T cell subsets with regulatory function is the expression of the lectin-like receptors (Ly49) in CD8+CD122+ T cells in mice and an expression of their functional human equivalent, the killer immunoglobulin-like receptors (KIR) in humans (Carter, 2011, 2020; Croy et al., 2003; Li et al., 2022; Penman et al., 2016; Saligrama et al., 2019). CD122 is the receptor for both IL-2 and IL-15, thus the ligand availability likely influences the CD122 mediated signalling in CD8+CD122+ regulatory T cells and therefore, the T cell response.

Other CD8+ regulatory T cell subsets have been reported, based on restriction to Qa1 in mice, the expression of FOXP3 and the CD8αα receptor in mice and humans, the absence of CD28, expression of HLA+DR+, and the specificity for hemoxygenase-1 (HMOX-1) derived peptides in humans (Andersen et al., 2009; Angin et al., 2017; Niederlova et al., 2021; Saligrama et al., 2019; Solano et al., 2015; Tilburgs, van der Mast, et al., 2009). The expression of further

inhibitory molecules, such as CTLA4, Lag3 and Tigit has also been used to identify CD8+ regulatory T cells (Bézie et al., 2018; Saligrama et al., 2019), which creates a dilemma as they also serve to identify the previously mentioned exhausted CD8+ T cells.

Due to the accumulating evidence of regulatory properties of CD8+ T cells expressing CD122, in this dissertation we focus on their investigation in pregnancy. As a starting point, we generated preliminary data on the abundance of CD8+CD122+ T cells in diverse lymphoid and non-lymphoid tissues across the lifespan of a mouse, spanning from fetal life (GD 18.5), reproductive age (3-5 months old) to an old age (8 months old). CD8+CD122+ T cells appear to be generated post-thymically in fetuses, as they were abundant within the liver and blood but low in the thymus **(Figure 4A)**. Also, they were found in higher frequency in the peripheral blood in fetal life and in old age compared to young adulthood, during the peak of the mouse reproductive window **(Figure 4A)**. In adulthood the frequencies of CD8+CD122+ T cells are enriched in the peripheral organs analysed, liver and uterus, compared to lymphoid organs. Their frequencies may not be influenced by the sex of the mice, as they did not differ in female and male blood and para-aortic lymph nodes **(Figure 4B)**. Although immune cells can fluctuate during the estrous cycle, the frequency of CD8+CD122+ T cells were not significantly altered between the four different stages of the estrous cycle of virgin mice, thus the virgin mice used in this dissertation were not selected based on a particular estrous stage (Appendix 1). Taken together, this preliminary information highlighted a cell subset whose origins require further elucidation and that may be involved in tissue specific responses.

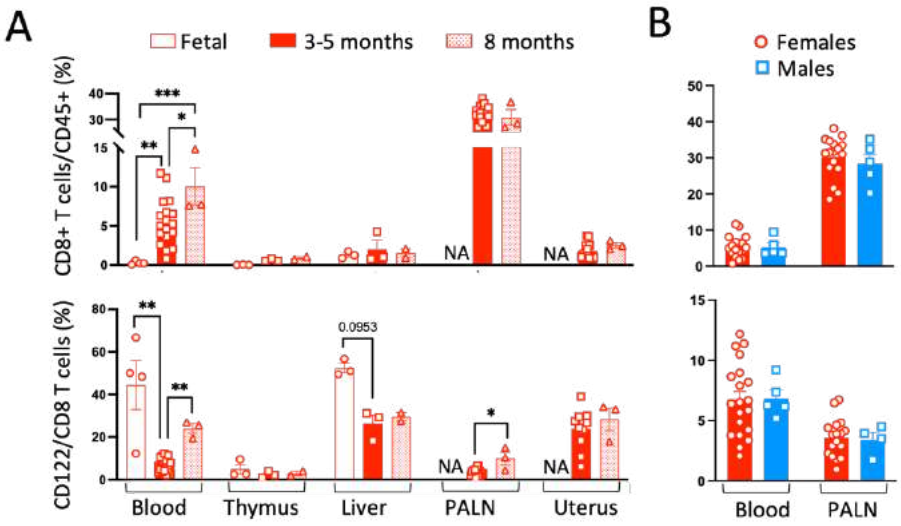

Figure 4. CD8+CD122+ T cells across the lifespan of a mouse.
A) *The ratio of CD8+ T cells in CD45+ leucocytes (top) and the ratio of CD8+CD122+ T cells CD8+ T cells (bottom) in females from fetal age of GD 18.5, mice of reproductive ag (3-5 months old) and aging mice at 8 months old in selected tissues.* ***B)*** *The ratio of CD8+ T cells in CD45+ leucocytes (top)*

and the ratio of CD8+CD122+ T cells CD8+ T cells (bottom) in females (red) and age matched males (blue) in blood and para-aortic lymph nodes (PALN). N/A: Not available.

1.4.2 CD8+ regulatory T cell function and mechanisms

CD8+ regulatory T cells have been shown to exert their regulatory function by various means. Those include suppression of cytotoxic or autoreactive T cells by suppressing proliferation and secretion of inflammatory cytokines of conventional CD8+ T cells, as well as triggering their apoptosis via Fas (Tumor necrosis factor receptor superfamily member 6) and FasL (Fas ligand) and with secretion of cytotoxic granules containing Perforin and Granzyme B (Akane et al., 2016; Li et al., 2022; Saligrama et al., 2019). They have even been claimed to maintain T cell homeostasis with a higher potential than CD4+ regulatory T cells (Dai et al., 2014; Endharti et al., 2011; Okuno et al., 2013; Rifa'i et al., 2004; Shimokawa et al., 2020). Furthermore, CD8+ regulatory T cells have been shown to secrete anti-inflammatory cytokines IL-10 (Interleukin-10) and TNFα and the inflammatory cytokine IFNγ (Elizondo et al., 2019; Endharti et al., 2005; Mangalam et al., 2012). CD8+Ly49+ T cells have been regarded as a regulatory population, that are Qa-1 restricted (HLA-E in humans), controlling various autoimmune diseases, by killing Qa-1 expressing follicular helper T cells via degranulation (Hu et al., 2004; Jiang et al., 1995, 2010; Kim et al., 2010; Kim et al., 2011; Leavenworth et al., 2013) Recently CD8+CD122+Ly49+ /CD8+KIR+ regulatory T cells were recently shown to suppress CD4+ T cells specific for myelin oligodendrocyte glycoprotein and gliadin-specific CD4+ T cells, in mouse model for multiple sclerosis and in patients with celiac disease (Li et al., 2022), respectively, thus keeping the CD4+ T cells contributing to disease severity under control. This was mediated via direct killing by CD8+ regulatory T cells of pathogenic CD4+ T cells with cytotoxic molecules, upon recognition of both classical and non-classical MHC I molecules. Also, CD8+ regulatory T cells may mediate their regulatory function indirectly via interaction with other immune cells, for instance by suppression of costimulatory molecules in dendritic cells. However, the detailed mechanism of CD8+ regulatory cells is not fully understood.

Collectively, to date, there is no consensus about which molecules unambiguously can identify CD8+ regulatory T cells due to the heterogeneity of reported CD8+ regulatory T cells and the phenotypical and functional overlapping features with other CD8+ T cell subsets and functional states. Their classification and nomenclature as "regulatory CD8+ T cells" have been debated among immunologists (Dai et al., 2014). However, the immune regulatory properties of CD8+ T cells in important biological phenomena cannot be denied. It cannot be excluded that more

than one CD8+ regulatory T cells exists, with distinct characteristics and function. Thus, perhaps, looking for the one and only CD8+ regulatory T cell subset across the whole organism, as complex as we know it is, in health and disease, may not be the ideal ultimate goal. Nevertheless, understanding which CD8+ regulatory subset/s under which circumstances play a critical role is essential for fully understanding T cell immunity, modulation, and function within and beyond pregnancy context.

1.5 CD8+ T cells in pregnancy

Interestingly, patients with multiple sclerosis, an autoimmune disease of the central nervous system, containing autoreactive CD8+ and CD4+ T cells against central nervous system peptides (Salou et al., 2015) experience reduced disease activity during pregnancy. This is due to an altered inflammatory response as a result of pregnancy-related hormones (Confavreux et al., 1998; Varyté et al., 2020). The pregnancy hormones progesterone and estradiol rise in pregnancy. They can modulate immune responses in the endometrium acting either directly on CD8+ T cells and indirectly via the uterine microenvironment (Shen et al., 2021) Glucocorticoids likewise rise during pregnancy, although their role in pregnancy is less understood (Solano & Arck, 2020). The target receptor for progesterone has been reported to be both the progesterone and glucocorticoid receptor. Interestingly, immune adaptations to pregnancy are induced by binding of progesterone to the glucocorticoid receptor on T cells (Engels et al., 2017; Hierweger et al., 2019), thus underscoring the importance of the glucocorticoid receptor in T cells during pregnancy.

Collectively, this suggests that pregnancy does not only affect immune cell behaviour at the feto-maternal interface but also systemically, further supported by the presence of immunological memory in the peripheral circulation as fetal antigens and memory cells from previous pregnancy circulate the body before and during future pregnancies (Kinder et al., 2020). It is known that stress exposure during pregnancy negatively affects fetal development in mice. Interestingly, this is accompanied by significantly higher frequency of CD8+ T cells, and increased ratio of CD107a+IFNγ cytotoxic CD8+ T cells, in uterine-draining lymph nodes. Furthermore, depletion of CD8+ T cells significantly reduced fetal development and fetal weight (Solano et al., 2015). Although these are certainly interesting and insightful findings, in order to progress our understanding of CD8+ T cells in pregnancy, gaining knowledge about the CD8+ T cells localized at the feto-maternal interface is crucial.

1.5.1 Uterine immune cells

Various immune cell types have been detected at the feto-maternal interface. They include granulocytes, containing neutrophils and mast cells, NK cells, dendritic cells, macrophages, and T cells (Sanguansermsri & Pongcharoen, 2008). Macrophages have been extensively investigated in the decidua where they portray great plasticity in the changing micro-environment of the feto-maternal interface. They are known to be involved in immune regulation, tissue homeostasis tissue remodelling allowing for the necessary spiral artery formation (Faas & De Vos, 2018; Jantsch et al., 2017; Solano, 2019; Svensson-Arvelund et al., 2015). Although conventional dendritic cells are found in low frequencies in human decidua, a subpopulation called conventional dendritic cells 1, are enriched in the decidua compared to blood, which can cross-present fetal antigens bound to HLA-I molecules, to CD8+ T cells. However, decidual dendritic cells tend to display an immature phenotype, potentially limiting local activation of CD8+ T cells (Blois et al., 2007; Faas & De Vos, 2018; Vento-tormo et al., 2018). An innate lymphoid cells population, termed NK cells, are the most frequent leucocyte population in the decidua early in pregnancy (Bartmann et al., 2014). Unique NK cells have been detected in the uterus, not found in other organs, called uterine NK cells which can interact with HLA-C molecules on trophoblast cells. They are rich in inhibitory receptors, such as inhibitory KIR/Ly49 and NKG2A which prime NK cells for a proper function in pregnancy (Björkström et al., 2012; Shreeve et al., 2021). In addition to playing a role in immune tolerance towards the fetus, they play a critical role in uterine arterial remodelling including facilitating angiogenesis and spiral artery invasion (Faas & de Vos, 2017; Faas & De Vos, 2018; Moffett & Colucci, 2014). Furthermore, other lymphocyte subsets at the feto-maternal interface have been shown to be important for pregnancy, including NKT cells (Miko et al., 2021; Yao et al., 2019) and B cells (Guzman-Genuino et al., 2019).

Importantly, T cells have been identified in the pregnant uterus in mice and humans where identification of uterine CD4+ Treg cells (CD4+Fox3+CD25+) has been of particular interest. They are enriched in the decidua, compared to peripheral blood, where they display a more differentiated phenotype along with higher levels of inhibitory receptors PD1, Tim3, CTLA4 and Lag3, and higher expression of the CXCR3 ligand suggesting a leucocyte recruitment in human pregnancy (Powell et al., 2017; Sasaki et al., 2004). They secrete IFNγ and IL-17 and are involved in uterine spiral artery remodelling and trophoblast invasion (Powell et al., 2017). As previously mentioned, CD4+ T cells recognise antigens bound to MHC- II molecules, which

are presented by APC's but not by trophoblast cells (Powell et al., 2017). As the focus of this dissertation is uterine CD8+ T cells, they will be covered in their own subchapter.

Collectively, the decidual lymphocytes come in very close contact with the EVT. What many uterine leucocytes have in common is a unique phenotype, which could be promoted by the communication with EVT, decidual cells and the unique microenvironment. They often present an altered immune profile with distinct immune response and function, as well as many promote the necessary placentation and tissue homeostasis, involving tissue regeneration. Thus, uterine leucocytes contain both an immune-related function and a non-immune function in pregnancy. Due to the nature of the complex direct and indirect interactions of distinct leucocytes at the feto-maternal interface, each population should be viewed from the perspective of the whole immune system for understanding the orchestrated modulation to pregnancy. Thus, understanding the understudied uterine CD8+ T cell features and function is crucial for painting the whole picture of the decidual immune cell responses.

1.5.2 Uterine CD8+ T cells

CD8+ T cells have highly diverse roles involving interactions with other cells, including the above-mentioned immune cells. They are found in a non-pregnant uterus and their activity oscillates during the menstrual cycle in humans (White et al., 1997). In early pregnancy, CD8+ T cells constitute approximately 45% of T cells and T cells are approximately 5-20% of decidual cells in humans (Tilburgs et al., 2010; Zeng et al., 2018), while CD8+ T cells constitute approximately 15-20% of T cells in mouse decidua (Li et al., 2018). Although decidual NK cells have received great attention in pregnancy, it is the T cells that with the progress of pregnancy actively increase their frequency while NK cells remain stable after mid pregnancy (Lissauer et al., 2017; Stallmach et al., 1999; Williams et al., 2009).

1.5.2.1 Uterine CD8+ T cells in mice

Decidual CD8+ T cells have been much less investigated in mice compared to humans. In fact, the lack of an in dept phenotyping represents a major gap in knowledge for understanding CD8+ T cell function in mouse pregnancies. Although the end goal is to understand CD8+ T cell roles in human pregnancies for development of novel interventions of pregnancy complication, the advantage of characterizing uterine CD8+ T cells in mice would allow for better interpretation of important functional mouse studies in mice which for ethical reasons are not possible in

humans. However, a relatively new study mapped decidual dendritic cells and T cell subsets in syngeneic pregnancy with flow cytometry. They reported a complex dendritic cell dynamics during pregnancy, with stable frequencies of CD8+ T cells out of total T cells across pregnancy. They used CD44, CD62L and CD69 to identify naive cells as CD44-CD62L+, memory cells as CD44+CD62L- and activated cells as CD69+ (Li et al., 2018). Classification of CD8+ T cell subsets with this gating strategy is misleading as memory cells fall in CD44+CD62L+ population, effectors fall into the CD44+CD62L- population and CD69 is not solely reliable as activation marker due to its expression in tissue resident memory cells. Therefore, although insightful, the findings do not give adequate insights into decidual CD8+ T cell subtypes and a deeper analysis is still missing.

Data on the regulatory function and mechanisms of CD8+ regulatory T cells in maternal tolerance towards fetal antigens are limited, in both mice and humans. Evidence support that CD8+ regulatory T cells are pivotal players in pregnancy in mice (Solano et al., 2015). For example, mid gestational stress challenge in mice resulted in IUGR, placental insufficiency and increased CD8+ T cell cytotoxicity in uterine-draining lymph nodes which was due to a decreased frequency of the CD8+ regulatory T cells (Solano et al., 2015). Furthermore, adoptive transfer of CD8+CD122+ T cells into pregnant mice prevented inflammation-induced IUGR, improving placental and fetal growth, suggesting an important regulatory function in pregnancy (Solano et al., 2015), thus providing the first indication of importance of regulatory CD8+ T cells in pregnancy in mice. Expression of the regulatory markers, CD122 and PD1 have been detected in mucosal associated invariant T (MAIT) cells, atypical T cells which are predominantly CD8+ T cells (Dusseaux et al., 2011; Solders et al., 2017). MAIT cells are present in placenta and decidua (Solders et al., 2017) where they may contribute to the immune environment by cytokine secretion. Expression of various inhibitory receptors in CD8+ T cells have been reported in mouse decidua (Tilburgs, Scherjon, et al., 2009; S. C. Wang et al., 2015). In fact, abortion prone mice have significantly lower frequency of Tim3+CTLA4+ decidual CD8+ T cells in pregnancy, which produced higher levels of the inflammatory cytokine IFNγ, compared to normal pregnancies in Bl6 (C57BL/6J strain) controls. Also, Tim3 and PD1 blockage by antibodies in normal pregnancies were more susceptible to fetal loss (Wang et al., 2019; Xu et al., 2017) highlighting the beneficiary effect of expression of such inhibitory receptors in CD8+ T cells for a successful pregnancy.

1.5.2.2 Uterine CD8+ T cells in humans

Decidual CD8+ T cell subpopulations in humans was recently reviewed in Hardardottir et al. (2021). In humans, naive, memory and effector phenotypes have been identified and characterized in the decidua by several independent research groups. Collectively, decidual CD8+ T cells appear to be largely antigen-experienced cells with more advanced differentiation compared to peripheral blood, containing particularly higher frequency of effector memory subsets and tissue resident CD8+ T cells. The similarity of methodological aspects such as cell isolation and antibody panel selection between the research groups allows for adequate comparison of the findings, but some differences between experiments, and more importantly common misconception, halt the proper interpretation of the accumulated findings. For instance, effector memory cells are commonly characterized as CD45RA-CCR7-, while tissue resident memory cells are commonly characterized as CD103+CD69+, however tissue resident memory cells would fall into the CD45RA-CCR7- gate, thus not taking all four markers into account, tissue resident memory cells might be mistakenly referred to as effector memory cells. Therefore, although the current criteria and marker selection gives important insights into decidual CD8+ T cells, it does not give an accurate image of their subpopulations.

Identified regulatory subsets in the human decidua include CD8+ T cells restricted to HLA+DR+ cells (Angin et al., 2017) and CD8+CD28- (Machicote et al., 2016; Tilburgs, Scherjon, et al., 2009; Tilburgs, van der Mast, et al., 2009), which were found to be enriched in the decidua compared to peripheral blood. Although studies on decidual CD8+ regulatory T cells as such are scarce, current literature strongly reports tissue specific features of decidual CD8+ T cells, of which some resemble CD8+ regulatory T cell characteristics reported in contexts outside of pregnancy. Tissue specific features of decidual CD8+ T cells include low cytotoxicity due to low basal levels of secreted perforin and granzyme B. However, in addition to presence of activated effector and memory cells, decidual CD8+ T cells display a potent secretory profile, including high levels of IFNγ, indicating an active response to pregnancy. Furthermore, the functional states are also distinct from the peripheral blood CD8+ T cells, as expression of inhibitory receptors, PD1, Tim3 and CTLA4 are enhanced in highly differentiated cell subsets within the decidua.

1.5.2.3 Mechanisms of immune tolerance mediated by CD8+ T cells

The feto-maternal interface promotes peculiar CD8+ T cell responses, which are critical for immune tolerance towards the fetus as faulty CD8+ T cell recruitment and differentiation

disturbs establishment of proper immune tolerance (Arck et al., 1996; Blois et al., 2004; Clark et al., 1989; Solano et al., 2015). The tightly controlled features of CD8+ T cell compartment in the decidua, with regards to finely tuned differentiation paths, expression of inhibitory receptors and a precise secretion profile are altered in pathological pregnancies, such as preeclampsia, miscarriage and IUGR (Dunk et al., 2019; Kieffer et al., 2020; Lager et al., 2020; Southcombe et al., 2017; Wang et al., 2019; Wang et al., 2015; Xu et al., 2017). CD4+ regulatory T cell mechanism has been shown to involve inhibition of autologous T cell proliferation of conventional CD4+ T cells via cell-to-cell contact (Sasaki et al., 2004). Although not fully understood, a few tolerance mechanisms of CD8+ regulatory T cells might be at play at the feto-maternal interface.

One tolerance mechanism include the presence of fetal trophoblast cells which lack the polymorphic classical HLA-A and HLA-B molecules (Apps et al., 2009; Tilburgs & Strominger, 2013), expressing only HLA-C and the non-classical HLA-E, HLA-F and HLA-G. The classical MHC-I molecules present antigens in the form of peptide ligands to CD8+ T cells while non-classical MHC-I molecules, which contain lower genetic diversity generally mediate activating or inhibiting signals to cells such as NK cells, NKT and T cells (Bahri et al., 2006; Halenius et al., 2015; Kochan et al., 2013). Thus, rendering fetal trophoblasts almost "invisible" to human CD8+ T cell cytotoxic responses specific for paternal antigens mediated by HLA-A and HLA-B recognition, where the only visibility by CD8+ T cells could be by HLA-C. HLA-C restricted virus specific CD8+ T cells have been detected in the uterus (van der Zwan, van der Meer-Prins, et al., 2018), but the question of whether CD8+ T cells can directly recognize fetal (paternal) HLA-C, is still unanswered. Even less is known about the MHC expression in mouse placental trophoblast cells and antigen specificity of CD8+ T cells within the uterus. Madeja et al. (2011) demonstrated that placental trophoblast cells mainly express the classical MHC-I H2-K and H2-D, the former being the ortholog of HLA-C, and unlike in humans, that Qa1 and Qa2, orthologs of HLA-E and HLA-G, respectively, were not detected in fetal trophoblast cells (Madeja et al., 2011) **(Table 2).** The expression of the human HLA-C and the murine H2-K in fetal trophoblast cells gives weight to the expression of KIR and Ly49 in CD8+ T cells, as those are the respective receptors for this MHC-I molecule, resulting in stimulatory or inhibitory effect within the CD8+ T cell, depending on the nature of the receptor **(Table 2).** However, whether Ly49 are expressed in uterine CD8+ T cells is not known.

Table 2. Expression of classical and non-classical MHC-I in humans, Bl6 mice and Balb/c mice. *MHC marked with a star (*) has been detected in fetal trophoblast cells. Arrow indicates known murine H-2 ortholog of respective human HLA* (Affymetrix eBioscience, n.d.; Rahim et al., 2014).

MHC-I	Human	Mouse (B6)	Mouse (Balb/c)
Classical	HLA-A	***H2-D^{b}**	H2-D^{d}
	HLA-B		H2-L^{d}
	***HLA-C** →	***H2-K^{b}**	H2-K^{d}
Non-classical	HLA-D		
	***HLA-E** →	Qa1^{b}	Qa1^{b}
	***HLA-F** →	Qa2^{a}	Qa2^{a}
	***HLA-G**		

A second tolerance mechanism could be via immune checkpoint receptors **(Figure 5).** The expression of the inhibitory receptors such as PD1, Tim3, CTLA4, Lag3 and Tigit can modulate CD8+ T cell function. This is achieved by binding of respective ligands modulating the function. These ligands have been detected at the feto-maternal interface in humans and some in mice, strongly suggesting active immune checkpoint mechanism for fetal tolerance. PD1 expression might bind PD-L1 (Programmed cell death protein ligand 1) bound on APC and trophoblast cells with numerous possibilities, including limiting their own T cell activation (Jiang et al., 2019), altering the interaction with target cells, and enhancing the proliferation of PD1+ CD8+ T cells (Pardoll, 2012). CD8+Lag3+ cells binding to HLA class II molecule expressed on various immune cells at the feto-maternal interface may interfere with antigen presentation, while binding of CD8+ T cells expressing CTLA4 or Tigit to their ligands, CD80/CD86 and CD155/CD112, respectively may interfere with co-stimulation (Qin et al., 2019). Interestingly, Tim3 expression on CD8+ T cells is generally known to induce apoptosis upon binding to Gal9, but co-expression of PD1 with Tim3, found in tumour environment, modulates the Tim3/Gal9 mediated apoptosis into the proliferation instead. Other inhibitory receptors, such as CTLA4 and Tim3 have been reported to synergize inhibitory response with amplified anti-inflammatory cytokine release. Thus, understudied synergism and crosstalk of inhibitory receptors on a single CD8+ T cell can create unique CD8+ T cells functions in certain micro-environments, which might be taking place at the feto-maternal interface. As inhibitory receptors have been associated with exhaustion, dysfunction and CD8+ regulatory T cells, relying on those inhibitory markers for distinguishing CD8+ T cell subsets can be treacherous. Although one may imagine exhausted CD8+ T cells and the functional CD8+ regulatory T cells may overlap to some extent, for instance via the function of inhibitory receptors, evidence pinpoint functional differences.

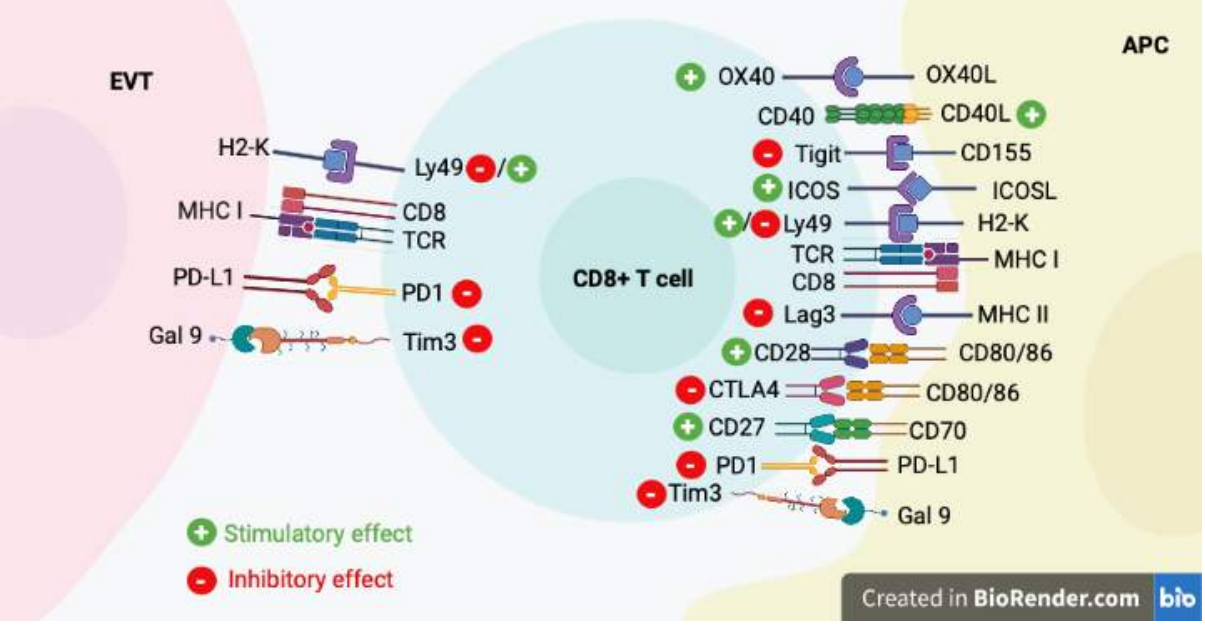

Figure 5. Potential interactions of uterine CD8+ T cells with extravillous trophoblast cells (EVT) and antigen presenting cells (APC) at the feto-maternal interface.
A green plus and a red minus indicates a stimulatory effect and an inhibitory effect, respectively, of the corresponding receptor-ligand binding. Figure was created in Biorender. Figure was influenced by (InvivoGen, n.d.; Moffett & Shreeve, 2022; Vento-tormo et al., 2018; Wykes & Lewin, 2018).

A third possible regulatory mechanism is by secretion of anti-inflammatory cytokine secretion. Decidual CD8+ T cells, in particular tissue resident memory cells, are potent producers of anti-inflammatory TGFβ (Transforming growth factor beta) and IL-4 (34). TGFβ is highly associated with immune evasion, for instance by modulating the differentiation of CD4+ T cells and dendritic cells into a tolerogenic phenotype (Moffett & Shreeve, 2022). IL-4 and IL-10 are pleiotropic cytokines which generally suppress a pro-inflammatory microenvironment, including the feto-maternal interface (Chatterjee et al., 2014). However, whether CD8+ regulatory T cells secrete IL-10, as is the case for CD4+ Treg cells (Dai et al., 2014; Elizondo et al., 2019; O'Garra et al., 2004), is controversial.

The fourth potential regulatory mechanism is a pro-inflammatory cytokine secretion profile modulating leucocytes that pose a threat to pregnancy and/or modulating other somatic cells at the feto-maternal interface. Indeed, it is widely accepted view that inflammation is an important part for pregnancy milestones, such as implantation and placentation (Alijotas-Reig et al., 2017). Decidual CD8+ T cells are known to express high levels of IFNγ and TNFα. Although IFNγ is a typically considered a potent anti-viral cytokine, at the feto-maternal interface it has a distinct function for instance by promoting vascular remodelling and angiogenesis, necessary for successful pregnancy (Murphy et al., 2009).

The fifth possible regulatory mechanism is cytotoxicity towards leucocytes that pose a threat to pregnancy. Although decidual CD8+ T cells in human express low levels of the cytolytic molecules Granzymes B and Perforin, killing pregnancy-threatening leucocytes with cytotoxic granules may be a regulatory mechanism contributing to tolerance, as seen in CD8+CD122+Ly49 and CD8+KIR+ regulatory T cells in mice and humans, respectively, in other contexts (Kim et al., 2011; Leavenworth et al., 2013; Li et al., 2022; Saligrama et al., 2019). Killing via Fas/FasL might be another killing mechanism of uterine CD8+ T cells (Janeway Jr et al., 2001).

Moreover, the unique microenvironment at the feto-maternal interface, besides the local immune system, is a major component of acquiring fetal tolerance as stromal cells, endothelial cells and decidual cells influence the differentiation of the immune system. For instance, IL-15 levels, one of the ligands for CD122, have been reported to be high at the feto-maternal interface (Gordon, 2021), which could have an indication for a presence of local CD8+CD122+ T cells. Whether CD8+CD122+ T cells are found at the feto-maternal interface has so far not been reported.

The feto-maternal interface has some similarities with a tumor microenvironment, representing a genetically different cell mass striving to evade the hosts immune system in order to survive. Also, similarities can be found between the feto-maternal interface and chronic infections due to prolonged exposure to the foreign antigens. It is not surprising that all three situations may induce similar CD8+ T cell exhaustion state and induction of CD8+ regulatory T cells. Although the expression of inhibitory receptors within decidua in mice and humans (Huang et al., 2020; Liu et al., 2020; Morita et al., 2020; Powell et al., 2017; Slutsky et al., 2019; Tilburgs et al., 2010; van der Zwan, Bi, et al., 2018; Zeng et al., 2018) indicate exhausted or dysfunctional states, and regulatory function, the expression of more accurate transcription factors for exhausted cells in the decidua has not been investigated. With current knowledge, CD8+ regulatory T cells cannot accurately be distinguished from other CD8+ T cell subsets due to the overlapping characteristics with effector and memory subsets, MAIT cells and exhausted cells, giving misleading reporting of CD8+ T cells. The solution to this dilemma within the scientific community, would be to combine an in-dept phenotypic characterisation with functional analysis (Feyaerts et al., 2017).

1.6 Antigen specificity of uterine CD8+ T cells

The CD8+ T cell immune response following recognition of peptide fragments of an antigen bound to the MHC molecule is dependent on the diversity of the CD8+ T cell repertoire, also termed T cell clonality (Chiffelle et al., 2020), in each individual, organ or micro-environment. Upon activation of a particular TCR clone, CD8+ T cell undergoes clonal expansion resulting in a population of identical cells yielding in sufficient numbers of antigen specific CD8+ T cells mounting an immune response for the threat (Janeway Jr et al., 2001). Antigen specificity of TCR repertoires among uterine CD8+ T cells is of interest as it gives information about the history of local CD8+ T cell responses. As fetal antigens are known to shed to the circulation during pregnancy in both mice and humans, it is not surprising that fetal antigen specific T cells exist (Moffett et al., 2015; van Kampen et al., 2002). Indeed, antigen specific CD4+ Treg cells have been detected in pregnancy, activated by antigens in the seminal fluid and from placenta (Sharkey et al., 2012) and have been shown to clonally expand in human pregnancies (Tsuda et al., 2018). As previously mentioned, several studies have unveiled an accumulation of antigen experienced CD8+ T cells in the uterus, with particular CD8+ T cell clones found to be specific for fetal and viral antigens which were enriched in the decidua compared to peripheral blood (Egmond et al., 2016; Morita et al., 2020; Powell et al., 2017; Vento-tormo et al., 2018) thus, refuting Medawar's hypothesis of the maternal immune system ignoring fetal antigens. Interestingly, locally expanded fetal specific CD8+ T cells were detected in human decidua, by identifying CD8+ T cells specific for peptides derived from male (fetal) specific HY chromosome (Powell et al., 2017). These clonally expanded fetal specific decidual CD8+ T cells had a highly differentiated profile (mainly effector memory and effector memory re-expressing CD45RA phenotype) with indications of tissue residency and altered responsive state due to expression profile of CD69 and PD1 (Morita et al., 2020; Powell et al., 2017).

Important insights into fetal-specific CD8+ T cells were achieved by a research group that used the Act-mOVA/OT-I system to investigate fetal specific CD8+ T cell by mating Act-mOVA male mice with B6 females, generating fetuses and placentas expressing ovalbumin (OVA) (Moldenhauer et al., 2017). They adoptively transferred into the pregnant females in vitro activated OVA-specific CD8+ OT-I T cells which were either exposed to TGFβ1 and IL-10, or with IL-2, to investigate the effect of an inhibitory/tolerogenic environment or activatory/inflammatory environment, respectively. Interestingly, IL-2 stimulated fetal specific CD8+ T cells resulted in elevated fetal loss, which was mediated in an antigen specific manner,

while TGFβ1/IL-10 stimulated CD8+ T cells did not, suggesting that a particular priming of CD8+ T cell activation and differentiation is important for successful pregnancy. Moreover, adoptively transferred OT-I CD8+ T cells, irrespective of activation method, were detected in the decidua, at resorption sites and uterus-draining para-aortic lymph nodes contradicting claims that effector CD8+ T cells do not migrate into the decidua (Moldenhauer et al., 2017).

Human CD8+ T cell clones specific for viruses (bound to HLA-A or HLA-B), such as human cytomegalovirus and Epstein Barr virus are enriched in the decidua, compared to blood (Egmond et al., 2016). Also, heterologous immunity might take place, where virus-specific decidual CD8+ T cells might be cross-reactive against the fetal HLA mismatch (Egmond et al., 2016). Although evidence indicate that the decidual microenvironment reduces decidual CD8+ T effector responses to maintain fetal tolerance (van der Zwan, Bi, et al., 2018), CD8+ T cell tolerance at the feto-maternal interface can be broken, as CD8+ T cells are susceptible to activation during gestation (Perchellet et al., 2013). For example, life threatening infections and stress exposure can exacerbate CD8+ T cell activation in pregnant mice, resulting in fetal loss (Kim et al., 2012) or uterine growth restriction (Solano et al., 2015).

Collectively, these findings suggest a unique CD8+ T cell repertoire in the decidua, some having the capability to fight infections and others possibly bearing tolerance towards the fetus. Yet, an extensive analysis of the total CD8+ T cell repertoire in human and mouse decidua is lacking which would give deeper insights into CD8+ T cell immunity in pregnancy, including which CD8+ T cell subtypes respond to pregnancy related events and their triggers.

2 Objectives

Our general hypothesis is that uterine CD8+ T cells can respond to the progressing pregnancy, and that CD8+CD122+ T cells regulate the T cell comparment in order to promote tolerance towards the fetus and that they play an additional role in promoting placental vascularization, rendering uterine CD8+ T cells an important component in a successful pregnancy. We hypothesize that the intrauterine environment promotes the generation of CD8+CD122+ regulatory T cells, whether it is by differentiation or proliferation, or even migration of these cells.

The aim of this doctorate project is twofold. First, we aimed to characterise uterine CD8+ T and CD8+CD122+ T cells, including the expression of cell surface proteins and the functional phenotype, to investigate the possibility of these cells possesing regulatory function. Second, we aimed to understand the dynamic response of uterine CD8+ T cells and CD8+CD122+ T cells in pregnancy, their migration, proliferation potential, differentiation, and finally whether play a role in pregnancy success.

To test the hypothesis and address the aims, further specific objectives were defined:

1. Characterise uterine and peripheral CD8+ T cells across mouse pregnancy, with the focus of cell differentiation trajectories and exhaustion state
2. Characterise uterine and peripheral CD8+CD122+ T cells across mouse pregnancy, with the focus of cell differentiation trajectories and regulatory potential
3. Characterise the functional phenotype of uterine CD8+ T cell and CD8+CD122+ T cells with single-cell RNA sequencing
4. Characterise peripheral CD8+ T cells across human pregnancy, with focus on cell differentiation trajectories and regulatory potential
5. Investigate proliferation, migration and differentiation patterns as well as effect on pregnancy outcome of adoptively transferred placental specific CD8+ T and CD8+CD122+ T cells in mouse pregnancy
6. Investigate the differences of CD8+ T cell subsets in distinct uterine compartments
7. Investigate uterine CD8+ T and CD8+CD122+ T cells in the peripartal period

3 Materials and methods

3.1 Material

3.1.1 Mice

The mice used for this dissertation are according to the following table.

Strain	Breeder
C57BL/6J CD45.2	Charles River, Sulzfeld, Germany
C57BL/6J CD45.1	Charles River, Sulzfeld, Germany
Balb/c CD45.2	Charles River, Sulzfeld, Germany
$GR^{flox}Lck^{cre}$ ($Nr3c1^{tm2GSc}$; $Tg^{(Lck\text{-}cre)1Cwi}$)	Provided by Prof. Dr. Manuel Friese University Medical Center Hamburg- Eppendorf, Germany
B6-OT1tg (C57BL/6-Tg (TcraTcrb)1100Mjb/J)	University Medical Center Hamburg- Eppendorf, Germany (originally from Jackson, Bar Harbor, ME)
Act-mOVA	The Jackson Laboratory (Jax: 005145)
Rag2-/-yc-/-	The Jackson Laboratory (Jax: 014593)

3.1.2 Human specimen

Isolated PBMC's from pregnant women (n =15) were provided from the PRINCE (Prenatal Determinants of Children's Health study) cohort at the University Clinic Hamburg-Eppendorf. The samples contained PBMC's from healthy pregnant patients from two consecutive pregnancies (first and second), from first, second and third trimesters. The six samples from each woman were labelled with a pseudo number providing anonymity but allowing for identification of paired samples. All study subjects gave informed consent and the study protocol was approved by the ethics committee of the Hamburg Chamber of Physicians.

3.1.3 Reagents and solutions

Reagent	Company	Catalog no.
AbC™Total Antibody Compensation Bead Kit	Invitrogen	A10497
Accutase	Sigma-Aldrich	SCR005
Acetic acid (glacial) 100%	Merck	1.00063
Acid Fuchsin	Sigma-Aldrich	F8129
Aquatex (aqueous mounting agent)	Merck	1.08562.0050
Bovine Serum Albumin (BSA)	SIGMA Life Science	A7030-100G
Citrate buffer	Sigma-Aldrich	C9999
ChromPure Human IgG	Jackson ImmunoResearch Laboratories, Inc.	009-000-003
Collagenase	Merck/ Sigma-Aldrich	SCR103
Dako antibody diluent	Agilent	S3022
DynabeadsTM My One TM SILANE	10x Genomics, Inc.	2000048

EDTA	Sigma-Aldrich	E9884-500G
Entellan new (xylene based- cover medium)	Sigma-Aldrich	1.07961
Eosin	Sigma-Aldrich	1.15935.0025
Ethanol (99.8%)	Roth	K928.4
GelRed Nucleic Acid stain 10000X in water	Biotium	41003
GeneRuler/DNA ladder	Fermentas, Thermo Scientific	SM0313, SM0373
Hematoxilin	Mayer/Sigma-Aldrich	51275
Hyaluronidase	European Pharmacopoeia Reference Standard	H11115000
Hydrogen peroxide 30%	Sigma-Aldrich	1.07209
IC fixation buffer	Life technologies	FB001
LE Agarose	Biozym Scientific GmbH	840000
Light green yellowish	Sigma-Aldrich	1.15941
Methanol 99,9%	Sigma-Aldrich	CAS 67-56-1
Normal donkey serum	PAN Biotech	P30-0101
Normal rat serum	Thermo Fischer	10710C
Normal goat serum	R&D System	DY005
Orange G	Merck	1.15925
Percoll	Sigma-Aldrich	P1644
Permeabilization buffer	Invitrogen	00-8333-56
Phosphotungstic acid hydrate	Sigma-Aldrich	79690
Ponceau S	Sigma-Aldrich	1.15927
RBC Lysis Buffer	eBioscience/Invitrogen	00-4333-57
RNA later Soln.	invitrogen	AM7021
RPMI medium 1640 (1X)	Gibco	21875034
Streptavidin HRP	Abcam	ab64269
TBS (10X)	Biorad	1706435
Tris-acetate-EDTA (TAE buffer)	Sigma-Aldrich	T9650-1L
TruStain FcX™ (anti-mouse CD16/32) Antibody	Biolegend	101320
Tryphan Blue solution	SIGMA Life Science	T8154-100ML
Xylol (Isomere)	Roth	9713.5

3.1.4 Kits

Kit name	Company	Catalog no.
Chromium ™ Next GEM Chip K Single Cell Kit, 16 rxns	10x Genomics, Inc.	1000287
Chromium Next GEM Single Cell 5' Kit v2, 4 rxns	10x Genomics, Inc.	1000265
Chromium Next GEM Single Cell 5' Gel Bead Kit v2, 4 rxns	10x Genomics, Inc.	1000267
Chromium Next GEM Single Cell 5' GEM Kit v2, 4 rxns	10x Genomics, Inc.	1000266
Chromium Single Cell Mouse TCR Amplification Kit, 16 rxns	10x Genomics, Inc.	1000254
DNeasy Blood & Tissue Kit (250)	Qiagen	69506

5' Feature Barcode Kit, 16 rxns	10x Genomics, Inc.	1000256
Library Construction Kit, 4 rxns	10x Genomics, Inc.	1000196
NextSeq 500/550 High Output Kit v2.5 (150 Cycles)	Illumina	20024907
Rneasy FFPE Kit (50)	Qiagen	73504
KAPA2G Fast ReadyMix	Roche	KK5101

3.1.5 Mouse antibodies for flow cytometry

Specificity	fluorochrome	clone	company	Catalog no.
CD4	FITC	RM4-5	Biolegend	100509
CD4	BV605	RM4-5	Biolegend	100547
CD8α	BV650	53-6.7	Biolegend	92297
CD8α	PE-Cy7	53-6.7	Biolegend	100709
CD8β	FITC	H35-17.2	Invitrogen	11-0083-85
CD11b	BV605	M1/70	Biolegend	101237
CD11c	FITC	N418	Biolegend	117306
CD19	BV605	6D5	Biolegend	115539
CD44	BUV395	IM7	BD Bioscience	740215
CD44	BV785	IM7	BD Bioscience	103041
CD45	AF700	30-F11	Biolegend	103128
CD45.1	FITC	A20	Biolegend	110705
CD45.1	BUV496	A20	BD Bioscience	741093
CD45.2	APC-Cy7	104	Biolegend	109823
CD49b	PE	DX5	BD Pharmingen	553858
CD49d	BUV737	R1-2	BD Optibuild	741713
CD49d	PE-Cy7	R1-2	Biolegend	103617
CD62L	BV421	16A8	Biolegend	104435
CD69	PE-Cy7	H1.2F3	BD Pharmingen	552879
CD69	PE	H1.2F3	Biolegend	104507
CD90.2	BV786	30-H12	Biolegend	105331
CD103	PE	2E7	Biolegend	121405
CD122	PE	5H4	Biolegend	105905
CD122	PerCP_efluor™710	TM-b1	eBioscience	46-1222-82
CD127	PE/Dazzle	A7R34	Biolegend	135031
CTLA4	PE	UC10-4F10-11	BD pharmingen	553720
CX3CR1	PE	SA011F11	Biolegend	149005
F4/80	FITC	BM8	Biolegend	123107
Fixable Viability Dye	efluor 506	-	Invitrogen	65-0866-14
Ki67	BV650	11F6	Biolegend	151215
KLRG1	BUV661	2F1	BD Optibuild	71586
KLRG1	FITC	2F1	Biolegend	138409
Lag3	BV421	C9B7W	Biolegend	125221
Ly49C/F/I/H	PE	14B11	Biolegend	108208
Ly49A	PE	YE1/48.10.6	Biolegend	116808

Ly49D	PE	4E5	Biolegend	138307
Ly49H	PE	3D10	Biolegend	144705
MR1: 5-OP-RU monomer	Biotinylated	-	NIH Tetramer core facility	-
MR1 negative control: 6-FP	Biotinylated	-	NIH Tetramer core facility	-
PD1	FITC	J43	eBioscience	11-9985-82
PD1	PE	RPM1-30	Biolegend	109103
Streptavidin	PE	-	BD Pharmingen	554061
TCRβ	APC	H57-597	BD Bioscience	553174
TCRγδ	APC	eBioGL3	eBioscience	17-5711-82
TCR Vα2	APC	B20.1	Biolegend	127810
TCR Vβ5.1, 5.2	PE	MR9-4	Biolegend	139504
Tigit	PE-DazzleTM594	1G9	Biolegend	142109
Tim3	BV785	RMT3-23	Biolegend	119725
Tim3	PE	RMT3-23	Biolegend	119703

3.1.6 Mouse antibodies for CITE-sequencing/hashtagging

Specificity	clone	company	Catalog no.
TotalSeq™ -C 0003 anti-mouse CD366 (Tim-3)	RMT3-23	Biolegend	119739
TotalSeq™ -C 0004 anti-mouse CD279 (PD1)	RMP1-30	Biolegend	109127
TotalSeq™ -C 0197 anti-mouse CD69	H1.2F3	Biolegend	104551
TotalSeq™ -C 0201 anti-mouse CD103	2E7	Biolegend	121443
TotalSeq™ -C 0227 anti-mouse CD122 (IL-2Rβ)	5H4	Biolegend	105915
TotalSeq™ -C 0563 anti-mouse CX3CR1	SA011F11	Biolegend	149043
TotalSeq™ -C 0839 anti-mouse Ly49H	3D10	Biolegend	144719
TotalSeq™ -C 0840 anti-mouse Ly49G	AT8	Biolegend	137405
TotalSeq™ -C 0841 anti-mouse Ly49D	4E5	Biolegend	138311
TotalSeq™ -C 0842 anti-mouse Ly-49A	YE1/48.10.6	Biolegend	116813
TotalSeq™ -C 0301 anti-mouse Hashtag 1	M1/42; 30-F11	Biolegend	155861
TotalSeq™ -C 0302 anti-mouse Hashtag 2	M1/42; 30-F11	Biolegend	155863
TotalSeq™ -C 0303 anti-mouse Hashtag 3	M1/42; 30-F11	Biolegend	155865

3.1.7 Mouse antibodies and kits for IHC

Specificity	Company	Catalog no.
CD31 (PECAM-1) (D8V9E) XP rabbit mAb	Cell Signaling Technology	77699
DAB Substrate kit	Abcam	Ab64238
IgG goat anti-rabbit Biotin	Invitrogen	10179442
Lyve-1 (Biotilinylated)	R&D systems	BAF2125
New Fuchsin substrate kit: Histofine New Fuchsin Substrate Kit	Nichirei Biosciences	415161F
Streptavidin HRP	Abcam	ab64269
Vectastatin ABC-AP Kit, Alkaline Phospahtase (Standard)	Vector labs	AK-5000

3.1.8 Human antibodies for flow cytometry

Antibody marker	Fluorophore	Clone	Company	Catalog no.
CD3	BV650	OKT3	Biolegend	317324
CD4	PE-Dazzle™594	RPA-T4	Biolegend	300548
CD8α	AF700	HIT8a	Biolegend	300920
CD19	BV510	HIB19	Biolegend	302242
CD25	BV785	BC96	Biolegend	302638
CD27	APC-Cy7	O323	Biolegend	302816
CD39	PE-Cy7	A1	Biolegend	328212
CD45RA	BV711	HI100	Biolegend	304138
CD127	PerCP_Cyanine5.5	A019D5	Biolegend	351322
Fixable Viability Dye	efluor 506	-	eBioscience	65-0866-14
KLRG1	BV605	2F1/KLRG1	Biolegend	138419
PD1	APC	EH12.2H7	Biolegend	329908
Tim3	BV421	F38-2E2	Biolegend	345008
2B4	FITC	C1.7	Biolegend	329506

3.1.9 Primers for genotyping

Primer name	Primer number	Sequence	Company
15226 TransgFoward	Z8034F03	CTT CCA GGA TTC GGA GAC AG	Invitrogen
15227 TransgReverse	Z8034F04	TCT GAA AGG CAT TGC TTG TG	Invitrogen
oIMR8744 IntPosContrFoward	Z8034F05	CAA ATC TTG CTT GTC TGG TG	Invitrogen
oIMR8745 IntPosContrReverse	Z8034F06	GTC AGT CGA GTG CAC AGT TT	Invitrogen

3.1.10 Instruments

Equipment	Company
PCR machine	Mastercycler Nexus, Eppendorf
BD LSRFortessaTM Cell Analyzer	BD Biosciences
BD FACSymphony A3 Cell analyzer	BD Biosciences
BD FACSAriaTM Fusion	BD Biosciences
10x GENOMICS Chromium Controller	10x Genomics Inc.
Image Lab Software version 5.2.1	BIO-RAD
Microtome, RM2125 RTS	Leica

3.1.11 Software

Software	Company
Biorender	Biorender, Toronto, Canada
Graphpad Prism version 9	GraphPad Software, La Jolla, CA, USA

FlowJo Version 10 for Mac	TreeStar, Asland, OR, USA
FACSDiva Software V.8.0.1	BD Bioscience, Heidelberg, Germany
RStudio 2022.02.3+492	PBC, Boston, MA, USA
SlideViewer 2.6	3DHISTECH, Budapest, Hungary

3.2 Methods

3.2.1 Mouse handling

Animals were kept under 12 h light/ dark circles at constant temperature, with food and water ad libitum. Mice were acclimatized for at least one week prior to start of mating/experiments. All experiments were performed in accordance with the animal ethics approval given by the State Authority of Hamburg (N046/2020) and State Authority of Regensburg (RUF-55.2.2-2532-2-1488).

Experimental setup of mouse experiments and groups are explained in the result chapter 4.

3.2.1.1 Timed mating

Timed mating was set up by placing two female mice (age 12-20 weeks old) into a cage containing one stud male, in the afternoon. Vaginal copulation plugs were detected the following morning and considered as GD 0.5. To confirm successful pregnancy, body weight was registered on GD 0.5, GD 8.5 and 10.5. Females showing a consistently increasing body weight were considered pregnant. Females of the same age serve as non-pregnant controls.
For the single-cell RNA sequencing experiment, male beddings were added to the female cage containing multiple females, in order to synchronize the estrus cycle and improve pregnancy rate, known as the Whitten effect (Jemiolo et al., 1986).

3.2.1.2 Determination of estrus stage

As non-pregnant mice go through the four-stage estrus cycle (lasting 4-5 days), the estrus stage for each virgin mouse was determined by a vaginal smear, where 20 µl of sterile PBS was gently inserted into the vaginal wall and the liquid containing vaginal leucocytes were aspirated and smeared on a slide either directly viewed under a light microscope or prepared for cytology for a later determination, explained in chapter 3.2.5.1. The determination of the estrus cycle is based on the following criteria: proestrus: small nucleated epithelial cells and few leucocytes, estrus: cornified anucleated epithelial cells, metaestrus: few cornified anucleated epithelial cells

and many leukocytes, diestrus: few nucleated epithelial cells and many leucocytes (Solano et al., 2011).

3.2.1.3 Intravital staining

For intravital staining, allowing for determination of extra-vascular leucocytes, mice were injected intravenously into the tail with 2.5 µg of anti-CD45 AF700 antibody, diluted in 200 µl of sterile PBS, three minutes prior to euthanasia, explained in chapter 3.2.1.5.

3.2.1.4 Adoptive transfer

FACS sorted cells were washed twice with 15 ml of sterile PBS, in order to eliminate all FBS from the sample, and resuspended in 200 µl sterile PBS, which were intravenously injected into the tail. Prior to injection, the tail was warmed with 37°C hot water to cause vasodilation, facilitating a successful injection.

3.2.1.5 Tissue collection

The mice were first anaesthetised with CO_2/O_2 for 30 seconds prior to euthanasia with CO_2 followed by either decapitation or cervical dislocation, confirming death. The mouse was sprayed with 70% ethanol and opened with sterile scissors and a pincet. This procedure took place under a sterile laminar flow hood for collection of tissues used for adoptive transfer experiments.

3.2.2 Isolation of leucocytes from mice

Cell isolation procedure took place on ice, unless otherwise stated. For most experiments, PBS was used for washing and resuspension but FACS buffer containing 0.5 % BSA was used for cell isolation of lymphocytes for sorting CD8+ T cells for adoptive transfer. Cell isolation took place under a sterile laminar flow hood when the cells were intended for adoptive transfer experiments. The procedures described apply to adult virgin and pregnant mice in the gestation period ranging from GD 6.5 to GD 18.5 and postpartum days PPD 4 and 21-30, unless otherwise stated.

3.2.2.1 Blood

Whole blood acquired from decapitation was collected in a blood collection microtube containing EDTA K (max 500 µl of whole blood). In a 50 ml Falcon tube, 1 ml of 1x RBC lysis

buffer was added to every 100 µl of whole blood and incubated on ice for 5 minutes. The reaction was stopped by filling the tube with PBS and centrifuged at 450 rcf for 8 minutes, the supernatant discarded, and the cell pellet was resuspended in 0.5 ml PBS.

3.2.2.2 Spleen

Spleen was collected into a 15 ml FACS tube containing cold PBS. Spleen was placed on a 40 µM cell strainer attached to a 50 ml Falcon tube and meshed with the inner part of a 1 ml syringe followed by a wash of PBS. The solution was centrifuged at 450 rcf for 8 minutes and supernatant was discarded. The cell pellet was resuspended in 5 ml of 1x RBC lysis buffer for 5 minutes on ice. The reaction was stopped by filling the tube with PBS and filtered through a 40 µM cell strainer and centrifuged at 450 rcf for 8 minutes. The supernatant was discarded, and the cell pellet was resuspended in 2 ml PBS.

3.2.2.3 Lymph nodes

Lymph nodes were collected into a 15 ml Falcon tube containing cold PBS. Lymph nodes where then placed on a 40 µM cell strainer placed on a petri dish and meshed with the inner part of a 1 ml syringe followed by a wash of PBS. The solution was placed into a 15 ml Falcon tube and centrifuged at 450 rcf for 8 minutes, the supernatant was discarded, and the cell pellet was resuspended in 0.5 ml PBS.

3.2.2.4 Liver

Liver from adult mice was collected and put into a petri dish filled with PBS and cleaned from adherent blood by shaking the organ in PBS. The liver was cut with a scalpel into little pieces and transferred into a 15 ml tube with 10 ml RPMI + DNase I (1:1000) + Collagenase D (10mg/ml) and incubated for 30 minutes at 37°C in water bath while stirred by a magnet. Thereafter, the cell suspension was filtered through a 70 µm cell strainer and tissue was mashed with the inner part of a 1 ml syringe into a 50 ml Falcon tube and washed with PBS (up to 50 ml). The cell suspension was centrifuged at 300 rcf, 4°C for 10 minutes and the supernatant discarded. The cell pellet was resuspended with 5 ml 1x RBC lysis buffer for 4 minutes on ice and the reaction was stopped with 45 ml of PBS. The cell suspension was centrifuge at 300 rcf, 4°C for 10 minutes and the supernatant discarded. The cell pellet was resuspended in 10 ml of 37 % Percoll solution, transferred to 15 ml Falcon tube and centrifuged at 800 rcf, 4°C for 20 minutes (brake 5). The upper band was removed and the remaining Percoll discarded. The cell

pellet was washed with PBS, centrifuged at 300 rcf, 4°C for 10 minutes, the supernatant discarded, and the cells resuspended in 3 ml PBS.

3.2.2.5 Fetal tissues

Fetal livers and fetal thymus were collected on GD 18.5 into Eppendorf tubes containing PBS and put into a 40 μM cell strainer placed on a petri dish on ice and meshed with the inner part of a 1 ml syringe followed by a wash of PBS. The solution was centrifuged at 450 rcf for 8 minutes and supernatant was discarded. The cell pellet from a fetal thymus was resuspended in 0.5 ml PBS, while the cell pellet from fetal liver was resuspended in 300 μl of 1x RBC lysis for 3 minutes and the reaction stopped with PBS. The cell suspension was centrifuged at 450 rcf for 8 minutes and supernatant was discarded, and the cell pellet resuspended in 0.5 ml PBS.

3.2.2.6 Uterus

Uterine dissection was performed according to a previously published protocol with minor alterations (Arenas-Hernandez et al., 2015). The whole uterus was collected and placed in a petri dish full of PBS. Fat was trimmed from the uterine horns. For GD 10.5, 14.5 and 18.5, an implantation was removed, and a small incision was made in the uterine wall adjacent to the placental and mesometrial uterus and further cut around the placenta/uterus until they were separated from the chorioallantoic membrane that included the fetus. Thereafter, the mesometrial uterine tissue was peeled/cut from the placental tissue and placed into petri dish full of cold PBS. The anti-mesometrial uterus, which surrounded the chorioallantoic membrane/fetus, was peeled off and placed in a separate petri dish full of cols PBS. This procedure was repeated for all implantations, one at a time. For virgin uterus, uterus on GD 6.5, and postpartal uterus, the whole uterus, cleaned from fat, was placed in a 15 ml Falcon tube with cold PBS, where a small incision was made into implantation sides on GD 6.5 uterus and the implantations were pushed out. Depending on the downstream application, two methods were used for isolation of uterine leucocytes. For experiments requiring higher yield of cells, the protocol using Accutase for enzymatic digestion was used, while for experiments requiring higher viability of cells, such as for single-cell RNA sequencing and adoptive transfer of cells, a protocol using collagenase and hyaluronidase was used.

Enzymatic digestion with Accutase:
The uterine tissues were placed in an Eppendorf tube containing 500 μl of cold Accutase solution. The tissue was then disassociated with fine sterile scissors and another 500 μl of cold

Accutase solution was added to the tube. The homogenized tissue sample was next transferred to a 15 ml Falcon tube and further 2 ml of cold Accutase solution were used to wash the remaining uterine tissue from the Eppendorf tube. The sample was placed in a water bath at 37ºC and incubated for 35 minutes while being stirred by magnets. The reaction was stopped by placing the samples on ice. The homogenized uterine sample was run through a 40 µM cell strainer into a 50 ml Falcon tube and meshed with an inner part of a 1 ml syringe and washed with PBS. The cell suspension was next centrifuged for 1250 rcf for 10 minutes at 4 ºC and the supernatant discarded. Two following options were used for further processing depending on experiment.

A) The cell pellet was resuspended with 1 ml of RPMI medium. The sample was carefully overlayed by 500 µl of FBS and centrifuged for 10 minutes at 1100 rcf without the break at room temperature. The RPMI/FBS interface containing cellular debris was aspirated along with the rest of the RPMI and the cell pellet was resuspended with 1 ml PBS.
B) The cell pellet was resuspended with 2 ml of 1x RBC lysis buffer for 4 minutes on ice. The cells were then washed with approximately 48 ml of PBS, centrifuged at 450 rcf for 10 minutes at 4 ºC and resuspended with 1 ml PBS.

Enzymatic digestion with Collagenase and hyaluronidase:

The uterine tissues were placed in an Eppendorf tube containing 500 µl PBS and disassociated with fine sterile scissors. The sample was then transferred to a 15 ml Falcon tube containing 5 ml HBSS with 200 U/ml hyaluronidase, 1 mg/ml collagenase VIII and 1 mg/ml BSA. The sample was placed in a water bath at 37º C and incubated for 20 minutes while being stirred by magnets. Next, the sample was removed from the water bath and 2 ml from the tissue-digestion solution were filtered through a 40 µM cell strainer into a 50 ml Falcon tube and left on ice, while 2 ml of HBSS were added to the tissue-digestion tube and placed back into the water bath for another 20 minutes of incubation at 37º C. The rest of the tissue-digestion solution was filtered into the same 50 ml Falcon tube along with meshing with an inner part of a 1 ml syringe, on ice. The sample was centrifuged at 450 rcf for 8 minutes at 4ºC, the supernatant discarded, and the cell pellet resuspended in 2 ml of 1x RBC lysis buffer for 4 minutes on ice. The reaction was stopped with cold PBS, up to 50 ml, followed by centrifugation at 450 rcf for 8 minutes at 4ºC, and resuspension by 1 ml PBS.

3.2.3 Isolation of leucocytes from human blood

PBMC's were provided as frozen leucocytes stored at -80 °C. The cells were thawed in pre-warmed 37°C waterbath and placed into 10 ml of pre-warmed 10% FBS in RPMI and centrifuged at 450 rcf for 8 minutes at room temperature. The supernatant was discarded, and the cell pellet resuspended in 15 ml of RPMI, centrifuged again at 450 rcf for 8 minutes at room temperature, supernatant discarded and resuspended in 1 ml PBS.

3.2.4 Flow cytometry

3.2.4.1 Spectral compensation for flow cytometry

Compensation beads were used for generating single stained controls and therefore setting the flow cytometry compensation. The kit contains Component A, which binds all isotypes of mouse, rat, hamster and rabbit immunoglobulins, and Component B, negative beads with no antibody binding capacity. Beads were vortexed for 10 seconds and one drop of component A was added to a FACS tube. A pre-titrated amount of each mouse antibody was added to the bead suspension, mixed, and incubated for 15 minutes at room temperature in dark. Thereafter, 3 ml of PBS were added and centrifuged for 5 minutes at 250 rcf. The supernatant was discarded, and the bead pellet was resuspended in 0.5 ml of PBS and one drop of Component B was added to the suspension and mixed. An additional unstained sample containing only Component B was used as a negative control. Single stained control for the viability antibody was generated with 1 million cells, where half of them had been heated at 56° for 10 minutes, generating mixture of dead and living cells. On the flow cytometer, the voltages for each channel were set based on appropriate cellular staining, the single stained controls were recorded, and the compensation was calculated, and the compensation matrix applied to the experiment. The post-compensation matrix was further optimised in FlowJo version 10.

3.2.4.2 FACS staining of mouse tissues

Cells were counted by placing 10 µl of the sample diluted in Tryptan Blue (I:10) into a hemacytometer and number of cells per ml were determined. FACS tubes were prepared, containing 1 ml of PBS and 1 million cells and centrifuged for 450 rcf for 8 minutes at 4ºC. The supernatant was discarded, and the cells were resuspended in 10 µl of blocking buffer, containing 1:200 True Stain (Fc block) and 1:100 Normal rat serum in PBS and incubated for 15 minutes on ice. Extracellular antibody panel mix, containing pre-titrated antibodies, was added to each sample and incubated for 30 minutes on ice in dark. Thereafter the cells were

washed with 1 ml PBS and centrifuged at 450 rcf for 8 minutes at 4ºC. Cells were either resuspended in 200 µl of PBS. In case of intracellular staining, the cells were fixed and permeabilized by an incubation in 100 µl of IC fixation buffer for 30 minutes and washed twice with 2 ml of 1x Permeabilization buffer (centrifugation: 450 rcf, 8 minutes at 4ºC) followed by incubation of an intracellular antibody for 30 minutes on ice in dark, a wash with 1 ml PBS (centrifugation: 450 rcf, 8 minutes at 4ºC) and resuspension in 200 µl PBS.

3.2.4.3 Preparation of PE- labelled MR1 tetramer

OP-RU (MR1) and 6-FP (negative control) biotinylated monomers were tetramerised by addition of 2.11 µg PE-Streptavidin, ten times at 10-minute intervals (total 21.1 µg), into 20 µg of the monomer, in the dark at room temperature. The tetramer was stored at 4ºC, and the staining was verified in liver samples.

3.2.4.4 Antibody panels used for mouse experiments

CD8+ T effector and memory		
Specificity	Fluorochrome	Dilution
KLRG1	FITC	1:100
CD122	PerCP efluor 710	1:200
CD127	PE/dazzle	1:100
CD69	PE-Cy7	1:100
MR1	PE	1:300
TCRβ	APC	1:100
CD45.2	APC-Cy7	1:200
CD45	AF700	intravital
CD19	BV605	1:100
CD11b	BV605	1:100
CD8α	BV650	1:100
CD44	BV785	1:100
CD62L	BV421	1:200
Viability	efluor 506	1:100

CD8+ T regulatory/inhibitory		
Specificity	Fluorochrome	Dilution
PD-1	FITC	1:100
CD122	PerCP efluor 710	1:200
Tigit	PE/dazzle	1:100
CD49d	PE-Cy7	1:200
TCRβ	APC	1:100
CD45.2	APC-Cy7	1:200

CD45	AF700	intravital
CD4	BV605	1:100
Lag3	BV421	1:100
CD8α	BV650	1:100
Tim3	BV785	1:100
CTLA4	PE	1: 50
Viability	efluor 506	1:100

OT-I genotyping		
Specificity	Fluorochrome	Dilution
CD8α	BV650	1:100
TCRValpha2	APC	1:100
TCRVb5.1,5.2	PE	1:100
CD45.1	FITC	1:300
CD45.2	APC-Cy7	1:100

OT-I Sorting panel		
Specificity	Fluorochrome	Dilution
CD4	FITC	1:100
CD11c	FITC	1:100
CD122	PerCP efluor 710	1:200
CD11b	BV605	1:100
CD19	BV605	1:100
CD49b	PE	1:100
Viability	efluor 506	1:100

Adoptive transfer D4 panel		
Specificity	Fluorochrome	Dilution
CD49d	BUV737	1:100
KLRG1	BUV661	1:200
CD45.1	BUV496	1:100
CD44	BUV395	1:200
CD90.2	BV786	1:200
CD11b	BV 605	1:100
CD62L	BV421	1:200
CD122	PerCP efluor 710	1:200
PD1	FITC	1:100
CD8α	PE-Cy7	1:100
CD127	PE/dazzle	1:100
Ly49	PE	1:100

CD45.2	APC-Cy7	1:200
TCRβ	APC	1:100
Viability	efluor 506	1:100
Ki67	BV 650	1:100
CD45	AF700	intravital

CD8aa/ab panel		
Specificity	Fluorochrome	Dilution
CD122	PerCP efluor 710	1:200
CD45.2	APC-Cy7	1:200
TCRβ	APC	1:100
CD45	AF700	intravital
CD8β	FITC	1:200
CD8α	BV421	1:200
CD4	BV605	1:100
Viability	efluor 506	1:100

Lectin panel		
Specificity	Fluorochrome	Dilution
Viability	efluor 506	1:100
CD45	AF700	intravital
CD45.2	APC-Cy7	1:200
TCRβ	APC	1:100
CD8α	BV650	1:100
CD122	PerCP efluor 710	1:200
Lectin panel 1		
MAA	FITC	1:200
SNA-I (biotinylated)	-	1:100
Lectin panel 2		
PHA-L (biotinylated)	AF700	1:100
Lectin panel 3		
LEA	FITC	1:200
PNA (biotinylated)	FITC	1:200
Secondary staining		
Streptavidin	PE	1:000

For the lectin panel, antibodies including relevant lectins were incubated for 1 hour at 4°C, washed with PBS followed by a secondary staining with PE-Streptavidin for 30 minutes on ice, followed by wash with PBS.

3.2.4.5 Staining of human PBMC

For staining human PBMC‘s, 1 ml of FACS buffer containing 0.5 % BSA in PBS and 1 million cells were added to each FACS tubes and centrifuged at 450 rcf for 8 minutes at room temperature. The supernatant was discarded and 2 µl of the IgG blocking agent (ChromPure Human IgG) was added for 5 min. The antibody mix, containing pre-titrated antibodies, was added to the cell suspension, and incubated for 20 minutes on ice in darkness, followed by wash with 2 ml FACS buffer and resuspension in 200 µl FACS buffer. Samples were directly measured by flow cytometry.

3.2.4.6 Antibody panel used for human PBMC’s

Specificity	Fluorochrome	Dilution
CD3	BV650	1:167
CD4	PE-Dazzle™594	1:500
CD8α	AF700	1:250
CD19	BV510	1:100
CD25	BV785	1:16.7
CD27	APC-Cy7	1:250
CD39	PE-Cy7	1:100
CD45RA	BV711	1:250
CD127	PerCP Cy5.5	1:400
KLRG1	BV605	1:100
Tim3	BV421	1:50
Viability	efluor 506	1:250
PD1	APC	1:100
2B4	FITC	1:250

3.2.5 Histology

3.2.5.1 Haematoxylin and eosin staining of vaginal smears

Vaginal smears were allowed to try at room temperature and fixed in 100% methanol for 20 minutes. The samples were rehydrated in ethanol in descending dilutions for five minutes each (100% > 100 % > 95% > 90% > 80% > 70%) and washed in PBS for 5 minutes. The samples were next stained with Mayer‘s Haematoxylin solution (staining nuclei blue) for 3 minutes and washed in running tap water for 15 minutes and stained with Eosin (staining cytoplasm pink) for 5 minutes. The samples were dehydrated in ethanol in ascending dilutions for 2 minutes

each (70 % > 80% > 90% > 95 % > 100 % > 100 %) and in three separate xylene solutions for 5 minutes each. The samples were mounted with xylene based mounting medium.

3.2.5.2 Tissue preparation

Tissues were placed in 4% formaldehyde for 24-46 hours, then transferred to PBS until embedded into a paraffin block, performed at the Pathology department at University Medical Center Hamburg-Eppendorf or University Hospital Regensburg. Tissues were cut into 3 µm thick sections on a microtome and placed on glass slides, dried at room temperature for at least 12 hours and incubated at 60°C for 1 hour.

3.2.5.3 Masson-Goldner trichrome staining

The paraffin embedded tissues were deparaffinated in three Xylol solutions for 10 minutes each. Thereafter the tissues were rehydrated in ethanol in descending dilutions for five minutes each (100% > 100 % > 95% > 90% > 80% > 70%) and washed in PBS for 5 minutes. The samples were next stained with Mayer‘s Haematoxylin solution for 5 minutes and washed in running tap water for 15 minutes , then submerged in Ponceau S solution for 2 minutes and washed with 1% acetic acid (3-10 seconds). The tissue was next submerged in Phosphotungstic acid for 3 minutes and washed wit 1% acetic acid. Thereafter, the tissue was submerged in Light green solution (stains collagenous fibres) for 5 minutes, washed with 1 % acetic acid and dehydrated in ethanol in ascending dilutions for 5 minutes each (95% > 100 % > 100 %) and in three separate xylene solutions for 10 minutes each. The samples were mounted with xylene based mounting medium.

3.2.5.4 Immunohistochemistry

The paraffin embedded tissues were deparaffinated in three Xylol solutions for 10 minutes each. Thereafter the tissues were rehydrated in ethanol in descending dilutions for five minutes each (100% > 100 % > 95% > 90% > 80% > 70%) and washed with three separate TBS solutions for 5 minutes each. Antigen retrieval was performed by covering the tissue in 1x Citrate buffer (pH 6.0), which was brought 98°C in a microwave (800W for 5 min) and allowed to cool down and washed twice with TBS for 5 min each. Tissues were circled with a hydrophobic PapPen. The downstream protocol for detection of CD31 and Lyve-1 differed and is explained separately in the following two subchapters.

3.2.5.4.1 Detection of blood vessels by detection of CD31

The tissue was treated with 3% hydrogen peroxide for 5 minutes for blocking endogenous peroxidase activity and washed three times with TBS for 5 minutes each wash. The tissue was next blocked with 50 µl of blocking solution (1% BSA + 20% normal goat serum in Dako diluent) for 1 hour in a humid chamber at room temperature. CD31 antibody diluted in Dako diluent (1:50) was added to the sample and incubated overnight in 4°C in a humid chamber. The following day, the tissue was allowed to reach room temperature and washed three times in TBS, for 5 min each. Thereafter, 50 µl of secondary antibody, a goat anti-rabbit biotin, diluted in Dako diluent (1:200) was added to the tissue and incubated for 1 hour in humid chamber at room temperature, followed by 3x TBS washing steps. Thereafter, 1 drop of DAB Chromogen was added to 1 ml of DAB substrate which was added to the tissue under a microscope and after sufficient time, the reaction was stopped in dH2O and washed two times in dH2O for 5 minutes each. The tissue was counterstained with filtered haematoxylin (diluted 1:2) and incubated for 1 minute. The tissue was washed in water for 15 minutes and dehydrated in ethanol in ascending dilutions for 2 minutes each (70 % > 80% > 90% > 95 % > 100 % > 100 %) and in three separate xylene solutions for 5 minutes each. Finally, slides were covered with xylene based mounting medium.

3.2.5.4.2 Detection of lymphatic vessels by detection of Lyve-1

The tissue was blocked with 50 µl of blocking solution (10% normal goat serum in Dako diluent) for 1 hour in a humid chamber at room temperature. Biotinylated Lyve-1 antibody diluted in Dako diluent (1:30) was added to the sample and incubated overnight in 4°C in a humid chamber. The following day, the tissue was allowed to reach room temperature and washed three times in TBS, for 5 min each. Thereafter, 50 µl of alkaline phosphatase from APC-AP kit (prepared according to manufacturer's recommendations) was added to the tissue and incubated for 30 minutes in humid chamber at room temperature, followed by 3x TBS washing steps. Next, New Fuschin substrate was prepared according to manufacturer's recommendation and applied to the tissue at room temperature for 10-20 minutes, monitored under the microscope. The reaction was terminated with tap water for 5 minutes, followed by two washes with dH2O for 15 minutes each wash. The slides were covered with aqueous based mounting medium.

3.2.6 Genotyping of OVA implantations

Fetal liver from each implantation was collected and stored in -80°C for confirmation of OVA positive placentas. The fetal liver was thawed, and DNA was isolated with DNeasy Blood & Tissue Kit according to the manufacturer's protocol. DNA yield was measured Nanodrop where the A260/280 absorbance ratio of ~1.8 and 260/230 ratio of ~2-2.2 was accepted as pure DNA without contamination. Polymerase chain reaction (PCR) was performed with the components and PCR settings according to the following two tables.

PCR reaction		
Component	Final concentration/ notes	Final volume (µl)
Primer forward 10 uM	0.5 µM	1.25
Primer reverse 10 uM	0.5 µM	1.25
Internal positive control primer forward	0.5 µM	1.25
Internal positive control primer forward	0.5 µM	1.25
KAPA2G Fast ReadyMix with Dye 2X	5 U (1X)	12.5
DNA	40 ng	1
Ultra-pure water		Up to 25

Cycling			
Step	Temperature (°C)	Time (minutes)	Notes
1	94	3	
2	94	15	
3	65	15	- 0.5°C per cycle decrease
4	68	30	
5			Repeat steps 2-4 for 10 cycles (Touchdown)
6	94	15	
7	60	15	
8	72	30	
9			Repeat steps 2-4 for 10 cycles (Touchdown)
10	72	2	
11	10	hold	

The PCR products (12 µl of sample) along with 5 µl DNA of ladders (100 and 50 base pair ladders) were loaded onto agarose gel containing 3g Agarose, 150 µl Tris-acetate-EDTA buffer and 15 µl GelRed Nucleic Acid Stain 10000X in water. The gel was run at 130 V for 55 minutes and imaged using an Image Lab Software version 5.2.1.

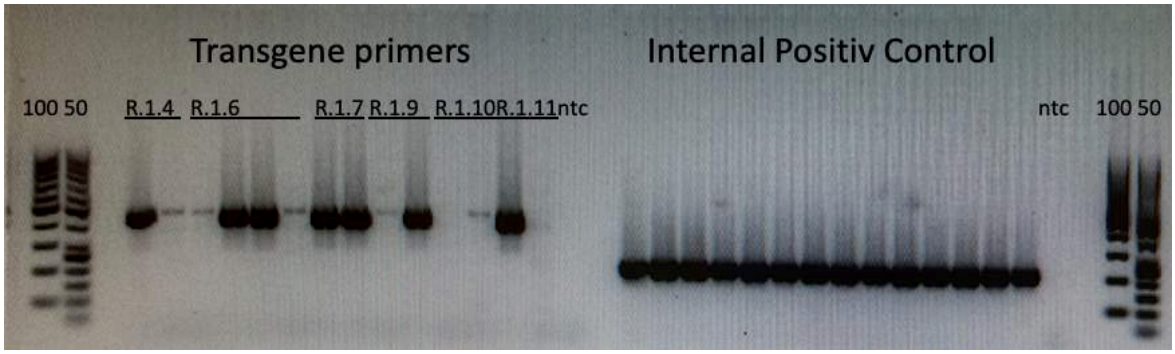

Figure 6. A representative gel showing OVA positive implantations.
First two columns show the two DNA ladders (100 and 50 base pairs) Each adoptively transfer receiver mouse (R.X.Y), is underlined and 2-4 implantations from each mouse was genotyped at a time. For instance, mouse R.1.6 has two OVA positive implantations out of four. Ntc stands for no template control, a sample without addition of DNA. The observed band for the internal positive control demonstrates appropriate quality of the DNA.

3.2.7 Single-cell RNA sequencing

All the steps of the procedure took place under a sterile laminar hood. Leucocytes were isolated from blood and mesometrial uterine samples from three pregnant Bl6 females (13 weeks old) on GD 14.5 were collected and isolated according to chapter 3.2.2.6, using collagenase and hyaluronidase for enzymatic digestion for uterus. Each sample was processed individually, the cells were counted by placing 10 µl of the sample diluted in Tryptan Blue (I:10) into a hemacytometer and number of cells per ml were determined. FACS tubes were prepared, containing 1 ml of cell isolation buffer containing 0.5% BSA and 2mM EDTA in PBS (adjusted to pH 7.2 - 8), along with 1-2 million cells and centrifuged for 450 rcf for 8 minutes at 4ºC. The supernatant was discarded, and the cells were resuspended in 10 µl of blocking buffer, containing 1:200 True Stain (Fc block) and 1:100 Normal rat serum in PBS and incubated for 15 minutes on ice. Two antibody mixes were prepared, one containing antibodies for CD8+ T cells, and the other containing the CITE-sequencing barcoded antibodies. The two antibody panels were added to each sample for 30 minutes on ice in dark, along with a relevant Hashtag antibody allowing for identification of each mouse. Thereafter the cells were washed with 1 ml cell isolation buffer and centrifuged at 450 rcf for 8 minutes at 4ºC and resuspended in 1 ml of cell isolation buffer.

Sorting panel for single-cell RNA sequencing		
Specificity	Fluorochrome	Dilution
CD8α	BV650	1:100
F480	FITC	1:200

TCRβ	APC	1:200
TCRγδ	APC	1:100
CD45	AF700	intravital
Viability	efluor 506	1:100

CITE-sequencing panel	
Specificity	Dilution
TotalSeq™ -C 0003 CD366 (Tim-3)	1:80
TotalSeq™ -C 0004 CD279 (PD1)	1:160
TotalSeq™ -C 0197 CD69	1:160
TotalSeq™ -C 0201 CD103	1:320
TotalSeq™ -C 0227 CD122 (IL-2Rβ)	1:320
TotalSeq™ -C 0563 CX3CR1	1:1080
TotalSeq™ -C 0839 Ly49H	1:320
TotalSeq™ -C 0840 Ly49G	1:480
TotalSeq™ -C 0841 Ly49D	1:1080
TotalSeq™ -C 0842 Ly-49A	1:1080

Hashtag antibodies		
Specificity	Mouse no.	Dilution
TotalSeq™ -C 0301 Hashtag 1	1	1:720
TotalSeq™ -C 0302 Hashtag 2	2	1:720
TotalSeq™ -C 0303 Hashtag 3	3	1:720

Isolated leucocytes from blood and uterus were brought to the FACS core facility at the RCI Regensburg centre for immunology for FACS sorting. CD8+ T cells were sorted from each sample individually into low bind 1.5 ml eppendorf tubes containing 10% FCS in PBS, resulting in pooled CD8+ T cells from the three blood samples into one tube and pooled CD8+ T cells from the three uterine samples into another tube. The two samples, each containing 12000 sorted CD8+ T cells were directly handed over to the NGS Core facility "Omics" at the RCI, which performed the downstream procedure for single-cell RNA sequencing, along with the CITE-sequencing and TCR sequencing application, with kits and reagents from 10X Genomics. The procedure was according to the manufacturer's standard protocol.

3.2.8 Data analysis

3.2.8.1 Flow cytometry

All flow cytometry data were analysed with FlowJo version 10. Flow cytometry data were analysed by manual gating of individual cell populations and/or by unsupervised analysis utilizing dimensionality reduction approach. In the latter case, cells from each sample were

downsampled (Downsample V3 plugin) and concatenated and given a keyword so that each group contained the same number of cells for accurate comparison between groups. Dimensionality reduction was acquired by using the t-distributed stochastic neighbour embedding (tSNE) algorithm, an unsupervised machine learning technique which generates a tSNE plot allowing for visualisation of the structure of high dimensionality data in three dimensions and therefore, visualisation of patterns (Maaten & Hinton, 2008). Data were visualised as dot plots, contour plots, histograms and tSNE plots generated by FlowJo, as well as visualised as bar plots generated by Graphpad prism 9.

3.2.8.2 Histology

Tissue slides were sent to the pathology department at University Hospital Regensburg for scanning. The slides were visualised with SlideViewer 2.6 for qualitative evaluation of the tissue.

3.2.8.3 Single-cell RNA sequencing

The data from the single-cell RNA sequencing experiment was pre-processed by Dr. Nicholas Strieder at the NGS core facility "Omics" using Cell Ranger software. This involved loading and demultiplexing the data. Hashtag oligos (HTO) were cross-linked with antibodies that bind to ubiquitous cell surface proteins. All batches were multiplexed and processed into the same 10X Chromium Chip Channel (GEM well), hence sequencing together HTO and single-cell gene expression reads (cDNA). Next, inter-batch doublets were detected as those cell barcodes have high counts of two or more HTO. Next, the barcodes (cells) were demultiplexed back to its original batch to discard doublets and negative cells. Also, the protein name of each CITE-sequencing barcode was allocated to the dataset. Further data processing and analysis was performed in close contact with Dr. Strieder using Seurat (R package). The data processing was performed in parallel with Dr. Strieder and Dr. Strieder's integration and data cleaning of uterine and blood samples were used for analysis and visualisation presented in this dissertation, while the processing/analysis of uterine sample processed alone was done by this dissertation's author. Further information about data processing and data cleaning is according to Appendix 2. The chosen relevant genes in CD8+ T cell biology were based on gene lists provided on NanoString's website (https://nanostring.com), and from various publications (Chen et al., 2021; Hardardottir et al., 2021; Li et al., 2022; Saligrama et al., 2019; Szabo et al., 2019; van der Zwan, Bi, et al., 2018; Vento-tormo et al., 2018; Zeng et al., 2018) and from detected highly

expressed genes found in the current dataset. Gene expression was visualised with heatmaps showing relative expression of selected groups, and an average gene expression was calculated for each group and presented as a heatmap. Analysis of TCR sequencing was performed by Dr. Strieder using R programming software and the Immunarch package.

3.2.9 Statistics

Statistical significance was calculated by Graphpad Prism version 9. For data containing two groups, non-parametric (Mann-Whitney) test or parametric t-test was used, depending on normal distribution. In the case of comparing mesometrial to anti-mesometrial uterus, a paired t-test was used. For data containing more than two groups statistical analyses were performed with non-parametric (Kruscal-Wallis test) or parametric One-way ANOVA and the p values were corrected for multiple comparison. In the case of comparing the different time points of pregnant women, a paired One-way ANOVA was used. Statistical significance is indicated by stars: *p< 0.05; **p< 0.01; ***p< 0.001 ; ***p< 0.0001.

3.2.10 Data visualisation

Figures were created in both Power Point and in BioRender.

4 Results

4.1 The uterine immune compartment in pregnancy

A semi-allogenic mouse model was used for investigation of CD8+ T cells across pregnancy in order to imitate human pregnancies. For this, male Balb/c and female Bl6 females were used, which contain distinct classical H2-K allele ($H2K^d$ and $H2\text{-}K^b$, respectively), the murine equivalent of HLA-C expressed by extravillous trophoblast cells. Here, three time points of pregnancy, following important pregnancy milestones with involvement of maternal immune responses were chosen. Those include gestation day (GD) 6.5, where the implantation of the blastocyst into the uterus has taken place, GD 10.5, where the placenta has formed, and GD 14.5, where the placenta is fully vascularized, additionally representing late gestation. Furthermore, virgin mice served as controls representing a state where no reproductive related immune changes have been induced within the uterus. Four organs were chosen for immunophenotyping CD8+ T cells. Those include peripheral blood, for investigation of systemic changes during pregnancy, the spleen and uterine draining para-aortic lymph node, for investigation within secondary lymphoid organs, and the uterus for investigation of local immune responses at the feto-maternal interface. For this experiment, 7-13 mice were used per group **(Figure 7A)**. Prior to tissue collection, the females were intravenously injected with anti-CD45 antibody for staining and exclusion of intravascular leucocytes. The implantation including the distinct uterine layers and compartments, the placenta and fetus are shown schematically in **Figure 7B** and by histological (Masson-Goldner) staining on GD 10.5 and 14.5 in **Figure 7C**. Here, a regressing myometrium, with thicker decidual layer, was evident in pregnancy, along with regressing anti-mesometrial uterus with progressing pregnancy on GD 14.5.

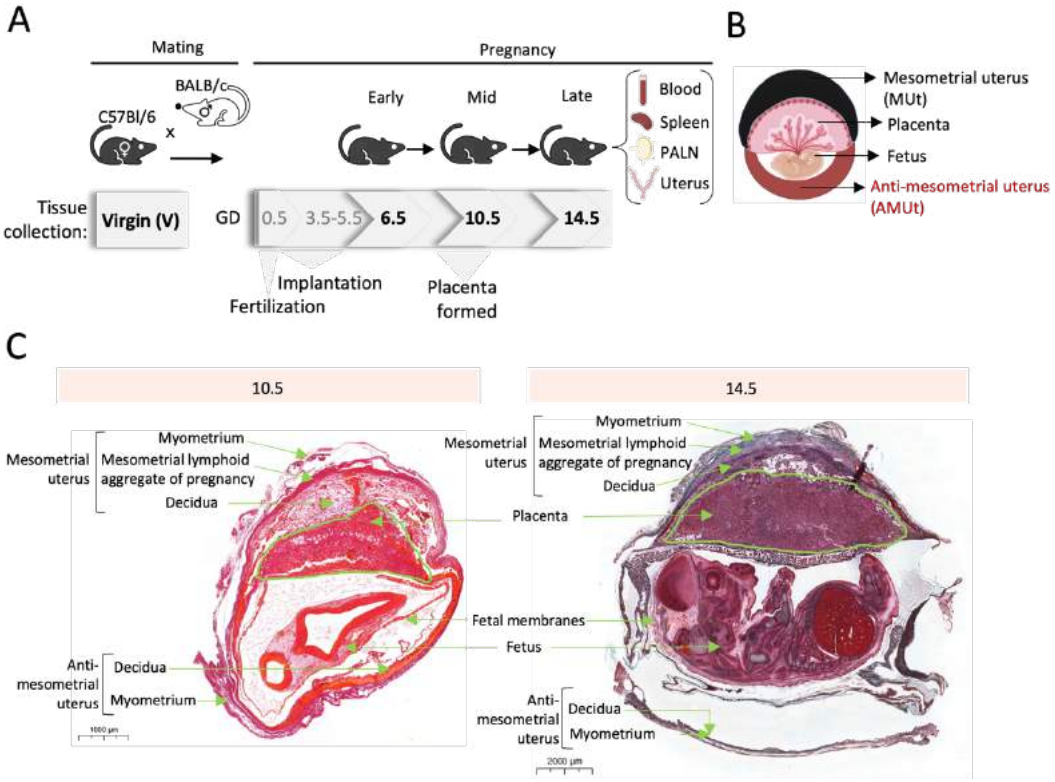

Figure 7. Experimental setup and main features of the intrauterine environment
A) *A schematic overview of the experimental setup. Blood, spleen, para-aortic lymph nodes (PALN) and uterus were harvested on gestation days (GD) 6.5, 10.5 and 14.5 from Balb/c mated C57Bl/6 females, and virgin controls, n:7-13. Females were injected with anti-CD45 antibody prior to tissue collection, for exclusion of intravascular leucocytes. Leucocytes were isolated, quantified and characterized by flow cytometry using supervised and dimension reduction analyses.* ***B)*** *A schematic overview of a mouse implantation site showing the mesometrial uterus (MUt; black) adjacent to the placenta, the underlying fetus and the distal anti-mesometrial uterus (AMUt; dark red).* ***C)*** *Masson-Goldner histological staining of implantation tissue sections on GD 10.5 (left) and GD 14.5 (right), showing the placenta, fetus, fetal membranes, the mesometrial uterus containing myometrium, mesometrial lymphoid aggregate of pregnancy and decidua, and the anti-mesometrial uterus containing myometrium and decidua*

We first aimed to investigate whether lymphocytes, including CD8+ T cells expand in pregnancy and if so, whether an expansion would be due to homeostatic proliferation due to enlarged uterine tissue. We found that total uterine weight increased in pregnancy, approximately 8x fold **(Figure 8A),** accompanied with a massive increase in leucocyte counts in the uterus. Particularly T cells and CD8+ T cell counts expanded in the uterus across pregnancy between GD 6.5 and 10.5, which spans the time of formation of the definitive chorioallantois placenta, when fetal antigens come in close contact with maternal circulation, but not in other organs **(Figure 8B-C)**. This expansion, as shown by approximately 100x fold increase in uterine CD8+ T cells, vastly exceeds the tissue expansion, and therefore cannot be explained by homeostatic proliferation due to an enlarged uterus **(Figure 8A)**. Hence, we aimed to investigate this massive expansion of uterine CD8+ T cells by an in-depth phenotypical

characterization, their activation levels, cytotoxic potential, their regulatory potential, fetal antigen specificity and whether their expansion is due to recruitment and/or proliferation. These questions will be addressed in the coming chapters.

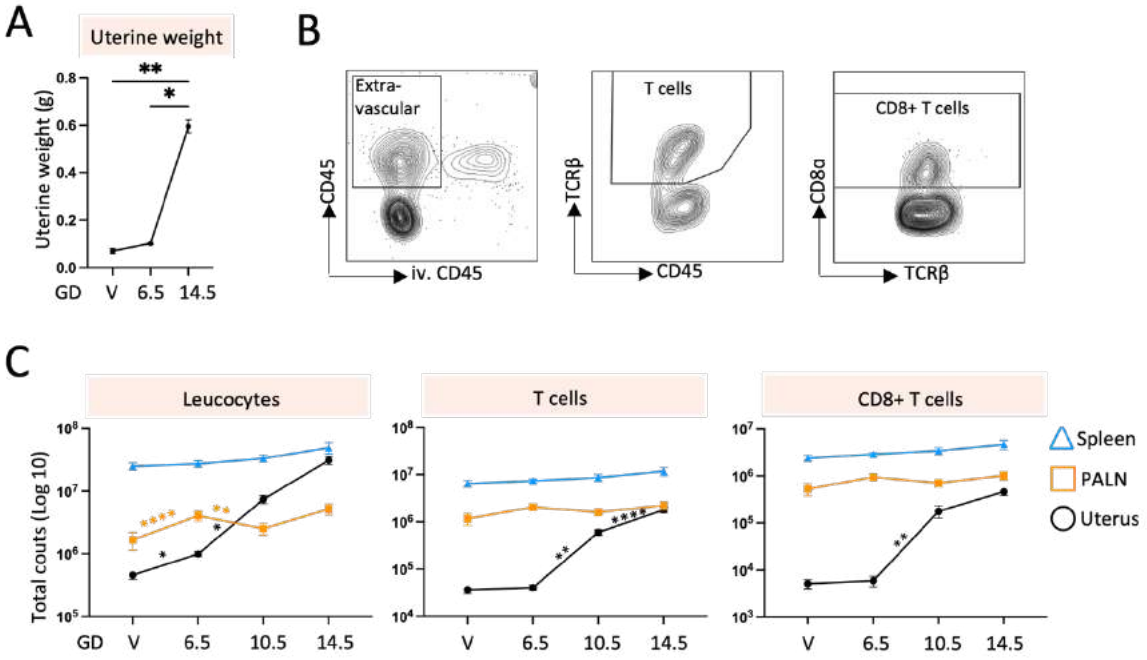

Figure 8. The expansion of the immune compartment exceeds vastly the uterine tissue expansion. ***A)*** *Uterine weigh (Y axis) across pregnancy (X axis) including virgin controls (V), calculated upon removal of the placenta, fetus and membranes.* ***B)*** *Representative countour plots showing gating of extra-vascular leucocytes (left), T cells (center), and CD8+ T cells (right).* ***C)*** *Total counts of leucocytes, T cells and CD8+ T cells throughout pregnancy in spleen (blue triangle), PALN (yellow square) and uterus (black circle). Y axis is log_{10} scale of total counts, X axis represents gestational day. Statistical analyses were performed with a t-test comparing two adjoining time points. *p< 0.05; **p< 0.01; ***p< 0.001; ****p< 0.0001.*

4.1.1 Characterization and dynamics of CD8+ T cells across mouse pregnancy

CD8+ T cells from all time points and organs (shown in Figure 1A) were first concatenated for unsupervised analysis and a dimensionality reduction method (further explained in chapter 3.2.8.1) was applied to generate a tSNE (t-distributed Stochastic Neighbor Embedding) plot which enables the simultaneous comparison of the expression of the selected markers for effector and memory differentiation **(Figure 9A).** The tSNE contained CD8+ T cells with a contribution of equal numbers from each group. CD44 and CD62L expression was used to separate CD8+ T cells from the concatenated file into three populations: CD44+CD62L- (including CD44 high and intermediate populations) containing effector and memory cells coloured in pink, CD44+CD62L+ (including CD44 high population) containing central memory cells, coloured in purple and CD44-CD62L- (including CD44 intermediate and low

populations) mainly containing naive cells, coloured in turquoise. A fourth population of CD44-CD62L- cells (including the low CD44 expression) coloured in grey, contained uterine cells with a naive phenotype (lacking KLRG1 and CD69 expression), where we hypothesize that CD62L had been shed from the cell surface, during enzymatic cell isolation procedure, containing cells that were not activated in vivo. Thus, cells within this gate were not regarded in further analysis, often presented as such within the scientific literature (Kawabe et al., 2020; Klebanoff et al., 2016; Winterberg et al., 2019) as they do not represent the physiological state of the cells within the mouse. These gates were applied to the tSNE plot for visualisation of these three general CD8+ T cell subtypes across pregnancy in the analysed tissues **(Figure 9B)**. Visualisation of the color-coded tSNE for each time point and tissue shows the difference and dynamics of the subpopulations between tissues, pinpointing a striking and surprising abundance a of CD44+CD62L- effector and memory populations in the uterus **(Figure 9C)**. The pattern of higher CD44 and lower CD62L expression in the uterus compared to blood was confirmed in single-cell RNA sequencing data of sorted CD8+ T cells **(Figure 9D)**.

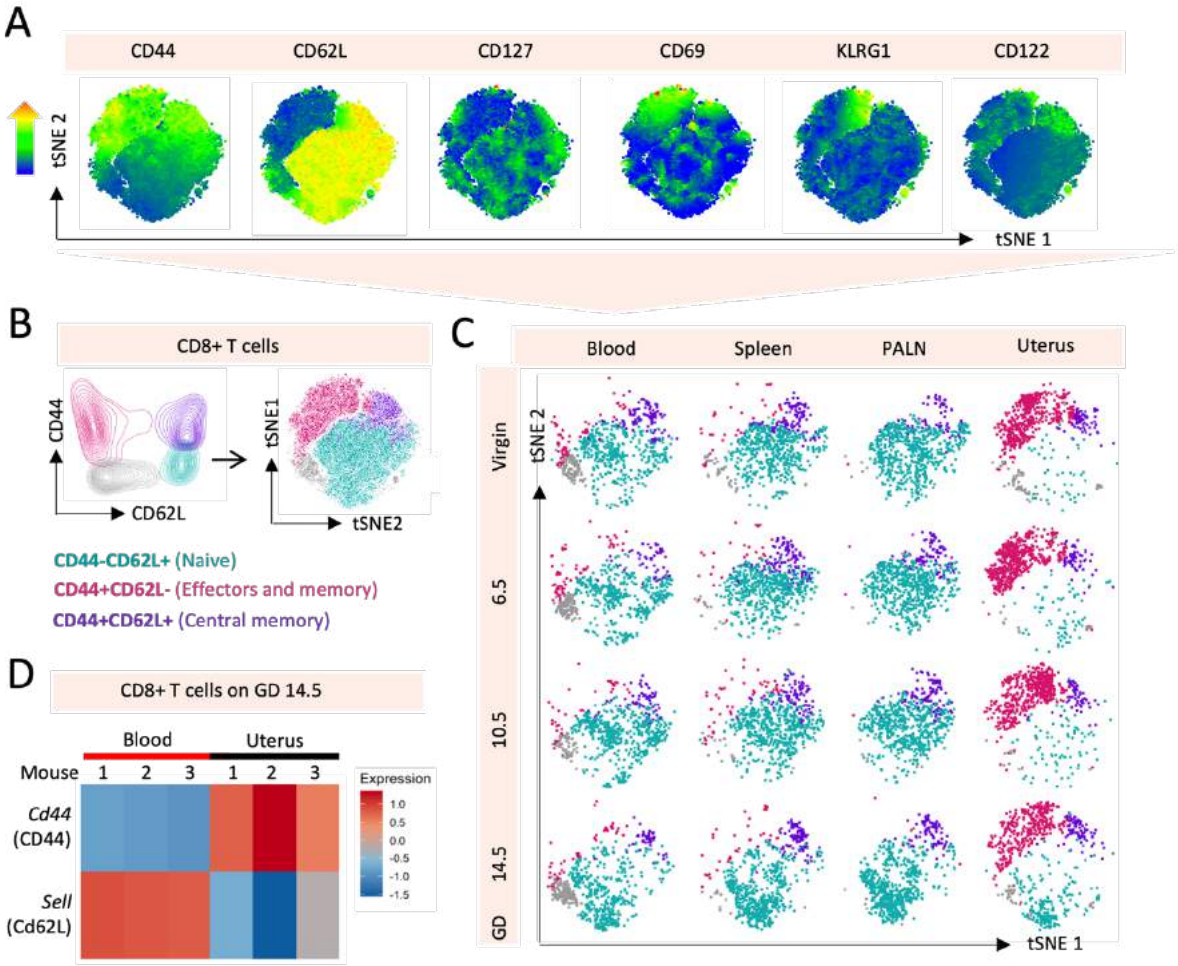

Figure 9. CD8+ T cell subpopulations based on CD44 and CD62L expression in pregnancy.
A) *tSNE plots generated by dimension reduction analysis of flow cytometry data which include concatenated data from blood, spleen, para-aortic lymph nodes and uterus on gestation day (GD) 6.5,*

10.5, 14.5 and in virgin mice. Heatmaps show the expression of markers included and used for clustering of CD8+ T cell populations. ***B)*** *CD44 and CD62L expression (left) in all CD8+ T cells determines color codes applied to the tSNE plots (right). Green indicates CD44-CD62L+ cells used to identify naive cells, purple indicates CD44+CD62L+ used to indicate central memory cells, pink indicates CD44+CD62L- used to indicate effectors and memory populations* ***C)*** *tSNE plots showing CD44 and CD62L expression in all organs: blood, para-aortic lymph node (PALN), spleen and uterus on gestation days (GD) 6.5, 10.5, 14.5 and virgin (V) mice.* ***D)*** *Heatmap showing average gene expression of Cd44 (CD44) and Sell (CD62L) in CD8+ T cells in blood and uterus on GD 14.5, from single-cell RNA sequencing analysis, n:3.*

For an in-dept analysis of effector and memory CD8+ T cells (αβ T cells) in pregnancy, a supervised analysis was conducted on the flow cytometry data **(Figure 11)**. The gating strategy is according to **Figure 10A**, MR1 tetramer was verified and used to identify MAIT cells, see Appendix 5. **Figure 10B** shows the potential developmental relationship between the analysed CD8+ T cell populations mainly based on to the circular model (explained in chapter 1.3.2.1).

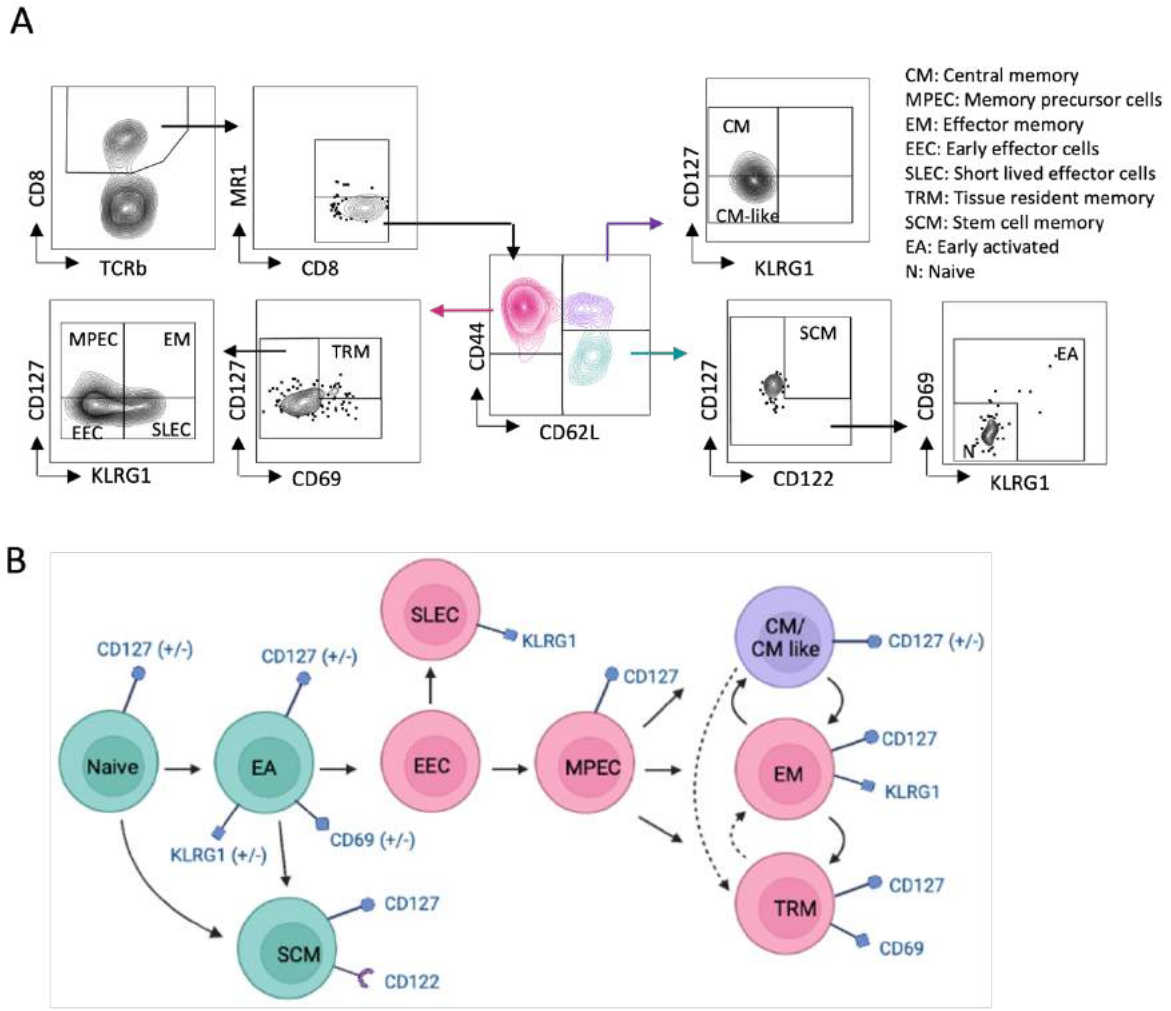

Figure 10. Characterization and dynamics of CD8+ T cells in pregnancy in mice.
A) *Gating strategy for identifying CD8+ T cell subpopulations after prior gating on living cells, followed by extravascular CD45 positive and CD11bCD19 negative cells. Contour plots are representative of staining in uterus on GD 14.5.* ***B)*** *A schematic overview of identified CD8+T cell*

populations and their possible lineage relationship, based on the circular model. Solid lines indicate a known differentiation path, dotted lines indicate a potential differentiation path.

Naive cells were low in the uterus but high in other tissues. During pregnancy, naive cells increased in the uterus with the peak on GD 14.5 which could mean that naive cells are migrating into the uterus to a high extent. This is supported by the fact that naive cells are decreased on GD 14.5 in the other tissues, significantly in para-aortic lymph node and that naive cells in blood, spleen and para-aortic lymph node are being activated. Early activated cells tend to increase in later stages of pregnancy in spleen, para-aortic lymph node. Also, the uterine early activated cells increased which may result from the accumulation of naive cells on GD 14.5. Stem cell memory cells, which hold a high renewal capability and the capacity to give rise to other memory cells were low in all tissues, but significantly increased on GD 14.5 in spleen and uterus. Central memory cells tend to increase in the peripheral organs, peaking on GD 14.5 while their level remained stable in the uterus. Central memory cells that have downregulated CD127 are here termed central memory-like cells. These cells could be activated central memory cells embarking on an effector path but have also been associated with impairing immune function in chronic viral infections (Lv et al., 2010; Mercier et al., 2008). Central memory-like cells significantly increased in para-aortic lymph node in mid-late pregnancy but were in general of highest abundance in the uterus. Hence, we proposed that they had differentiated from central memory cells in the uterus and uterine draining lymph nodes upon encounter to fetal antigens or have migrated from the periphery.

Early effector cells were strikingly the most prominent cells in the uterus, with frequency of up to 40% of uterine CD8+ T cells, while virtually absent in other tissues. Their ratio remained high throughout pregnancy, slightly decreasing in mid and late pregnancy, although not significantly. One explanation for this could be a constant activation of naive cells which give rise to effector and memory cells. Their hight abundance might also be due to proliferation. Another explanation could be that although technically falling under a gate of early effector cells they derive from central memory/central memory-like cells which have shed CD62L expression when entering the uterus. These cells might be of importance for uterine homeostasis throughout the lifespan of a mouse, irrelevant of pregnancy, for example for tissue remodelling and regeneration during the estrous cycle, presenting a non-cytotoxic function. Surprisingly, short-lived effector cells are exclusively abundant in the uterus, thus pregnancy does not induce such cytotoxic cells in the periphery. They seem to increase in the uterus in early pregnancy, although not significantly, which goes in line with the reducing frequencies of early effector

cells, as some of them might have transitioned to short-lived effector cells. The peak of short-lived effector cells at GD 10.5 is surprising but might reflect the immune response upon establishment of the placenta as fetal antigens come in close contact with maternal circulation and subsequent adaptation as the frequency return to normal in a few days. Memory precursor effector cells were found in all tissues, lowest in para-aortic lymph node and highest in the uterus. Although low in the para-aortic lymph node, they significantly decreased on GD 6.5 and 10.5, possibly differentiating into memory cells, and increased again on GD 14.5. In the uterus, memory precursor effector cells peaked on GD 6.5, possibly due to immune activation upon fertilization and/or implantation. Of note, as these graphs represent percentages of CD8+ T cells, an increase or decrease of populations could be indirectly due to differences in other populations, for example, the lowest frequency of memory precursor effector cells on GD 10.5 could be explained by the frequency of naive and short-lived effector cells escalating at this time point. Effector memory and tissue resident memory cells were almost exclusively found in the uterus. The significant rise in both population on GD 6.5 indicates another example of immune activation upon fertilization and/or implantation and might derive from uterine early effector cells, memory precursor cells and/or central memory cells. Also, memory precursor effector cells in para-aortic lymph node could be migrating to the uterus (after their return to the blood circulation) where they differentiate into memory populations (effector memory and tissue resident memory cells) on GD 6.5. CD8+ MAIT cells were mainly found in uterus, however not in a virgin uterus, and peak at GD 6.5 which might be a result of rapid innate response to implantation.

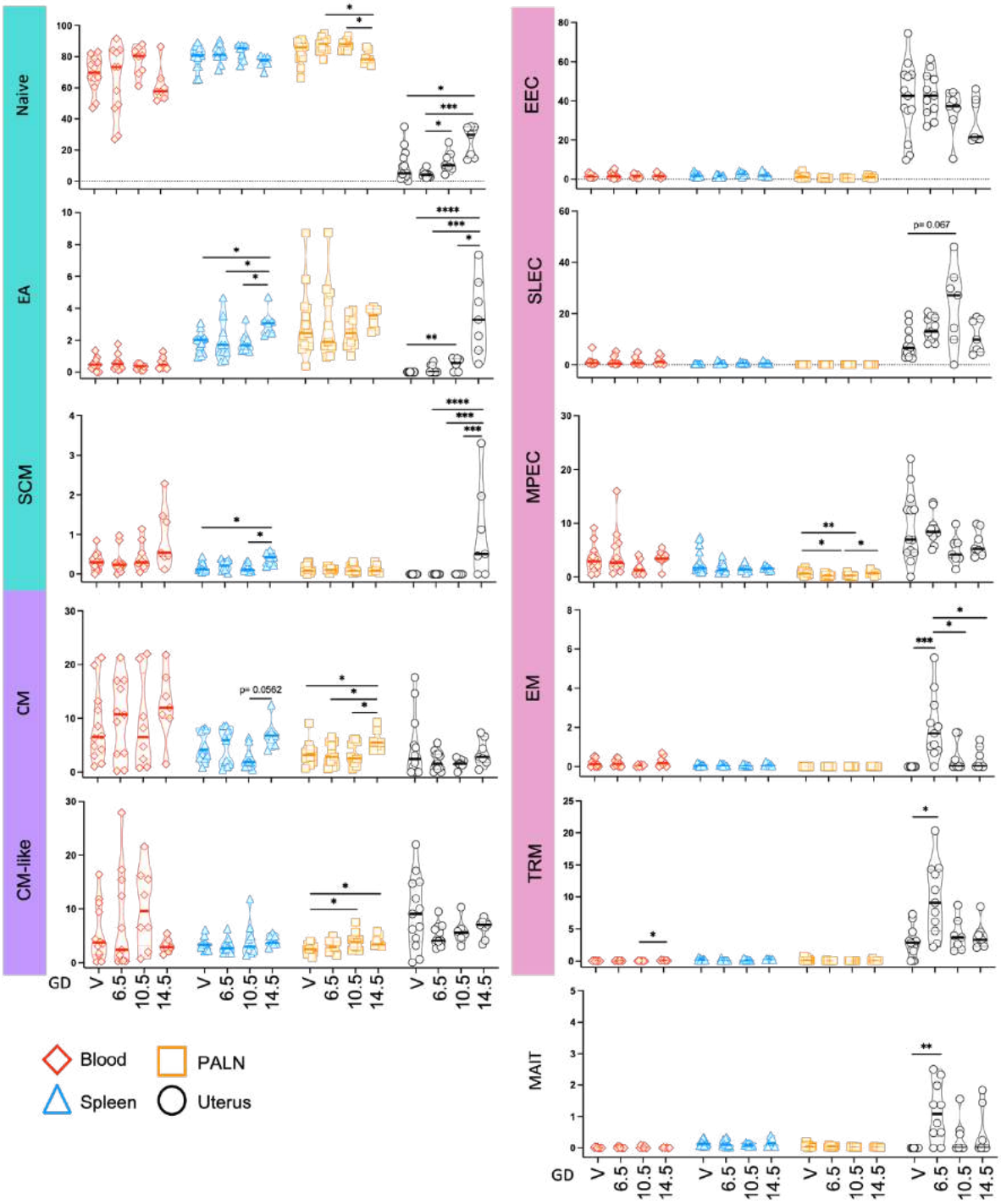

Figure 11. Characterization and dynamics of CD8+ T cells in pregnancy in mice.

*Dynamic changes were observed in different CD8+ T cell subpopulations across pregnancy in the investigated organs. Y axis represent percentage of CD8+ T cells. X axis represents gestational day. EA: Early Effectors, SCM: Stem Cell Memory, CM: Central Memory, EEC: Early Effector Cells, SLEC: Short-Lived Effector Cells, MPEC: Memory Precursor Effector Cells, EM: Effector Memory, TRM: Tissue Resident Memory, MAIT: Mucosal Associated Invariant T cells. Statistical analyses were performed with non-parametric One-way ANOVA and the p values were corrected for multiple comparison (Kruscal-Wallis test), *p< 0.05; **p< 0.01; ***p< 0.001; ****p< 0.0001.*

As immune cell phenotyping by flow-cytometry is restricted to a limited number of markers, single-cell RNA sequencing analysis of sorted CD8+ T cells was conducted to validate the findings of differences observed in blood and uterine CD8+ T cells from the flow cytometry data, and to gain further insights into the functional phenotype of uterine CD8+ T cells (See method chapter 3.2.8.3 and Appendix 2). Here, sorted CD8+ T cells from three mice were compared in blood and mesometrial uterus on GD 14.5. This time point was chosen for the majority of experiments in this dissertation, due to the high numbers of uterine CD8+ T cells and from observations of the heterogeneous CD8+ T cell subsets from the characterisation study. Here, cell clusters were determined by Seurat R package showing 10 clusters of CD8+ T cells and we evaluated the gene expression in the particular clusters to uncover their identity. We could confirm the previously observed presence of naive cells in the uterus, which frequency were lower compared to blood, and higher frequencies of heterogeneous effector and memory populations (Appendix 3). Table with the gene list and protein names is according to Appendix 4. Furthermore, single-cell RNA sequencing data underscored that uterine CD8+ T cells contain gene signatures of activation and broad CD8+ T cell function, while CD8+ T cells in the blood do not contain such gene signatures to the same extent (Appendix 3). Further identification and analysis of each of the 10 clusters are not included in this dissertation but will be further analysed in the future.

Collectively, uterine CD8+ T cells present an activation status as shown by accumulation of naive cells followed by an increase in early activated cells, dynamic effector cell frequencies and formation or recruitment of memory cells, in particular, tissue resident memory cells. The data indicate an immune response upon fertilization and implantation on GD 6.5, as shown by elevated frequencies of short-lived effector cells, memory precursor effector cells, effector memory, tissue resident memory and MAIT cells, of which short-lived effector cells peak on GD 10.5 which might reflect an immune response upon the establishment of the placenta as fetal antigens come into close contact with maternal circulation. Furthermore, peripheral blood and lymphatic organs do not mirror the changes in CD8+ T cells observed in the uterus indicating a local response to fetal antigens rather than a systemic response.

4.1.2 Characterization and dynamics of CD8+ T cells across human pregnancy

We next aimed to investigate and compare CD8+ T cell subpopulations in human pregnancy to CD8+ T cells in mouse pregnancy. For this, peripheral blood mononuclear cells (PBMC) were obtained from pregnant women in first, second and third trimester of pregnancy in their first

pregnancy followed by phenotypic analysis of CD8+ T cells with flow cytometry **(Figure 12A)**. Expression pattern of the markers used for characterization was visualised with a tSNE plot, generated by concatenation of CD8+ T cells from all time points of pregnancy **(Figure 12B)**. Due to differences in mouse and human CD8+ T cells, different markers are commonly used for detection of CD8+ T cell subpopulations in humans. Gating strategy identifying naive cells, central memory/T cell peripheral memory, effector memory, effector memory re-expressing CD45RA and effectors is according to **Figure 12C**. As in mice, CD8+ T cells in peripheral blood in first trimester in humans consisted mainly of naive cells **(Figure 12D)**. However, in humans, the frequency of effectors was higher compared to mouse. Dynamic analysis showed a rather stable frequencies of the CD8+ T cell populations across pregnancy, with the exception of an increase in naive cells and a decrease in effectors, which might be explained by a recruitment of effectors from the peripheral circulation to the implantation side.

Although activated CD8+ T cell subpopulations, including effectors were present in pregnant uterus in physiological mouse pregnancies, they clearly do not pose a threat to the developing fetus. This raises the question of the functional phenotype and the functional state of the uterine CD8+ T cells and their role in the pregnant uterus. Based on the striking observation of activated uterine CD8+ T cells, we hypothesize that they might be modulated to allow for a successful pregnancy.

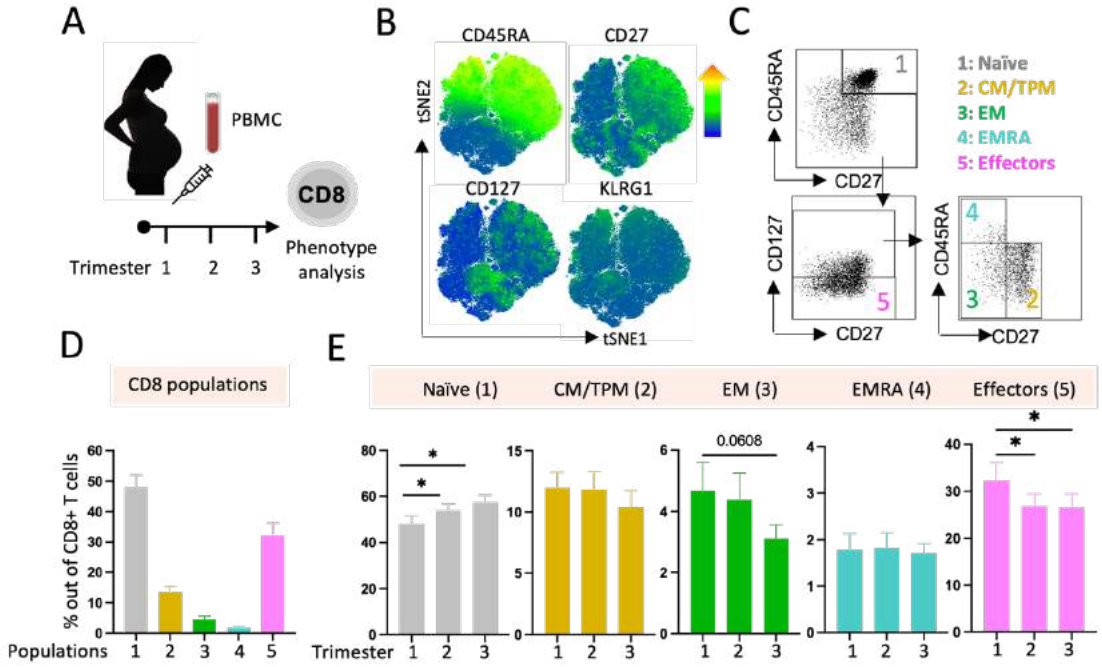

Figure 12. Characterization of human PBMC CD8+ T cells across pregnancy.
A) *Experimental setup: Peripheral blood mononuclear cells (PBMC) obtained from healthy women on first, second and third trimester of pregnancy were stained and analysed by flow cytometry.* ***B)*** *tSNE plots generated by dimension reduction analysis of flow cytometry data including concatenated CD8+*

T cells from all three trimesters of pregnancy. Heatmaps of markers used for determining CD8+ T cell subpopulations. ***C)*** *Gating strategy for identifying CD8+ T cell populations, Naive, CM (Central memory)/TPM (T cell peripheral memory), EM (Effector memory), EMRA (Effector memory re-expressing CD45RA), and effectors.* ***D)*** *Percentage of each population in first trimester PBMC.* ***E)*** *Percentage of each CD8+ T cell population in first, second and third trimester PBMC. Y axis represents percentage of CD8+ T cells. Statistical analyses were performed with non-parametric One-way ANOVA and the p values were corrected for multiple comparison, n= 15. *p< 0.05.*

4.2 CD8+ T cell modulation in pregnancy

A potential modulation of uterine CD8+ T cells could be mediated by i) acquiring an exhausted state, as often seen in tumour biology, and/or ii) by the activity of CD8+ regulatory T cells. The presence of both "fetal-friendly" modulation possibilities were investigated in the following two subchapters.

4.2.1 Inhibitory receptors/exhaustion in pregnancy

In order to investigate expression and dynamics of inhibitory receptors associated with exhaustion, and their dynamics during pregnancy, a flow cytometry panel consisting of commonly known inhibitory receptors, associated with exhaustion: PD1, Tim3, CTLA4, Lag3 and Tigit, were studied in uterine and blood CD8+ T cells in semi-allogenic pregnancies, as explained in **Figure 7A,** to evaluate and to compare local immune modulation to systemic immune modulation in pregnancy. Out of these inhibitory receptors, PD1 had the highest expression in both organs **(Figure 13A)**. PD1 expression was significantly increased on GD 14.5 in blood while it slightly rose on GD 6.5 in the uterus, although not significantly. Expression of the other inhibitory receptors were not significantly altered in blood across pregnancy while Tim3 and CTLA4 were significantly increased on GD 14.5 and GD 10.5, respectively. This suggests that different inhibitory mechanisms might be activated after different pregnancy milestones. As PD1 is generally considered the main marker for exhaustion, and as among the other investigated inhibitory receptors it had the highest frequency of CD8+ T cells in both blood and uterus, it was further studied. PD1 expression was highest in CD44+CD62L- containing effectors and memory cells, particularly in the uterus, further supporting the presence of enrichment of exhausted effector cells in the uterus **(Figure 13B)**. Co-expression of PD1 and Tim3, which are commonly co-expressed in exhausted cells, was also enriched in the uterus compared to blood and its ratio tended to rise in the uterus across pregnancy, although not significantly **(Figure 13C)**. Cell subsets with single and co-expression of PD1 and Tim3 in general had higher expression of Lag3, CTLA4 and Tigit compared to cells

lacking both PD1 and Tim3 **(Figure 13D),** suggesting a synergistic exhaustion signature. Single-cell RNA sequencing analysis of sorted CD8+ T cells likewise showed higher exhaustion signature in uterus compared to blood, with higher average expression of the above-mentioned inhibitory molecules, in addition to Tox, transcription factor associated with exhaustion **(Figure 13E)**. The observed low expression of the *Tcf7* gene, coding for TCF1, in the uterus, suggests a terminally differentiated exhausted profile while its high expression in blood and relative low expression of inhibitory molecules further supports a naive phenotype. Furthermore, PD1+Tim3- and PD1+Tim3+ had relatively higher Tox expression compared to PD1-Tim3- and PD1-Tim3+, suggesting they are truly exhausted, where PD1+Tim3- may contain the stem cell-like exhaustion progenitors which self-renew and generate the terminally differentiated exhausted PD1+Tim3+ population, based on Tcf7 gene expression. As the level of exhaustion has been correlated with higher PD1 expression (Kim et al., 2018), we further investigated PD1 high and intermediate levels in pregnancy. We observed that the majority of PD1 positive cells had intermediate PD1 expression, and only the uterus contained high PD1 expression, which was virtually absent in blood (Appendix 6). This further confirms a presence of exhausted cells locally at the feto-maternal interface and lack of exhaustion mechanism in the periphery, suggesting a particular local immune response not reflected systemically. As PD1 intermediate and PD1 high cells were detected in the uterus, and the intermediate population might hold important functions in pregnancy, both will be presented together as PD1 positive population for most part of the dissertation.

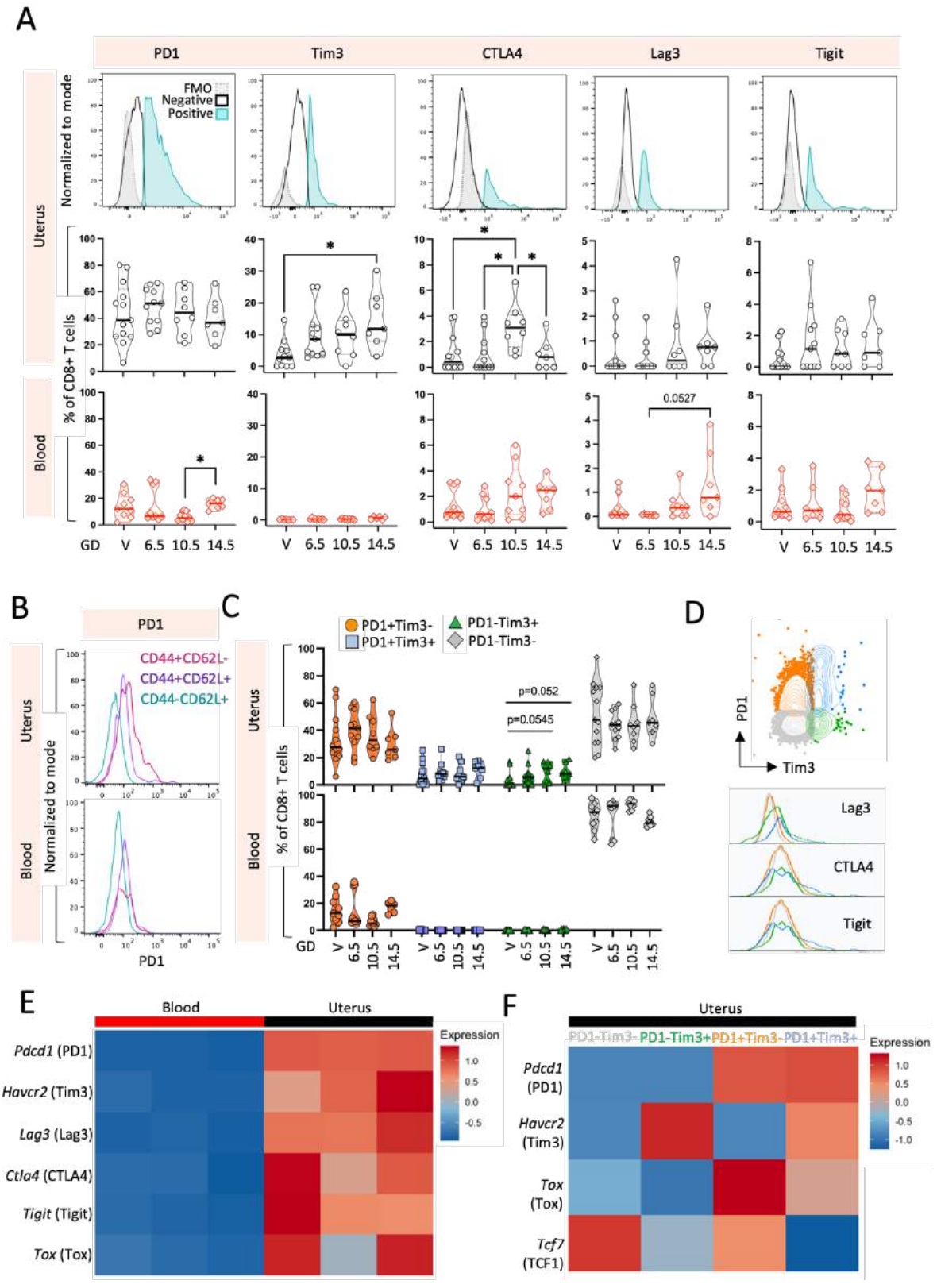

Figure 13. CD8+ T cell exhaustion in pregnancy in mice.

A) *Histograms of the inhibitory receptors PD1, Tim3, CTLA4, Lag3 and Tigit expression in uterus (top row), from a concatenated file of multiple uterine samples. X axis represents expression levels of a given inhibitory receptor. Y axis represents values as Normalised to mode where each peak is normalised to its mode for each overlayed population. Expression of inhibitory receptors in CD8+ T cells across pregnancy in the uterus (center row) and blood (bottom row), Y axis represent percentage of CD8+ T*

cells, Y axis represent gestation day. ***B)*** *Comparison of PD1 expression in CD44+CD62L- (containing central memory cells), CD44+CD62L+ (containing effectors and memory cells) and CD44-CD62L+ (containing naive cells) in uterus and blood.* ***C)*** *Dynamics of single and co-expression of PD1 and Tim3 in CD8+ T cells in uterus and blood across pregnancy.* ***D)*** *Contour plot showing single and co-expression of PD1 and Tim3 in uterus (top) and expression level of Lag3, CTLA4 and Tigit in each subpopulation.* ***E)*** *A heatmap showing average gene expression of genes associated with exhaustion in CD8+ T cells in blood and uterus on GD 14.5, from ScRNA sequencing analysis, n:3.* ***F)*** *A heatmap showing average gene expression of the same genes as in F in PD1-Tim3-, PD1-Tim3+, PD1+Tim3- and PD1+Tim3+ CD8+ T cell populations in uterus on GD 14.5, from ScRNA sequencing analysis. In* ***A)*** *middle and bottom, and* ***C)*** *Y axis represents percentage of CD8+ t cells and X axis represents gestational day. Statistical analyses were performed with non-parametric One-way ANOVA and the p values were corrected for multiple comparison (Kruscal-Wallis test), *p< 0.05.*

CD8+ T cell exhaustion in the uterus has been more extensively studied in human pregnancy compared to murine pregnancy. The current findings on uterine CD8+ T cell exhaustion in mouse uterus supports the scarce literature about its presence and importance at the feto-maternal interface. In order to compare CD8+ T cell exhaustion levels in mice to humans, the expression of inhibitory receptors in CD8+ T cells from human peripheral blood mononuclear cells (PBMC's) was investigated. Here, inhibitory receptors commonly associated with exhaustion in humans: PD1, Tim3, 2B4 and CD39 were studied **(Figure 14A)** and applied to the tSNE plot **(Figure 14B)** with the previously reported CD8+ T cell populations in **Figure 12**. As in mice, PD1 expression was highest in effectors, indicating exhausted CD8+ T cells **(Figure 14B-C)**. Tim3 expression was highest in naive and effector memory re-expressing CD45A cells while 2B4 was found in various populations but to the highest extent in effector memory, effector memory re-expressing CD45A and effectors. CD8+ T cells expressing CD39 were few, but CD39+ cells were mainly central memory /T cell peripheral memory and effectors. The dynamics of the inhibitory receptors were evaluated across pregnancy **(Figure 14C)** where PD1 and CD39 expression in all CD8+ T cells were stable across pregnancy, while Tim3 significantly increased and 2B4 decreased **(Figure 14D)**. When the dynamics of PD1 expression were further investigated in the effector and memory phenotypes they had the tendency of increasing in late pregnancy, in all populations except for naive cells, however not significantly, suggesting a slight upregulation of PD1 expression particularly in effectors which might indicate an elevated exhaustion in late pregnancy in human PBMC's. Additionally, CD8+ T cells from the subsequent second pregnancy from same women were also analysed. Similar trends were observed in second pregnancy compared to first pregnancy (Appendix 7). In general, expression of the inhibitory receptors, particularly PD1 expression, were higher in second pregnancy suggesting higher level of exhaustion and memory from the first pregnancy.

Collectively, these findings indicate that exhaustion is one mechanism of CD8+ T cell modulation in the uterus.

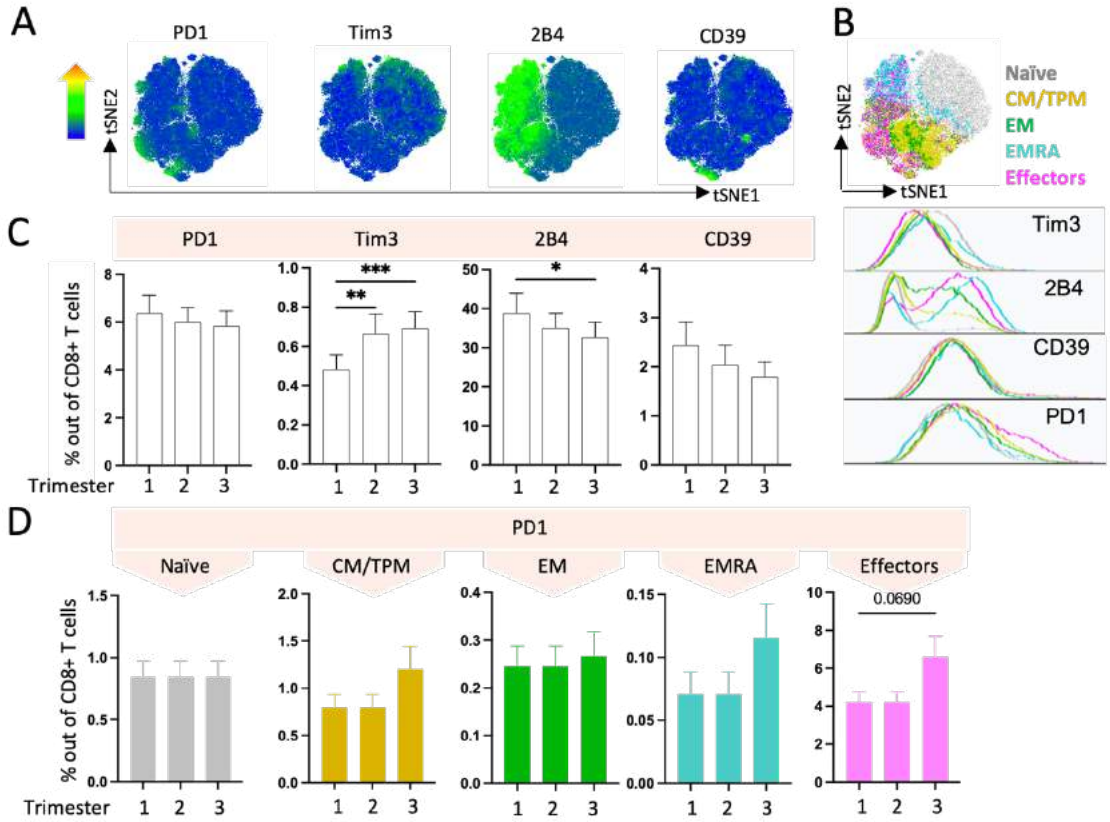

Figure 14. CD8+ T cell exhaustion in human PBMCs across pregnancy.
*__A)__ Heatmaps represent the expression of inhibitory molecules PD1, Tim3, 2B4 and CD39 in the tSNE plots generated in Figure 6. __B)__ tSNE showing clustering of the populations from figure 4 within the tSNE plot (top) and histograms of inhibitory molecules in each population (bottom). __C)__ Percentage of inhibitory receptors in first, second and third trimester out of CD8+ T cells. __D)__ Percentage of PD1+ cells within CD8+sub populations in first, second and third trimester PBMC. One way ANOVA and the p values were corrected for multiple comparison (Kruscal-Wallis test), n= 15, *p< 0.05; **p< 0.01; ***p< 0.001.*

4.2.2 Characterization and dynamics of CD8+CD122+ T cells across pregnancy.

Another possible explanation of the striking abundance of uterine CD8+ T cells, without posing a harm to the fetus, is a presence of CD8+ T cells a regulatory function. To our knowledge, no information is available about the presence or characteristic of uterine CD8+CD122+ T cells. As the literature suggests that CD8+ T cells expressing CD122 hold a suppressive or regulatory capacity, and the discovery of a potential role of CD8+CD122+ T cells in pregnancy (Solano et al., 2015), CD8+CD122+ T cells were next investigated in pregnancy.

First, we aimed to understand general characteristics of uterine CD8+CD122+ T cells, that is, whether uterine CD8+CD122+ T cells belong to conventional or unconventional CD8+ T cells. Therefore, the composition of the CD8 receptor chains α and β were assessed by flow cytometry in blood and uterus on GD 14.5 to determine the ratio of conventional CD8αβ and unconventional CD8αα T cells. The majority of CD8+ and CD8+CD122+ T cells in blood and uterus were CD8αβ cells, thus containing a low frequency (< 5 %) of CD8αα T cells (Appendix 8A). Also, CD8 expression can be gradual and an indicator of particular immune responses, for instance, CD8 low expressing CD8+ T cells have been identified as a subset of activated CD8+ T cells, associated with cytotoxicity in humans (Trautmann et al., 2003). Therefore, CD8+ T cells with high CD8α expression ($CD8\alpha^{hi}$) and low CD8α expression ($CD8\alpha^{lo}$) were assessed. Here, majority of CD8αβ+ and CD8αβ+CD122+ T cells in both organs had high CD8α expression, although the frequency of low CD8α expression appears higher in the uterus. The unconventional CD8αα T cells however contained higher frequency of low CD8α in both organs, compared to CD8αβ cells (Appendix 8B). Therefore, we conclude that splenic and uterine CD8+CD122+ T cells are conventional CD8αβ T cells and that it is not necessary to distinguish between CD8αα and CD8αβ cells in further experiments.

Next, the general effector and memory phenotype was investigated in CD8+CD122+ T cells for comparison of CD8+ T cell phenotype, between organs and time points as previously explained in **Figure 7A**. CD122 expression was detected in all three subsets based on CD44 and CD62L expression, however to the highest extent in CD44+CD62L+ (containing central memory cells) subset and to the lowest extent in CD44-CD62L+ (containing naive cells) subset **(Figure 15A).**

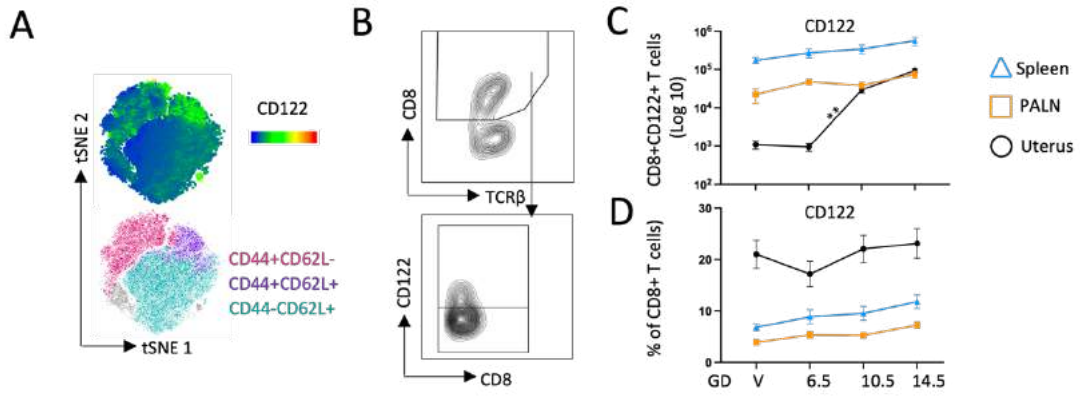

Figure 15. CD8+CD122+ T cells across pregnancy in mice.
A) *Heatmap of CD122 expression (top) and colour codes for CD44 and CD62L expression (bottom) within the tSNE plots for CD8+ T cells in all tissues and time points as generated for Figure 8.* ***B)*** *Representative dot plots of CD8+CD122+ T cells in virgin (top) and GD. 14.5 (bottom) females.* ***C)*** *Frequency of CD8+CD122+ T cell subsets throughout pregnancy expressed as total counts, y axis is log_{10} scale D) Percentages of CD122 expression in CD8+ T cells across pregnancy x axis indicates gestation day in C-D. *p< 0.05; **p< 0.01; ***p< 0.001.*

Like CD8+ T cells, total counts of CD8+CD122+ T cells escalated in the pregnant uterus which was not observed in the other tissues **(Figure 15B-C)**. However, their frequency among CD8+ T cells remained stable across pregnancy at approximately 20% in the uterus **(Figure 15D).** We investigated whether the frequency of CD8+CD122+ T cells could be modulated using a mouse model for glucocorticoid receptor deficiency in T cells. Such a knockout has been reported to introduce various physiological changes, most prominently reduced immunological fitness (Mittelstadt et al., 2012). This percentage seem to be constant as despite knocking out the glucocorticoid receptor in T cells **(Figure 16A)** it negatively affected fetal weight **(Figure 16B)** and caused differences in CD122 percentages in the peripheral circulation, while CD122 percentages in the pregnant uterus remained stable **(Figure 16C-D)**. This suggests a tightly regulated CD8+CD122+ T cell compartment, and a critical homeostasis of this subset at the feto-maternal interface.

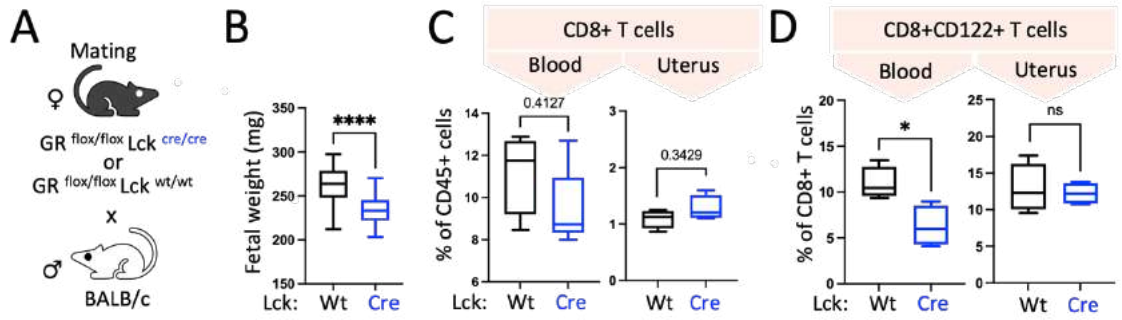

Figure 16. Glucocorticoid receptor in CD8+ T cells on GD. 14.5

A) *Experimental overview: females lacking glucocorticoid receptor (GR) in T cells ($GR^{flox/flox}$ $Lck^{cre/cre}$) and control females ($GR^{flox/flox}$ $Lck^{wt/wt}$) were mated to BALb/c males and analysed on GD 14.5.* ***B)*** *Fetal weight in milligrams (mg) in control mice (Wt) and transgenic mice lacking glucocorticoid receptor (Cre), n=26-28.* ***C)*** *Percentage of CD8+ T cells out of CD45+ cells in blood and uterus in Wt and Cre pregnant females, n=4.* ***D)*** *Percentage of CD8+CD122+ T cells out of CD8+ T cells in blood and uterus in Wt and Cre pregnant females, n=4. Statistical analyses were performed with t-test, *p< 0.05; ****p< 0.0001.*

The same gates as in **Figure 10** were applied to CD8+CD122+ T cells in order to investigate in-depth the phenotype of CD8+CD122+ T cells in regards of memory and effector differentiation **(Figure 17)**. As MAIT cells can express CD122, the positivity of MR1 tetramer was used to identify and exclude MAIT CD8+ T cells prior to phenotyping of CD8+CD122+ T cells. Indeed, uterine MAIT cells were mainly negative for CD122 expression confirming that they do not interfere with further analysis of CD8+CD122+ T cells and do not need to be taken into consideration or excluded in further experiments. The data showed that CD8+CD122+ T cells were not naive or early activated, although CD122+ naive cells significantly increased on GD 14.5, which might be an indication of the formation of early stem cell memory cells. Consistent with the literature, the majority of central memory cells express CD122. Central memory-like cells follow a similar pattern as central memory cells where they in general peak on GD 14.5 in all tissues. Interestingly, in the uterus, they tended to gradually rise during pregnancy and express CD69, while CD122- did neither (Appendix 9). This could mean that central memory cells are recruited into the uterus, where they downregulate CD127 expression and gain CD122 and CD69 expression, the latter indicating acquirement of tissue residency features or a recent activation.

CD122 expression was low in early effector cells in all tissues but increased in the peripheral tissues in pregnancy, however CD122+ early effector cells are absent in the uterus. Notably, CD122+ short-lived effector cells have a different curve than total short-lived effector cells as CD122+ population peaks before, on GD 6.5, while CD122- short-lived effector cells peak on

GD 10.5 indicating a more rapid, and innate-like, response of CD122+ short-lived effector cells. These cells also express CD69 (Appendix 9). In general, memory precursor effector cells, effector memory and tissue resident memory were mainly CD122 negative, although on GD 6.5, approximately half of effector memory and tissue resident memory cells expressed CD122, when compared to these populations in total CD8+ T cells. If differentiation takes place within the uterus, upon implantation, CD122-. Early effector cells may differentiate into either memory precursor effector cells and subsequently to effector memory and tissue resident memory cells around GD 6.5, or directly into short-lived effector cells accompanied with upregulation of CD122 expression in approximately half of the cells. Alternatively, these effector and memory cells expressing CD122 may have migrated from the low numbers in peripheral tissues, and possibly proliferated locally.

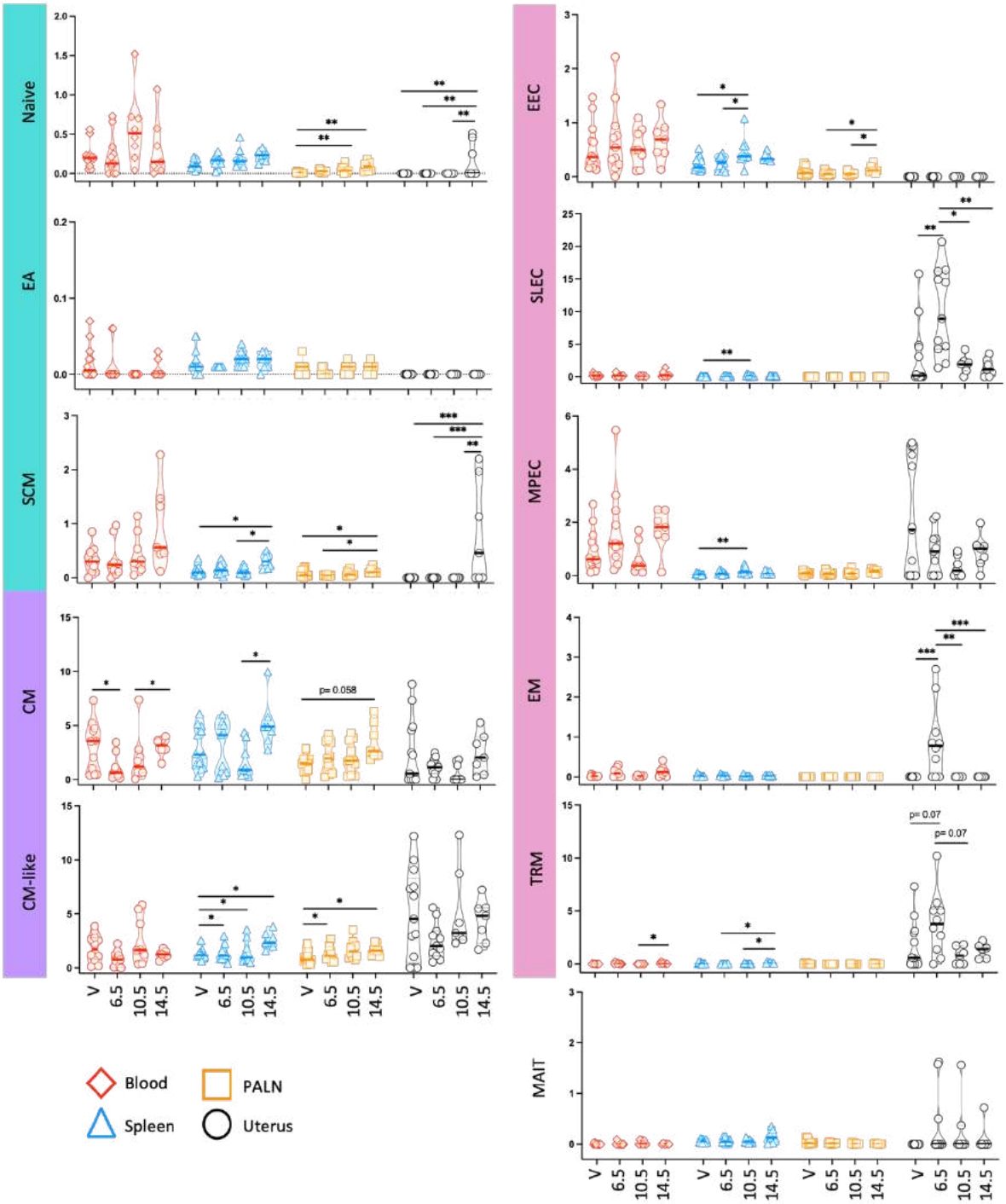

Figure 17. Characterization and dynamics of CD8+CD122+ T subpopulations across pregnancy in mice.

*Dynamics of different CD8+CD122+ T cell subpopulations across pregnancy in all organs. Y axis represent percentage of CD8+ T cells. X axis represents gestational day. EA: Early Effectors, SCM: Stem Cell Memory, CM: Central Memory, EEC: Early Effector Cells, SLEC: Short-Lived Effector Cells, MPEC: Memory Precursor Effector Cells, EM: Effector Memory, TRM: Tissue Resident Memory, MAIT: Mucosal Associated Invariant T cells. Statistical analyses were performed with non-parametric One-way ANOVA and the p values were corrected for multiple comparison (Kruscal-Wallis test). *p< 0.05; **p< 0.01; ***p< 0.001.*

Collectively, memory cells and effectors express CD122, but to a higher extent in the uterus. The dynamics of CD8+CD122+ T cells do in general not represent the changes in blood and

lymphoid organs except for the cell types expressing CD62L, suggesting that these cell types might have migrated from the periphery where they further differentiated upon uterine specific cues. Clearly, it is evident that CD8+ T cells and CD8+CD122+ T cells exist in the uterus, and they possess a distinct phenotype compared to CD8+ and CD8+CD122+ T cells found in the peripheral circulation and in secondary lymphoid organs. Although this data provides important new insights into uterine CD8+ T cell differentiation and dynamics, it raises further questions about migration, proliferative and differentiation capacity of CD8+ T cells during pregnancy. Thus, we aimed next to understand the mechanism behind this abundance in the uterus, that is whether it is due to migration, which occurrence has been debated (Erlebacher et al., 2007; Moldenhauer et al., 2017; Nancy et al., 2012), or proliferation. Therefore, their migration potential and proliferation potential were next addressed along with CD122 differentiation, antigen specificity, and importantly their function and whether they have a role in pregnancy.

4.3 Mechanism of placental specific CD8+CD122- and CD8+CD122+ T cells

For investigation of the mechanism and behaviour of CD8+ T cells and CD8+CD122+ T cells in pregnancy, the OVA/OT-I system was used in order to generate a pregnancy mouse model with fetal/placental specific CD8+ T cells, which can be accurately traced and characterized. This was achieved by mating Act-mOVA males, which carry the ovalbumin (OVA) protein in the surface of all cells, with Rag2γcKO females, which lack lymphocytes **(Figure 18A)**. This combination generates placentas expressing OVA in females harbouring no endogenous CD8+ T cells. These females were used as recipients of OT-I placental specific cells, which contain a transgenic T cell receptor specific for OVA expressed in placenta. Briefly, CD8+ T cells were sorted from spleen, para-aortic lymph nodes and uterus from OT-I females. These cells served as donor cells, which were adoptively transferred (AT) intravenously to pregnant recipients on GD 8.5-10.5, the window where we observed expansion of uterine CD8+ T cells as shown in **Figure 8C**. OT-I donor cells were either CD8+CD122- T cells, or co-transferred with 17% (1:5) OT-I CD8+CD122+ T cells (total of 300.000 AT cells), which resembles typical frequency of CD122 expression in uterine CD8+ T cells. For generation of control groups lacking placental specificity, two different combinations were generated: i) Rag2γcKO females were mated with Balb/c males, resulting in pregnancies lacking OVA expression and ii) wild type (wt) donor cells were adoptively transferred into OVA+ pregnancies, resulting in a pregnancy lacking the OVA-specific OT-I T cells. Additionally, some mice received phosphate buffered saline (PBS) instead of donor cells. Four days later (GD 12.5-14.5), adoptively transferred CD8+ T cells were tracked in blood, spleen and uterus, characterized by flow cytometry and their effect on

pregnancy success was evaluated. Information about the donor cells and gating strategy is according to (Appendix 10). For confirmation of the existence of OVA positive implantations in recipient females, fetal livers from each implantation were genotyped for the OVA antigen and considered as OVA positive pregnancy if at least one implantation from the mother contained the OVA antigen (see chapter 3.2.6).

4.3.1 Placental specificity, migration, and proliferation of adoptively transferred CD8+ T cells

First, we aimed to answer the debated question of whether peripheral CD8+ T cells can migrate to the uterus. Adoptively transferred CD8+CD122- T cells and CD8+CD122+ T cells were tracked by detecting whether they were found in the selected organs. They were found in blood and spleen, however to a higher extent when placental specific cells were adoptively transferred compared to cells with no placental specificity. Interestingly, exclusively adoptively transferred placental specific CD8+CD122- with or without CD8+CD122+ T cells were found in the pregnant uterus **(Figure 18B-C)**. Strikingly, CD8+ T cells lacking placental specificity were absent in the uterus. Expression levels of CD49d and Ki67 were used to evaluate lymphocyte migration and proliferation, respectively. CD49d is a component of the α4β1 integrin, called very late antigen 4 (VLA-4). By binding to vascular cell adhesion molecule 1 (VCAM-1) expressed on endothelial cells, VLA-4 facilitates leucocyte trafficking into the tissue (Muller, 2013). Ki67 is a nuclear protein, expressed in the cell cycle phases G1,S, G2 and M, but not in the quiescent G0 giving information about the proliferative state of a cell (Tanaka et al., 2011) and whether it has recently proliferated. Both CD49d and Ki67 expression was detected in placental specific CD8+ T cells, but to the highest extent in the uterus, supporting that CD8+ T cells can migrate into the uterus where they proliferate extensively **(Figure 18C-D)**.

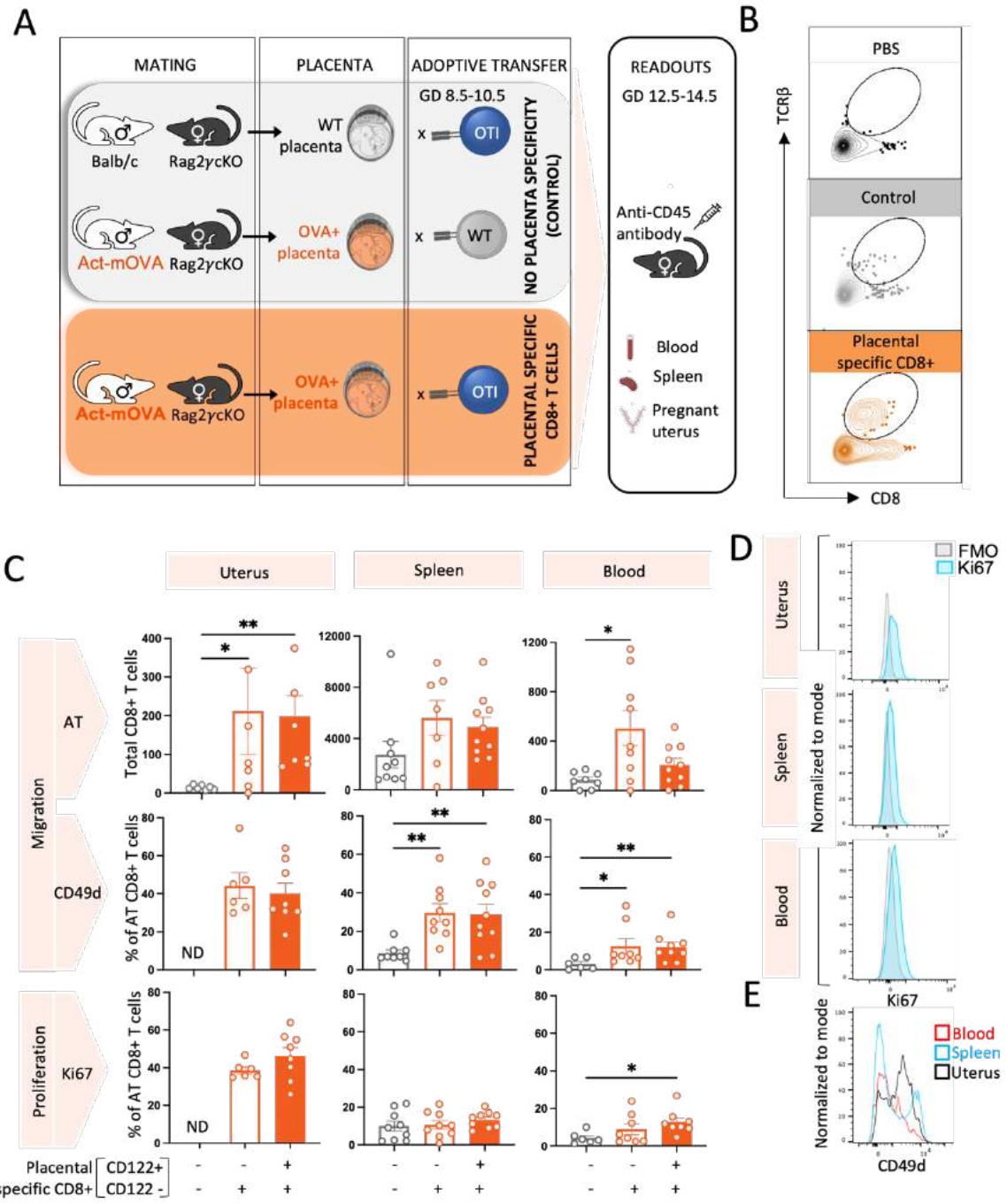

Figure 18. Recruitment, proliferation, and antigen specificity of adoptively transferred CD8+ T cells in pregnant Rag2γcKO females.

A) *A schematic overview of the experimental setup. Either Act-mOVA or Balb/c males were mated with Rag2γcKO females. Sorted CD8+ donor T cells were adoptively transferred intravenously to pregnant females on GD 8.5-10.5. Donor cells were either wild type (WT) or OT-I CD8+CD122- T cells, co-transferred with or without 17% OT-I CD8+CD122+ T cells (total 300.000 CD8+ T cells). This generates a control group without placental specific CD8+ T cells (grey) and a group with placental specific CD8+ T cells (orange). On GD. 12.5-14.5, blood, spleen, and uterus were harvested for flow cytometry analysis.* ***B)*** *Representative contour plots showing AT CD8+ T cells recruited to the uterus in control and placental specificity group.* ***C)*** *Total AT CD8+ T cells detected in uterus, spleen, and blood (top row), ratio of CD49d (center row) and Ki67 (bottom row) expression in AT CD8+ T cells, Y axis represents total counts in top row and percentages of AT CD8+ T cells in center and bottom row.*

Number of AT spleen cells are per 1 million splenic cells analysed, while the number of AT PBMCs are per 500 ul whole blood. X axis represents different groups with no placental specificity (grey bar) and placental specificity (orange bar) and whether donor cells were CD122+ or CD122-. ***D)*** *Representative histograms of Ki67 expression (blue) compared to FMO (Fluorescence Minus One) (grey).* ***E)*** *Representative histogram of CD49d expression in blood (red), spleen (blue) and uterus (black). Y axis on histograms is presented a Normalised to mode, while X axis indicates expression levels of a given marker. Statistical analyses were performed with non-parametric One-way ANOVA and the p values were corrected for multiple comparison (Kruscal-Wallis test). *p< 0.05; **p< 0.01.*

4.3.2 Phenotype of adoptively transferred CD8+ T cells

Next, we aimed to address the formation of CD8+CD122+ T cells, that is, whether they are induced by upregulation of CD8+CD122- T cells or whether they are formed by CD8+CD122+ T cell proliferation. Therefore, whether CD8+CD122- T cells upregulate CD122 expression and likewise whether CD8+CD122+ T cells downregulate CD122 expression was next investigated. Surprisingly, CD122 expression in adoptively transferred CD8+ T cells in blood and spleen was extremely high, much higher than normally seen in these organs and remained the same percentages independent of placental specificity or whether CD8+CD122- or CD8+CD122+ T cells were adoptively transferred **(Figure 19A)**. In contrast, CD122 expression within the uterus remained at a percentage typically seen in this organ, further supporting a tightly controlled population in the uterus reaching a homeostasis within the uterine compartment, while a distinct mechanism seems to take place within the periphery. Furthermore, three mice received adoptively transferred CD8+CD122+ which carried one CD45.1 and one CD45.2 allele (hence, here called $CD45^{1/2}$) co-transferred with CD8+CD122- which were $CD45^{2/2}$, allowing for tracking of each subset for investigation of CD122 differentiation **(Figure 19B)**. It became evident that CD8+CD122- T cells upregulated CD122 expression in all organs while some CD8+CD122+ cells downregulated CD122 in all organs **(Figure 19C-D)**, in fact, the majority of CD122+ T cells in the group receiving the co-transfer of CD8+CD122- with CD8+CD122+ T cells, originated from the adoptively transferred CD8+ CD122- T cells suggesting that the accumulation of CD8+CD122+ T cells is mainly due to a robust upregulation of CD122 expression, rather than proliferation of CD122+ T cells.

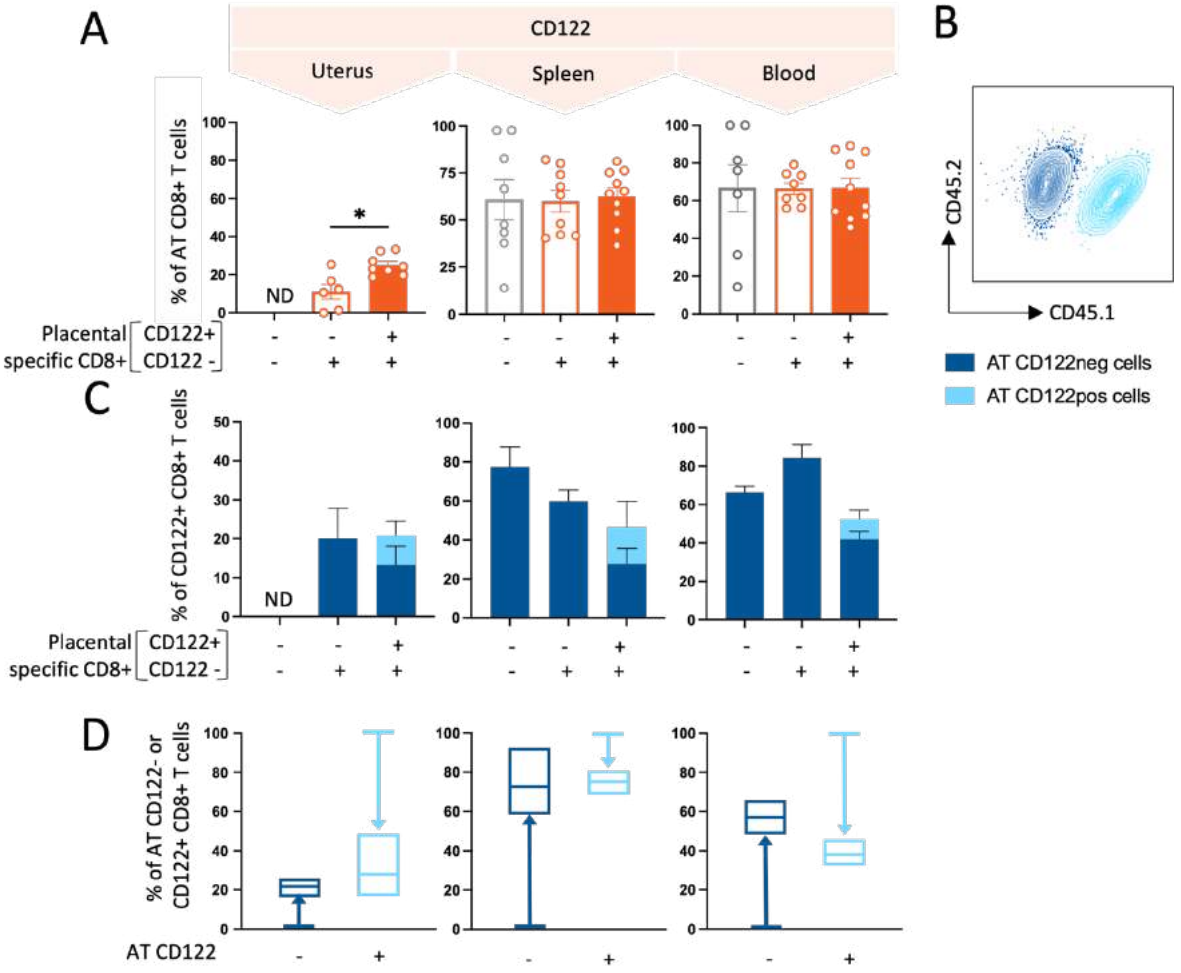

Figure 19. CD122 expression of adoptively transferred CD8+ T cells in pregnant Rag2γcKO females.

A) *CD122 expression in AT CD8+ T cells in uterus, spleen, and blood in control (grey bar) and placental specific (orange bar) groups, Y axis indicates percentages of AT CD8+ T cells. X axis represents different groups with no placental specificity (grey bar) and placental specificity (orange bar) and whether donor cells were CD122+ or CD122-.* ***B)*** *A representative contour plot showing the separation of donor AT CD8+CD122+ T cells ($CD45^{1/2}$: light blue) and donor AT CD8+CD122- T cells ($CD45^{2/2}$: dark blue) allowing for their separation and analysis of CD122 expression.* ***C)*** *Stacked bar plots showing CD122 expression in uterus, spleen and blood, n=3. Y axis indicates percentages of CD122+CD8+ T cells, with the blue colour code explained in C representing the donor origin of the CD122+ expressing cells.* ***D)*** *Box plots showing the upregulation of CD122 in CD8+CD122- T cells from 0% (dark blue), and downregulation of CD122 in CD8+CD122+ T cells from 100% (light blue), n=3. Y axis indicates the percentage of CD122 expression out of the parent population (either AT CD122- or AT CD122+), X axis indicates CD122 expression in donor cells. Statistical analyses were performed with non-parametric One-way ANOVA and the p values were corrected for multiple comparison (Kruscal-Wallis test). ND: Not detectable. *p< 0.05.*

4.3.3 Physiological pregnancy

The OVA/OT-I experiment was repeated with Bl6 females in order to confirm the above-mentioned findings in a physiological pregnancy. Here, co-transfer of $CD45^{1/2}$ OT-I

CD8+CD122- with 3% CD8+CD122+ T cells was done with a total of 1 million cells, that ensured that they would be differentiated among the endogenous $CD45^{2/2}$ CD8+ T cells **(Figure 20A-B).** As 17% of CD8+CD122+ T cells was not feasible for technical reasons, the chosen percentage of CD8+CD122+ T cells was based on physiological percentage of these cells observed in OT-I donors (from pooled spleen, para-aortic lymph nodes, and uterus). As observed in Rag2γcKO females, exclusively placental specific adoptive transferred cells were able to migrate to, endure and proliferate in the uterus **(Figure 20C-E)**. Adoptively transferred placental specific CD8+ T cells had higher CD49d and Ki67 compared to endogenous CD8+ T cells in all organs. Also, in line with findings from Rag2γcKO females, the frequency of CD122 expression in adoptively transferred CD8+ T cells was strikingly high in blood and spleen but were found within physiological range in the uterus confirming above mentioned theory of CD122 homeostasis within the uterus. Furthermore, the expression of Ki67 and CD49d was assessed in CD44+CD62L- (containing effector and memory cells), CD44+CD62L+ (containing central memory cells) and CD44-CD62L+ (containing naive cells) in both spleen and uterus in pregnant Bl6 females **(Figure 20F)**. This data confirms elevated expression of Ki67 and CD49d expression in the uterus compared to peripheral organs and shows that CD44+CD62L- (containing effector and memory cells) possess the highest expression of Ki67 and CD49d, followed by CD44+CD62L+ cells (containing central memory cells). To confirm these findings, gene expression of selected markers from the single-cell RNA sequencing data was visualized in a UMAP (Uniform manifold approximation and projection) plot within the uterus of Bl6 females on GD 14.5, see Appendix 11, confirming the expression of CD49d and Ki67 in the uterus on mRNA level.

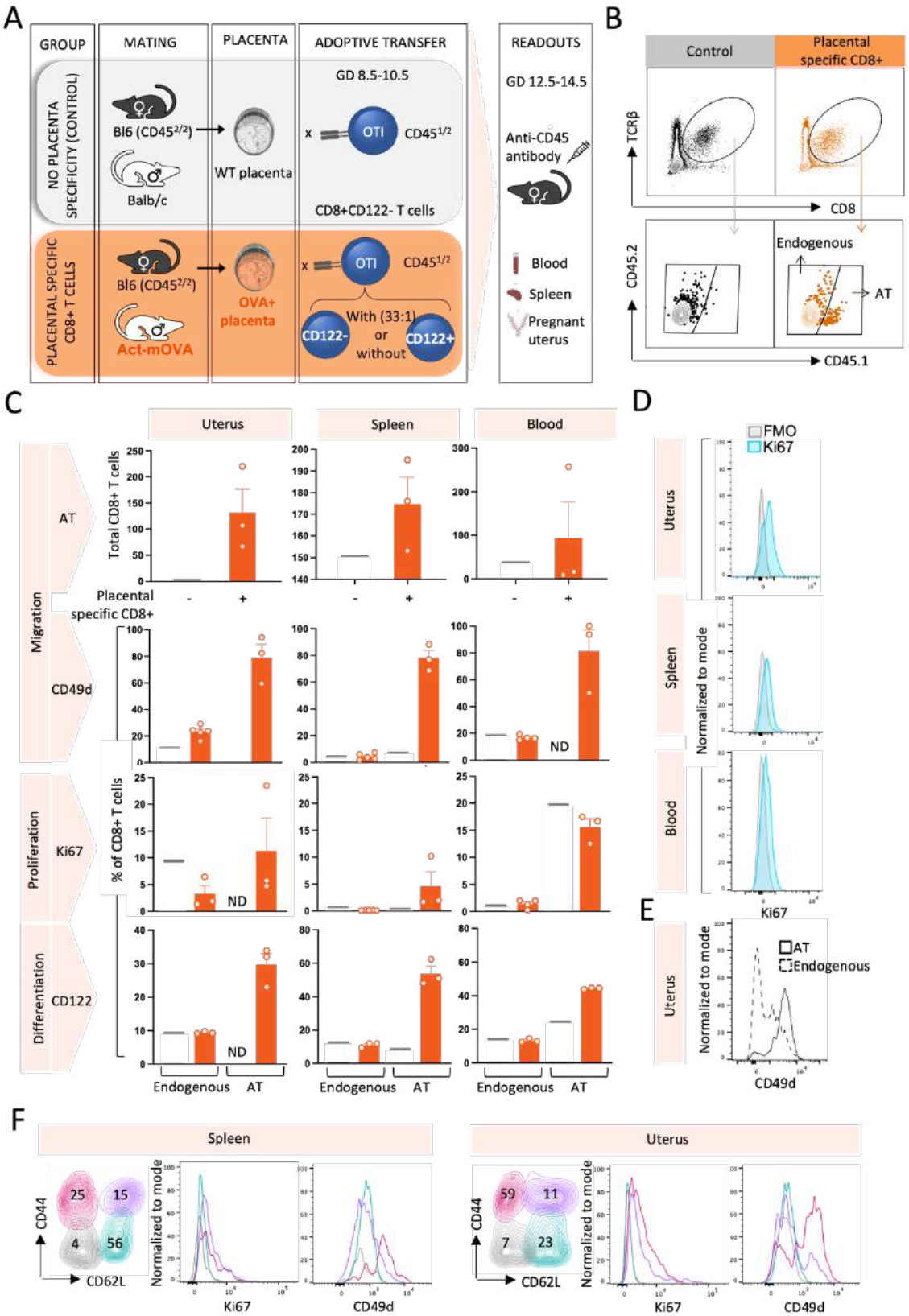

Figure 20. Migration, proliferation, antigen specificity and differentiation in physiological pregnancy.

A) *A schematic overview of the experimental setup. Either Act-mOVA or Balb/c males were mated with Bl6 females. Sorted CD8+ donor T cells were adoptively transferred intravenously to pregnant females on GD 8.5-10.5. Donor cells were OT-I CD8+CD122- T cells, co-transferred with 3% OT-I CD8+CD122+ T cells (Total 1 million cells). Donors were* $CD45^{1/2}$*, allowing for separation of*

adoptively transferred (AT) cells from endogenous CD45$^{1/2}$. This generates a control group without placental specific CD8+ T cells (grey) and a group with placental specific CD8+ T cells (orange). On GD. 12.5-14.5, blood, spleen and uterus were harvested for flow cytometry analysis. ***B)*** *Contour plots showing CD8+ T cells recruited to the uterus in control (top left) and placental specificity (top right) group. Endogenous cells express CD45$^{2/2}$ while AT express CD45$^{1/2}$ allowing their separation.* ***C)*** *Total AT CD8+ T cells detected in uterus, spleen and blood (top row), Y axis of the top row indicates total counts while X axis indicates placental specificity of the AT CD8+ T cells (grey line: no placental specificity, orange bar: placental specificity). Ratio of CD49d (second row), Ki67 (third row) and CD122 (bottom row) expression in endogenous and AT CD8+ T cells in uterus, spleen and blood, Y axis represent percentages of the parent population (CD8+ T cells in endogenous cells and AT CD8+ T cells in AT donor CD8+ T cells), X axis indicates both placental specificity and origin of CD8+ T cells.* ***D)*** *Representative histograms of Ki67 expression (blue) compared to FMO (Fluorescence Minus One) (grey).* ***E)*** *Representative histogram of CD49d expression in AT and endogenous CD8+ T cells in the uterus. Y axis in E-F represent values Normalised to mode, while X axis represents the expression levels of a given marker.* ***F)*** *Comparison of Ki67 and CD49d expression in CD44+ CD62L- (including effector and memory cells: pink), CD44+CD62L+ (including central memory cells: purple) and CD44-CD62L+ (including naive cells: turquoise), in concatenated endogenous CD8+ T cells from spleen (left) and uterus (right) on GD 12.5-14.5. Data are represented as contour plots showing frequency of each population and histograms showing expression levels of Ki67 and CD49d (X axis) with values Normalised to mode (Y axis).*

4.3.4 Effect of adoptively transferred CD8+ T cells on pregnancy success

In order to understand the consequence of adoptively transferred placental specific CD8+CD122- with or without CD8+CD122+ T cells, abortion rate was evaluated in Rag2γcKO females. Of note, Rag2γcKO females are considered good breeders, not regarded as abortion prone mouse model. When injected with PBS, abortion rate was on average 10%, typically observed in physiological mouse pregnancies in our laboratory, but embryonic genetic abnormalities are one of the main reason for spontaneous resorptions (Flores et al., 2014; Gu et al., 2021; Yakut et al., 2015). Although not significantly, the abortion rate of adoptively transferred CD8+CD122- T cells appeared slightly higher, irrespective of placental specificity. This suggests that placental specific CD8+CD122- T cells did not harm the pregnancy outcome more than non-placental specific cells, although some of those may contain naturally occurring placental specific CD8+ T cells. Thus, although the naturally occurring abortion rate is at least partly due to non-immune related triggers, we cannot exclude that the addition of CD8+CD122- T cells, might negatively affect the abortion rate to some extent. Interestingly, adoptively transferred placental specific CD8+CD122- co-transferred with CD8+CD122+ T cells significantly reduced abortion rate compared to adoptive transfer of control or placental specific CD8+CD122- T cells **(Figure 21A)**. This suggests that CD8+CD122+ T cells somehow improved the pregnancy outcome, however whether it is due to immune related function and/or non-immune related function is up for speculation. It is clear that all groups receiving

adoptively transferred CD8+ T cells, do contain CD8+ CD122+ T cells on tissue collection day, due to previously mentioned CD122 upregulation. Interestingly, it seems like it was only the original adoptively transferred CD8+CD122+ T cells that were able to improve the pregnancy outcome, by preventing fetal loss, indicating a beneficial role in pregnancy, while the recently upregulated CD122+ T cells did not.

Thus, we aimed to understand whether the original adoptively transferred CD8+CD122+ T cells contained a regulatory phenotype that could explain the effect on pregnancy outcome. Therefore, the two regulatory subtypes, CD8+CD122+Ly49+ and CD8+CD122+PD1+ were investigated in the spleen and uterus in all groups. Interestingly the uterus of the mice receiving the co-transfer of CD8+CD122+ T cells, presented higher levels of both CD8+ T regulatory subtypes, although only significantly for CD8+CD122+Ly49+ T cells, than in mice without co-transfer of CD8+CD122+ T cells **(Figure 21B)**. Notably, Ly49 expression was almost exclusively found in the original adoptively transferred CD8+CD122+ T cells, but not in the newly CD122 upregulated CD8+CD122+ T cells (Appendix 12), suggesting that the "true" CD8+CD122+Ly49+ regulatory cells are not simply generated by a recent upregulation of CD122, and Ly49, but may have other origin and specific characteristics for their regulatory function or beneficiary function in pregnancy. These findings put CD8+ T regulatory cells into the spotlight and raise further questions about uterine CD8+CD122+ T cells, their characteristics and function in pregnancy, which will now be further addressed.

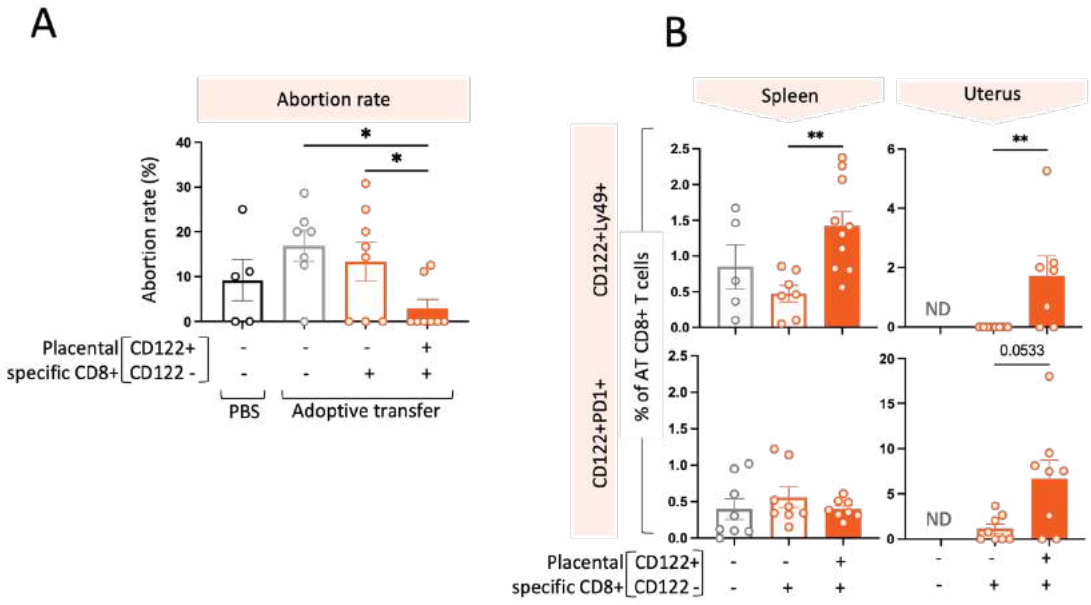

Figure 21. The effect of adoptively transferred (AT) CD8+ T cells on pregnancy success.
A) *Abortion rate in pregnant Rag2γcKO females receiving AT placental specific CD8+CD122- T cells or co-transfer of CD8+CD122+ T cells. Y axis represents the abortion rate in percentages* ***B)***

*Percentages of CD122+Ly49+ and CD122+PD1+ expression in spleen and uterus from pregnant females receiving AT placental specific CD8+CD122- T cells or co-transfer of CD8+CD122+ T cells. Y axis represents percentages of AT CD8+ T cells. X axis in A-B represents different groups with no placental specificity (grey bar) and placental specificity (orange bar) and whether donor cells were CD122+ or CD122-. ND: not detectable. Statistical analyses were performed with non-parametric One-way ANOVA and the p values were corrected for multiple comparison (Kruscal-Wallis test). *p< 0.05; **p< 0.01.*

4.4 Identification of regulatory/tolerogenic CD8+CD122+ T cells in pregnancy

4.4.1 Characterization with single-cell RNA sequencing

In order to gain deeper understanding of uterine CD8+CD122+ T cells in pregnancy, their functional phenotype was studied from single-cell RNA sequencing data from FACS- sorted CD8+ T cells in blood and mesometrial uterus on GD 14.5 in mice. First, CD8+ T cells were assigned into five subgroups based on CD122, PD1 and Ly49 expression (Appendix 13), resulting in two CD122 negative populations: CD122-PD1- (conventional CD122-), CD122-PD1+ (exhausted CD122-), and three CD122+ populations: CD122+PD1-Ly49, CD122+Ly49-PD1+ (CD122+PD1+ regulatory) and CD122+Ly49+ (CD122+Ly49+ regulatory) **(Fig. 22A)**. Here, consistent with flow cytometry data, CD122 percentage was enriched in the uterus compared to blood, however and surprisingly, to a much higher extent than observed by flow cytometry, approximately 60% **(Fig 22A-B)**. The majority of CD122+ T cells lacked PD1 and Ly49 expression, and both CD122+PD1+ and CD122+Ly49+ subsets were detected in the uterus, but barely in blood.

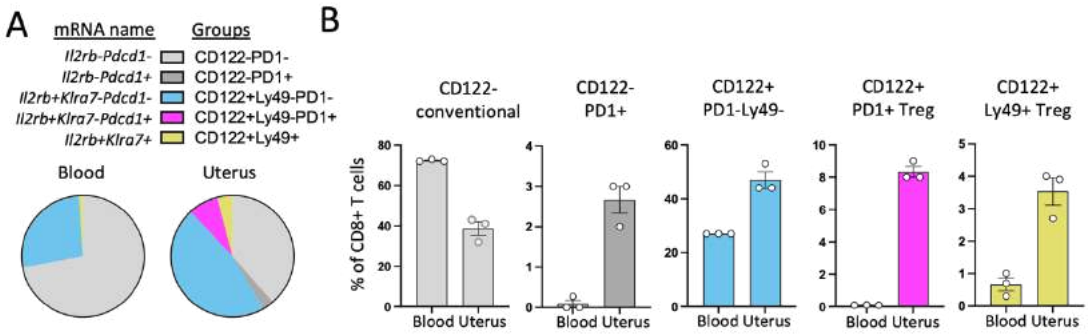

Figure 22. CD8+CD122+ and CD8+CD122- subsets in blood and uterus on GD 14.5 from single-cell RNA sequencing data.

Five subgroups of CD8+ T cells were generated based on gene expression of Il2rb (CD122), Pdcd1 (PD1) and Klra7 (Ly49G), described in Appendix 13. ***A)*** *Pie plots of the five subgroups of CD8+ T cells: CD122-PD1- (including conventional CD8+ T cells: light grey), CD122-PD1+ (including exhausted cells: dark grey), CD122+Ly49-PD1- (non-regulatory CD8+ T cells: blue), CD122+Ly49-PD1+ (CD122+PD1+ T regulatory cells: pink), CD122+Ly49+ (CD122+Ly49+ T regulatory cells), in blood (left) and uterus (right).* ***B)*** *Percentages of each subgroup of CD8+ T cells (Y axis) in blood and uterus (X axis).*

As mRNA gene expression does not directly predict protein expression of a given gene, barcoded CITE-sequencing antibodies were used for selected genes for comparison of gene expression and protein expression (see chapter 3.1.6). Unfortunately, an accurate integration and normalisation of blood and uterine CITE-sequencing data was not possible, most likely due to the difference in the purity of the cell suspension and the difference in cell isolation protocols, affecting the antibody staining and causing incorrect data integration of the different organs. Thus, the uterus data was processed individually as explained in Appendix 14, allowing for correct comparison between mRNA and protein expression. A high CD122 expression was confirmed by high positivity of uterine CD122 protein expression measured by a CITE-sequencing barcoded antibody (Appendix 15), however by a lower extent than mRNA levels. Of note, some markers are better detected on the protein level than on mRNA level, for instance when high mRNA levels of a given gene may not result in protein expression due to post-translation modification mechanisms. Likewise, some markers are not detected on mRNA level, thus, having the information of both RNA and protein level is advantageous. Comparison of mRNA and protein expression of other relevant markers was included in Appendix 15, showing varying correlation of mRNA and protein expression. For both simplicity and for maximising cell numbers, a deeper analysis of the uterine data was carried out with the mRNA expression data.

We hypothesise that uterine CD8+CD122+Ly49+ and CD8+CD122+PD1+ cell subsets contain a distinct functional phenotype compared to not only CD8+CD122- subsets, but also to each other. To explore this, gene expression patterns of relevant gene signature were compared between the five CD8+ T cell groups, (same groups as in **Figure 22**), including activation status, their phenotypical differentiation into effectors or memory cells, inhibitory receptors, levels of apoptosis and proliferation, migration, cytokine secretion and cytotoxicity **(Figure 23)**, and then compared to published findings of these subsets in other organs and contexts. Here, average gene expression was calculated and relative gene expression across the five groups are presented as a heatmap, and additionally as original values in a heatmap in Appendix 16.

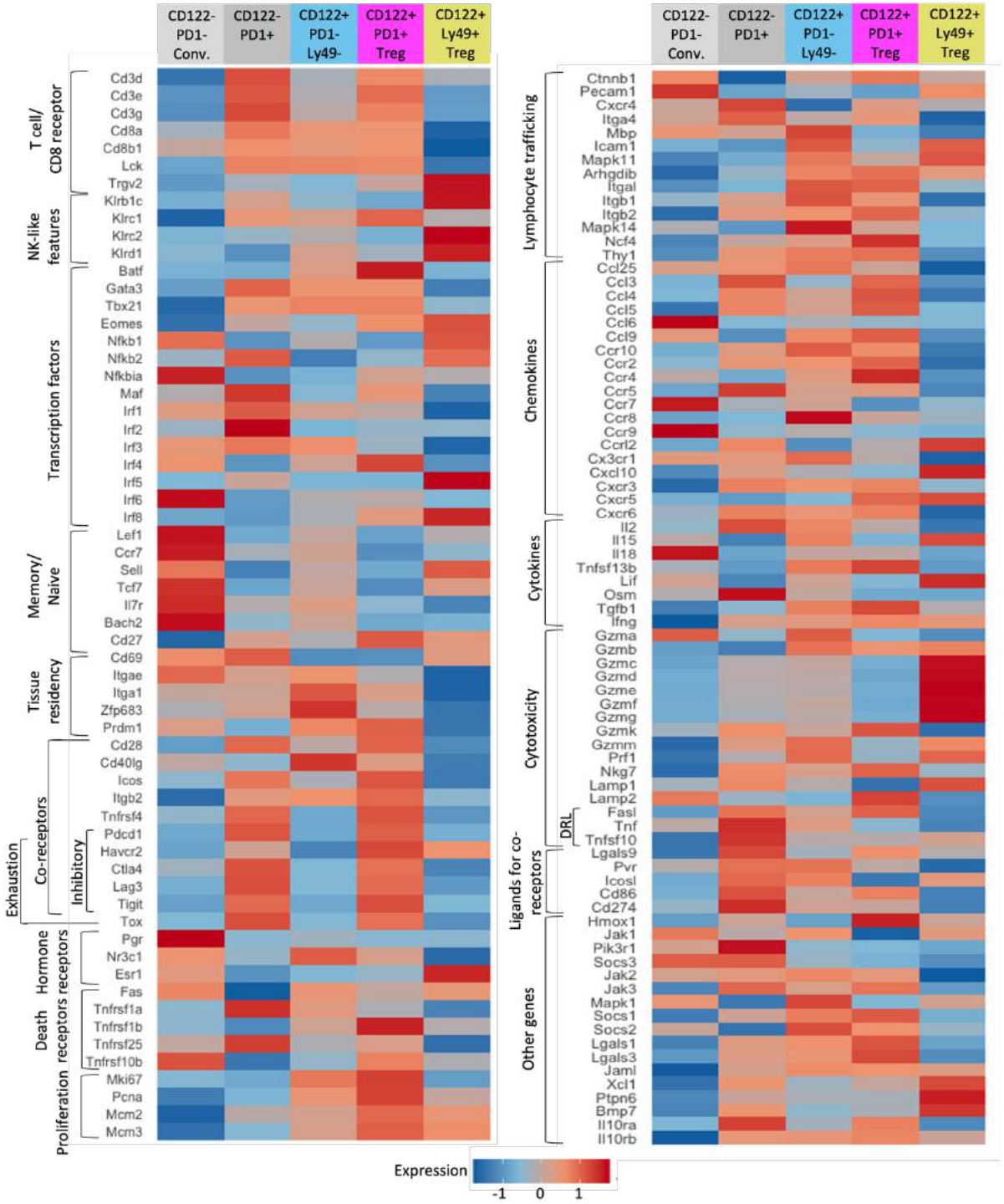

Figure 23. Gene expression in CD8+CD122+ and CD8+CD122- subsets in uterus on GD 14.5 from single-cell RNA sequencing data

Heatmaps representing average expression of selected genes relevant for CD8+ T cells differentiation and function in five subgroups of CD8+ T cells: CD122-PD1- (including conventional CD8+ T cells: light grey), CD122-PD1+ (including exhausted cells: dark grey), CD122+Ly49-PD1- (non-regulatory CD8+ T cells: blue), CD122+Ly49-PD1+ (CD122+PD1+ T regulatory cells: pink), CD122+Ly49+ (CD122+Ly49+ T regulatory cells). DRL: Death receptor ligands. List of the genes and their corresponding protein name can be found in Appendix 4.

In general, CD122-PD1- cells, contain a gene signature of naive and memory cells, which lack co-stimulatory receptors and are not undergoing proliferation. They have relatively low expression of cytokines, chemokines, and cytotoxic genes. CD122-PD1+ cells have gene expression pattern of activation, and co-receptors including both activation receptors and inhibitory receptors, such as *Tox*, suggesting an exhausted phenotype. However, this group also contains relatively high expression of death ligands and ligands for co-receptors, suggesting that they can influence the behaviour of target cells. CD122+PD1-Ly49- T cells seem less activated compared to other CD122+ groups, but contain gene signature of tissue residency, lymphocyte trafficking, and broad chemokine and cytokine expression.

The two CD8+CD122+ regulatory subsets appear different in terms of functional phenotype. CD122+PD1+ T regulatory cells, which contain a low gene expression of *Sell* (CD62L) indicating a memory/effector phenotype rather than central memory, may mediate their regulatory function via an exhaustion mechanism, based on elevated expression of inhibitory co-receptors and *Tox*, producing *Tgfb* and *Ifng*. Although this subset seems similar to CD122-PD1+ to some extent, their functional gene signature appears different, for instance in transcription programs, and chemokine and cytokine production, and contain further enrichment of interesting genes further discussed in chapter 5.3.4. Based on the gene expression signature, they might mediate cytotoxicity against targets via production of the cytolytic molecules *Gzmb, Gzmk*, and *Nkg7* mediated via the degranulation protein CD107b *(Lamp-2)*, and via the FasL/Fas pathway. Furthermore, the elevated gene expression of the transcription factors *Batf, Gata3, Tbx2*, *Maf, Irf4* and *Eomes* have been linked with effector function and/or exhaustion (Harberts et al., 2021; Kurachi et al., 2014; Li, He, et al., 2018; Man et al., 2017; Verdeil, 2016). Collectively, the expression pattern of CD122+PD1+ T cells provides intriguing evidence of modulation of the CD8+ T subset at the feto-maternal interface.

When compared to published gene signature of CD8+CD122+Ly49+ regulatory T cells in mice (Li et al., 2022; Saligrama et al., 2019), uterine CD8+CD122+Ly49+ T cells contain a similar gene signature, with NK-like features (*Klrb1c, Klrc2, Klrd1*), lack of *CD28*, high expression of *Eomes* transcription factor, the chemokine *Cxcr5* and the cytotoxic molecules Granzymes (*Gzm-b, c,d,e,f,g,m*), Perforin (*Prf1)*, as well as degranulation molecule CD107a (*Lamp1*). Opposed to CD122+PD1+ subset, these cells contain the phenotype of central memory cells based on relatively high gene expression of *Sell* (CD62L). The top genes expressed in this subset further support a differential function to the CD122+PD1+ cells, where the *Fcer1g* gene,

reported to distinguish particular cytotoxic CD8+ T cell tumour infiltrating lymphocytes from CD8+PD1+ tumour infiltrating lymphocyte cells (Morrish & Ruland, 2022), was upregulated. Other upregulated genes were the inhibitory receptor *Cd160* and genes involved in limiting effector response such as *Ptpn6* (which limits production of CD8+ effector T cells) (Fowler et al., 2010), *Ms4a4c* (a negative feedback loop of activation and proliferation) (Xu et al., 2010), but also genes associated with effector function such as *Ikzf2, Itma2 and Pglyrp1* (Li et al., 2022; Naluyima et al., 2019; Sharapova et al., 2017, 2018). They further differ from CD122+PD1+ Treg cells in their lower expression of markers for exhaustion, proliferation and lymphocyte trafficking and lower expression of chemokines and cytokines. These finding support the hypothesis that CD122+Ly49+ Tregs may mediate their regulatory function via another means than CD122+PD1+ T regulatory cells.

Glycosylation is a posttranslational modification of proteins which generates binding sites for lectins and galectins (Boscher et al., 2011). When studying galectins, considering the Galectin-glycan interaction can be helpful. Therefore, glycosylation was evaluated in CD8+CD122+ and CD8+CD122- T cells by measuring lectins which recognise specific O-glycan and N-glycan structures, as well as by sialyation by flow cytometry (Appendix 18). The data suggest distinct difference in glycosylation pattern between the two subsets, suggesting distinct interactions and modulation with other immune cells at the feto-maternal interface. Although intriguing findings, further investigation is needed to conclude the functional meaning of the expression pattern of the galectins in CD8+CD122+ T cells in pregnancy.

Collectively, CD8+CD122+PD1+ and CD8+CD122+Ly49+ regulatory T cell subsets were identified in pregnant uterus and contained a particular phenotype, as described in the literature in other contexts. Although containing distinct gene signature, both regulatory subsets contained an activated phenotype associated with both effector function and inhibitory function/immune suppression as well as cytotoxicity. This supports claims of CD8+ T regulatory cells, in particularly CD8+CD122+Ly49+ cells, mediating immune tolerance via a cytotoxic mechanism towards respective targets, for example other T cell subsets.

Table 3. Overview and comparison of CD122+Ly49-PD1+ and CD122+Ly49+ T cells in pregnant uterus on GD 14.5 from single-cell RNA sequencing data.

CD122+ regulatory subset	CD122+PD1+	CD122+Ly49+
Phenotype (CD44 & CD62L)	Effector/memory	Central memory
Inhibitory phenotype/function, immunesuppressive	Inhibitory receptors Lgal1/Lgal3 Exhaustion: - *Tox* - *Bst2, Hmgb2, Tuba1b* *Tgfb1*	*CD160,* *Ptpn6, Ms4a4c* *Ikzf2, Itma2, Pglyrp1,* *Havcr2, Bmp7*
Activation/effector	*Batf, Gata3, Tbx2*, *Maf, Irf4* and *Eomes* (effector and exhaustion) Interferon signaling: *Ifng, Ifi2712a, Zbp1, Isg20, Isg15*	*Nfkb1/Nfkb2, Irf8,* *Ifng*
Cytotoxicity	*Gzmb, Gzmk, Nkg7, CD107b* *FasL*	*Granzymes (Gzm-b, c,d,e,f,g,m), Perforin 1, CD107a*
Found in tumours	*Sh2d2a, Crip1, Ccl4, Ccl5,* *Lgal1/Lgal3*	*Bmp7*
NK-like features	*Klrc1, Nkg7*	*Klrb1c, Klrc2, Klrd1*

4.4.2 Flow cytometry analysis of CD8+CD122+ T cells in pregnancy.

As it is evident that mRNA levels do not directly indicate cell membrane protein expression, protein levels of selected cell membrane inhibitory receptors were validated in pregnancy. Therefore, a flow cytometry panel including the most likely markers for a CD8+ T regulatory potential, based on current literature, was used in a semi-allogenic pregnancy experiment as described in Figure 7A. The literature strongly suggests that CD8+ T regulatory cells are CD8+CD122+Ly49+ and/or CD8+CD122+PD1+ T cells. Ly49 and PD1 are generally not co-expressed in CD8+ T cells (Shytikov et al., 2021), supported by the current single-cell RNA sequencing data in uterus. This was confirmed on protein level with flow cytometry as uterine CD8+ T cells did not co-express those inhibitory molecules but contained cells expressing either PD1 or Ly49 **(Figure 24A)**.

Here, expression of inhibitory receptors associated with exhaustion was further studied in CD8+CD122+ T cells. Expression of inhibitory receptors was first visualised with dimensionality reduction analysis in CD8+CD122+ T cells for identification of CD8+CD122+ T cells expressing PD1, Tim3, CTLA4, Lag3 and Tigit. CD8+ T cells from all time points and all organs (as explained in **Figure 7A**) were concatenated, containing 16470 CD8+ T cells from 155 samples, each group contributing equal numbers of CD8+ T cells to the concatenated file. A tSNE plot was generated based on expression of CD122 and the above-mentioned inhibitory receptors which clearly clustered CD122 into one population within the tSNE plot **(Figure 24B)**, which was further divided into three populations, CD122+PD1 high (CD122+PD1^{hi}), CD122+PD1 intermediate (CD122+PD1^{int}) and CD122+PD1 negative (CD122+PD1^{neg}) **(Figure 24C)**. Only the PD1^{hi} population expressed the other inhibitory receptors Tim3, Lag3, CTLA4 and Tigit **(Figure 24D)** which along with the PD1^{int} population were strikingly enriched in the uterus compared to the peripheral organs **(Figure 24E-F)** and remained stable across pregnancy**,** (Appendix 19). The same approach was applied to CD8+CD122- cells, which did not show the same enrichment of Tim3, Lag3, CTLA4 and Tigit in PD1^{hi} cells, suggesting this feature is unique to CD8+CD122+ T cells on protein level (Appendix 19). Taken together, CD122+PD1+ and CD122+Ly49+ regulatory T cells were detected in the pregnant uterus on both mRNA expression level and protein expression level.

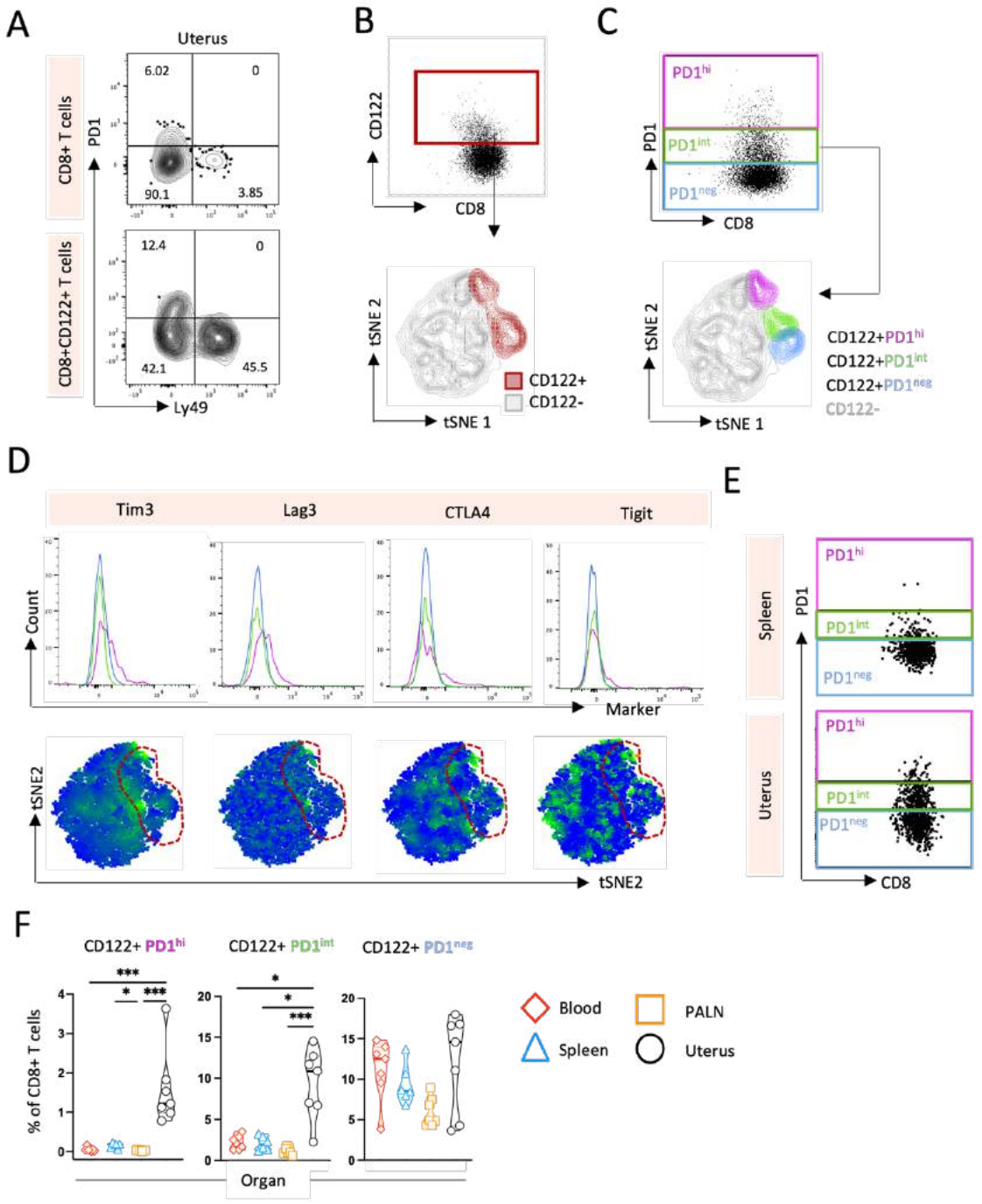

Figure 24. Flow cytometry analysis of inhibitory molecules on CD8+CD122+ T cells.

A) *Contour plot of single and co-expression of PD1 and Ly49 in CD8+ T cells (top) and in CD8+CD122+ T cells (bottom) in GD 14.5 uterus.* ***B)*** *A dotplot of CD122+ CD8+ T cells (top) applied to the tSNE plot, dictating the clustering of CD122+ CD8+ T cells (bottom).* ***C)*** *A dot plot of PD1 expression, separated to PD1 high ($PD1^{hi}$): pink, PD1 intermediate ($PD1^{int}$): green and PD1 negative ($PD1^{neg}$): blue (top), to the tSNE plot showing three subpopulations of CD122+ CD8+ T cells (bottom). CD122- CD8+ T cells are coloured grey.* ***D)*** *Histograms of the inhibitory molecules Tim3, Lag3, CTLA4 and Tigit in CD122+$PD1^{hi}$, CD122+$PD1^{int}$, CD122+$PD1^{neg}$ cells (top row). Y axis represents counts, X axis represents expression levels of a given marker. Bottom row shows tSNE heatmaps of the same inhibitory receptors used for clustering CD8+ populations, red dottet line showing CD122+ cells.* ***E)*** *Dot plots of PD1 expression in spleen (top) and uterus (bottom).* ***F)*** *Percentages of CD122+$PD1^{hi}$, CD122+$PD1^{int}$, CD122+$PD1^{neg}$ and CD122- CD8+ T cells in blood (red), spleen (blue), PALN (yellow) and uterus (black) on GD 14.5. Y axis represents percentage of CD8+ T cells. X axis represents the*

*color-coded organ. Statistical analyses were performed with non-parametric One-way ANOVA and the p values were corrected for multiple comparison (Kruscal-Wallis test). *p< 0.05***; p< 0.001.*

4.5 T cell receptor clonality in pregnancy

Clearly, CD8+ T cells expand in the pregnant uterus. It is of high relevance to understand the clonal expansion, meaning which CD8+ T cell clones expand in pregnant uterus, compared to the peripheral circulation. This could give information about which CD8+ T cell subset have responded to fetal antigens, undergone clonal expansion and what functional characteristics they contain. Therefore, the samples used for single-cell RNA sequencing were also used for sequencing the T cell receptor in blood and mesometrial uterus on GD 14.5.

Complementary determining region 3 (CDR3) is the highly variable sequence encoded by the V(D)J junction and the CDR3 length can be used as an indicator of diversity within the TCR repertoire, where distinct CDR3 repertoires can be detected in distinct pathologies such as in infection diseases, tumours and autoimmune diseases (Hou et al., 2016; Wang et al., 2017). Therefore, the CDR3 length was assessed in blood and uterine samples. CDR3 length in both organs followed a normal distribution curve, but uterine clonotypes tend to have higher CDR3 length compared to clonotypes found in blood **(Figure 25A).** Next the number of unique clonotypes and rare clonal proportion in both organs was investigated. By plotting the distribution of clonotype abundance in each organ, it became evident that blood contains more clonotypes of low abundance, while uterine CD8+ T cells contain more clonotypes of high abundance compared to blood. This goes in hand with uterine CD8+ T cells containing fewer number of unique clonotypes compared to blood **(Figure 25B)** and lower ratio of rare clones **(Figure 25D)**. Also, clonotypes with medium, large and hyperexpanded clonotypes were detected in the uterus to a higher extent compared to blood **(Figure 25E)**. The top ten clonotypes were visualised in uterus and compared to blood, showing higher proportion of those clonotypes in the uterus **(Figure 25F)**. Collectively this suggests a higher level of clonal expansion of uterine CD8+ T cells, while blood contains higher levels of non-expanded clones. It is tempting to speculate that the uterine clonotypes are specific for fetal antigens, but further experiments are needed to determine fetal specificity of the clonally expanded uterine CD8+ T cells. It is also tempting to speculate that clonally expanded uterine CD8+ T cells are the CD8+CD122+ regulatory T cells, expressing PD1 or Ly49. Due to complexity of such data analysis, this question will not be addressed in this dissertation, but such analysis is underway as a

continuation of this project and will provide further information about the clonally expanded uterine CD8+ T cells for further progression of this project.

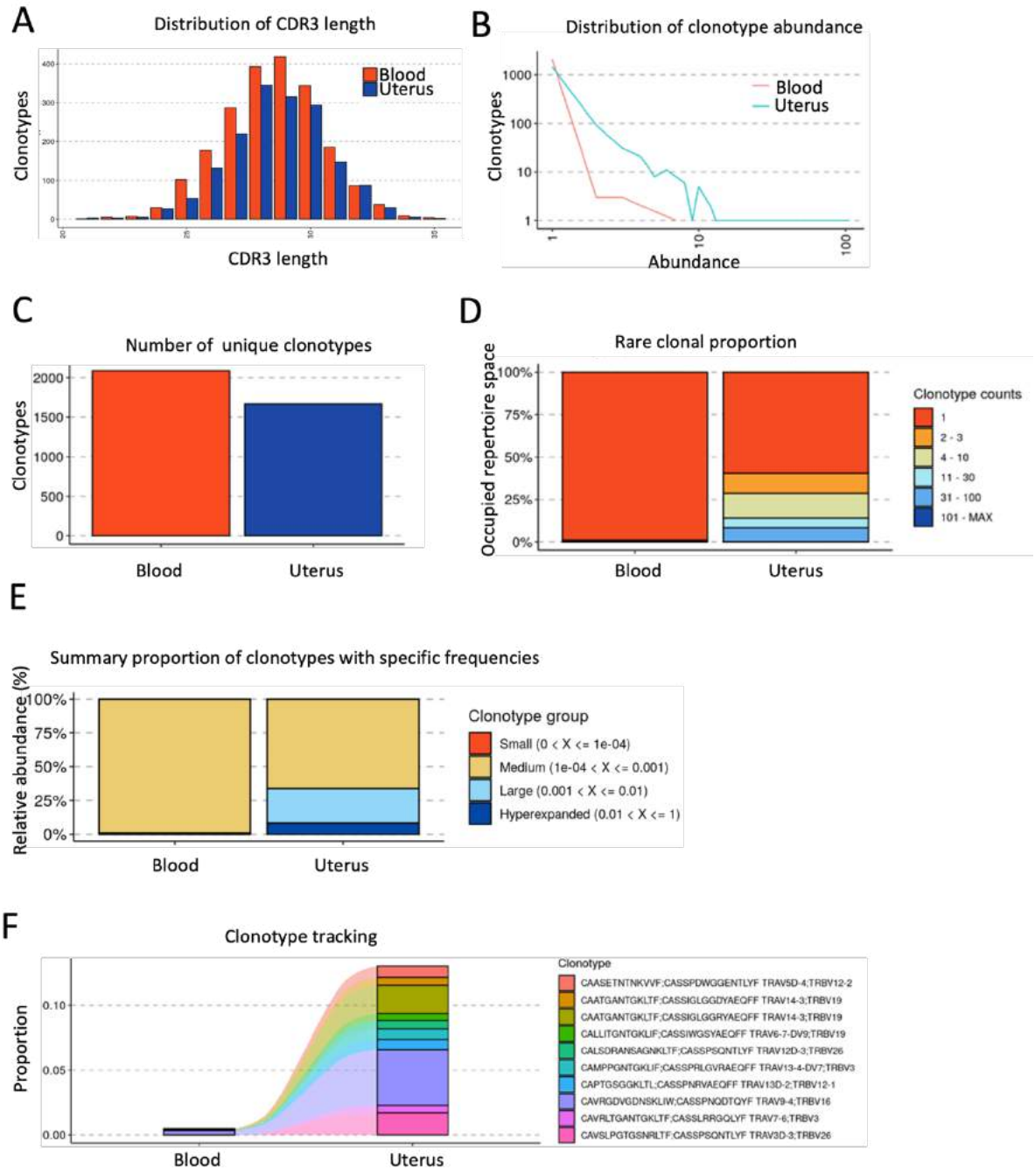

Figure 25. T cell receptor sequencing of CD8+ T cells from blood and uterus on GD 14.5.
A) *Distribution of CDR3 length in blood (red) and uterus (blue).* ***B)*** *Distribution of clonotype abundance in blood (red) and uterus (green).* ***C)*** *Number of unique clonotypes in the input data in blood(red) and uterus(blue).* ***D)*** *Summary proportion of clonotypes with specific counts in blood and uterus. E). Relative abundance in percentages of four clonotype groups containing small, medium, large and hyperexpanded CD8+ T cell clonotype group, based on frequency of clones.* ***F)*** *Clonotype tracking showing the top ten clonotypes as a relative proportion of clonotypes for each sample. Each colour represents a unique clonotype.*

4.6 Mesomesometrial and anti-mesometrial uterine compartment

So far, the flow cytometry data of the uterus on GD 10.5 and 14.5 derive from the mesometrial side of the uterus, which contains thicker decidual layer with closer proximity to the placenta and therefore fetal antigens than the anti-mesometrial side. However, the anti-mesometrial uterus was also analysed and compared to the mesometral uterus. Of note, the flow cytometry data refer to mesometrial uterus, which contain mesometrial decidua, MLAp and mesometrial myometrium, while anti-mesometrial uterus contains anti-mesometrial decidua ad anti-mesometrial myometrium.

The data presented in this dissertation have demonstrated that CD8+ T cells migrate to the mesometrial uterus, where they proliferate and represent a heterogenous population of effector and memory CD8+ T cells along with CD8+CD122+ T cells with a regulatory potential. Whether CD8+ T cells are also found in the anti-mesometrial uterus and whether they follow similar characteristics was next investigated by evaluating blood vessel and lymphocyte vessels in both uterine compartments, along with comparing CD8+ T cell subset frequencies between both compartments.

4.6.1 Histological staining of blood vessels and lymphoid vessels at implantation sites

In order to assess vascularisation within uterine layers and compartments, and therefore possible lymphocyte migration, blood vessels were evaluated by CD31 detection **(Figure 26A).** It became evident that GD 10.5 and 14.5 mesometrial decidua and MLAp are highly vascularized. CD31 positivity was also detected in the anti-mesometrial decidua, however seemingly to a lesser extent compared to mesometrial decidua, especially on GD 10.5. Due to the greater size of the mesometrial uterus, this site automatically allows for greater migration of CD8+ T cells. The surrounding myometrium seems less vascularised suggesting that the migration of CD8+ T cells from the periphery into the uterus takes place more abundantly within the decidua than in the myometrium, indicating that the vessels are indeed in close proximity to extravillous trophoblast cells **(Figure 26A).**

To understand possible lymphatic trafficking of lymphocytes, including CD8+ T cells to and from the uterus, lymphatic vessels were evaluated by Lyve-1 detection. Lymphatic vessels are mainly located in the myometrium of both mesometrial and anti-mesometrial side and seem enriched on GD 14.5 compared to GD 10.5. This goes in line with previously published

observations that although present in the mouse myometrium, lymphatic vessels are absent within the decidua, hindering migration of decidual dendritic cells to uterine draining lymph nodes (Collins et al., 2009). This might suggest a low involvement of secondary lymph nodes in the local response of uterine CD8+ T cells. Collectively, while leucocyte trafficking via blood vessels mainly takes place within the mesometrial decidua and MLAp, the leucocyte lymphatic trafficking into the uterine draining lymph nodes takes place in the myometrium **(Figure 26B).**

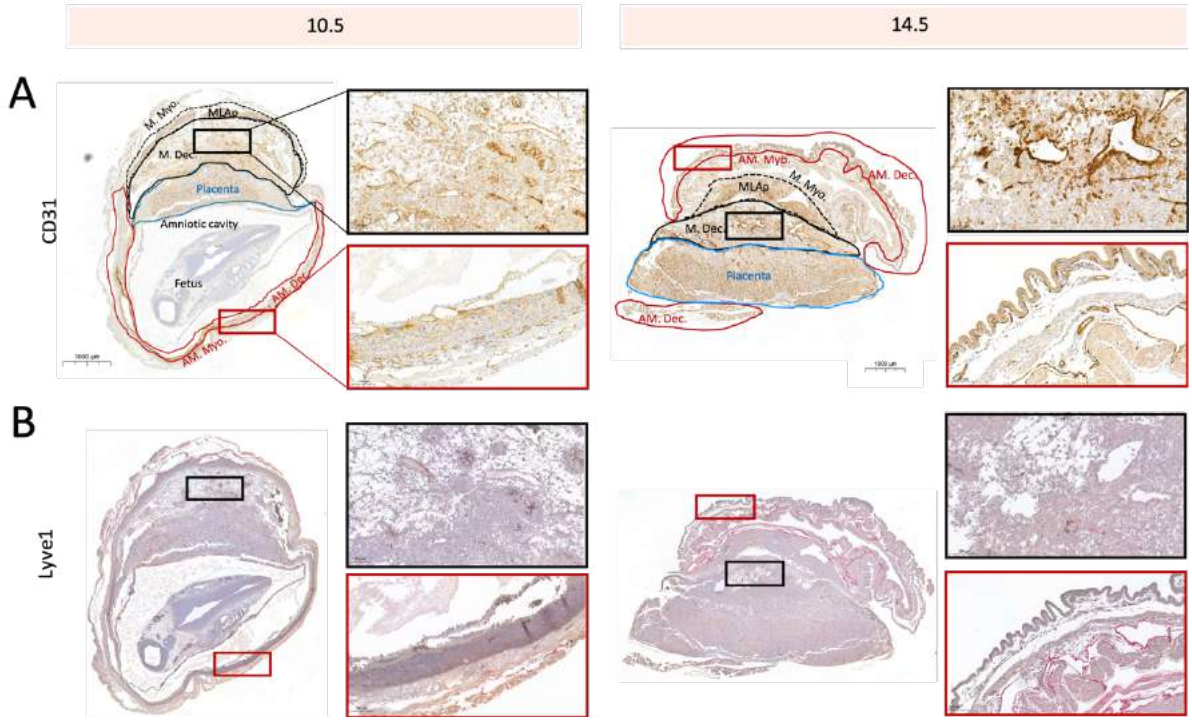

Figure 26. Immunohistochemical analysis of the uterine compartment.
A) *CD31 staining of implantation on GD 10.5 (left) and GD 14.5 (right). Mesometrial decidua (M.dec.; black) and anti-mesometrial decidua (AM. Dec.; dark red) are shown in a higher magnification. The fetus has been removed from the implantation on GD 14.5. M. Myo: Mesometrial myometrium, MLAp: Mesometril lymphoid aggregate of pregnancy, AM. Myo: Anti-mesometrial myometrium, AM. Dec: Anti-mesometrial decidua.* ***B)*** *Lyve-1 staining of the same implantations as shown in A.*

4.6.2 Comparison of CD8+ T cells in uterine compartments

Although total counts of leucocytes, T cells and CD8+ T cells were found in good numbers in the anti-mesometrial uterus, they remained higher in the mesometrial uterus. However, the ratio of CD8+ T cells in the mesometrial versus anti-mesometrial was higher than for leucocytes and T cells **(Figure 27A)**. The ratio of CD8+ T cell subsets within the anti-mesometrial uterus were next compared to their ratio in mesometrial uterus, to determine if the observed dynamics were compartment specific **(Figure 27B-D)**. Indeed, the observation of increased levels of naive cells

on GD 14.5 was not seen in anti-mesometrial uterus. This could be explained by higher area of vascularization within the mesometrial uterus, allowing for greater non-selective leakage within the tissue. Similarly, the increase of early activated and stem cell memory cells in mesometrial uterus on GD 14.5 was also not seen in anti-mesometrial uterus likely for same reasons as for naive cells, and higher levels of fetal antigens on the mesometrial side likely results in higher activation.

Central memory and central memory-like cells were not significantly different between mesometrial and anti-mesometrial uterus although central memory cells seem lower in the latter on GD 14.5, possibly due less migration of those cells to regressing decidua on the anti-mesometrial side. In contrast, early effector cell ratio was higher in mesometrial uterus. One possible explanation could be that activated CD8+ T cells are differentiating towards memory populations on the anti-mesometrial side, supported by seemingly higher ratio of memory precursor effector cells, effector memory, and tissue resident memory cells. Alternatively, it might be an indirect result of the low ratio of naive and early activated cells. The observed peak of short-lived effector cells on GD 10.5 in mesometrial uterus was not observed in anti-mesometrial uterus, which could be due to the lack of fetal antigens on the anti-mesometrial side and/or to the influx of short-lived effector cells or their precursors, primarily recruited into the mesometrial side. Collectively, naive and effector cells tend to reside in the mesometrial uterus while memory subsets tend to reside to a slightly higher extent in the mesometrial side. Furthermore, CD8+PD1+ cells, particularly CD8+PD1^{hi} T cells were found to be significantly higher in the anti-mesometrial uterus, suggesting enhancement of exhaustion at the anti-mesometrial side. **(Figure 27E)**.

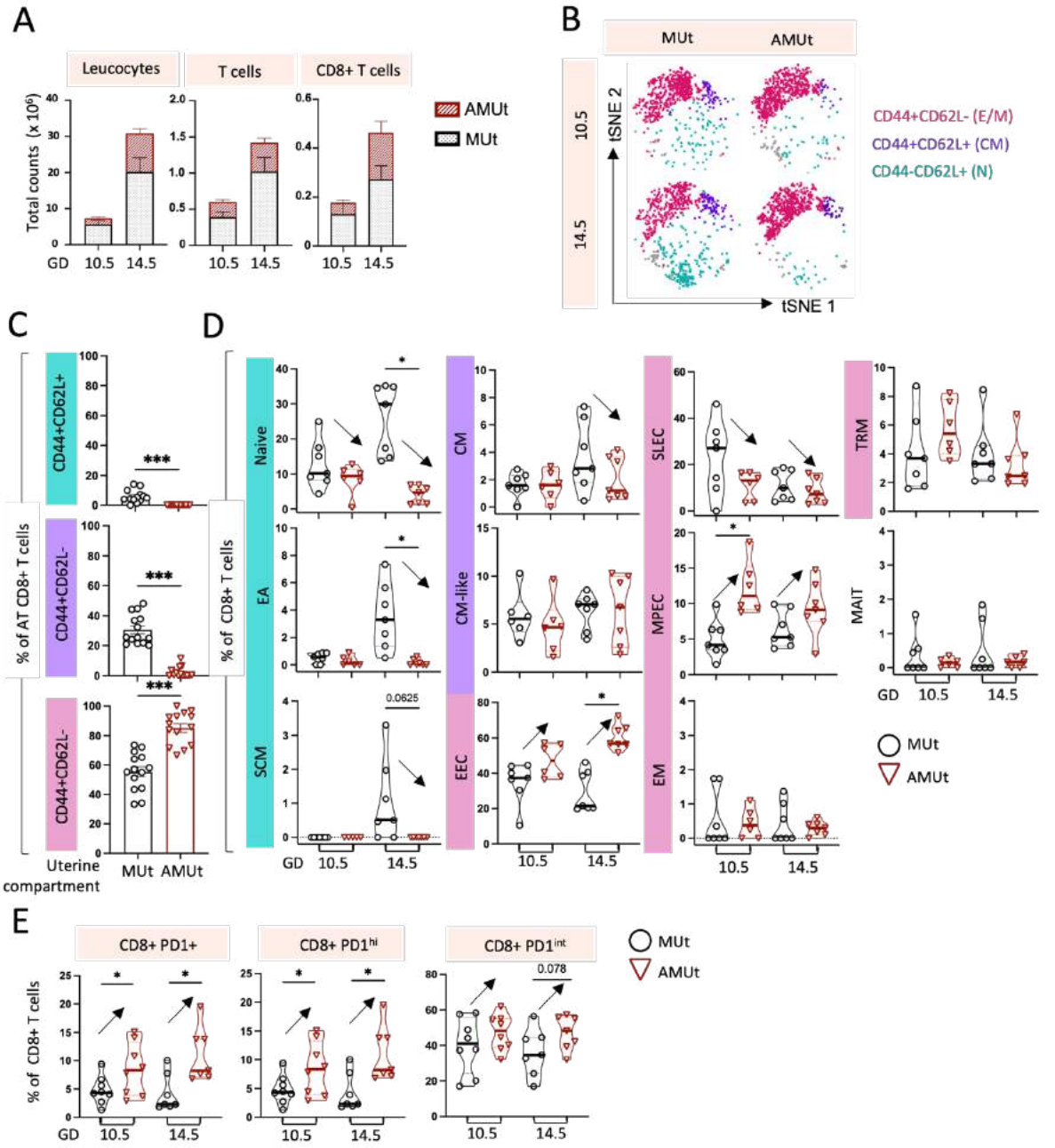

Figure 27. CD8+ T cell subsets in uterine compartments.

A) *Total counts of leucocytes, T cells and CD8+ T cells throughout pregnancy in mesometrial (MUt; black) and anti-mesometrial (AMUt; dark red) uterus in Bl6 females. Y axis represents total cell counts of a given population as x10⁶. X axis indicates gestational day.* ***B)*** *tSNE plots from a concatenated file of CD8+ T cells comparing CD44 and CD62L expression in mesometrial and anti-mesometrial uterus in Bl6 females.* ***C)*** *Frequency of CD44+CD62L- (including effector and memory cells: pink), CD44+CD62L+ (including central memory cells: purple) and CD44-CD62L+ (including naive cells: turquoise) in adoptively transferred (AT) placental specific CD8+ T cells in mesometrial and anti-mesometrial uterus in Rag2γcKO females on GD 12.5-14.5. Y axis represent percentages of AT CD8+ T cells, X axis indicates the uterine compartment.* ***D)*** *Percentages of different CD8+ T cell subpopulations on GD 10.5 and GD 14.5 in mesometrial and anti-mesometrial uterus. Y axis represent percentage of CD8+ T cells. X axis represents gestational day. EA: Early Effectors, SCM: Stem Cell Memory, CM: Central Memory, EEC: Early Effector Cells, SLEC: Short-Lived Effector Cells, MPEC: Memory Precursor Effector Cells, EM: Effector Memory, TRM: Tissue Resident Memory, MAIT:*

Mucosal Associated Invariant T cells. ***E)*** *Percentage of CD8+ T cells expressing PD1 (left), separated into high PD1 expression ($PD1^{hi}$, center) and intermediate PD1 expression ($PD1^{int}$, right). Y axis represents percentage of CD8+ T cells, X axis indicate gestational day. Statistical analyses were performed with a nonparametric paired t test. *p< 0.05;***p< 0.001.*

Next, uterine compartmental differences of frequency and characteristics of CD8+CD122+ T cells were assessed. CD8+CD122+ T cells were also present in the anti-mesometrial uterus, although to a slightly lower extent, compared to the mesometrial uterus **(Figure 28A)**. The frequency of CD8+CD122+ T cells was enriched in both mesometrial and anti-mesometrial uterus compared to other tissues, and as previously shown, remained at a stable percentage in the uterus throughout pregnancy **(Figure 28A)**. Next, the ratio of the two CD8+CD122+ T regulatory subsets were compared in mesometrial and anti-mesometrial uterus **(Figure 28B)**. Although these data are not statistically significant (likely due to low number of mice), it appears that among CD8+CD122+ T cells in the mesometrial uterus, CD122+Ly49+ T regulatory cells increased in mid pregnancy, while CD122+PD1+ T regulatory cells increased in late pregnancy, possibly due to differential role upon differential pregnancy milestones. However, this pattern appears different in the anti-mesometrial side in CD122+Ly49+ T regulatory cells. While CD8+CD122+Ly49+ percentage out of total CD8+CD122+ T cells seem lower in the anti-mesometrial side compared to mesometrial side in mid pregnancy, they catch up in late pregnancy resulting in similar frequency. The ratio of CD8+CD122+ PD1+ cells rose to a similar extent in both uterine compartments, perhaps slightly higher in anti-mesometrial side. Moreover, Ki67 expression in CD8+CD122+ T cells appears higher in the anti-mesometrial side, suggesting higher local proliferation of this subset, possibly due to homeostatic proliferation.

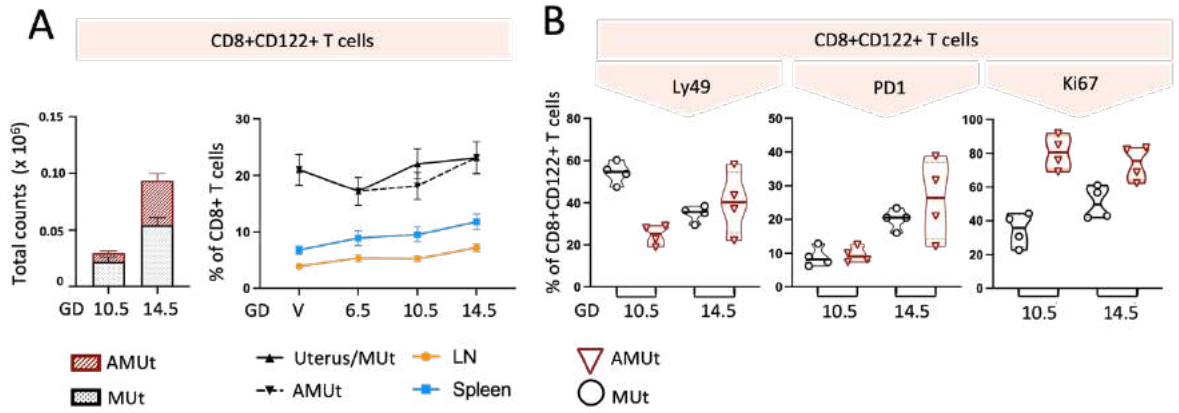

Figure 28. CD8+CD122+ T cells in uterine compartments.
A) *Total counts of CD8+CD122+ T cells in mesometrial and anti-mesometrial uterus (left). Percentage of CD122 expression in CD8+ T cells (right) in mesometrial uterus (black solid line) anti-mesometrial uterus (dotted black), para-aortic lymph node (PALN) (yellow) and spleen (blue).* ***B)*** *Percentages of*

PD1, Ly49 and Ki67 expression in CD8+CD122+ T cells in mesometrial and anti-mesometrial uterus, on GD 10.5 and 14.5, represented as a percentage of CD8+CD122+ T cells. Statistical analysis in B were performed with a nonparametric paired t test.

Furthermore, CD8+ T cells from the adoptive transfer study of placental specific CD8+ T cells were evaluated in the anti-mesometrial side and compared to the mesometrial side, showing comparable counts of total CD8+ T cells in both compartments **(Figure 29A)**. The observation of mesometrial uterine CD8+CD122+Ly49+ regulatory T cells within the group receiving the co-transfer of placental specific CD8+CD122- and CD8+CD122+ T cells was not observed in the anti-mesometrial uterus, while CD8+CD122+PD1+ regulatory T cells were also found in the anti-mesometrial uterus to a similar extent as in the mesometrial uterus **(Figure 29B)**. Moreover, CD49d expression was higher in the mesometrial side, while Ki67 and KLRG1 was lower, confirming higher migration into the mesometrial side, and higher proliferation accompanied with less effector function in the anti-mesometrial side. The frequency of CD122 expression did not differ in anti-mesometrial uterus **(Figure 29C)**.

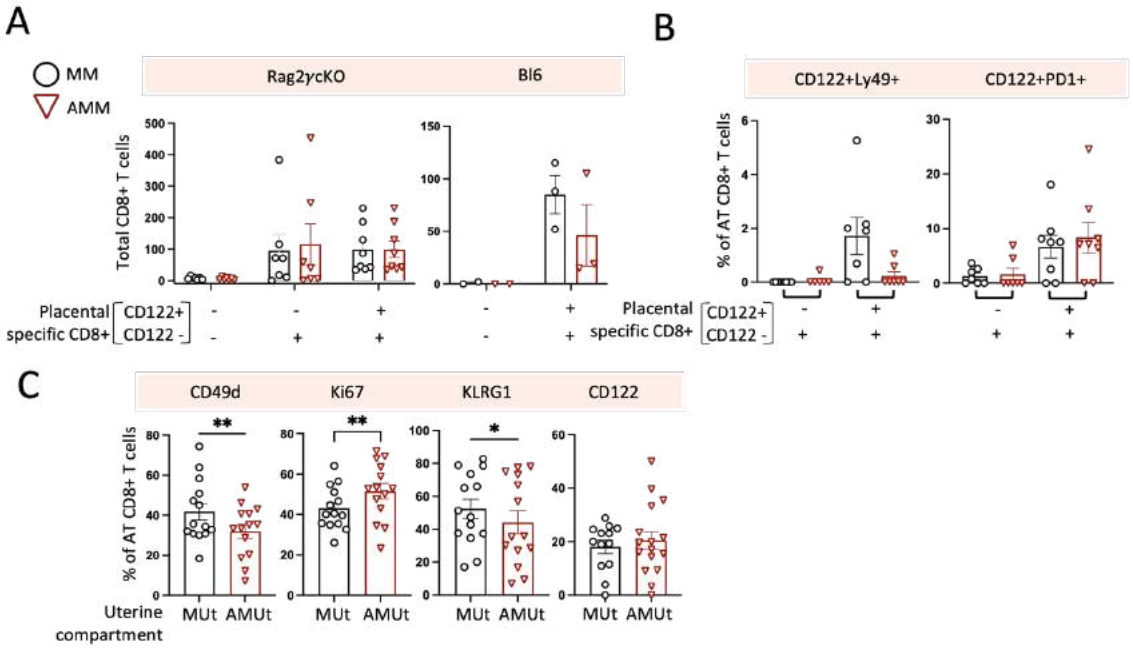

Figure 29. Comparison of adoptively transferred CD8+ T cells in uterine compartments.
A) *Total count of recruited CD8+ T cells in control and placental specific Rag2γcKO (left) and Bl6 (right) females in mesometrial (black) and anti-mesometrial (dark red) uterus.* ***B)*** *Percentages of placental specific CD8+CD122+Ly49+ T cells and CD8+CD122+PD1+ T cells in mesometrial and anti-mesometrial uterus. X axis indicates CD122 expression of donor AT CD8+ T cells, and the uterine compartment.* ***C)*** *Expression of CD49d, Ki67, KLRG1 and CD122 in placental specific CD8+ T cells in mesometrial and anti-mesometrial uterus, Y axis represent percentages of AT CD8+ T cells, X axis indicates the colour coded uterine compartment. Statistical analyses were performed with a nonparametric paired t test. *p< 0.05; **p< 0.01.*

Figure 30 summarizes the main differences detected between the two uterine compartments. Taken together, the mesometrial decidua contained higher blood vessel vascularization and higher migration potential of CD8+ T cells compared to the anti-mesometrial uterus, while proliferation levels were higher on the anti-mesometrial side. Ratios of CD44-CD62L+ subsets (naive, early activated, and stem cell memory), CD44+CD62L+ subsets (central memory, central memory-like) and short-lived effector cells, as well as CD122+Ly49+Tregs (in mid pregnancy) tend to be higher at the mesometrial uterus while other CD44+CD62L- subsets (early effector, tissue resident memory, memory precursor effector and effector memory cells) ratios were enriched at the mesometrial side. Lymphatic vessel trafficking mainly takes place in myometrium in both uterine compartments. Collectively, this indicates that the two uterine compartments are different in terms of CD8+ T cell characteristics and should be taken into consideration when studying uterine CD8+ T cells.

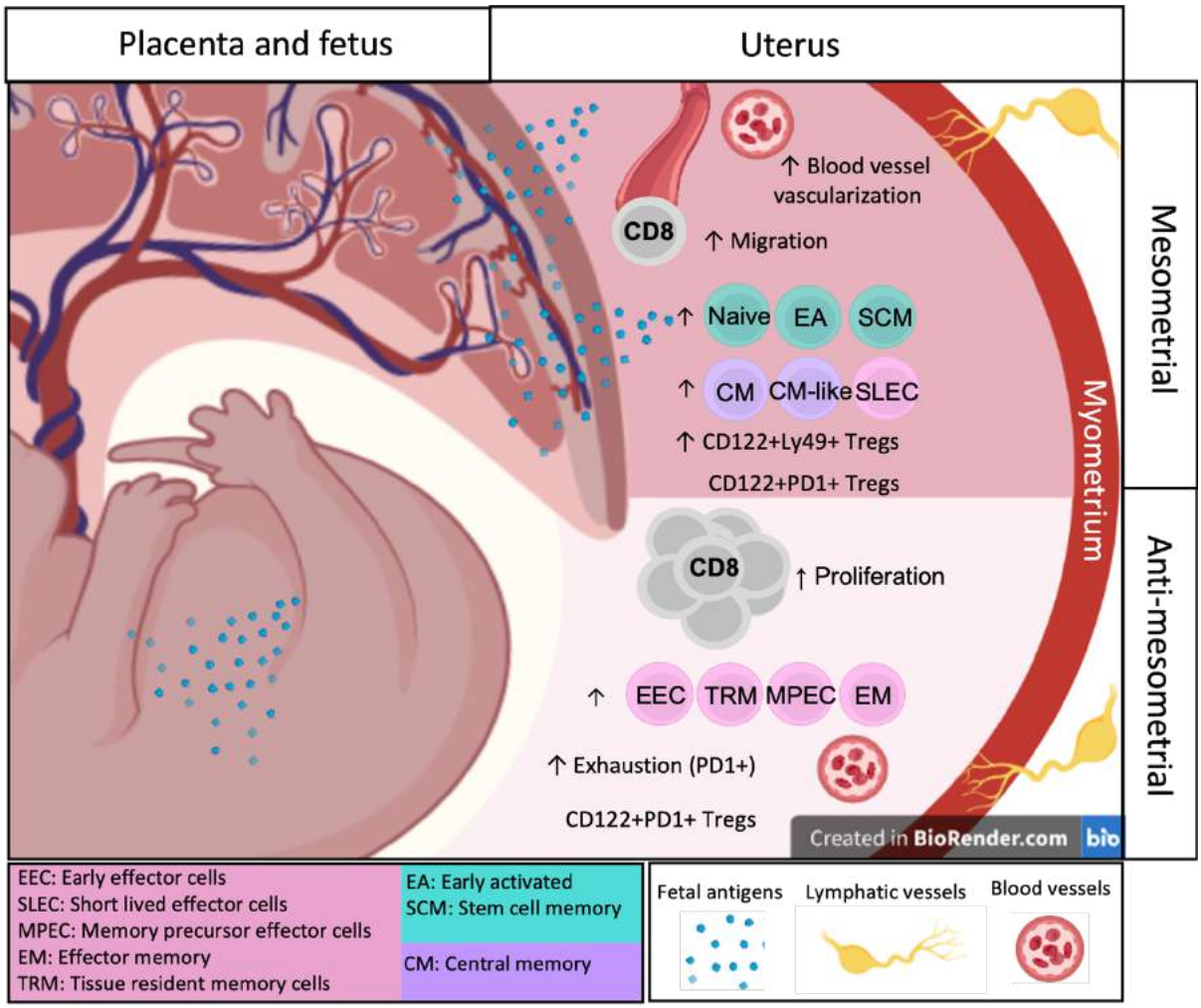

Figure 30. A schematic summary of differences between the uterine compartments.
The mesometrial decidua contains higher blood vessel vascularization and higher migration potential of CD8+ T cells compared to the anti-mesometrial uterus. Ratios of Naive, EA, SCM, CM, CM-like and SLEC, and CD122+Ly49+Tregs tend to be higher at mesometrial uterus while EEC, TRM, MPEC, EM ratios are enriched at the mesometrial side. Although high on both sides, proliferation levels are higher

on the anti-mesometrial side. Lymphatic trafficking mainly takes place in myometrium on both sides. Figure was created with Biorender.

4.7 Characterization and dynamics of CD8+ T cell peripartum.

Clearly, pregnancy poses dynamic changes in CD8+ T cells throughout pregnancy. Post birth, a wound is left at the former implantation site followed by a scar-free regeneration of the endometrial layer, essential for successful subsequent pregnancies. As lymphocytes have been proposed to play a role in the postpartal uterine tissue remodelling, the modulation of CD8+ T cell frequencies and their phenotype in the peripartal period (the period shortly before, during and after birth), was investigated in the uterus as well as in para-aortic lymph nodes. The para-aortic lymph node was chosen as a refence organ due to peak exposure of fetal antigens locally and systemically during birth, an immune response more likely involving secondary lymphoid organs. Here, the selected time points included GD 18.5, for investigation of uterine CD8+ T cells at term pregnancy, postpartal day (PPD) 4, for investigation of uterine CD8+ T cells shortly after birth and PPD 21-30, when we expect tissue regeneration to be completed.

After a massive expansion of uterine leucocytes in pregnancy, the counts of leucocytes gradually decreased after labour, on PPD 4 and 21-30, maintaining however 20x higher cell counts than in uterus from virgin mice. In contrast, T cells continued expanding until PPD 4 and reduced their frequencies on PPD 21-30, particularly in CD8+ T cells **(Figure 31A).** Leucocytes, T cells and CD8+ T cells were found in higher levels in mesometrial uterus compared to the anti-mesometrial uterus **(Figure 31B)**, likely explained by the very regressed anti-mesometrial uterus this late in pregnancy. CD8+CD122+ T cell percentage out of leucocytes increased in para-aortic lymph nodes in term pregnancy suggesting lymphatic draining from the uterus during pregnancy **(Figure 31D)**. Surprisingly, uterine CD8+CD122+ percentages out of leucocytes increasing in the postpartal period, particularly on PPD 4. The fraction of CD8+CD122+ T cells expressing PD1 was however not affected in PPD 4 **(Figure 31E).** A more in-depth flow cytometry analysis identified differentiation trajectories in uterine CD8+ T cells **(Figure 31F)** and CD8+CD122+ T cells **(Figure 31G)** in the postpartum period which consists of reduced frequencies of less differentiated cells, expressing enhanced tissue resident memory cells on PPD 21-30. Central memory-like cells in the uterus peaked on PPD 4, suggesting that these cells, that have downregulated CD127 and likely gained an effector function, may play a role in early tissue homeostasis and the regeneration process, while early effector cells peak on PPD 21-30, suggesting a role in late tissue homeostasis and the

regeneration process. In most cases, the differentiation followed a different dynamic in the para-aortic lymph nodes, further underscoring the importance of the local immune responses in the uterus. **(Figure 31F)**. Furthermore, CD8+ T cell subsets in the two uterine compartments showed similar differences as was observed during pregnancy (Appendix 20).

Among CD8+CD122+ T cells, their phenotype and dynamics mainly differed from total CD8+ T cells in early effector cells, peaking earlier than total CD8+ early effector cells, possibly suggesting an earlier response to the tissue injury at the former implantation site. Also, CD8+CD122+ do not seem to contain phenotype of tissue residency, based on this gating strategy **(Figure 10A)**. Ideally this could be confirmed with the additional detection of CD103. To conclude, the expansion of CD8+ T cells with a regulatory phenotype may facilitate the formation of the vasculature and tissue regeneration, often associated with tolerogenic responses. The postpartal remodelling culminates with the establishment of a prominent antigen experienced tissue resident memory CD8+ T cell subset, suggesting an achievement of a new local immune homeostasis.

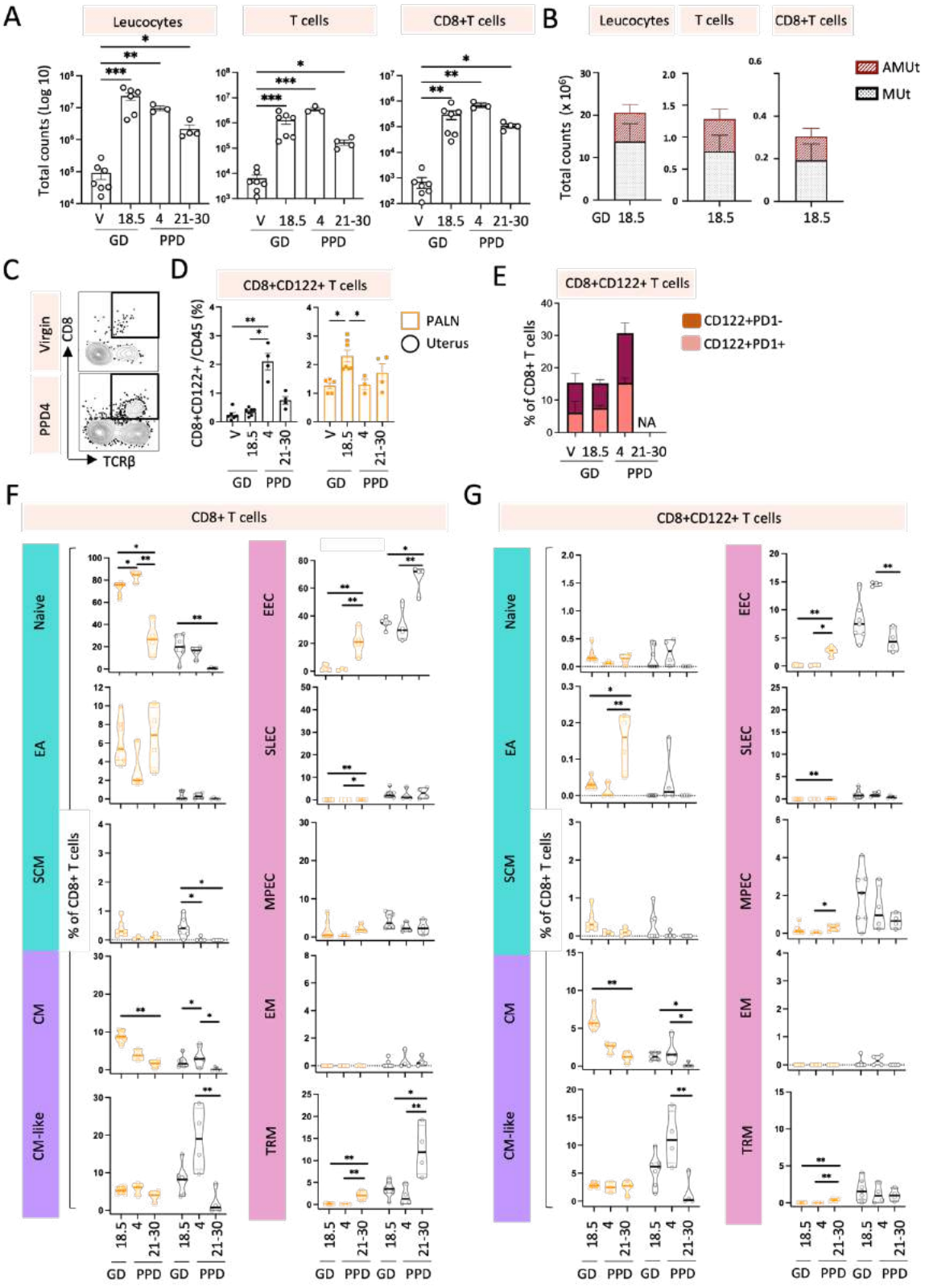

Figure 31. Characterization and dynamics of CD8+ T cells peripartum

A) *Total counts of leucocytes, T cells and CD8+ T cells peripartum, including gestation day (GD) 18.5 and postpartal days (PPD) 4 and 21-30, in addition to virgin (V) controls. Y axis represent the total counts as a* Log_{10} *scale, X axis indicates the time point. B) Total counts of Leucocytes, T cells CD8+ T cells and CD8+CD122+ T cells in mesometrial uterus (MUt; black) and anti-mesometrial uterus (AMUt; dark red) on GD 10.5. Y axis represents total counts x10*^{6}*.* ***C)*** *A contour plot showing CD8+ T*

cell gate in virgin (top) and PPD 4 (bottom) uterus. ***D)*** *Percentage of CD8+CD122+ T cells in leucocytes in uterus (left) and para-aortic lymph node (PALN) (right). Y axis represents percentages of CD45+ cells (extravascular leucocytes) X axis indicates time point.* ***E)*** *PD1 expression in CD8+CD122+ T cells, represented as a percentage of CD8+ T cells.* ***F)*** *Dynamics of different CD8+CD122+ T cell subpopulations peripartum in uterus (black) and PALN (yellow). Y axis represent percentage of CD8+ T cells. X axis represents gestational day. EA: Early Effectors, SCM: Stem Cell Memory, CM: Central Memory, EEC: Early Effector Cells, SLEC: Short-Lived Effector Cells, MPEC: Memory Precursor Effector Cells, EM: Effector Memory, TRM: Tissue Resident Memory, MAIT: Mucosal Associated Invariant T cells.* ***G)*** *Dynamics of populations in CD8+CD122+ T cells peripartum. Y axis represents percentages out of CD8+ T cells, X axis indicates time point. Statistical analyses were performed with non-parametric One-way ANOVA and the p values were corrected for multiple comparison (Kruscal-Wallis test). *p< 0.05; **p< 0.01; ***p< 0.001.*

5 Discussion

5.1 Research problem

The presence of the commonly known cytotoxic CD8+ T cells at the feto-maternal interface, in healthy pregnancies, without posing harm to the fetus, is an intriguing phenomenon. This can partly be explained by the fact that not all CD8+ T cells are cytotoxic. Indeed, emerging evidence pinpoint additional functions of CD8+ T cells besides their killing mechanism against foreign objects, such as pathogens and tumour cells. Such alternative function involves not only altered or reduced effector functions upon sustained chronic stimulation in chronic infections, but also certain microenvironments can modulate CD8+ T cell responses, as observed in the tumour environment. Uterine CD8+ T cells with a regulatory function, particularly in mice, are disappointingly understudied. One of the main challenges of studying CD8+ regulatory T cells in any context, is that there is no consensus within the scientific community about which markers to use for their identification. Therefore, we aimed to understand the phenotype of uterine CD8+ T cells, in terms of not only cell differentiation trajectories, meaning subsets of naive, effector and memory subsets, but also of selected markers typically used to identify CD8+ regulatory T cells. Also, as CD8+ T cells have been reported in high numbers in the uterus we aimed to understand the mechanism behind their existence and potential expansion. Finally, we aimed to investigate whether CD8+ regulatory T cells may have a role in pregnancy.

5.2 Key findings

We investigated the phenotype of uterine CD8+ T cells, with a particular focus on CD8+ regulatory T cells. Our atlas of CD8+ T cell subsets and their dynamics in the uterus and in peripheral organs across mouse pregnancy with flow cytometry, revealed a heterogeneous CD8+ T cell subsets within the uterus, surprisingly mainly consisting of effector and memory subsets which was not reflected in the peripheral organs. Among them, CD122 expression within CD8+ T cells was enriched in uterus, compared to the other investigated organs. The phenotype was confirmed, and the knowledge further deepened with single-cell RNA sequencing of uterine and blood CD8+ T cells in pregnant mice, revealing two uterine CD8+CD122+ T cell subsets with a reported regulatory phenotype.

We observed a massive expansion in uterine CD8+ T cells during pregnancy. To address the question of how CD8+ T cells expand in pregnancy we took the advantage of the OVA/OT-I

system and observed that adoptively transferred placental specific CD8+ T cells were capable of migrating to, and enduring in the uterus, while CD8+ T cells lacking placental specificity did not. Our data indicate that the previously observed expansion of uterine CD8+ T cells is not only due to migration, but also due to proliferation.

Importantly, the OVA/OT-I experiment shed a light on a role of CD8+CD122+ T cells in pregnancy as adoptively transferred placental specific CD8+CD122- co-transferred with CD8+CD122+ T cells significantly reduced abortion rate compared to adoptive transfer of control or placental specific CD8+CD122- T cells, suggesting a beneficiary role of CD8+CD122+ T cells in pregnancy. The dams that received CD8+CD122+ T cell co-transfer contained higher levels of CD8+CD122+ regulatory T cells in spleen and uterus, particularly expressing Ly49, underlining the importance of CD8+CD122+Ly49+ regulatory T cells in pregnancy. The frequency of CD8+CD122+ T cells remained stable during various conditions suggesting a tight control of this cell subset abundance. Interestingly, CD8+CD122+ T cell frequency in the uterus peaks shortly after birth, suggesting a further role within the uterus beyond pregnancy related events.

5.3 Interpretation

5.3.1 Expansion, migration, and proliferation of CD8+ T cells in pregnancy

How and why CD8+ T cells seed into the uterine tissue in pregnancy was one of our main questions for understanding CD8+ T cells in pregnancy **(Figure 8)**. The unexpected massive expansion of uterine CD8+ T cells underlines the need to investigate how this expansion is mediated and why, as effector CD8+ T cells have been reported to have limited capacity to migrate to the decidua (Nancy et al., 2012). The observed increase in accumulation of naive cells **(Figure 11)** did not express CD49d **(Figure 20F)**, suggesting an alternative mode of entering the uterus than binding to endothelial VCAM-1, possibly via a non-selective recruitment, as at this time point the blood vessels might be more permeable allowing for greater “leakage” into the tissue. The fact that adoptively transferred CD8+ T cells were found within the uterine tissue demonstrates that uterine CD8+ T cells can enter the uterus, further supported by CD49d mediated migration, enabling CD8+ T cell trafficking into the tissue. Nancy et al. (2012) claimed that effector CD8+ T cell access to the decidua is greatly limited due to chemokine gene silencing in decidual stromal cells, with stronger fluorescent signal of CD8+ T cells within the myometrium than in the decidua. However, based on histological staining

presented in this dissertation **(Figure 7C and 26)**, the decidual component of the uterus has much greater volume compared to a very thin myometrial layer, thus, although if it is true that the frequency of myometrial CD8+ T cells per given area is higher than within the decidua, it does not exclude that substantial numbers of CD8+ T cells are found in the decidua due to its much greater volume. Thus, CD8+ T cell trafficking into the decidua may be limited to some extent, but it is certainly not absent. We aspire to visualize the localization of CD8+ T cells in uterine tissues for shedding further light on these speculations. Indeed, Dr. Wenqin Shi, the successor of this project, could recently demonstrate that CD8+ T cells are found in the decidual tissue, not to a lesser extent than found in the myometrial tissue (data not shown, personal communication). The migration and endurance of only placental specific CD8+ T cells was somewhat surprising **(Figure 18)**. We hypothesize that CD8+ T cells lacking placental specificity do not endure in the uterus as they may be patrolling the organism, leaving the uterus upon a non-eventful encounter with the placental cells, while activation of placental specific CD8+ T cells, causes them to stay in the uterus and proliferate. In line with our findings, other studies have demonstrated a recruitment of adoptively transferred OT-I CD8+ T cells into mouse decidua (Moldenhauer et al., 2017), and a selective recruitment of fetal-specific regulatory CD4+ T cells to the human decidua (Tilburgs et al., 2008). We conclude that fetal specific CD8+ T cells are more likely to migrate and endure in the uterus than non-specific CD8+ T cells.

The observed high expression of Ki67 in adoptively transferred CD8+ T cells in the uterus indicates high proliferation of these cells, indeed almost half of uterine CD8+ T cells had proliferated, which was at least twofold higher ratio than found in blood and spleen. The proliferation was however independent of whether the adoptively transferred T cells were CD8+CD122- or CD8+CD122+ T cells, suggesting the CD8+CD122+ T cells were not particularly suppressing CD8+CD122- T cell proliferation. Unfortunately, whether the adoptively transferred CD8+ T cells proliferated within the periphery and subsequently migrated to the uterus, or whether they proliferated within the uterus cannot be concluded with this dataset, however both possibilities are plausible. In line with our findings, a research group demonstrated that human decidual CD8+ T cells strongly proliferate, to a higher extent compared to peripheral blood CD8+ T cells, in response to fetal antigens (Powell et al., 2017). Distinct proliferative triggers and mechanisms have been reported for CD8+ T cells. They include homeostatic proliferation, spontaneous proliferation, and clonal expansion. Homeostatic proliferation is a mechanism of restoring T cell deficiency, independent of cognate

antigen stimulation, although low affinity self-antigens and microbiota derived antigens have been suggested to play a part, where cells can acquire a memory-like phenotype (Kieper et al., 2005; Min, 2018). Spontaneous T cell proliferation can be triggered by a lack of memory T cells and result in an extremely fast and robust proliferation, resulting in phenotypically distinct CD8+ T cell populations. Spontaneous T cell proliferation has been observed in physiological settings (Min et al., 2003). Although both homeostatic and spontaneous proliferation may explain to some extent the expansion of uterine CD8+ T cells within expanding uterus, the observed rise of CD8+ T cells in uterus during pregnancy was not solely due to homeostatic proliferation as the increase of CD8+ T cells reached far beyond the increase of uterine weight **(Figure 8)**. Thus, clonal expansion triggered by cognate antigen and co-stimulation is the most likely proliferation mechanism behind the high accumulation of uterine CD8+ T cells. This is supported by our observation of higher levels of clonally expanded CD8+ T cells in the uterus compared to peripheral blood **(Figure 25)**. As CD8+ T cells are present in a virgin uterus, one may wonder whether the massive expansion of uterine CD8+ T cells is mainly due to local proliferation of already present CD8+ T cells, which could also explain the presence of fewer clones within the uterus compared to blood. However, at this this point we can conclude it is also due to some level of migration of CD8+ T cells from the periphery.

5.3.2 CD8+ T cell phenotype in pregnancy

Another of our main questions regarding CD8+ T cells in pregnancy, was regarding their phenotype in the pregnant uterus and how it differs from other peripheral organs. The presence of CD44+CD62L- (containing effector and memory cells) within the uterus **(Figure 9-10)** was striking, although their presence has been reported in mouse decidua (Li et al., 2018), as well as their human counterparts, detected with the markers CD45RA and CCR7 (Liu et al., 2020; Tilburgs et al., 2010). This indicates an accumulation of antigen experienced cells within the uterine tissue as circulating CD8+ T cells within the uterus were excluded from the analysis. Another possibility for the observed CD8+ T cell dynamics in pregnancy, aside from being induced by fetal antigens, are modulation of CD8+ T cells by pregnancy hormones. We observed that short-lived effectors peaked on GD 10.5, reaching surprisingly high frequencies (approximately 25%), which might be due to an immune response upon establishment of the placenta. On one hand, although falling into the gate of short-lived effector cells, we cannot ensure that their function is typical of cytotoxic cells as the functional phenotype was not investigated in this subset on GD 10.5. On the other hand, if they are truly cytotoxic, perhaps they play an important inflammatory role in pregnancy, as it is well established that

inflammation is a critical part of achieving successful pregnancy milestones, such as implantation (Griffith et al., 2017). The high frequency of memory cells, particularly effector memory and tissue resident memory cells in a virgin uterus in a laboratory mouse (housed in conditions of high hygiene) was surprising. Possibly, these memory cells were induced locally upon fertilization, due to exposure to seminal fluid which contains paternal antigens. Also, they may have been recruited from the periphery following exposure to seminal fluid as observed in human cervix following coitus (Sharkey et al., 2012). Typically, the formation of memory cells following viral infection, takes place approximately 30 days post infection (Kaech & Cui, 2012), thus it would be farfetched to speculate whether they could have been generated in 10 days via similar means, including contraction period following a memory generation period. Of note, as differentiation of memory cells is a more complex phenomenon than following the "simple" circular model, a direct differentiation into memory cells following antigen exposure, should not be ruled out as a possibility. Theoretically, they could also simply be specific for non-pregnancy related antigens, temporarily scanning the uterine tissue for their respective match. Information about the possibility of decidual CD8+ T having an exhausted state in mice are scarce, however, expression of the inhibitory receptors PD1, Tim3 and CTLA4, often associated with exhaustion, in mouse decidual CD8+ T cells has been reported, where particularly their co-expression (of PD1 with either Tim3 or CTLA4) was associated with pregnancy success (Wang et al., 2019; Wang et al., 2015), harmonizing with our findings of enhanced exhausted state in the uterus compared to blood, and a possible induction of local exhaustion during mouse pregnancy **(Figure 13)**.

The observed findings of the differences in the tissue, CD8+ T cell phenotype, migration and proliferation pattern between the mesometrial and anti-mesometrial side underscores the merit in investigating both sides separately. For instance, based on this information we opted for performing the single-cell RNA sequencing on the mesometrial side of the uterus as our priority was to investigate the functional phenotype of uterine CD8+ T cells in closer proximity to the placenta and therefore fetal antigens, more likely capturing the snapshot of uterine CD8+ T cell effector and regulatory subsets.

Research on decidual CD8+ T cell phenotype, in terms of both differentiation trajectories and exhaustion state, in human pregnancy is much more extensive than for mice. Data on dynamics of CD8+ T cell phenotype in PBMC's across the first, second and third trimesters of human pregnancy within the same individuals, has however to our not knowledge not been published.

Our observation of the composition of PBMC's in first trimester pregnancy is comparable to reported findings (Liu et al., 2020), with majority of CD8+ T cells containing a naive phenotype (~50-60%), followed by effector cells (~20-30%). However, the observed frequency of central memory cells presented in this dissertation was lower compared to published findings, likely due to different selection of markers and gating strategy. Although our main observations of increasing peripheral naive CD8+ T cells and decreased effectors during pregnancy provides some insights, performing such a temporal phenotyping of decidual CD8+ T cells, including matched non-pregnant controls is enticing.

Comparing findings of CD8+ T cell subsets in mice to subsets observed in humans can be challenging, one reason being that different markers are used due to species specific cell biological differences. As access to human uterine/decidual samples can be troublesome, one would hope that studying human PBMC's from pregnant women, a much easier material to access, would give some information about pregnancy related immune responses. However, based on the observed differences of PD1 expression and dynamics in blood and uterus in mice, it might be challenging to use human PBMC data to accurately predict the functional state of CD8+ T cells within human uterus, therefore, uterine biopsy would be optimal for fully determining the tissue specific CD8+ T cell phenotype. The same can be said for an attempt to predict uterine CD8+ T cell subset composition based on information in blood. However, some information from CD8+ T cells in PBMC's might be useful for extrapolating the information to the uterus, such as considering the expression of adhesion molecules which can give information about their potential trafficking patterns. Likewise, pregnancy hormones increase not only in uterus, but also in peripheral blood and could therefore to some extent affect peripheral CD8+ T cells differentiation and function, which might be reflected in the uterus.

5.3.3 Origin of CD8+CD122+ T cells

CD8+CD122+ T cells have been hypothesised to originate from thymic emigrates in young individuals (Li et al., 2014) and have been shown to increase again with age (Messaoudi et al., 2006). This harmonizes with our data in peripheral blood **(Figure 4)**, our data also suggests a post-thymic generation. Furthermore, CD8+CD122+ T cells have been reported to be clonally expanded cells (Okuno et al., 2013), further suggesting a peripheral generation, and generation by proliferation, rather than upregulation of CD122. Our data indicate that CD8+CD122+ T cells do proliferate **(Figure 23),** (Appendix 10 and 12), but also that CD8+CD122- T cells readily upregulate CD122 **(Figure 19)** but whether these cells gain the regulatory function

reported for CD8+CD122+T cells cannot be concluded at this point, although our data suggest that may not be the case **(Figure 21),** (Appendix 12).

One might think that the strikingly high percentage we observed of CD122 in blood and spleen in the OVA/OT-I experiment **(Figure 19)**, might be at least partly due to the fact that pregnant Rag2γcKO females lack lymphocytes, allowing for homeostatic proliferation and enhanced activation in an "empty" mouse. However, the frequency of CD122 expression in adoptively transferred CD8+ T cells found in blood and spleen in physiological Bl6 mice, which contain endogenous CD8+ T cells, were also high, indeed higher than observed in their endogenous CD8+ T cells, arguing against the CD122 upregulation being solely due to the Rag2γcKO phenotype. The reason for such an upregulation of CD122 in the periphery is up for discussion.

As CD122 is a rather general marker, not specific for CD8+ regulatory T cells only, as further inhibitory molecules and a specific functional phenotype is more likely the determining factor for the regulatory function, this raises the question of what role the CD122 molecule may have for CD8+ regulatory T cell. The CD122 receptor may play a role in extended survival of these cells. Another plausible explanation could be that high expression of CD122 captures circulating IL-2 upon activated immune response, resulting in a less harmful response of stimulated CD8+CD122+ T cells, rather than of CD8+CD122- conventional cells, thus CD122 acting as a "sponge", depriving other cells of the IL-2 ligand as has been reported as one mechanism of CD4+ regulatory T cells (Chinen et al., 2016; Pandiyan et al., 2007). Notably, the CD122 receptor is emerging as an important receptor for various uterine lymphocytes during pregnancy. In addition to the unique uterine CD8+CD122+ T cell population identified in the current dissertation, CD122+ macrophages were recently identified as an enriched population in the pregnant uterus of mice and humans, responsive to IL-15 signals (Gordon et al., 2020). Indeed, homeostasis of IL-15 is important for pregnancy as its disruptions can lead to poor pregnancy outcomes, which may be due to subsequent faulty immune responses of uterine leucocytes, including CD8+CD122+ T cells, as CD8+Ly49+ regulatory T cells have been reported to depend on IL-15 for the suppressive function (Kim et al., 2011).

Although CD8+CD122+ T cells massively expand in the pregnant uterus, their frequency out of CD8+ T cells remain stable, or approximately 20% **(Figure 15C-D)**. Throughout this dissertation, this frequency appears consistent between experimental conditions, adoptive transfer of CD8+CD122- and CD8+CD122+ T cells, and even when they lack the

glucocorticoid receptor, which affected CD122 frequencies in peripheral organs. This suggests that the uterine CD8+CD122+ T cell compartment is tightly controlled reaching an optimal percentage and homeostasis. It is tempting to speculate whether this particular percentage of these potential regulatory CD8+CD22+ T cells is optimal for mediating their function but need to be balanced with other CD8+ T cell subsets to reach fetal tolerance, without immunopathology and immunocompromises.

5.3.4 Functional phenotype of CD8+CD122+ T cells in pregnancy

An important aspect of addressing the CD8+ T cell phenotype, was to unveil whether CD8+ T cells with a regulatory potential are found within the pregnant uterus. We used the cutting-edge method of single-cell RNA sequencing for an in-depth investigation of uterine CD8+CD122+ T cells with a regulatory phenotype in pregnancy. Here, we had the means to compare the functional phenotype of CD8+CD122+ T cells to CD8+CD122- T cells, and additionally to compare CD8+CD122+PD1+ T cells to CD8+CD122+Ly49+ T cells. Supporting our hypothesis, we observed that these subsets do not overlap as they both exist in the pregnant uterus, where they contain distinct gene signatures.

CD8+CD122+PD1+ T cells are mainly CD44+CD62L- (containing effector and memory cells), express relatively higher levels of inhibitory receptors, such as *CTLA4, Lag3 and Tigit,* and other exhaustion related markers *(Tox, Bst2, Hmgb2, Tuba1b),* yet express activation and further effector molecules (*Batf, Gata3, Tbx2*, *Maf, Irf4* and *Eomes)* including those related to cytotoxicity *(Gzmb, Gzmk, Nkg7, Lamp-2).* Also, this subset has the highest average gene expression of *Lgal1* and *Lgal3*, strongly suggesting these cells are similar to the CD122+PD1+ T regulatory cells found to be expanded in cancers with immunosuppressive and pro-angiogenic function (Cagnoni et al., 2021). Indeed, emerging evidence indicate that galectins, including Galectin 1 (Gal-1) and Galectin 3 (Gal-3), coded by *Lgal1* and *Lgal3* genes, respectively, specifically bind to carbohydrate ligands which regulate immune cell adaptation to pregnancy and angiogenesis (Menkhorst et al., 2021). Gal-1 possesses broad anti-inflammatory properties which targets various immune cell subsets, resulting in immunomodulation favouring pregnancy success (Blois et al., 2007; Menkhorst et al., 2021). Uterine immune cells can express Gal-1, including NK cells which are proposed to induce apoptosis of Th1/Th17 cells (Kopcow et al., 2008), and CD8+ T cells, of which Gal-1 has been identified within their cytotoxic granules. Gal-3 can interact with various of ligands for specific modulation of cell functions important in pregnancy including immune function and

angiogenesis (Menkhorst et al., 2021). For instance, by inhibiting NK cells, promoting tolerogenic dendritic cells and by interfering with co-inhibitory signalling (Kouo et al., 2015; Suzuki et al., 2012; Tsuboi et al., 2011; Volarevic et al., 2019). The importance of Gal-1 and Gal-3 for pregnancy success is further supported by their deficiency resulting in various pregnancy complications associated with impaired immune tolerance and improper vascularization and placentation (Hirashima et al., 2018; Jeschke et al., 2007). When considering the highest expressed genes in the CD122+PD1+ subset (Appendix 17), genes associated with interferon signalling (*Ifi2712a, Zbp1, Isg20, Isg15*), genes often expressed in CD8+ T cells in tumours, (*Sh2d2a, Crip1, Ccl4, Ccl5*), or associated with exhaustion (*Bst2, Hmgb2, Tuba1b*), were upregulated. *IL-10* gene expression was barely detected in this data set, possibly due to technical rather than biological reasons. It cannot be excluded that these cells secrete IL-10 in pregnancy as they do in cancers, however the elevated expression of *Aw112010*, which appeared in the top expressed genes in the CD122+PD1+ subset, is known to suppress IL-10 (Yang et al., 2020) which might contribute to the low IL-10 detection. The expression pattern of the uterine CD8+CD122+PD1+ T cells match to a great extent the previously published findings of these subsets with a regulatory potential in contexts such as in tumours, suggesting a CD8+ T cell subset modulated in an immune privileged site. Also, the CD122+PD1+ CD8+ T cell subset may possess a role in pregnancy beyond immune tolerance, such as in angiogenesis and supporting proper placentation. This is in line with the observed elevated interferon signalling, in particular an enrichment of *IFNg* gene expression (IFNy), which is a known critical mechanism of uterine NK cells to promote angiogenesis and placental vascular remodelling (Murphy et al., 2009; Sojka et al., 2019). Furthermore, the CD122+PD1+ subset showed relatively higher gene expression of the *Hmox1 gene*, involved in regulation of placental vasculature development in mice (Zhao et al., 2011). CD122+PD1+ T cells contained also the relatively highest expression of *Klrc1* (NKG2A), an inhibitory receptor present on NK and on activated CD8+ T cells, which defines Ly49/KIR educated uterine NK cells. Tumour infiltrating NKG2A+CD8+ T cells in humans have signature of tissue residency and exhaustion (Chen et al., 2020) while in mice, NKG2A inhibitory receptor was shown to optimize the CD8+ T cell response during viral infection (Rapaport et al., 2015). NKG2A recognise HLA-E expressed by extravillous trophoblast cells in humans, however evidence suggest that the murine ortholog Qa-1 is not expressed by mouse extravillous trophoblast, therefore mouse uterine CD8+NKG2A+ T cells, are unlikely modulated by extravillous trophoblast cells (Madeja et al., 2011). Whether NKG2A expression in mouse uterine CD8+ T cells has alternative implications for immune tolerance in pregnancy is up for discussion.

Likewise, expression pattern of the uterine CD8+CD122+Ly49+ T cells highly resemble the previously published findings of this subset containing important regulatory function. This may be mediated particularly via cytotoxicity, as based on relatively high expression of genes coding for the cytotoxicity markers Granzyme B, Perforin 1 and CD107a. This subset likewise contained higher levels of Granzymes c, d, e, f, g and m, thus it is important to note that although granzymes are generally known as being cytotoxic, cytotoxicity is not the main role of all of them. For instance, extracellular granzymes are involved in remodelling of the extracellular matrix, wound healing and amplifying inflammatory and cytokine response, suggesting a potential alternative role for uterine remodelling in pregnancy (de Jong et al., 2021; Wensink et al., 2015). CD8+CD122+Ly49+ T cells are mainly CD44+CD62L+ (containing central memory cells). This subset does not express markers associated with exhaustion, rather they express other molecules associated to immune suppression (*Cd160, Ptpn6, Ms4a4c, Ikzf2, Itma2, Pglyrp1, Havcr2, Bmp7,*) as well as for effector function (*Nfkb1/Nfkb2, Irf8, Ifng*) and NK markers (*Klrb1c, Klrc2, Klrd1*). Likewise, their overall cytokine and chemokine profile differs from the profile of CD8+CD122+PD1+ T cells. Moreover, the enriched gene expression of the estrogen receptor alpha (*Esr1*) and genes involved in the NFκβ pathway (*Nfkb1, Nfkb2*), susceptible to be regulated by estrogens suggests a pregnancy related modulation of CD122+Ly49+ T cells. Estrogen receptor has been shown to be able to enhance and dampen immune signalling in innate immune cells and has been implied in regulating T cell immunity with increased TNFα and IFNγ production by virus specific CD8+ T cells in the lungs (Kovats, 2015; Robinson et al., 2014). Moreover, the elevated gene expression of the chemokine ligand *Xxl1*, which is secreted by NK and antigen-specific CD8+ T cells, binds to XCR1 expressed by conventional dendritic cells, facilitating cross-presentation of antigens (Dorner et al., 2009; Lei & Takahama, 2012). However, gene expression of *Irf5* in CD122+Ly49+ subset might impair dendritic cell function, as seen in leishmania infection (Hammami et al., 2015). The regulatory mechanism of CD8+CD122+Ly49+ T cells has been reported to be mediated via cytotoxicity, by suppressing antigen specific CD4+ T cells in the context of autoimmune diseases, particularly of Qa-1 (HLA-E in humans) restricted CD4+ T cells (Li et al., 2022; Saligrama et al., 2019). Whether this mechanism can be extrapolated to uterine CD8+CD122+Ly49 regulatory T cells, is an intriguing theory. As mouse extravillous trophoblast cells do not express Qa-1 and the human trophoblast cell type, syncitiotrophoblast cells, which is in direct contact with maternal blood, do not express any HLA, and none of the trophoblast cell types express HLA class II, direct recognition of trophoblast cells by CD4+ T cells cannot occur,

however an indirect recognition may take place as uterine APC's might take up paternal H2-K (HLA-C in humans) and initiate a CD4+ T cell response resulting in placental specific CD4+ T cell migration to the pregnant uterus (Moffett & Shreeve, 2022). Although placental specific CD4+ regulatory T cells have been reported to be selectively recruited in the uterus (Tilburgs et al., 2008), placental specific T_H1 CD4+ T cells, which are a considerable threat to pregnancy success, may also similarly migrate to the pregnant uterus, explaining a demand for local uterine CD8+CD122+Ly49+ regulatory T cell response.

5.3.5 Effect of CD8+CD122+ T cells in pregnancy

One of our main questions was to know whether CD8+CD122+ T cells may have a regulatory role in pregnancy, which would positively impact pregnancy outcome. A previous publication first demonstrated that CD8+CD122+ T cells had beneficiary effects on pregnancy by promoting fetal growth and placental development (Solano et al., 2015). Thus, we evaluated the pregnancy outcome by looking at the abortion ratio in the adoptive transfer experiment. The important observation of adoptively transferred placental specific CD8+CD122- co-transferred with CD8+CD122+ T cells significantly reduced abortion rate compared to adoptive transfer of control or placental specific CD8+CD122- T cells **(Figure 21A)**, underlines a beneficiary effect of CD8+CD122+ T cells in pregnancy. The mechanism underlying such an effect is not clear. We observed a basal level of abortion rate at ~10%, which is to be expected in a healthy mouse, due to spontaneous resorption, likely due to genetic defects (Flores et al., 2014; Gu et al., 2021; Yakut et al., 2015) rather than immunological attacks. As abortion rate was only slightly elevated following adoptive transfer of CD8+CD122- T cells, although not significantly, the abortion rate in general does not seem to be greatly influenced by adoptive transfer of CD8+CD122- cells (control or placental specific). Then how come co-transferring CD8+CD122+ T cells reduced the abortion rate? Based on our observations, it does not appear the mechanism involves keeping CD8+CD122- T cells under control for immune tolerance. Instead, possibly they mediate their effect by influencing the pre-existing environment, such as interacting with other immune cells. It is also tempting to speculate whether CD8+CD122+ T cells influence the uterine endometrium in a way further allowing implanted embryos, that might be less competent (for instance, containing genetic defects), that otherwise might be resorbed, to survive. Although, depending on the extent of the genetic defect, they may not be carried to term and may result in miscarriage later in pregnancy. This theory is supported by research demonstrating that recurrent implantation failure can be due to low uterine receptivity, where a genetically competent embryo cannot implant, while genetically defected embryos can

implant in women with high endometrial receptivity (Lessey & Young, 2019; Stevens Brentjens et al., 2022).

When the phenotype of originally adoptively transferred CD8+CD122+ T cells was compared to the one of originally adoptively transferred CD8+CD122- T cells that had upregulated CD122 expression by tissue collection day, it became evident that only the originally adoptively transferred CD8+CD122+ T cells expressed Ly49 but not the newly upregulated CD8+CD122+ T cells (Appendix 12). Possibly, the observed improved pregnancy outcome is due to the CD8+CD122+Ly49+ T cells. Possibly these cells have contained greater distinctive phenotype, perhaps with distinct origin where an upregulation of CD122 is not sufficient for, and not an indicator of formation of CD8+CD122+Ly49+ regulatory T cell subset. Another explanation could be that the immediate presence of CD122 and Ly49 is critical to prevent fetal loss and the upregulation of CD122 and Ly49 receptors on adoptively transferred CD122- cells was not quick enough for a CD8+CD122+ T cell mediated prevention of fetal loss.

5.3.6 CD8+ and CD8+CD122+ T cells peripartum

To our knowledge, there is no data on the role of uterine CD8+ T cells postpartum. Thus, we aimed to gain insights into whether the observed abundance of CD8+ T cells and CD8+ T cell dynamics end with pregnancy. We hypothesize that the expansion and changes in the CD8+ T cell compartment may prepare the uterine tissue for post-partum related processes. As observed in macrophages and CD4+ regulatory T cells, lymphocytes are known to play a role in tissue regeneration after organ injury (D'Alessio et al., 2019; Li, Tan, et al., 2018; Wynn & Vannella, 2016), which might be mediated by the uterine CD8+CD122+ T cells. In fact, their frequency remain high in the uterus after birth, picking in numbers shortly thereafter. Thus, it is important to note that uterine CD8+ T cells may have additional implications beyond supporting fetal tolerance and placental development during pregnancy, as they may be setting up for the subsequent regeneration process.

5.4 Limitations of the study

The main limitation of the study is that our main findings are based on mouse models. Mouse models can provide insights into the immune cell function in human pregnancies to a certain extent, but the demonstrated mechanisms must be investigated and confirmed in human pregnancies, notably because the placental specificity created here is certainly artificial and gains much more complexity in human pregnancy.

Also, adoptively transferring uterine cells from pregnant OT-I donor females instead from virgin females would have been ideal, to maximize the number of the unique uterine CD8+ T cell within the pooled donor cells, for maximizing an effect of the adoptively transferred CD8+CD122+ T cells on pregnancy outcome. However, this was not feasible due to complicated synchronization of pregnancies of OT-I females and Rag2γcKO along with other experimental aspects of this complicated experiment.

Furthermore, the differences observed on mRNA and protein levels in the single-cell RNA sequencing experiment complicated the analysis and interpretation of the data. Ideally, this could be improved by increasing the sequencing depth, particularly of the CITE-sequencing antibodies to increase the number of cells positive for the surface level CITE-sequencing barcodes.

5.5 Implementation and future research

The findings represented in this dissertation expands the knowledge of CD8+ T cells in pregnancy. To further expand the knowledge gained with this dissertation, several angles of this project can be further investigated. An obvious important aim is to further analyse the data from the single-cell RNA sequencing experiment, in terms of identifying the CD8+ T cell differentiation trajectories in greater depth in uterus and blood, and to compare those with published subpopulations from single-cell RNA sequencing in other tissues and contexts. It is also intriguing to continue with an in-depth analysis from the TCR sequencing, to reveal the phenotype of the expanded clones in the uterus. These two analyses are currently ongoing by the NGS Core facility “Omics” at the RCI, Regensburg. Also, it is enticing to visualise CD8+ T cells, preferably in transgenic mice with endogenously fluorescently labelled CD8+ T cells, utilizing the tissue clearing method (Kagami et al., 2017; Tian et al., 2021), which allows a three-dimensional visualisation of CD8+ T cells, along with additional fluorescence staining of vessels and other markers in a transparent tissue. Additional investigations of interactions with other leucocytes and stromal cells would be helpful in determining whether such interactions are one mechanism of the CD8+CD122+ T cells in pregnancy, both by visually investigating co-localisation of these cells, and ligand-receptor binding, as well as by setting up co-cultures to investigate immune responses. As the experiments conducted for this dissertation focused more on immunological aspects of CD8+ T cells in pregnancy, further investigating the role of CD8+CD122+ T cell on vascularisation is another angle to cover, which is one of the goals for

the successor of this project. Creating a transgenic mouse model in which CD8+ T cells lack CD122 is desirable but was not feasible for this dissertation due to extensive resources and work of creating such a mouse model, which to our knowledge is currently not available. Finally, investigating CD8+ regulatory T cells in human decidua is a crucial next step for this project. Here, pinpointing the CD8+ regulatory T cell phenotype would be the first step, where CD8+KIR+ T cells is a promising candidate, and should be investigated in the uterus in healthy and pathological pregnancies. Once uterine CD8+ T cells, in particular CD8+ regulatory T cell phenotype and function is unveiled in human pregnancies, they might become a novel target for future therapies in pathological pregnancies.

6 Summary

In physiological pregnancies, the semi-allogenic fetus does not induce adverse immune responses by the maternal CD8+ T cells in the pregnant uterus. However, immune responses can be triggered in pregnancy leading to detrimental consequences for fetal growth/survival. Emerging evidence pinpoint CD8+CD122+ T cells with a regulatory function as critical players in immune tolerance in multiple pathological contexts, yet not defined in immune tolerance towards the fetus. However, the phenotypical traits of uterine CD8+ T cells in mouse pregnancy, particularly those with a regulatory potential remain poorly defined. The present dissertation examines i) the in-depth phenotype of effector and memory CD8+ T cell subsets, including CD122+ subsets with regulatory potential across pregnancy, in peripheral organs and in the uterus, ii) the expansion, proliferation and migration pattern of uterine CD8+ T cells and iii) the role of CD8+CD122+ T cells in pregnancy. We used a semi-allogenic mouse model to investigate and characterize CD8+ T cells across pregnancy with flow cytometry. Here, we observed a massive expansion of uterine CD8+ T cells in pregnancy. They contained heterogenous CD8+ T cell subsets, including a unique profile of naive, various effector and memory subsets, of which composition and frequency was not reflected in the peripheral organs. By using the OVA/OT-I system, we adoptively transferred placental specific CD8+ T cells into either immunodeficient Rag2γcKO mice or wildtype C57BL/6 pregnant females and observed that the expansion of uterine CD8+ T cells was both due to proliferation and migration, where placental specificity was crucial for endurance in the uterus. With the use of single-cell RNA sequencing and flow cytometry we could identify two CD8+CD122+ T cell subsets in the uterus with a regulatory phenotype, as reported in the literature. Both subsets, CD8+CD122+Ly49+, and CD8+CD122+PD1+, were enriched in the uterus but their functional phenotype suggests distinct regulatory mechanisms. Importantly, adoptively transferring CD8+CD122- T cells with CD8+CD122+ T cells into pregnant females of the OVA/OT-I mouse model, prevented fetal loss which might be explained by lack of decidual CD122+Ly49+ T cells in the group only receiving CD8+CD122- cells. Collectively, the results suggest that pregnancy induced CD8+T cells immune responses portray a unique local response distinct from systemic processes, where CD8+CD122+ T cells co-expressing molecules associated with immune regulation and suppression, promote a successful pregnancy. This research sets the ground for and expands the knowledge of uterine CD8+ regulatory T cells and their beneficial roles in pregnancy. The findings call for further investigation, especially in human pregnancies

which could give valuable insights into immune mechanisms supporting fetal growth, and potentially providing novel preventive or therapeutic strategies for pregnancy complications.

7 Zusammenfassung

In physiologischen Schwangerschaften löst der semi-allogene Fötus keine immunologische Abstoßungsreaktion über die mütterlichen CD8+ T-Zellen in der Gebärmutter aus. Allerdings können in der Schwangerschaft Immunreaktionen ausgelöst werden, die sich ungünstig auf das Wachstum und Überleben des Fötus auswirken. Neue Erkenntnisse weisen darauf hin, dass CD8+CD122+ T-Zellen eine entscheidende regulatorische Funktion bei der Immuntoleranz in verschiedenen pathologischen Kontexten übernehmen. Bezüglich der Immuntoleranz gegenüber dem Fötus ist die Rolle dieser T-Zellen bisher nicht näher beschrieben. Auch die phänotypischen Merkmale der uterinen CD8+ T-Zellen in schwangeren Mäusen, insbesondere derjenigen mit einem regulatorischen Potenzial, sind unzureichend definiert. Die vorliegende Dissertation untersucht i) den detaillierten Phänotyp von Effektor- und Gedächtnis-CD8+ T-Zelluntergruppen, einschließlich CD122+ Untergruppen mit regulatorischem Potenzial während der Schwangerschaft, in peripheren Organen und im Uterus, ii) das Expansions-, Proliferations- und Migrationsverhalten von uterinen CD8+ T-Zellen und iii) die Rolle von CD8+CD122+ T-Zellen in der Schwangerschaft. Wir haben ein semi-allogenes Mausmodell verwendet, um CD8+ T-Zellen während der Schwangerschaft mittels Durchflusszytometrie zu untersuchen und zu charakterisieren. Dabei konnten wir eine massive Vermehrung von CD8+ T-Zellen in der Gebärmutter während der Schwangerschaft beobachten. Sie beinhalteten heterogene CD8+ T-Zell-Subpopulationen, darunter ein einzigartiges Profil von naiven T-Zellen sowie verschiedener Effektor- und Gedächtnis-Subpopulationen, deren Zusammensetzung und Häufigkeit sich in den peripheren Organen nicht widerspiegelte. Unter Verwendung des OVA/OT-I-Systems haben wir plazentaspezifische CD8+ T-Zellen sowohl in immundefiziente Rag2γcKO-Mäuse als auch in trächtige C57BL/6-Wildtyp-Mäuse adoptiv transferiert. Hier konnten wir beobachten, dass die Expansion der uterinen CD8+ T-Zellen sowohl auf Proliferation als auch auf Migration zurückzuführen war, wobei die Plazentaspezifität für den Verbleib in der Gebärmutter entscheidend war. Mithilfe von Einzelzell-RNA-Sequenzierung und Durchflusszytometrie konnten wir zwei CD8+CD122+ T-Zell-Untergruppen im Uterus ausmachen, welche eine regulatorische Erscheinungsform aufweisen, wie sie in der Literatur beschrieben wurde. Beide Untergruppen, CD8+CD122+Ly49+ und CD8+CD122+PD1+, waren in der Gebärmutter vermehrt aufzufinden, wobei ihr jeweiliger funktioneller Phänotyp unterschiedliche

Regulationsmechanismen vermuten lässt. Dabei ist wichtig, dass der adoptive Zelltransfer von CD8+CD122- T-Zellen zusammen mit CD8+CD122+ T-Zellen in die trächtigen Weibchen des OVA/OT-I-Mausmodells den Verlust des Fötus verhinderte. Dies könnte durch den Mangel an dezidualen CD122+Ly49+ T-Zellen in der Gruppe, die nur CD8+CD122- Zellen erhielt, erklärt werden. Insgesamt deuten die Ergebnisse darauf hin, dass die schwangerschaftsinduzierten Immunantworten der CD8+ T-Zellen eine einzigartige lokale Reaktion darstellen, die sich von systemischen Prozessen unterscheidet. Eine erfolgreiche Schwangerschaft wird gefördert durch CD8+CD122+ T-Zellen, welche Moleküle co-exprimieren, die mit der Immunregulation und -suppression assoziiert sind. Diese Forschungsarbeit schafft eine Grundlage und Erweiterung des Wissens über uterine CD8+ regulatorische T-Zellen und ihre positive Rolle in der Schwangerschaft. Die Ergebnisse machen weitere Forschung erforderlich, insbesondere in Blick auf menschliche Schwangerschaften. Dies könnte wertvolle Einblicke in diejenigen Mechanismen des Immunsystems geben, die das fetale Wachstum unterstützen, und möglicherweise zu neuen präventiven oder therapeutischen Strategien für Schwangerschaftskomplikationen führen.

8 Abbreviations

AMUt	Anti-mesometrial uterus
APC	Antigen presenting cell
AT	Adoptive Transfer
Bl6	C57BL/6J mouse strain
CD	Cluster of differentiation
CDR3	Complementary determining region 3
CM	Central Memory
CML	Central Memory Like
CTLA4	Cytotoxic T-lymphocyte-associated antigen 4
DRL	Death receptor ligands
EA	Early Activated
EEC	Early Effector Cells
EM	Effector Memory
EMRA	Effector memory re-expressing CD45RA
EVT	Extravillous trophoblasts
FACS	Fluorescence activated cell sorting
FasL	Fas ligand
Gal	Galectin
GD	Gestation day
GR	Glucocorticoid receptor
HLA	Human Leucocyte Antigen
HMOX-1	Hemoxygenase-1
HTO	Hashtag oligos
IFNγ	Interferon gamma
IL	Interleukin
IL-2Rβ	Interleukin 2 receptor beta
IUGR	Intrauterine growth restriction
KIR	Killer Immunoglobulin-like Receptors
Lag3	Lymphocyte activation gene 3
Ly49	Lectin-like receptors
MAIT	Mucosal associated invariant T cell
MHC	Major Histocompability complex

MLAp	Mesometrial lymphoid aggregate of pregnancy
MPEC	Memory Precursor Effector Cell
MUt	Mesometrial uterus
NA	Not available
ND	Not determined
NK	Natural killer
NKT	Natural killer T cells
NP	Not pregnant
OVA	Ovalbumin
PALN	Para-aortic lymph npde
PBMC	Peripheral blood mononuclear cells
PCR	Polymerase chain reaction
PD-L1	Programmed Cell Death Protein Ligand 1
PD1	Programmed Cell Death Protein 1
PPD	Postpartal day
SCM	Stem Cell Memory
SLEC	Short- Lived Effector Cell
TCF1	Transcription factor 1
TCR	T cell receptor
TGFβ	Transforming growth factor beta
Tigit	T-cell immunoglobulin and ITIM domain
Tim3	T cell immunoglobulin and mucin domain-containing protein 3
TNFα	Tumor necrosis factor alpha
TOX	Thymocyte selection-associated HMG bOX
TPM	Peripheral memory T cells
Treg	T regulatory
TRM	Tissue Resident Memory
tSNE	t-distributed stochastic neighbour embedding
UMAP	Uniform manifold approximation and projection
V	Virgin
VCAM-1	Vascular cell adhesion molecule 1
VLA-4	Very late antigen 4
WT	Wild type

Further abbreviations of gene and protein names are according to Appendix 4.

9 Bibliography

Abrahamsohn, P. A., & Zorn, T. M. (1993). Implantation and decidualization in rodents. *The Journal of Experimental Zoology*, *266*(6), 603–628. https://doi.org/10.1002/jez.1402660610

Affymetrix eBioscience. (n.d.). *Mouse Haplotype Table*. https://tools.thermofisher.com/content/sfs/brochures/Mouse_Haplotype_Table.pdf

Akane, K., Kojima, S., Mak, T. W., Shiku, H., & Suzuki, H. (2016). CD8 $^{+}$ CD122 $^{+}$ CD49d ^{low} regulatory T cells maintain T-cell homeostasis by killing activated T cells via Fas/FasL-mediated cytotoxicity. *Proceedings of the National Academy of Sciences*, *113*(9), 2460–2465. https://doi.org/10.1073/pnas.1525098113

Alfei, F., Kanev, K., Hofmann, M., Wu, M., Ghoneim, H. E., P, R., Utzschneider, D. T., von Hoesslin, M., Cullen, J. G., Fan, Y., Eisenberg, V., Wohlleber, D., Steiger, K., Merkler, D., Delorenzi, M., Knolle, P. A., Cohen, C. J., Thimme, R., Youngblood, B., & Zehn, D. (2019). TOX reinforces the phenotype and longevity of exhausted T cells in chronic viral infection. *Nature*, *571*, 265–269.

Alijotas-Reig, J., Esteve-Valverde, E., Ferrer-Oliveras, R., Llurba, E., & Gris, J. M. (2017). Tumor Necrosis Factor-Alpha and Pregnancy: Focus on Biologics. An Updated and Comprehensive Review. *Clinical Reviews in Allergy & Immunology*, *53*(1), 40–53. https://doi.org/10.1007/s12016-016-8596-x

Alivuhare, V., Kallikourdis, M., & Betz, A. (2004). Regulatory T cells mediate maternal tolerance to the fetus. *Nat Immunol*, *5*(3), 266–271.

Andersen, M., Sørensen, R., Brimnes, M., Svane, I., Jürgen, C., & Straten, P. (2009). Identification of heme oxygenase-1-specific regulatory CD8+T cells in cancer patients. *J Clin Invest.*, *119*(8), 2245–2256.

Angin, M., Fathi, A., King, M., Ledoux, M. B., Piechocka-Trocha, A., Altfeld, M., & Addo, M. M. (2017). Acute HIV-1 infection is associated with increased plasma levels of heme oxygenase-1 and presence of heme oxygenase-1-specific regulatory T cells. *Aids*, *31*(5), 635–641. https://doi.org/10.1097/QAD.0000000000001390

Apps, R., Murphy, S. P., Fernando, R., Gardner, L., Ahad, T., & Moffett, A. (2009). Human leucocyte antigen (HLA) expression of primary trophoblast cells and placental cell lines, determined using single antigen beads to characterize allotype specificities of anti-HLA antibodies. *Immunology*, *127*(1), 26–39. https://doi.org/10.1111/j.1365-2567.2008.03019.x

Arck, P. C., & Hecher, K. (2013). Fetomaternal immune cross-talk and its consequences for maternal and offspring's health. *Nature Medicine*, *19*(5), 548–556. https://doi.org/10.1038/nm.3160

Arck, P. C., Merali, F., Chaouat, G. R., & Clark, D. A. (1996). Inhibition of Immunoprotective CD8 / T Cells as a Basis for Stress-Triggered Substance P-Mediated Abortion in Mice 1. In *CELLULAR IMMUNOLOGY* (Vol. 171).

Arenas-Hernandez, M., Sanchez-Rodriguez, E. N., Mial, T. N., Robertson, S. A., & Gomez-Lopez, N. (2015). Isolation of Leukocytes from the Murine Tissues at the Maternal-Fetal Interface. *Journal of Visualized Experiments : JoVE*, *99*, e52866. https://doi.org/10.3791/52866

Arnaud, J., Huchenq, A., Vernhes, M. C., Caspar-Bauguil, S., Lenfant, F., Sancho, J., Terhorst, C., & Rubin, B. (1997). The interchain disulfide bond between TCR alpha beta heterodimers on human T cells is not required for TCR-CD3 membrane expression and signal transduction. *International Immunology*, *9*(4), 615–626. https://doi.org/10.1093/intimm/9.4.615

Bahri, R., Hirsch, F., Josse, A., Rouas-Freiss, N., Bidere, N., Vasquez, A., Carosella, E. D., Charpentier, B., & Durrbach, A. (2006). Soluble HLA-G Inhibits Cell Cycle Progression in Human Alloreactive T Lymphocytes1. *The Journal of Immunology*, *176*(3), 1331–1339. https://doi.org/10.4049/jimmunol.176.3.1331

Bartmann, C., Segerer, S. E., Rieger, L., Kapp, M., Sütterlin, M., & Kämmerer, U. (2014). Quantification of the predominant immune cell populations in decidua throughout human pregnancy. *American Journal of Reproductive Immunology (New York, N.Y. : 1989)*, *71*(2), 109–119. https://doi.org/10.1111/aji.12185

Bassing, C. H., Swat, W., & Alt, F. W. (2002). The mechanism and regulation of chromosomal V(D)J recombination. *Cell*, *109 Suppl*, S45-55. https://doi.org/10.1016/s0092-8674(02)00675-x

Bevilacqua, E. M., & Abrahamsohn, P. A. (1988). Ultrastructure of trophoblast giant cell transformation during the invasive stage of implantation of the mouse embryo. *Journal of Morphology*, *198*(3), 341–351. https://doi.org/10.1002/jmor.1051980308

Bevilacqua, E. M., & Abrahamsohn, P. A. (1989). Trophoblast invasion during implantation of the mouse embryo. *Archivos de Biologia y Medicina Experimentales*, *22*(2), 107–118.

Bézie, S., Anegon, I., & Guillonneau, C. (2018). *Advances on CD8 + Treg Cells and Their Potential in Transplantation*. *102*(9). https://doi.org/10.1097/TP.0000000000002258

Billingham, R. E., Brent, L., & Medawar, P. B. (1953). Actively acquired tolerance of foreign cells. *Nature*, *4379*(172), 603–606.

Billington, D. (2003). The immunological problem of pregnancy: 50 years with the hope of progress. A tribute to Peter Medawar. *J Reprod Immunol*, *60*, 1–11.

Björkström, N. K., Béziat, V., Cichocki, F., Liu, L. L., Levine, J., Larsson, S., Koup, R. A., Anderson, S. K., Ljunggren, H. G., & Malmberg, K. J. (2012). CD8 T cells express randomly selected KIRs with distinct specificities compared with NK cells. *Blood*, *120*(17), 3455–3465. https://doi.org/10.1182/blood-2012-03-416867

Blank, C., Haining, W. N., Held, W., Hogan, P., Kallies, A., Lugli, E., Lynn, R., Philip, M., Rao, A., Restifo, N. P., Schietinger, A., Schumacher, T. N., Schwartzberg, P. L., Sharpe, A. H., Speiser, D., Wherry, E. J., Youngblood, B. A., & Zehn, D. (2019). Defining T cell exhaustion. *Nat Rev Immunol*, *19*(11), 665–674. https://doi.org/10.1038/s41577-019-0221-9.

Blois, S. M., Ilarregui, J. M., Tometten, M., Garcia, M., Orsal, A. S., Cordo-Russo, R., Toscano, M. A., Bianco, G. A., Kobelt, P., Handjiski, B., Tirado, I., Markert, U. R., Klapp, B. F., Poirier, F., Szekeres-Bartho, J., Rabinovich, G. A., & Arck, P. C. (2007). A pivotal role for galectin-1 in fetomaternal tolerance. *Nature Medicine*, *13*(12), 1450–1457. https://doi.org/10.1038/nm1680

Blois, S. M., Joachim, R., Kandil, J., Margni, R., Tometten, M., Klapp, B. F., & Arck, P. C. (2004). Depletion of CD8+ Cells Abolishes the Pregnancy Protective Effect of Progesterone Substitution with Dydrogesterone in Mice by Altering the Th1/Th2 Cytokine Profile. *The Journal of Immunology*, *172*(10), 5893–5899. https://doi.org/10.4049/jimmunol.172.10.5893

Borowski, S., Tirado-Gonzalez, I., Freitag, N., Garcia, M. G., Barrientos, G., & Blois, S. M. (2020). Altered Glycosylation Contributes to Placental Dysfunction Upon Early Disruption of the NK Cell-DC Dynamics. *Frontiers in Immunology*, *11*. https://doi.org/10.3389/fimmu.2020.01316

Boscher, C., Dennis, J. W., & Nabi, I. R. (2011). Glycosylation, galectins and cellular signaling. *Current Opinion in Cell Biology*, *23*(4), 383–392. https://doi.org/https://doi.org/10.1016/j.ceb.2011.05.001

Bouneaud, C., Kourilsky, P., & Bousso, P. (2000). Impact of negative selection on the T cell repertoire reactive to a self- peptide: a large fraction of T cell clones escapes clonal deletion. *Immunity*, *13*, 829–840.

Cagnoni, A. J., Laura, M., Blidner, A. G., Cutine, A. M., & Gatto, S. G. (2021). *Galectin-1 fosters an immunosuppressive microenvironment in colorectal cancer by reprogramming CD8 + regulatory T cells*. https://doi.org/10.1073/pnas.2102950118

Carson, D. D., Bagchi, I., Dey, S. K., Enders, A. C., Fazleabas, A. T., Lessey, B. A., & Yoshinaga, K. (2000). Embryo Implantation. *Developmental Biology*, *223*(2), 217–237. https://doi.org/https://doi.org/10.1006/dbio.2000.9767

Carter, A. M. (2011). Comparative studies of placentation and immunology in non-human primates suggest a scenario for the evolution of deep trophoblast invasion and an explanation for human pregnancy disorders. *Reproduction (Cambridge, England)*, *141*(4), 391–396. https://doi.org/10.1530/REP-10-0530

Carter, A. M. (2020). Animal models of human pregnancy and placentation: alternatives to the mouse. *Reproduction*, *160*, R129–R143.

Chatterjee, P., Chiasson, V. L., Bounds, K. R., & Mitchell, B. M. (2014). Regulation of the Anti-Inflammatory Cytokines Interleukin-4 and Interleukin-10 during Pregnancy. *Frontiers in Immunology*, *5*, 253. https://doi.org/10.3389/fimmu.2014.00253

Chen, P., Zhou, L., Chen, J., Lu, Y., Cao, C., Lv, S., Wei, Z., Wang, L., Chen, J., Hu, X., Wu, Z., Zhou, X., Su, D., Deng, X., Zeng, C., Wang, H., Pu, Z., Diao, R., & Mou, L. (2021). The Immune Atlas of Human Deciduas With Unexplained Recurrent Pregnancy Loss. *Frontiers in Immunology*, *12*(June), 1–16. https://doi.org/10.3389/fimmu.2021.689019

Chen, Y., Xin, Z., Huang, L., Zhao, L., Wang, S., Cheng, J., Wu, P., & Chai, Y. (2020). CD8+ T Cells Form the Predominant Subset of NKG2A+ Cells in Human Lung Cancer. *Frontiers in Immunology*, *10*. https://doi.org/10.3389/fimmu.2019.03002

Chiffelle, J., Genolet, R., Perez, M. A., Coukos, G., Zoete, V., & Harari, A. (2020). T-cell repertoire analysis and metrics of diversity and clonality. *Current Opinion in Biotechnology*, *65*, 284–295. https://doi.org/10.1016/j.copbio.2020.07.010

Chinen, T., Kannan, A. K., Levine, A. G., Fan, X., Klein, U., Zheng, Y., Gasteiger, G., Feng, Y., Fontenot, J. D., & Rudensky, A. Y. (2016). An essential role for the IL-2 receptor in T(reg) cell function. *Nature Immunology*, *17*(11), 1322–1333. https://doi.org/10.1038/ni.3540

Clark, D. A., Brierley, J., Banwatt, D., & Chaouat~, G. (1989). Hormone-Induced Preimplantation Lyt 2+ Murine Uterine Suppressor Cells Persist after Implantation and May Reduce the Spontaneous Abortion Rate in CBA/J Mice'. In *CELLULAR IMMUNOLOGY* (Vol. 123).

Collins, M., Tay, C., & Erlenbacher, A. (2009). Dendritic cell entrapment within the pregnant uterus inhibits immune surveillance of the maternal/fetal interface in mice. *Journal of Clinical Investigation*, *119*(7), 2062–2073. http://www.ncbi.nlm.nih.gov/entrez/query.fcgi?cmd=Retrieve&db=PubMed&dopt=Citation&list_uids=6537210

Confavreux, C., Hutchinson, M., Houea, M. M., Cortinovis-Tournaire, P., & Moreau, T. (1998). RATE OF PREGNANCY-RELATED RELAPSE IN MULTIPLE SCLEROSIS. *The New England Journal of Medicine*, *339*(5), 285–291.

Croy, B. A., Esadeg, S., Chantakru, S., van den Heuvel, M., Paffaro, V. A., He, H., Black, G. P., Ashkar, A. A., Kiso, Y., & Zhang, J. (2003). Update on pathways regulating the activation of uterine Natural Killer cells, their interactions with decidual spiral arteries and homing of their precursors to the uterus. *Journal of Reproductive Immunology*, *59*(2), 175–191. https://doi.org/https://doi.org/10.1016/S0165-0378(03)00046-9

Croy, B. A., Yamanda, A. T., DeMayo, F. J., & Adamson, S. L. (2015). *The Guide To Investigation of mouse pregnancy*. Elsevier.

Cyktor, J., Carruthers, B., Beamer, G., & Turner, J. (2013). Clonal expansions of CD8+ T cells with IL-10 secreting capacity occur during chronic Mycobacterium tuberculosis infection. *PLoS ONE*, *8*(3), e58612.

D'Alessio, F. R., Kurzhagen, J. T., & Rabb, H. (2019). Reparative T lymphocytes in organ injury. *The Journal of Clinical Investigation*, *129*(7), 2608–2618. https://doi.org/10.1172/JCI124614

Dai, H., Wan, N., Zhang, S., Moore, Y., Wan, F., & Dai, Z. (2010). Cutting Edge: Programmed Death-1 Defines CD8 + CD122 + T Cells as Regulatory versus Memory T Cells . *The Journal of Immunology*, *185*(2), 803–807. https://doi.org/10.4049/jimmunol.1000661

Dai, Z., Zhang, S., Xie, Q., Wu, S., Su, J., Li, S., Xu, Y., & Li, X. C. (2014). Natural CD8+CD122+ T cells are more potent in suppression of allograft rejection than CD4+CD25+ regulatory T cells. *American Journal of Transplantation*, *14*(1), 39–48. https://doi.org/10.1111/ajt.12515

Das, A., Mantena, S. R., Kannan, A., Evans, D. B., Bagchi, M. K., & Bagchi, I. C. (2009). De novo synthesis of estrogen in pregnant uterus is critical for stromal decidualization and angiogenesis. *Proceedings of the National Academy of Sciences of the United States of America*, *106*(30), 12542–12547. https://doi.org/10.1073/pnas.0901647106

Davis, M. M., & Boyd, S. D. (2019). Recent progress in the analysis of αβT cell and B cell receptor repertoires. *Current Opinion in Immunology*, *59*, 109–114. https://doi.org/10.1016/j.coi.2019.05.012

de Jong, L. C., Crnko, S., Ten Broeke, T., & Bovenschen, N. (2021). Noncytotoxic functions of killer cell granzymes in viral infections. *PLoS Pathogens*, *17*(9), e1009818. https://doi.org/10.1371/journal.ppat.1009818

Dorner, B. G., Dorner, M. B., Zhou, X., Opitz, C., Mora, A., Güttler, S., Hutloff, A., Mages, H. W., Ranke, K., Schaefer, M., Jack, R. S., Henn, V., & Kroczek, R. A. (2009). Selective Expression of the Chemokine Receptor XCR1 on Cross-presenting Dendritic Cells Determines Cooperation with CD8+ T Cells. *Immunity*, *31*(5), 823–833. https://doi.org/https://doi.org/10.1016/j.immuni.2009.08.027

Dunk, C., Kwan, M., Hazan, A., Walker, S., Wright, J. K., Harris, L. K., Jones, R. L., Keating, S., Kingdom, J. C. P., Whittle, W., Maxwell, C., & Lye, S. J. (2019). Failure of decidualization and maternal immune tolerance underlies uterovascular resistance in intra uterine growth restriction. *Frontiers in Endocrinology*, *10*(MAR), 1–18. https://doi.org/10.3389/fendo.2019.00160

Dusseaux, M., Martin, E., Serriari, N., Péguillet, I., Premel, V., Louis, D., Milder, M., Le Bourhis, L., Soudais, C., Treiner, E., & Lantz, O. (2011). Human MAIT cells are xenobiotic-resistant, tissue-targeted, CD161hi IL-17–secreting T cells. *Blood*, *117*(4), 1250 LP – 1259. https://doi.org/10.1182/blood-2010-08-303339

Egmond, A. Van, Keur, C. Van Der, Swings, G. M. J. S., Scherjon, S. A., & Claas, F. H. J. (2016). The possible role of virus-specific CD8 + memory T cells in decidual tissue. *Journal of Reproductive Immunology*, *113*, 1–8. https://doi.org/10.1016/j.jri.2015.09.073

Elia, A., & Georgiades, P. (2021). Investigation of the pregnancy-induced muscle bundle dispersal of the inner myometrium of adult mouse uterus and its relationship to the metrial gland/MLAp. *Biochemical and Biophysical Research Communications*, *584*, 66–72. https://doi.org/10.1016/j.bbrc.2021.11.007

Elizondo, D. M., Andargie, T. E., Haddock, N. L., da Silva, R. L. L., de Moura, T. R., & Lipscomb, M. W. (2019). IL-10 producing CD8(+) CD122(+) PD-1(+) regulatory T cells are expanded by dendritic cells silenced for Allograft Inflammatory Factor-1. *Journal of Leukocyte Biology*, *105*(1), 123–130. https://doi.org/10.1002/JLB.1A0118-010RR

Endharti, A. T., Okuno, Y., Shi, Z., Misawa, N., Toyokuni, S., Ito, M., Isobe, K. -i., & Suzuki, H. (2011). CD8+CD122+ Regulatory T Cells (Tregs) and CD4+ Tregs Cooperatively Prevent and Cure CD4+ Cell-Induced Colitis. *The Journal of Immunology*, *186*(1), 41–52. https://doi.org/10.4049/jimmunol.1000800

Endharti, A. T., Rifa'I, M., Shi, Z., Fukuoka, Y., Nakahara, Y., Kawamoto, Y., Takeda, K.,

Isobe, K.-I., & Suzuki, H. (2005). Cutting edge: CD8+CD122+ regulatory T cells produce IL-10 to suppress IFN-gamma production and proliferation of CD8+ T cells. *Journal of Immunology (Baltimore, Md. : 1950)*, *175*(11), 7093–7097. https://doi.org/10.4049/jimmunol.175.11.7093

Engels, G., Hierweger, A. M., Hoffmann, J., Thieme, R., Thiele, S., Bertram, S., Dreier, C., Resa-Infante, P., Jacobsen, H., Thiele, K., Alawi, M., Indenbirken, D., Grundhoff, A., Siebels, S., Fischer, N., Stojanovska, V., Muzzio, D., Jensen, F., Karimi, K., … Gabriel, G. (2017). Pregnancy-Related Immune Adaptation Promotes the Emergence of Highly Virulent H1N1 Influenza Virus Strains in Allogenically Pregnant Mice. *Cell Host and Microbe*, *21*(3), 321–333. https://doi.org/10.1016/j.chom.2017.02.020

Engler, J. B., Kursawe, N., Solano, M. E., Patas, K., Wehrmann, S., Heckmann, N., Lühder, F., Reichardt, H. M., Arck, P. C., Gold, S. M., & Friese, M. A. (2017). Glucocorticoid receptor in T cells mediates protection from autoimmunity in pregnancy. *Proceedings of the National Academy of Sciences*, *114*(2), E181–E190. https://doi.org/10.1073/pnas.1617115114

Erlebacher, A. (2013). Mechanisms of T cell tolerance towards the allogeneic fetus. *Nature Reviews Immunology*, *13*(1), 23–33. https://doi.org/10.1038/nri3361

Erlebacher, A., Vencato, D., Price, K. A., Zhang, D., & Glimcher, L. H. (2007). Constraints in antigen presentation severely restrict T cell recognition of the allogeneic fetus. *Journal of Clinical Investigation*, *117*(5), 1399–1411. https://doi.org/10.1172/JCI28214

Faas, M. M., & de Vos, P. (2017). Uterine NK cells and macrophages in pregnancy. *Placenta*, *56*, 44–52. https://doi.org/https://doi.org/10.1016/j.placenta.2017.03.001

Faas, M. M., & De Vos, P. (2018). Innate immune cells in the placental bed in healthy pregnancy and preeclampsia. *Placenta*, *69*, 125–133. https://doi.org/10.1016/j.placenta.2018.04.012

Feyaerts, D., Benner, M., Cranenbroek, B. Van, & Heijden, O. W. H. Van Der. (2017). *Human uterine lymphocytes acquire a more experienced and tolerogenic phenotype during pregnancy*. *April*, 1–10. https://doi.org/10.1038/s41598-017-03191-0

Flores, L. E., Hildebrandt, T. B., Kühl, A. A., & Drews, B. (2014). Early detection and staging of spontaneous embryo resorption by ultrasound biomicroscopy in murine pregnancy. *Reproductive Biology and Endocrinology : RB&E*, *12*, 38. https://doi.org/10.1186/1477-7827-12-38

Fonseca, R., Beura, L. K., Quarnstrom, C. F., Ghoneim, H. E., Fan, Y., Zebley, C. C., Scott, M. C., Fares-frederickson, N. J., Wijeyesinghe, S., Thompson, E. A., Borges, H., Vezys, V., Youngblood, B., & Masopust, D. (2020). Developmental Plasticity Allows Outside-In Immune Responses by Resident Memory T cells. *Nature Immunology*, *21*, 412–421. https://doi.org/10.1038/s41590-020-0607-7

Fowler, C. C., Pao, L. I., Blattman, J. N., & Greenberg, P. D. (2010). SHP-1 in T cells limits the production of CD8 effector cells without impacting the formation of long-lived central memory cells. *Journal of Immunology (Baltimore, Md. : 1950)*, *185*(6), 3256–3267. https://doi.org/10.4049/jimmunol.1001362

Frebel, H., Nindl, V., Schuepbach, R. A., Braunschweiler, T., Richter, K., Vogel, J., Wagner, C. A., D, L.-C., Kurrer, M., Ludewig, B., & Oxenius, A. (2012). Programmed death 1 protects from fatal circulatory failure during systemic virus infection of mice. *The Journal of Experimental Medicine*, *209*(13), 2485–2499.

Gee, S. E., & Frey, H. A. (2020). Contractions: Traditional concepts and their role in modern obstetrics. *Seminars in Perinatology*, *44*(2), 151218. https://doi.org/10.1016/j.semperi.2019.151218

Gerlach, C., Moseman, E. A., Loughhead, S. M., Alvarez, D., Zwijnenburg, A. J., Waanders, L., Garg, R., & Torre, J. C. De. (2016). The chemokine receptor CX3CR1 defines three antigen-experienced CD8 T cell subsets with distinct roles in immune surveillance and

homeostasis. *Immunity*, *45*, 1270–1284. https://doi.org/10.1016/j.immuni.2016.10.018.The

Gerritsen, B., & Pandit, A. (2016). *The memory of a killer T cell : models of CD8 + T cell differentiation*. *January*, 236–241. https://doi.org/10.1038/icb.2015.118

Gershon, R. K., & Kondo, K. (1970). Cell interactions in the induction of tolerance: the role of thymic lymphocytes. *Immunology*, *18*(5), 723–737.

Gordon, S. M. (2021). Interleukin-15 in Outcomes of Pregnancy. *International Journal of Molecular Sciences*, *22*(20). https://doi.org/10.3390/ijms222011094

Gordon, S. M., Nishiguchi, M. A., Chase, J. M., Mani, S., Mainigi, M. A., & Behrens, E. M. (2020). IFNs Drive Development of Novel IL-15-Responsive Macrophages. *Journal of Immunology (Baltimore, Md. : 1950)*, *205*(4), 1113–1124. https://doi.org/10.4049/jimmunol.2000184

Griffith, O. W., Chavan, A. R., Protopapas, S., Maziarz, J., Romero, R., & Wagner, G. P. (2017). Embryo implantation evolved from an ancestral inflammatory attachment reaction. *Proceedings of the National Academy of Sciences*, *114*(32), E6566–E6575. https://doi.org/10.1073/pnas.1701129114

Gu, H., Li, L., Du, M., Xu, H., Gao, M., Liu, X., Wei, X., & Zhong, X. (2021). Key Gene and Functional Pathways Identified in Unexplained Recurrent Spontaneous Abortion Using Targeted RNA Sequencing and Clinical Analysis. *Frontiers in Immunology*, *12*, 717832. https://doi.org/10.3389/fimmu.2021.717832

Guzman-Genuino, R. M., Eldi, P., Garcia-Valtanen, P., Hayball, J. D., & Diener, K. R. (2019). Uterine B Cells Exhibit Regulatory Properties During the Peri-Implantation Stage of Murine Pregnancy. *Frontiers in Immunology*, *10*, 2899. https://doi.org/10.3389/fimmu.2019.02899

Halenius, A., Gerke, C., & Hengel, H. (2015). Classical and non-classical MHC I molecule manipulation by human cytomegalovirus: so many targets—but how many arrows in the quiver? *Cellular & Molecular Immunology*, *12*(2), 139–153. https://doi.org/10.1038/cmi.2014.105

Hammami, A., Charpentier, T., Smans, M., & Stäger, S. (2015). IRF-5-Mediated Inflammation Limits CD8+ T Cell Expansion by Inducing HIF-1α and Impairing Dendritic Cell Functions during Leishmania Infection. *PLoS Pathogens*, *11*(6), e1004938. https://doi.org/10.1371/journal.ppat.1004938

Harberts, A., Schmidt, C., Schmid, J., Reimers, D., Koch-Nolte, F., Mittrücker, H.-W., & Raczkowski, F. (2021). Interferon regulatory factor 4 controls effector functions of CD8(+) memory T cells. *Proceedings of the National Academy of Sciences of the United States of America*, *118*(16). https://doi.org/10.1073/pnas.2014553118

Hardardottir, L., Bazzano, M. V., Glau, L., Gattinoni, L., Köninger, A., Tolosa, E., & Solano, M. E. (2021). *The New Old CD8 + T Cells in the Immune Paradox of Pregnancy*. *12*(November), 1–14. https://doi.org/10.3389/fimmu.2021.765730

Head, J. R., & Billingham, R. E. (1986). Concerning the immunology of the uterus. *American Journal of Reproductive Immunology and Microbiology : AJRIM*, *10*(3), 76–81.

Herndon, J., Patrick, M., & Ferguson, T. (2005). Peripheral Deletion of Antigen-Specific T Cells Leads to Long-Term Tolerance Mediated by CD8+ Cytotoxic Cells. *J Immunol*, *174*, 4098–4104.

Hierweger, A. M., Engler, J. B., Friese, M. A., Reichardt, H. M., Lydon, J., DeMayo, F., Mittrücker, H.-W., & Arck, P. C. (2019). Progesterone modulates the T-cell response via glucocorticoid receptor-dependent pathways. *American Journal of Reproductive Immunology (New York, N.Y. : 1989)*, *81*(2), e13084. https://doi.org/10.1111/aji.13084

Hirashima, C., Ohkuchi, A., Nagayama, S., Suzuki, H., Takahashi, K., Ogoyama, M., Takahashi, H., Shirasuna, K., & Matsubara, S. (2018). Galectin-1 as a novel risk factor for both gestational hypertension and preeclampsia, specifially its expression at a low

level in the second trimester and a high level after onset. *Hypertension Research : Official Journal of the Japanese Society of Hypertension*, *41*(1), 45–52. https://doi.org/10.1038/hr.2017.85

Hirota, Y., Acar, N., Tranguch, S., Burnum, K. E., Xie, H., Kodama, A., Osuga, Y., Ustunel, I., Friedman, D. B., Caprioli, R. M., Daikoku, T., & Dey, S. K. (2010). Uterine FK506-binding protein 52 (FKBP52)-peroxiredoxin-6 (PRDX6) signaling protects pregnancy from overt oxidative stress. *Proceedings of the National Academy of Sciences of the United States of America*, *107*(35), 15577–15582. https://doi.org/10.1073/pnas.1009324107

Hou, X., Wang, M., Lu, C., Xie, Q., Cui, G., Chen, J., Du, Y., Dai, Y., & Diao, H. (2016). Analysis of the Repertoire Features of TCR Beta Chain CDR3 in Human by High-Throughput Sequencing. *Cellular Physiology and Biochemistry : International Journal of Experimental Cellular Physiology, Biochemistry, and Pharmacology*, *39*(2), 651–667. https://doi.org/10.1159/000445656

Hu, D., Ikizawa, K., Lu, L., Sanchirico, M. E., Shinohara, M. L., & Cantor, H. (2004). Analysis of regulatory CD8 T cells in Qa-1-deficient mice. *Nature Immunology*, *5*(5), 516–523. https://doi.org/10.1038/ni1063

Huang, X., Liu, L., Xu, C., Peng, X., Li, D., & Du, M. (2020). *Tissue-resident CD8 + T memory cells with unique properties are present in human decidua during early pregnancy*. *April*, 1–13. https://doi.org/10.1111/aji.13254

Hughes, G. C., Clark, E. A., & Wong, A. H. (2013). The intracellular progesterone receptor regulates CD4+ T cells and T cell-dependent antibody responses. *Journal of Leukocyte Biology*, *93*(3), 369–375. https://doi.org/10.1189/jlb.1012491

InvivoGen. (n.d.). *Immune Checkpoints*. https://www.invivogen.com/immune-checkpoints

Jameson, S. C., & Masopust, D. (2019). *Understanding subset diversity in T cell memory*. *48*(2), 214–226. https://doi.org/10.1016/j.immuni.2018.02.010.Understanding

Janeway Jr, C., Travers, P., & Walport, M. (2001). T cell-mediated cytotoxicity. In *Immunobiology: The Immune System in Health and Disease. 5th edition.*

Jantsch, J., L. Schultze, J., & Kurts, C. (2017). Immunophysiology: Macrophages as key regulators of homeostasis in various organs . *Pflügers Archiv - European Journal of Physiology*, *469*(3), 363–364. https://doi.org/10.1007/s00424-017-1963-5

Jeannet, G., Boudousquié, C., Gardiol, N., Kang, J., Huelsken, J., & Held, W. (2010). Essential role of the Wnt pathway effector Tcf-1 for the establishment of functional CD8 T cell memory. *Proc. Natl Acad. Sci. USA*, *107*(21), 9777–9782.

Jemiolo, B., Harvey, S., & Novotny, M. (1986). Promotion of the Whitten effect in female mice by synthetic analogs of male urinary constituents. *Proceedings of the National Academy of Sciences of the United States of America*, *83*(12), 4576–4579. https://doi.org/10.1073/pnas.83.12.4576

Jeschke, U., Mayr, D., Schiessl, B., Mylonas, I., Schulze, S., Kuhn, C., Friese, K., & Walzel, H. (2007). Expression of galectin-1, -3 (gal-1, gal-3) and the Thomsen-Friedenreich (TF) antigen in normal, IUGR, preeclamptic and HELLP placentas. *Placenta*, *28*(11–12), 1165–1173. https://doi.org/10.1016/j.placenta.2007.06.006

Jiang, H., Canfield, S. M., Gallagher, M. P., Jiang, H. H., Jiang, Y., Zheng, Z., & Chess, L. (2010). *HLA-E – restricted regulatory CD8 + T cells are involved in development and control of human autoimmune type 1 diabetes*. *120*(10), 3641–3650. https://doi.org/10.1172/JCI43522.mechanisms

Jiang, H., Ware, R., Stall, A., Flaherty, L., Chess, L., & Pernis, B. (1995). Murine CD8+ T cells that specifically delete autologous CD4+ T cells expressing V beta 8 TCR: a role of the Qa-1 molecule. *Immunity*, *2*(2), 185–194. https://doi.org/10.1016/s1074-7613(95)80079-4

Jiang, X., Wang, J., Deng, X., Xiong, F., Ge, J., Xiang, B., Wu, X., Ma, J., Zhou, M., Li, X.,

Li, Y., Li, G., Xiong, Guo, W., & C Zeng, Z. (2019). Role of the tumor microenvironment in PD-L1/PD-1-mediated tumor immune escape PMC6332843. *Mol Cancer*, *18*(1).

Kaech, S. M., & Cui, W. (2012). Transcriptional control of effector and memory CD8+ T cell differentiation. *Nature Publishing Group*, *October*. https://doi.org/10.1038/nri3307

Kagami, K., Ono, M., Iizuka, T., Matsumoto, T., Hosono, T., Sekizuka-Kagami, N., Shinmyo, Y., Kawasaki, H., & Fujiwara, H. (2020). A novel third mesh-like myometrial layer connects the longitudinal and circular muscle fibers -A potential stratum to coordinate uterine contractions-. *Scientific Reports*, *10*(1), 8274. https://doi.org/10.1038/s41598-020-65299-0

Kagami, K., Shinmyo, Y., Ono, M., Kawasaki, H., & Fujiwara, H. (2017). Three-dimensional visualization of intrauterine conceptus through the uterine wall by tissue clearing method. *Scientific Reports*, *7*(1), 1–9. https://doi.org/10.1038/s41598-017-06549-6

Kawabe, T., Yi, J., Kawajiri, A., Hilligan, K., Fang, D., Ishii, N., Yamane, H., Zhu, J., Jankovic, D., Kim, K. S., Trinchieri, G., & Sher, A. (2020). Requirements for the differentiation of innate T-bethigh memory-phenotype CD4+ T lymphocytes under steady state. *Nature Communications*, *11*(1), 3366. https://doi.org/10.1038/s41467-020-17136-1

Kieffer, T. E. C., Laskewitz, A., Vledder, A., Scherjon, S. A., Faas, M. M., & Prins, J. R. (2020). *Decidual memory T-cell subsets and memory T-cell stimulatory cytokines in early- and late-onset preeclampsia*. *April*, 1–14. https://doi.org/10.1111/aji.13293

Kieper, W. C., Troy, A., Burghardt, J. T., Ramsey, C., Lee, J. Y., Jiang, H.-Q., Dummer, W., Shen, H., Cebra, J. J., & Surh, C. D. (2005). Cutting Edge: Recent Immune Status Determines the Source of Antigens That Drive Homeostatic T Cell Expansion1. *The Journal of Immunology*, *174*(6), 3158–3163. https://doi.org/10.4049/jimmunol.174.6.3158

Kim, H.-D., Song, G.-W., Park, S., Jung, M. K., Kim, M. H., Kang, H. J., Yoo, C., Yi, K., Kim, K. H., Eo, S., Moon, D.-B., Hong, S.-M., Ju, Y. S., Shin, E.-C., Hwang, S., & Park, S.-H. (2018). Association Between Expression Level of PD1 by Tumor-Infiltrating CD8+ T Cells and Features of Hepatocellular Carcinoma. *Gastroenterology*, *155*(6), 1936-1950.e17. https://doi.org/https://doi.org/10.1053/j.gastro.2018.08.030

Kim, H.-J., Verbinnen, B., Tang, X., Lu, L., & Cantor, H. (2010). Inhibition of follicular T-helper cells by CD8(+) regulatory T cells is essential for self tolerance. *Nature*, *467*(7313), 328–332. https://doi.org/10.1038/nature09370

Kim, H., Wang, X., Radfar, S., Sproule, T. J., Roopenian, D. C., & Cantor, H. (2011). CD8+ T regulatory cells express the Ly49 Class I MHC receptor and are defective in autoimmune prone B6-Yaa mice. *Proceedings of the National Academy of Sciences of the United States of America*, *108*(5), 2010–2015. https://doi.org/10.1073/pnas.1018974108

Kim, K. H., Choi, B. K., Kim, J. D., Kim, Y. H., Lee, S. K., Suh, J. H., Lee, S. C., Kang, S. W., & Kwon, B. S. (2012). 4-1BB Signaling Breaks the Tolerance of Maternal CD8+T Cells That Are Reactive with Alloantigens. *PLoS ONE*, *7*(9), 1–8. https://doi.org/10.1371/journal.pone.0045481

Kinder, J. M., Turner, L. H., Stelzer, I. A., Miller-Handley, H., Burg, A., Shao, T. Y., Pham, G., & Way, S. S. (2020). CD8+ T Cell Functional Exhaustion Overrides Pregnancy-Induced Fetal Antigen Alloimmunization. *Cell Reports*, *31*(12), 107784. https://doi.org/10.1016/j.celrep.2020.107784

Klebanoff, C. A., Scott, C. D., Leonardi, A. J., Yamamoto, T. N., Cruz, A. C., Ouyang, C., Ramaswamy, M., Roychoudhuri, R., Ji, Y., Eil, R. L., Sukumar, M., Crompton, J. G., Palmer, D. C., Borman, Z. A., Clever, D., Thomas, S. K., Patel, S., Yu, Z., Muranski, P., … Restifo, N. P. (2016). Memory T cell-driven differentiation of naive cells impairs

adoptive immunotherapy. *The Journal of Clinical Investigation*, *126*(1), 318–334. https://doi.org/10.1172/JCI81217

Kochan, G., Escors, D., Breckpot, K., & Guerrero-Setas, D. (2013). Role of non-classical MHC class I molecules in cancer immunosuppression. In *Oncoimmunology* (Vol. 2, Issue 11, p. e26491). https://doi.org/10.4161/onci.26491

Kondělková, K., Vokurková, D., Krejsek, J., Borská, L., Fiala, Z., & Andrýs, C. (2010). REVIEW ARTICLE REGULATORY T CELLS (TREG) AND THEIR ROLES IN IMMUNE SYSTEM WITH RESPECT TO IMMUNOPATHOLOGICAL DISORDERS Detection of Tregs The crucial role of T cell system in the pathogenesis of. *ACTA MEDICA*, *53*(2), 73–77. https://doi.org/10.14712/18059694.2016.63

Konno, A., Okada, K., Mizuno, K., Nishida, M., Nagaoki, S., Toma, T., Uehara, T., Ohta, K., Kasahara, Y., Seki, H., Yachie, A., & Koizumi, S. (2002). CD8αα memory effector T cells descend directly from clonally expanded CD8α+βhigh TCRαβ T cells in vivo. *Blood*, *100*(12), 4090–4097. https://doi.org/10.1182/blood-2002-04-1136

Kopcow, H. D., Rosetti, F., Leung, Y., Allan, D. S. J., Kutok, J. L., & Strominger, J. L. (2008). T cell apoptosis at the maternal-fetal interface in early human pregnancy, involvement of galectin-1. *Proceedings of the National Academy of Sciences of the United States of America*, *105*(47), 18472–18477. https://doi.org/10.1073/pnas.0809233105

Kouo, T., Huang, L., Pucsek, A. B., Cao, M., Solt, S., Armstrong, T., & Jaffee, E. (2015). Galectin-3 Shapes Antitumor Immune Responses by Suppressing CD8+ T Cells via LAG-3 and Inhibiting Expansion of Plasmacytoid Dendritic Cells. *Cancer Immunology Research*, *3*(4), 412–423. https://doi.org/10.1158/2326-6066.CIR-14-0150

Kovats, S. (2015). Estrogen receptors regulate innate immune cells and signaling pathways. *Cellular Immunology*, *294*(2), 63–69. https://doi.org/10.1016/j.cellimm.2015.01.018

Kurachi, M., Barnitz, R. A., Yosef, N., Odorizzi, P. M., DiIorio, M. A., Lemieux, M. E., Yates, K., Godec, J., Klatt, M. G., Regev, A., Wherry, E. J., & Haining, W. N. (2014). The transcription factor BATF operates as an essential differentiation checkpoint in early effector CD8+ T cells. *Nature Immunology*, *15*(4), 373–383. https://doi.org/10.1038/ni.2834

Lager, S., Sovio, U., Eddershaw, E., Linden, M. W. Van Der, Yazar, C., Cook, E., Happerfield, L., Jessop, F. A., Sebire, N. J., Charnock-jones, D. S., & Smith, G. C. S. (2020). *Abnormal placental CD8 + T-cell infiltration is a feature of fetal growth restriction and pre-eclampsia*. *23*, 5555–5571. https://doi.org/10.1113/JP279532

Leavenworth, J. W., Tang, X., Kim, H.-J., Wang, X., & Cantor, H. (2013). Amelioration of arthritis through mobilization of peptide-specific CD8+ regulatory T cells. *The Journal of Clinical Investigation*, *123*(3), 1382–1389. https://doi.org/10.1172/JCI66938

Lei, Y., & Takahama, Y. (2012). XCL1 and XCR1 in the immune system. *Microbes and Infection*, *14*(3), 262–267. https://doi.org/https://doi.org/10.1016/j.micinf.2011.10.003

Lessey, B. A., & Young, S. L. (2019). What exactly is endometrial receptivity? *Fertility and Sterility*, *111*(4), 611–617. https://doi.org/10.1016/j.fertnstert.2019.02.009

Levy, A. R. R. A., Rojas-villarraga, A., & Levy, R. A. (2013). Autoimmunity From Bench to Bedside. In *Macmillan Publishers*. https://doi.org/10.1016/b978-0-444-50331-2.x5000-0

Li, J., He, Y., Hao, J., Ni, L., & Dong, C. (2018). High Levels of Eomes Promote Exhaustion of Anti-tumor CD8(+) T Cells. *Frontiers in Immunology*, *9*, 2981. https://doi.org/10.3389/fimmu.2018.02981

Li, J., Tan, J., Martino, M. M., & Lui, K. O. (2018). Regulatory T-Cells: Potential Regulator of Tissue Repair and Regeneration. *Frontiers in Immunology*, *9*, 585. https://doi.org/10.3389/fimmu.2018.00585

Li, J., Zaslavsky, M., Yapeng, S., Guo, J., Sikora, M. J., Unen, V. van, Christophersen, A., Chiou, S., Chen, L., Li, J., Ji, X., Wilhelmy, J., Mcsween, A. M., Palanski, B. A.,

Vamsee, V., Mallajosyula, A., Bracey, N. A., Dhondalay, G. K. R., Bhamidipati, K., … Davis, M. M. (2022). KIR + CD8 + T cells suppress pathogenic T cells and are active in autoimmune diseases and COVID-19. *Science*, *376*(265). https://doi.org/10.1126/science.abi9591

Li, S., Xie, Q., Zeng, Y., Zou, C., Liu, X., Wu, S., Deng, H., Xu, Y., Li, X. C., & Dai, Z. (2014). A naturally occurring CD8(+)CD122(+) T-cell subset as a memory-like Treg family. *Cellular & Molecular Immunology*, *11*(4), 326–331. https://doi.org/10.1038/cmi.2014.25

Li, Y., Lopez, G. E., Vazquez, J., Sun, Y., & Chavarria, M. (2018). *Decidual-Placental Immune Landscape During Syngeneic Murine Pregnancy*. *9*(September), 1–13. https://doi.org/10.3389/fimmu.2018.02087

Lissauer, D., Kilby, M. ., & Moss, P. (2017). Maternal effector T cells within decidua: The adaptive immune response to pregnancy. *Placenta*, *60*, 140–144.

Liu, H., Wang, Y., Zeng, Q., Zeng, Y.-Q., Liang, C.-L., Qiu, F., Nie, H., & Dai, Z. (2017). Suppression of allograft rejection by CD8+CD122+PD-1+ Tregs is dictated by their Fas ligand-initiated killing of effector T cells versus Fas-mediated own apoptosis. *Oncotarget*, *8*(15), 24187–24195. https://doi.org/10.18632/oncotarget.15551

Liu, L., Huang, X., Xu, C., Chen, C., Zhao, W., Li, D., Li, L., & Wang, L. (2020). Decidual - CD8 + T cells exhibit both residency and tolerance signatures modulated by decidual stromal cells. *Journal of Translational Medicine*, 1–14. https://doi.org/10.1186/s12967-020-02371-3

Lugli, E., Galletti, G., Boi, S. K., & Youngblood, B. A. (2021). *Stem, effector and hybrid states of memory CD8+ T cells*. *41*(1), 17–28. https://doi.org/10.1016/j.it.2019.11.004.Stem

Lv, G., Ying, L., Ma, W.-J., Jin, X., Zheng, L., Li, L., & Yang, Y. (2010). Dynamic analysis of CD127 expression on memory CD8 T cells from patients with chronic hepatitis B during telbivudine treatment. *Virology Journal*, *7*, 207. https://doi.org/10.1186/1743-422X-7-207

Maaten, L. van der, & Hinton, G. (2008). Visualising data using t-SNE. *Journal of Machine Learning Research*, *9*(86), 2579–2605.

Machicote, A., Podhorzer, A., Tolosa, E., Arck, P., Solano, M., & Fainboim, L. (2016). Characterization of a new subset of CD8+HLA-DR+ T cells in human decidua. In *Journal of Reproductive Immunology* (Vol. 115). https://doi.org/10.1016/j.jri.2016.04.009

Madeja, Z., Yadi, H., Apps, R., Boulenouar, S., Roper, S. J., Gardner, L., Moffett, A., Colucci, F., & Hemberger, M. (2011). Paternal MHC expression on mouse trophoblast affects uterine vascularization and fetal growth. *Proceedings of the National Academy of Sciences of the United States of America*, *108*(10), 4012–4017. https://doi.org/10.1073/pnas.1005342108

Male, V. (2021). *Medawar and the immunological paradox of pregnancy : in context*. *2*(October 2020), 1–5. https://doi.org/10.1093/oxfimm/iqaa006

Man, K., Gabriel, S. S., Liao, Y., Gloury, R., Preston, S., Henstridge, D. C., Pellegrini, M., Zehn, D., Berberich-Siebelt, F., Febbraio, M. A., Shi, W., & Kallies, A. (2017). Transcription Factor IRF4 Promotes CD8(+) T Cell Exhaustion and Limits the Development of Memory-like T Cells during Chronic Infection. *Immunity*, *47*(6), 1129-1141.e5. https://doi.org/10.1016/j.immuni.2017.11.021

Mangalam, A. K., Luckey, D., Giri, S., Smart, M., Pease, L. R., Rodriguez, M., & David, C. S. (2012). Two discreet subsets of CD8 T cells modulate PLP(91-110) induced experimental autoimmune encephalomyelitis in HLA-DR3 transgenic mice. *Journal of Autoimmunity*, *38*(4), 344–353. https://doi.org/10.1016/j.jaut.2012.02.004

Martin, M. D., & Badovinac, V. P. (2018). *Defining Memory CD8 T Cell*. *9*(November), 1–

10. https://doi.org/10.3389/fimmu.2018.02692
Menkhorst, E., Than, N. G., Jeschke, U., Barrientos, G., Szereday, L., Dveksler, G., & Blois, S. M. (2021). Medawar's PostEra: Galectins Emerged as Key Players During Fetal-Maternal Glycoimmune Adaptation. *Frontiers in Immunology*, *12*. https://doi.org/10.3389/fimmu.2021.784473
Mercier, F., Boulassel, M.-R., Yassine-Diab, B., Tremblay, C., Bernard, N.-F., Sekaly, R.-P., & Routy, J.-P. (2008). Persistent human immunodeficiency virus-1 antigenaemia affects the expression of interleukin-7Rα on central and effector memory CD4+ and CD8+ T cell subsets. *Clinical and Experimental Immunology*, *152*(1), 72–80. https://doi.org/10.1111/j.1365-2249.2008.03610.x
Messaoudi, I., Warner, J., & Nikolich-Zugich, J. (2006). Age-related CD8+ T cell clonal expansions express elevated levels of CD122 and CD127 and display defects in perceiving homeostatic signals. *Journal of Immunology (Baltimore, Md. : 1950)*, *177*(5), 2784–2792. https://doi.org/10.4049/jimmunol.177.5.2784
Miko, E., Barakonyi, A., Meggyes, M., & Szereday, L. (2021). The Role of Type I and Type II NKT Cells in Materno-Fetal Immunity. *Biomedicines*, *9*(12). https://doi.org/10.3390/biomedicines9121901
Min, B. (2018). Spontaneous T Cell Proliferation: A Physiologic Process to Create and Maintain Homeostatic Balance and Diversity of the Immune System. *Frontiers in Immunology*, *9*, 547. https://doi.org/10.3389/fimmu.2018.00547
Min, B., McHugh, R., Sempowski, G. D., Mackall, C., Foucras, G., & Paul, W. E. (2003). Neonates Support Lymphopenia-Induced Proliferation. *Immunity*, *18*(1), 131–140. https://doi.org/https://doi.org/10.1016/S1074-7613(02)00508-3
Mittelstadt, P. R., Monteiro, J. P., & Ashwell, J. D. (2012). Thymocyte responsiveness to endogenous glucocorticoids is required for immunological fitness. *The Journal of Clinical Investigation*, *122*(7), 2384–2394. https://doi.org/10.1172/JCI63067
Moffett, A., & Colucci, F. (2014). Uterine NK cells: active regulators at the maternal-fetal interface. *The Journal of Clinical Investigation*, *124*(5), 1872–1879. https://doi.org/10.1172/JCI68107
Moffett, A., Hiby, S. E., & Sharkey, A. M. (2015). The role of the maternal immune system in the regulation of human birthweight. *Philosophical Transactions of the Royal Society of London. Series B, Biological Sciences*, *370*(1663), 20140071. https://doi.org/10.1098/rstb.2014.0071
Moffett, A., & Shreeve, N. (2022). Local immune recognition of trophoblast in early human pregnancy: controversies and questions. *Nature Reviews Immunology*. https://doi.org/10.1038/s41577-022-00777-2
Moldenhauer, L. M., Diener, K. R., Hayball, J. D., & Robertson, S. A. (2017). An immunogenic phenotype in paternal antigen-specific CD8(+) T cells at embryo implantation elicits later fetal loss in mice. *Immunology and Cell Biology*, *95*(8), 705–715. https://doi.org/10.1038/icb.2017.41
Morita, K., Tsuda, S., Kobayashi, E., Hamana, H., & Tsuda, K. (2020). *Analysis of TCR Repertoire and PD-1 Expression in Decidual and Peripheral CD8 + T Cells Reveals Distinct Immune Mechanisms in Miscarriage and Preeclampsia*. *11*(June). https://doi.org/10.3389/fimmu.2020.01082
Morrish, E., & Ruland, J. (2022). Cytotoxic FCER1G+ innate-like T cells: new potential for tumour immunotherapy. *Signal Transduction and Targeted Therapy*, *7*(1), 204. https://doi.org/10.1038/s41392-022-01061-4
Muller, W. A. (2013). Getting leukocytes to the site of inflammation. *Veterinary Pathology*, *50*(1), 7–22. https://doi.org/10.1177/0300985812469883
Muñoz-Cruz, S., Togno-Pierce, C., & Morales-Montor, J. (2011). Non-reproductive effects of sex steroids: their immunoregulatory role. *Curr Top Med Chem*, *11*(13), 1714–1727.

Murphy, S. P., Tayade, C., Ashkar, A. A., Hatta, K., Zhang, J., & Croy, B. A. (2009). Interferon gamma in successful pregnancies. *Biology of Reproduction*, *80*(5), 848–859. https://doi.org/10.1095/biolreprod.108.073353

Naluyima, P., Lal, K. G., Costanzo, M. C., Kijak, G. H., Gonzalez, V. D., Blom, K., Eller, L. A., Creegan, M., Hong, T., Kim, D., Quinn, T. C., Björkström, N. K., Ljunggren, H.-G., Serwadda, D., Katabira, E. T., Sewankambo, N. K., Gray, R. H., Baeten, J. M., Michael, N. L., … Eller, M. A. (2019). Terminal Effector CD8 T Cells Defined by an IKZF2(+)IL-7R(-) Transcriptional Signature Express FcγRIIIA, Expand in HIV Infection, and Mediate Potent HIV-Specific Antibody-Dependent Cellular Cytotoxicity. *Journal of Immunology (Baltimore, Md. : 1950)*, *203*(8), 2210–2221. https://doi.org/10.4049/jimmunol.1900422

Nancy, P., Tagliani, E., Tay, C. S., Asp, P., Levy, D. E., & Erlebacher, A. (2012). Chemokine gene silencing in decidual stromal cells limits T cell access to the maternal-fetal interface. *Science*, *336*(6086), 1317–1321. https://doi.org/10.1126/science.1220030

Niederlova, V., Tsyklauri, O., Chadimova, T., & Stepanek, O. (2021). *CD8 + Tregs revisited : A heterogeneous population with different phenotypes and properties*. 512–530. https://doi.org/10.1002/eji.202048614

O'Garra, A., Vieira, P. L., Vieira, P., & Goldfeld, A. E. (2004). IL-10-producing and naturally occurring CD4+ Tregs: limiting collateral damage. *The Journal of Clinical Investigation*, *114*(10), 1372–1378. https://doi.org/10.1172/JCI23215

Okuno, Y., Murakoshi, A., Negita, M., Akane, K., Kojima, S., & Suzuki, H. (2013). CD8+CD122+regulatory T cells contain clonally expanded cells with identical CDR3 sequences of the T-cell receptor β-chain. *Immunology*, *139*(3), 309–317. https://doi.org/10.1111/imm.12067

Ono, M., & Maruyama, T. (2015). Stem Cells in Myometrial Physiology. *Seminars in Reproductive Medicine*, *33*(5), 350–356. https://doi.org/10.1055/s-0035-1563602

Pandiyan, P., Zheng, L., Ishihara, S., Reed, J., & Lenardo, M. J. (2007). CD4+CD25+Foxp3+ regulatory T cells induce cytokine deprivation-mediated apoptosis of effector CD4+ T cells. *Nature Immunology*, *8*(12), 1353–1362. https://doi.org/10.1038/ni1536

Pardoll, D. M. (2012). The blockade of immune checkpoints in cancer immunotherapy. *Nature Reviews Cancer*, *12*(4), 252–264. https://doi.org/10.1038/nrc3239

Parr, E. L., Tung, H. N., & Parr, M. B. (1987). Apoptosis as the Mode of Uterine Epithelial Cell Death during Embryo Implantation in Mice and Rats1. *Biology of Reproduction*, *36*(1), 211–225. https://doi.org/10.1095/biolreprod36.1.211

Penman, B. S., Moffett, A., Chazara, O., Gupta, S., & Parham, P. (2016). Reproduction, infection and killer-cell immunoglobulin-like receptor haplotype evolution. *Immunogenetics*, *68*, 755–764.

Perchellet, A. L., Jasti, S., & Petroff, M. G. (2013). Maternal CD4+ and CD8+ T Cell Tolerance Towards a Fetal Minor Histocompatibility Antigen in T Cell Receptor Transgenic Mice1. *Biology of Reproduction*, *89*(4), 1–12. https://doi.org/10.1095/biolreprod.113.110445

Philip, M., & Schietinger, A. (2019). Heterogeneity and fate choice: T cell exhaustion in cancer and chronic infections. *Current Opinion in Immunology*, *58*(i), 98–103. https://doi.org/10.1016/j.coi.2019.04.014

Powell, R. M., Lissauer, D., Tamblyn, J., Beggs, A., Cox, P., Moss, P., & Kilby, M. D. (2017). *Decidual T cells exhibit a highly differentiated phenotype and demonstrate potential fetal-specificity and a strong transcriptional response to interferon*. *199*(10), 3406–3417. https://doi.org/10.4049/jimmunol.1700114.Decidual

Qin, S., Xu, L., Yi, M., Yu, S., Wu, K., & Luo, S. (2019). Novel immune checkpoint targets: moving beyond PD-1 and CTLA-4. *Molecular Cancer*, *18*(1), 155. https://doi.org/10.1186/s12943-019-1091-2

Rahim, M. M., Tu, M., Mahmoud, A., Wight, A., Abou-Samra, E., Lima, P., & Makrigiannis, A. (2014). Ly49 Receptors: Innate and Adaptive Immune Paradigms. *Frontiers in Immunology*, *5*. https://doi.org/10.3389/fimmu.2014.00145

Rapaport, A. S., Schriewer, J., Gilfillan, S., Hembrador, E., Crump, R., Plougastel, B. F., Wang, Y., Le Friec, G., Gao, J., Cella, M., Pircher, H., Yokoyama, W. M., Buller, R. M. L., & Colonna, M. (2015). The Inhibitory Receptor NKG2A Sustains Virus-Specific $CD8^+$ T Cells in Response to a Lethal Poxvirus Infection. *Immunity*, *43*(6), 1112–1124. https://doi.org/10.1016/j.immuni.2015.11.005

Redline, R. W., & Lu, C. Y. (1989). Localization of fetal major histocompatibility complex antigens and maternal leukocytes in murine placenta. Implications for maternal-fetal immunological relationship. *Laboratory Investigation*, *61*, 27–36.

Rendell, V., Bath, N. M., & Brennan, T. V. (2020). Medawar's Paradox and Immune Mechanisms of Fetomaternal Tolerance. *OBM Transplant*, *4*(1). https://doi.org/10.21926/obm.transplant.2001104.Medawar

Rifa'i, M., Kawamoto, Y., Nakashima, I., & Suzuki, H. (2004). Essential Roles of $CD8^+$ $CD122^+$ Regulatory T Cells in the Maintenance of T Cell Homeostasis. *The Journal of Experimental Medicine*, *200*(9), 1123–1134. https://doi.org/10.1084/jem.20040395

Robinson, D. P., Hall, O. J., Nilles, T. L., Bream, J. H., & Klein, S. L. (2014). 17β-estradiol protects females against influenza by recruiting neutrophils and increasing virus-specific CD8 T cell responses in the lungs. *Journal of Virology*, *88*(9), 4711–4720. https://doi.org/10.1128/JVI.02081-13

Rosato, P. C., Wijeyesinghe, S., Stolley, J. M., & Masopust, D. (2020). *Integrating resident memory into T cell differentiation models*. 35–42. https://doi.org/10.1016/j.coi.2020.01.001.Integrating

Ruscher, R., Kummer, R. L., Lee, Y. J., Jameson, S. C., & Hogquist, K. A. (2017). CD8αα intraepithelial lymphocytes arise from two main thymic precursors. *Nature Immunology*, *18*(7), 771–779. https://doi.org/10.1038/ni.3751

Saligrama, N., Zhao, F., Sikora, M. J., Serratelli, W. S., Fernandes, R. A., Louis, D. M., Yao, W., Ji, X., Idoyaga, J., Mahajan, V. B., Steinmetz, L. M., Chien, Y. H., Hauser, S. L., Oksenberg, J. R., Garcia, K. C., & Davis, M. M. (2019). Opposing T cell responses in experimental autoimmune encephalomyelitis. *Nature*, *572*(7770), 481–487. https://doi.org/10.1038/s41586-019-1467-x

Salou, M., Nicol, B., Garcia, A., & Laplaud, D.-A. (2015). Involvement of CD8+ T Cells in Multiple Sclerosis. *Frontiers in Immunology*, *6*, 2–10. https://doi.org/10.3389/fimmu.2015.00604

Sanguansermsri, D., & Pongcharoen, S. (2008). Pregnancy immunology: decidual immune cells. *Asian Pacific Journal of Allergy and Immunology*, *26*(2–3), 171–181.

Sasaki, Y., Sakai, M., S, M., S, H., A, S., & Saito S. (2004). Decidual and peripheral blood CD4 + CD25 + regulatory T cells in early pregnancy subjects and spontaneous abortion cases. *Mol Hum Reprod*, *10*(5), 347–353. https://doi.org/10.1093/molehr/gah044

Schumann, J., Stanko, K., Schliesser, U., Appelt, C., & Sawitzki, B. (2015). Differences in CD44 Surface Expression Levels and Function Discriminates IL-17 and IFN-γ Producing Helper T Cells. *PloS One*, *10*(7), e0132479. https://doi.org/10.1371/journal.pone.0132479

Sharapova, T. N., Ivanova, O. K., Soshnikova, N. V, Romanova, E. A., Sashchenko, L. P., & Yashin, D. V. (2017). Innate Immunity Protein Tag7 Induces 3 Distinct Populations of Cytotoxic Cells That Use Different Mechanisms to Exhibit Their Antitumor Activity on Human Leukocyte Antigen-Deficient Cancer Cells. *Journal of Innate Immunity*, *9*(6), 598–608. https://doi.org/10.1159/000479382

Sharapova, T. N., Romanova, E. A., Sashchenko, L. P., & Yashin, D. V. (2018). Tag7 (PGLYRP1) Can Induce an Emergence of the CD3+CD4+CD25+CD127+ Cells with

Antitumor Activity. *Journal of Immunology Research*, *2018*, 4501273. https://doi.org/10.1155/2018/4501273

Sharkey, D. J., Tremellen, K. P., Jasper, M. J., Gemzell-Danielsson, K., & Robertson, S. A. (2012). Seminal Fluid Induces Leukocyte Recruitment and Cytokine and Chemokine mRNA Expression in the Human Cervix after Coitus. *The Journal of Immunology*, *188*(5), 2445–2454. https://doi.org/10.4049/jimmunol.1102736

Shen, Z., Garcia, M. R., Patel, M. V, & Wira, C. R. (2021). Direct and Indirect endocrine - mediated suppression of human endometrial CD8 + T cell cytotoxicity. *Scientific Reports*, *11*(1773), 1–14. https://doi.org/10.1038/s41598-021-81380-8

Shi, Z., Okuno, Y., Rifa'i, M., Endharti, A. T., Akane, K., Isobe, K. I., & Suzuki, H. (2009). Human CD8+CXCR3+ T cells have the same function as murine CD8+CD122+ Treg. *European Journal of Immunology*, *39*(8), 2106–2119. https://doi.org/10.1002/eji.200939314

Shimokawa, C., Kato, T., Takeuchi, T., Ohshima, N., Furuki, T., Ohtsu, Y., Suzue, K., Imai, T., Obi, S., Olia, A., Izumi, T., Sakurai, M., Arakawa, H., Ohno, H., & Hisaeda, H. (2020). CD8+ regulatory T cells are critical in prevention of autoimmune-mediated diabetes. *Nature Communications*, *11*(1), 1922. https://doi.org/10.1038/s41467-020-15857-x

Shreeve, N., Depierreux, D., Hawkes, D., Traherne, J. A., Sovio, U., Huhn, O., Jayaraman, J., Horowitz, A., Ghadially, H., Perry, J. R. B., Moffett, A., Sled, J. G., Sharkey, A. M., & Colucci, F. (2021). The CD94/NKG2A inhibitory receptor educates uterine NK cells to optimize pregnancy outcomes in humans and mice. *Immunity*, *54*(6), 1231-1244.e4. https://doi.org/10.1016/j.immuni.2021.03.021

Shytikov, D., Rohila, D., Li, D., Wang, P., Jiang, M., Zhang, M., Xu, Q., & Lu, L. (2021). Functional Characterization of Ly49(+)CD8 T-Cells in Both Normal Condition and During Anti-Viral Response. *Frontiers in Immunology*, *11*, 602783. https://doi.org/10.3389/fimmu.2020.602783

Slutsky, R., Romero, R., Xu, Y., Galaz, J., Miller, D., Done, B., Tarca, A. L., Gregor, S., Hassan, S. S., & Leng, Y. (2019). *Exhausted and Senescent T Cells at the Maternal-Fetal Interface in Preterm and Term Labor*. *2019*. https://doi.org/10.1155/2019/3128010

Smith, T., & Kumar, V. (2008). Revival of CD8+ Treg-mediated suppression. *Trends Immunol*, *29*(7), 337–342.

Sojka, D. K., Yang, L., & Yokoyama, W. M. (2019). Uterine Natural Killer Cells. *Frontiers in Immunology*, *10*, 960. https://doi.org/10.3389/fimmu.2019.00960

Solano, M. E. (2019). Decidual immune cells: Guardians of human pregnancies. *Best Practice & Research. Clinical Obstetrics & Gynaecology*, *60*, 3–16.

Solano, M. E., & Arck, P. C. (2020). Steroids, Pregnancy and Fetal Development. *Frontiers in Immunology*, *10*(January), 1–13. https://doi.org/10.3389/fimmu.2019.03017

Solano, M. E., Kowal, M. K., O'Rourke, G. E., Horst, A. K., Modest, K., Plösch, T., Barikbin, R., Remus, C., Berger, R. ., Jago, C., Ho, H., Sass, G., Parker, V. ., Lydon, J. ., DeMayo, F. ., Hecher, K., Karimi, K., & Arck, P. . (2015). Progesterone and HMOX-1 promote fetal growth by CD8+ T cell modulation. *Journal of Clinical Investigation*, *125*(4), 1726–1738. https://doi.org/10.1172/JCI68140

Solano, M. E., Sander, V. A., Ho, H., Motta, A. B., & Arck, P. C. (2011). Systemic inflammation, cellular influx and up-regulation of ovarian VCAM-1 expression in a mouse model of polycystic ovary syndrome (PCOS). *Journal of Reproductive Immunology*, *92*(1–2), 33–44. https://doi.org/10.1016/j.jri.2011.09.003

Solders, M., Gorchs, L., Erkers, T., Lundell, A. C., Nava, S., Gidlöf, S., Tiblad, E., Magalhaes, I., & Kaipe, H. (2017). MAIT cells accumulate in placental intervillous space and display a highly cytotoxic phenotype upon bacterial stimulation. *Scientific Reports*, *7*(1), 1–13. https://doi.org/10.1038/s41598-017-06430-6

Southcombe, J. H., Mounce, G., Mcgee, K., Elghajiji, A., Brosens, J., & Quenby, S. (2017). An altered endometrial CD8 tissue resident memory T cell population in recurrent miscarriage. *Nature Publishing Group*, *October 2016*, 1–8. https://doi.org/10.1038/srep41335

Speiser, D. E., Utzschneider, D. T., Oberle, S. G., Münz, C., Romero, P., & Zehn, D. (2014). T cell differentiation in chronic infection and cancer: functional adaptation or exhaustion? *Nat. Rev. Immunol*, *14*(11), 768–774.

Stallmach, T., Hebisch, G., Orban, O., & Lü, X. (1999). Aberrant positioning of trophoblast and lymphocytes in the feto-maternal interface with pre-eclampsia. *Virchows Arch*, *434*(3), 207–211.

Stevens Brentjens, L., Habets, D., Den Hartog, J., Al-Nasiry, S., Wieten, L., Morré, S., Van Montfoort, A., Romano, A., & van Golde, R. (2022). Endometrial factors in the implantation failure spectrum: protocol of a MUltidisciplinary observational cohort study in women with Repeated Implantation failure and recurrent Miscarriage (MURIM Study). *BMJ Open*, *12*(6), e056714. https://doi.org/10.1136/bmjopen-2021-056714

Suzuki, Y., Sutoh, M., Hatakeyama, S., Mori, K., Yamamoto, H., Koie, T., Saitoh, H., Yamaya, K., Funyu, T., Habuchi, T., Arai, Y., Fukuda, M., Ohyama, C., & Tsuboi, S. (2012). MUC1 carrying core 2 O-glycans functions as a molecular shield against NK cell attack, promoting bladder tumor metastasis. *International Journal of Oncology*, *40*(6), 1831–1838. https://doi.org/10.3892/ijo.2012.1411

Svensson-Arvelund, J., Mehta, R. B., Lindau, R., Mirrasekhian, E., Rodriguez-Martinez, H., Berg, G., Lash, G. E., Jenmalm, M. C., & Ernerudh, J. (2015). The human fetal placenta promotes tolerance against the semiallogeneic fetus by inducing regulatory T cells and homeostatic M2 macrophages. *Journal of Immunology (Baltimore, Md. : 1950)*, *194*(4), 1534–1544. https://doi.org/10.4049/jimmunol.1401536

Szabo, P. A., Levitin, H. M., Miron, M., Snyder, M. E., Senda, T., Yuan, J., Cheng, Y. L., Bush, E. C., Dogra, P., Thapa, P., Farber, D. L., & Sims, P. A. (2019). Single-cell transcriptomics of human T cells reveals tissue and activation signatures in health and disease. *Nature Communications*, *10*(1), 4706. https://doi.org/10.1038/s41467-019-12464-3

Tanaka, R., Tainaka, M., Ota, T., Mizuguchi, N., Kato, H., Urabe, S., Chen, Y., Fustin, J.-M., Yamaguchi, Y., Doi, M., Hamada, S., & Okamura, H. (2011). Accurate determination of S-phase fraction in proliferative cells by dual fluorescence and peroxidase immunohistochemistry with 5-bromo-2'-deoxyuridine (BrdU) and Ki67 antibodies. *The Journal of Histochemistry and Cytochemistry : Official Journal of the Histochemistry Society*, *59*(8), 791–798. https://doi.org/10.1369/0022155411411090

Tian, T., Yang, Z., & Li, X. (2021). Tissue clearing technique: Recent progress and biomedical applications. *Journal of Anatomy*, *238*(2), 489–507. https://doi.org/10.1111/joa.13309

Tilburgs, T., Roelen, D. L., van der Mast, B. J., de Groot-Swings, G. M., Kleijburg, C., Scherjon, S. A., & Claas, F. H. (2008). Evidence for a selective migration of fetus-specific CD4+CD25bright regulatory T cells from the peripheral blood to the decidua in human pregnancy. *Journal of Immunology (Baltimore, Md. : 1950)*, *180*(8), 5737–5745. https://doi.org/10.4049/jimmunol.180.8.5737

Tilburgs, T., Scherjon, S., Roelen, D., & Claas, F. (2009). Decidual CD8+CD28- T cells express CD103 but not perforin. *Hum Immunol*, *70*(2), 96–100.

Tilburgs, T., Schonkeren, D., Eikmans, M., Nagtzaam, N. M., Datema, G., Swings, G. M., Prins, F., Lith, J. M. Van, Mast, B. J. Van Der, Roelen, L., Scherjon, S. A., & Claas, F. H. (2010). *Human Decidual Tissue Contains Differentiated CD8 + Effector-Memory T Cells with Unique Properties*. https://doi.org/10.4049/jimmunol.0903597

Tilburgs, T., & Strominger, J. L. (2013). CD8+ Effector T Cells at the Fetal-Maternal

Interface, Balancing Fetal Tolerance and Antiviral Immunity. *American Journal of Reproductive Immunology*, *69*(4), 395–407. https://doi.org/10.1111/aji.12094

Tilburgs, T., van der Mast, B. J., Nagtzaam, N. M. A., Roelen, D. L., Scherjon, S. A., & Claas, F. H. J. (2009). Expression of NK cell receptors on decidual T cells in human pregnancy. *Journal of Reproductive Immunology*, *80*(1–2), 22–32. https://doi.org/10.1016/j.jri.2009.02.004

Trautmann, A., Rückert, B., Schmid-Grendelmeier, P., Niederer, E., Bröcker, E.-B., Blaser, K., & Akdis, C. A. (2003). Human CD8 T cells of the peripheral blood contain a low CD8 expressing cytotoxic/effector subpopulation. *Immunology*, *108*(3), 305–312. https://doi.org/10.1046/j.1365-2567.2003.01590.x

Tsuboi, S., Sutoh, M., Hatakeyama, S., Hiraoka, N., Habuchi, T., Horikawa, Y., Hashimoto, Y., Yoneyama, T., Mori, K., Koie, T., Nakamura, T., Saitoh, H., Yamaya, K., Funyu, T., Fukuda, M., & Ohyama, C. (2011). A novel strategy for evasion of NK cell immunity by tumours expressing core2 O-glycans. *The EMBO Journal*, *30*(15), 3173–3185. https://doi.org/10.1038/emboj.2011.215

Tsuda, S., Zhang, X., Hamana, H., Shima, T., Ushijima, A., Tsuda, K., Muraguchi, A., Kishi, H., & Saito, S. (2018). Clonally Expanded Decidual Effector Regulatory T Cells Increase in Late Gestation of Normal Pregnancy, but Not in Preeclampsia, in Humans. *Frontiers in Immunology*, *9*, 1934. https://doi.org/10.3389/fimmu.2018.01934

van der Zwan, A., Bi, K., Norwitz, E. R., Crespo, Â. C., Claas, F. H. J., Strominger, J. L., & Tilburgs, T. (2018). Mixed signature of activation and dysfunction allows human decidual CD8 + T cells to provide both tolerance and immunity. *Proceedings of the National Academy of Sciences*, *115*(2), 201713957. https://doi.org/10.1073/pnas.1713957115

van der Zwan, A., van der Meer-Prins, E. M. W., van Miert, P. P. M. C., van den Heuvel, H., Anholts, J. D. H., Roelen, D. L., Claas, F. H. J., & Heidt, S. (2018). Cross-Reactivity of Virus-Specific CD8+ T Cells Against Allogeneic HLA-C: Possible Implications for Pregnancy Outcome. *Frontiers in Immunology*, *9*, 2880. https://doi.org/10.3389/fimmu.2018.02880

van Kampen, C. A., Versteeg-vd Voort Maarschalk, M. F. J., Langerak-Langerak, J., Roelen, D. L., & Claas, F. H. J. (2002). Kinetics of the pregnancy-induced humoral and cellular immune response against the paternal HLA class I antigens of the child. *Human Immunology*, *63*(6), 452–458. https://doi.org/https://doi.org/10.1016/S0198-8859(02)00396-8

Varyté, G., Zakarevicienė2, J., Ramašauskaitė, D., Laužikienė, D., & Arlauskienė, A. (2020). Pregnancy and Multiple Sclerosis : An Update on the Disease Modifying Treatment Strategy and a Review of Pregnancy ' s Impact on Disease Activity. *Medicina*, *56*(49).

Vento-tormo, R., Efremova, M., Botting, R. A., Turco, M. Y., Vento-tormo, M., Meyer, K. B., Park, J., Stephenson, E., Polański, K., Goncalves, A., Gardner, L., Holmqvist, S., Henriksson, J., Zou, A., Sharkey, A. M., Millar, B., Innes, B., Wood, L., Ivarsson, M. A., … Rebecca, P. (2018). *Single-cell reconstruction of the early maternal – fetal interface in humans*. https://doi.org/10.1038/s41586-018-0698-6

Verdeil, G. (2016). MAF drives CD8(+) T-cell exhaustion. *Oncoimmunology*, *5*(2), e1082707. https://doi.org/10.1080/2162402X.2015.1082707

Volarevic, V., Zdravkovic, N., Harrell, C. R., Arsenijevic, N., Fellabaum, C., Djonov, V., Lukic, M. L., & Simovic Markovic, B. (2019). Galectin-3 Regulates Indoleamine-2,3-dioxygenase-Dependent Cross-Talk between Colon-Infiltrating Dendritic Cells and T Regulatory Cells and May Represent a Valuable Biomarker for Monitoring the Progression of Ulcerative Colitis. *Cells*, *8*(7). https://doi.org/10.3390/cells8070709

Wang, C.-Y., Fang, Y.-X., Chen, G.-H., Jia, H.-J., Zeng, S., He, X.-B., Feng, Y., Li, S.-J., Jin, Q.-W., Cheng, W.-Y., & Jing, Z.-Z. (2017). Analysis of the CDR3 length repertoire and

the diversity of T cell receptor α and β chains in swine CD4+ and CD8+ T lymphocytes. *Molecular Medicine Reports*, *16*(1), 75–86. https://doi.org/10.3892/mmr.2017.6601

Wang, S. C., Li, Y. H., Piao, H. L., Hong, X. W., Zhang, D., Xu, Y. Y., Tao, Y., Wang, Y., Yuan, M. M., Li, D. J., & Du, M. R. (2015). PD-1 and Tim-3 pathways are associated with regulatory CD8+ T-cell function in decidua and maintenance of normal pregnancy. *Cell Death and Disease*, *6*(5), 1–10. https://doi.org/10.1038/cddis.2015.112

Wang, S., Sun, F., Li, M., Qian, J., Chen, C., Wang, M., Zang, X., Li, D., Yu, M., & Du, M. (2019). The appropriate frequency and function of decidual Tim-3+CTLA-4+CD8+ T cells are important in maintaining normal pregnancy. *Cell Death and Disease*, *10*(6). https://doi.org/10.1038/s41419-019-1642-x

Wensink, A. C., Hack, C. E., & Bovenschen, N. (2015). Granzymes Regulate Proinflammatory Cytokine Responses. *The Journal of Immunology*, *194*(2), 491–497. https://doi.org/10.4049/jimmunol.1401214

White HD, Crassi KM, Givan AL, Stern JE, Gonzalez JL, Memoli VA, Green WR, & Wira CR. (1997). CD3+ CD8+ CTL activity within the human female reproductive tract: influence of stage of the menstrual cycle and menopause. *J Immunol*, *158*, 3017–3027.

Williams, P., Searle, R., Robson, S., Innes, B., & Bulmer, J. (2009). Decidual leucocyte populations in early to late gestation normal human pregnancy. *J Reprod Immunol*, *82*(1), 24–31.

Winterberg, P. D., Robertson, J. M., Kelleman, M. S., George, R. P., & Ford, M. L. (2019). T Cells Play a Causal Role in Diastolic Dysfunction during Uremic Cardiomyopathy. *Journal of the American Society of Nephrology : JASN*, *30*(3), 407–420. https://doi.org/10.1681/ASN.2017101138

Wykes, M. N., & Lewin, S. R. (2018). Immune checkpoint blockade in infectious diseases. *Nature Reviews Immunology*, *18*(2), 91–104. https://doi.org/10.1038/nri.2017.112

Wynn, T. A., & Vannella, K. M. (2016). Macrophages in Tissue Repair, Regeneration, and Fibrosis. *Immunity*, *44*(3), 450–462. https://doi.org/10.1016/j.immuni.2016.02.015

Xu, H., Yan, Y., Williams, M. S., Carey, G. B., Yang, J., Li, H., Zhang, G.-X., & Rostami, A. (2010). MS4a4B, a CD20 homologue in T cells, inhibits T cell propagation by modulation of cell cycle. *PloS One*, *5*(11), e13780. https://doi.org/10.1371/journal.pone.0013780

Xu, W., & Larbi, A. (2017). Markers of T Cell Senescence in Humans. *International Journal of Molecular Sciences*, *18*(8), 1–13. https://doi.org/10.3390/ijms18081742

Xu, Y., Wang, S., Lin, Y., & Du, M. (2017). Tim-3 and PD-1 regulate CD8+ T cell function to maintain early pregnancy in mice. *Journal of Reproduction and Development*, *63*(3), 289–294.

Yakut, S., Toru, H. S., Çetin, Z., Özel, D., Şimşek, M., Mendilcioğlu, İ., & Lüleci, G. (2015). Chromosome abnormalities identified in 457 spontaneous abortions and their histopathological findings. *Turk Patoloji Dergisi*, *31*(2), 111–118. https://doi.org/10.5146/tjpath.2015.01303

Yang, S., Liu, F., Wang, Q. J., Rosenberg, S. A., & Morgan, R. A. (2011). *The Shedding of CD62L (L-Selectin) Regulates the Acquisition of Lytic Activity in Human Tumor Reactive T Lymphocytes*. *6*(7). https://doi.org/10.1371/journal.pone.0022560

Yang, X., Bam, M., Becker, W., Nagarkatti, P. S., & Nagarkatti, M. (2020). Long Noncoding RNA AW112010 Promotes the Differentiation of Inflammatory T Cells by Suppressing IL-10 Expression through Histone Demethylation. *Journal of Immunology (Baltimore, Md. : 1950)*, *205*(4), 987–993. https://doi.org/10.4049/jimmunol.2000330

Yao, Y., Xu, X.-H., & Jin, L. (2019). Macrophage Polarization in Physiological and Pathological Pregnancy. *Frontiers in Immunology*, *10*. https://doi.org/10.3389/fimmu.2019.00792

Zeng, W., Liu, X., Liu, Z., Zheng, Y., Yu, T., Fu, S., Li, X., Zhang, J., Zhang, S., Ma, X., Liu,

X. R., Qin, X., Khanniche, A., Zhang, Y., Tian, F., & Lin, Y. (2018). Deep surveying of the transcriptional and alternative splicing signatures for decidual CD8+T cells at the first trimester of human healthy pregnancy. *Frontiers in Immunology*, *9*(MAY), 1–16. https://doi.org/10.3389/fimmu.2018.00937

Zhang, N., & Bevan, M. J. (2011). CD8+ T Cells: Foot Soldiers of the Immune System. *Immunity*, *35*(2), 161–168. https://doi.org/10.1016/j.immuni.2011.07.010

Zhao, H., Azuma, J., Kalish, F., Wong, R. J., & Stevenson, D. K. (2011). Maternal Heme Oxygenase 1 Regulates Placental Vasculature Development via Angiogenic Factors in Mice1. *Biology of Reproduction*, *85*(5), 1005–1012. https://doi.org/10.1095/biolreprod.111.093039

10 Appendix

Appendix 1: Estrous cycle in virgin mice.

Total counts of leucocytes, T cells, CD8+ T cells and CD8+CD122+ T cells (A), as well as frequency of CD122 expression in CD8+ T cells was evaluated across the four stages of the estrous cycle (B): Proestrus (PE), Estrus (E), Metaestrus (ME) and Diestrus (DE). High variability was observed within each estrous cycle stage, thus no significant differences were observed across the four stages of the estrus cycle. However, CD122 percentages seem slightly higher in the estrus stage, the stage when ovulation takes place, which might be modulated by recent peak in the pregnancy hormones follicular stimulating hormone, luteinizing hormone, progesterone, and estradiol, which might reach statistical significance with higher number of samples.

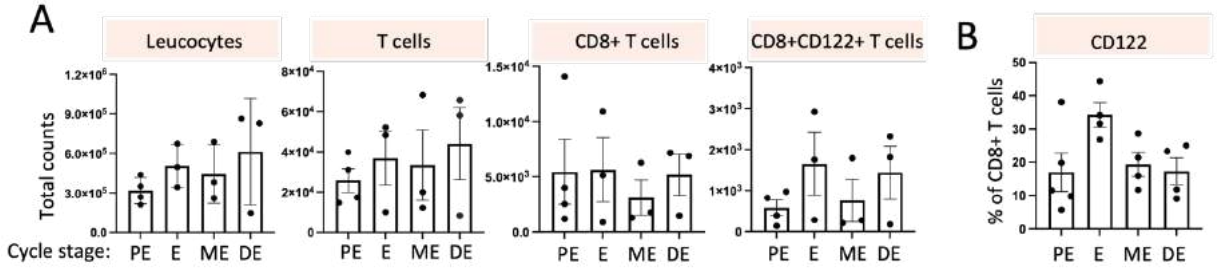

Appendix 2: Processing and integration of single-cell RNA sequencing data of blood and uterine samples on GD 14.5

The raw data from single-cell RNA sequencing was pre-processed by Dr. Nicholas Strieder, as a collaboration with the RCI NGS core facility at the University Hospital Regensburg. The data was first pre-processed using Cell Ranger software and further processed by Seurat. The quality of the data was assessed and found to be of satisfactory quality for analysis. The data was cleaned and filtered so that a threshold for number of genes per cell , mitochondrial content and doublets were filtered out of the dataset. The filtered data was normalized, scaled and principal components were calculated and assessed. The two samples (blood and uterus, here referred as decidua) were integrated by the function Harmony, in order to correctly compare the cells from the two samples. Thereafter, each sample was separated by the use of the hashtagging antibody, enabling a visualisation of cells from each mouse in each tissue (three blood samples and three uterine samples: n=3). The ribosomal percentage was further visualised in each cluster generated by Seurat.

QC_report

Inma Hernandez & Nicholas Strieder

1. Quality plots

```
## [1] "2022-08-06"
```

```
## multicore:
## - args: function (..., envir = parent.frame(), workers = 6)
## - tweaked: TRUE
## - call: plan("multicore", workers = 6)
```

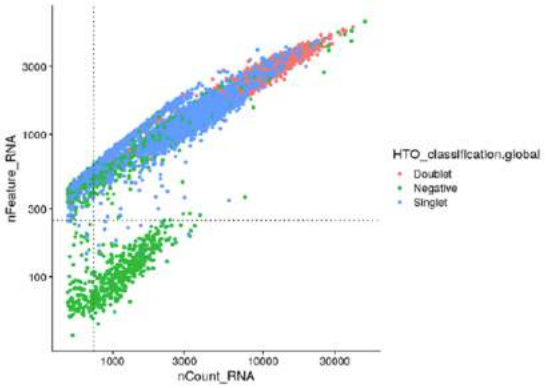


```
##
##                 Doublet Mouse1 Mouse2 Mouse3 Negative
##   Blood-library     740   1186   1199   1103      439
##   Decidua-library   361    919   2103   1111      572
##
##                 Mouse1 Mouse2 Mouse3
##   Blood-library   1186   1199   1103
##   Decidua-library  919   2103   1111
```

```
##
##   Blood-library Decidua-library
##            3488             4133
```

QC Metrics

The main qc metrices for single cell data a number of genes per cell (aka nFeature_RNA), number of reads per cell (aka nCount_RNA) and percentage of Mitochondrial genes (percent.mt).

nCount and nFeature Statitics

orig.ident	group	nCount_RNAmean	nCount_RNAmedian	nFeature_RNAmean	nFeature_RNAmedian
Blood-library	Mouse1	5107.937	4925	1573.621	1566
Blood-library	Mouse2	4867.969	4790	1546.002	1542
Blood-library	Mouse3	4947.942	4868	1540.009	1536
Decidua-library	Mouse1	4025.676	3419	1414.292	1317
Decidua-library	Mouse2	4227.420	3693	1535.724	1460
Decidua-library	Mouse3	4244.386	3553	1486.525	1371

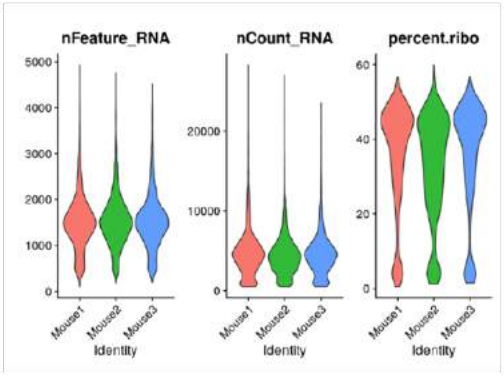

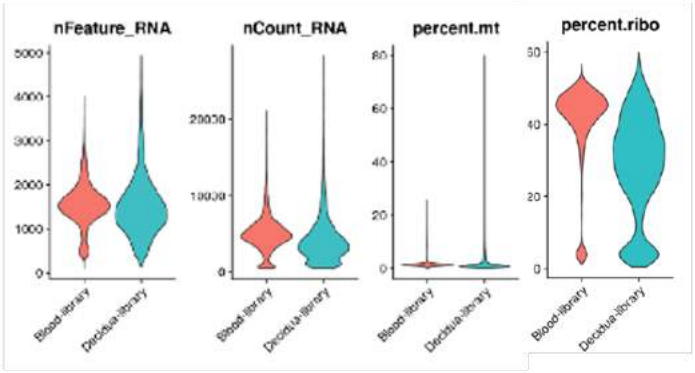

Distibution of number of counts and features

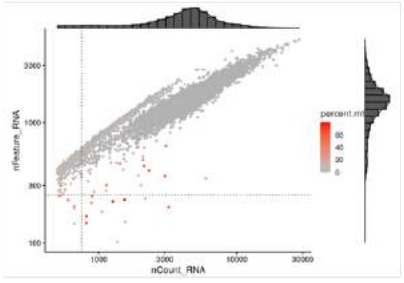

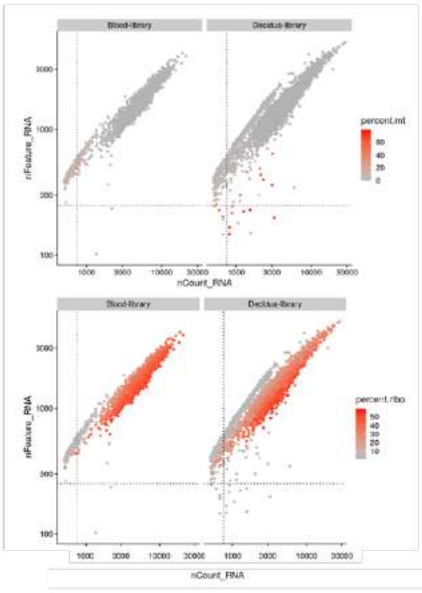

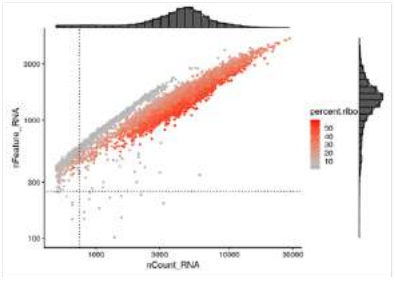

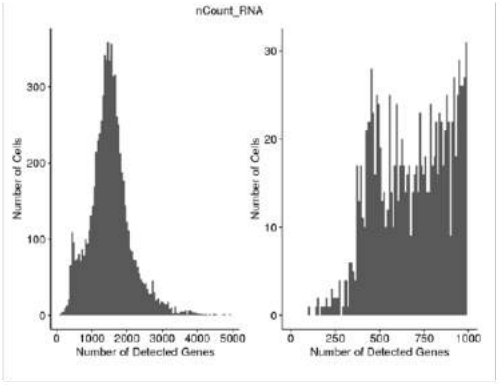

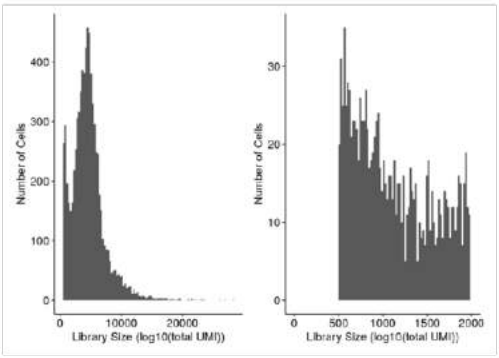

1a. After Filtering

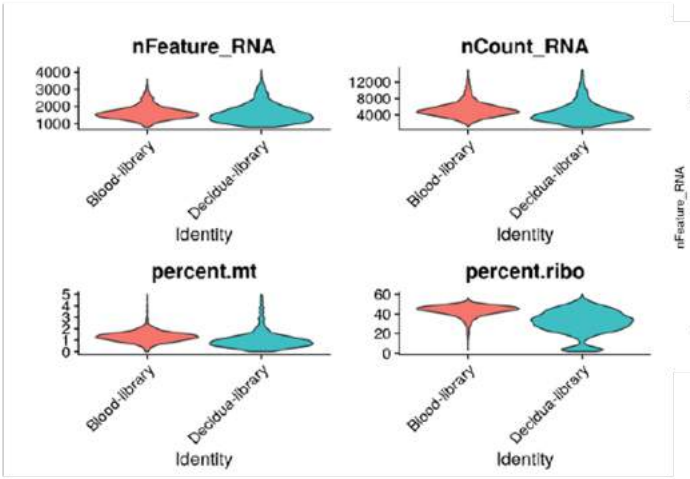

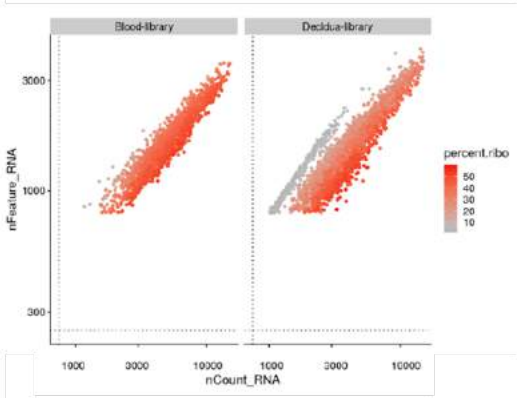

2. Normalization and PCA

```
## PC_ 1
## Positive:  S100a6, Ccl5, Lgals1, Itgb1, Cxcr3, Anxa2, S100a4, Ahnak, Nkg7, Top2a
##     Il2rb, Id2, Pclaf, Actg1, Mki67, Ly6c2, Cxcr6, Ctsw, Ly6a, Slamf7
##     Actb, Hopx, Birc5, Ctla2a, Klrk1, Vim, Stmn1, Ccna2, Lcp1, Rrm2
## Negative:  Ccr7, Klf2, Rps19, Rps20, Tsc22d3, Lef1, Rplp0, Rps26, Sell, Rps2
##     Igfbp4, Rflnb, Npm1, Fam241a, Il7r, Satb1, Ighm, Txnip, Actn1, Junb
##     Dapl1, Tmem108, Tdrp, Rps12, 2410006H16Rik, Gm43698, Cd55, Klf3, Rgcc, H2-Ob
## PC_ 2
## Positive:  Ms4a4b, Thy1, AW112010, Nkg7, Cd8a, Ccl5, Ctsw, Il7r, Klrd1, Rplp0
##     Hopx, Epsti1, Npm1, Ly6c2, Ifngr1, Tmsb10, Trbc2, Ctsd, S1fn1, Cst7
##     Lef1, Cxcr6, Hspa8, Cxcr3, Il2rb, Ifi47, Syx, Cd7, Hspa1b, Gimap4
## Negative:  H2-Ab1, Cd79a, H2-Eb1, H2-Aa, Cd74, Iglc2, Fcmr, Ly6d, H2-DMb2, Ebf1
##     Iglc3, Ms4a1, Mef2c, Bank1, Ly86, Cd79b, Napsa, Fcer2a, Cd19, Igkc
##     Blnk, Ctsh, Syk, Ighd, Fcrla, Mzb1, Siglecg, Cd81, Blk, Lyn
## PC_ 3
## Positive:  Birc5, Pclaf, Ccna2, Rrm2, Stmn1, Nusap1, Cdca3, Mki67, Ube2c, Kif11
##     Top2a, Spc24, Tpx2, Cenpf, Knl1, Esco2, Cdk1, Tubb5, Plk1, Cdca8
##     Cks1b, Neil3, Hist1h1b, Ccnb2, Aurkb, Ncapg, Hmmr, Nxd3, Hist1h2ae, Pbk
## Negative:  Ccl5, Malat1, Ly6a, Ahnak, Hopx, Itgb1, Ifit3, Fas1, Ptprc, S1fn5
##     Ccr5, Ifit1, Klrc1, Gzmk, S100a6, Klrk1, Cxcr3, Il10ra, Ccl4, Il2rb
##     Unc93b1, Cxcr6, Slamf7, Gm4070, Ctla2a, Ttc39b, Isg20, Rgs1, Dennd4a, Sorl1
## PC_ 4
## Positive:  Tmsb4x, Tmsb10, Pfn1, Cd52, Rps12, Rps26, Ppia, Myl6, Sh3bgrl3, Rps2
##     Rplp0, Actb, Fth1, Cfl1, Rps20, S100a10, Calm1, Rps19, Cyba, Crip1
##     S100a11, Gapdh, Nme2, Lgals1, Cox5b, AW112010, Sub1, Eif5a, Rbm3, Srgn
## Negative:  Malat1, Macf1, mt-Co1, Ptprc, mt-Atp6, Huwe1, Kmt2c, Jmjd1c, Kcnq1ot1, A
akl
##     Lyst, mt-Cytb, Etnk1, Hipk1, Lncpint, Chd2, Itga4, Dock2, Fry1, Herc1
##     Man2a1, Phip, Ugcg, Rnf111, Itpkb, Ankrd17, Pds5a, Ranbp2, mt-Nd4l, Atf7ip
## PC_ 5
## Positive:  Isg15, Ifit3, Ifit1, Rsad2, Usp18, Ifit3b, Irf7, Isg20, Sbp1, S1fn5
##     Bst2, Cmpk2, Rtp4, Ifi27l2a, Gbp6, Oasl2, Stat1, Iigp1, Ifih1, Xaf1
##     Phf11b, Cxcl10, Herc6, Oasla, Dhx58, Ifi208, Igtp, Trim30a, Ifi213, Daxx
## Negative:  Ahnak, Vim, Bcl2, S100a6, Lgals1, Ptpn4, Il2rb, Ifitm10, Syx, Ctsd
##     Ptprc, Il18r1, Osbpl3, Itgb1, S100a4, Hnrnpu, Flna, Thy1, Septl1, S1pr5
##     Cd160, Tmem163, Cx3cr1, Emp3, Lyst, Ccr2, Lgals3, Atp2b1, Efhd2, Klrc1
```

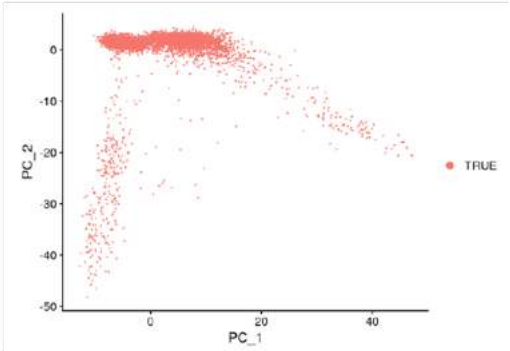

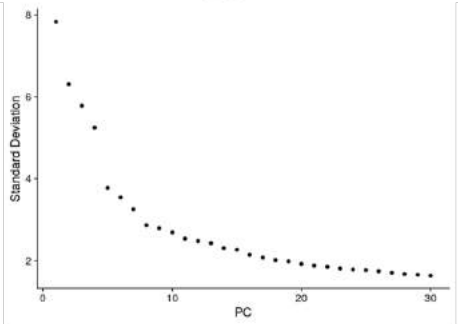

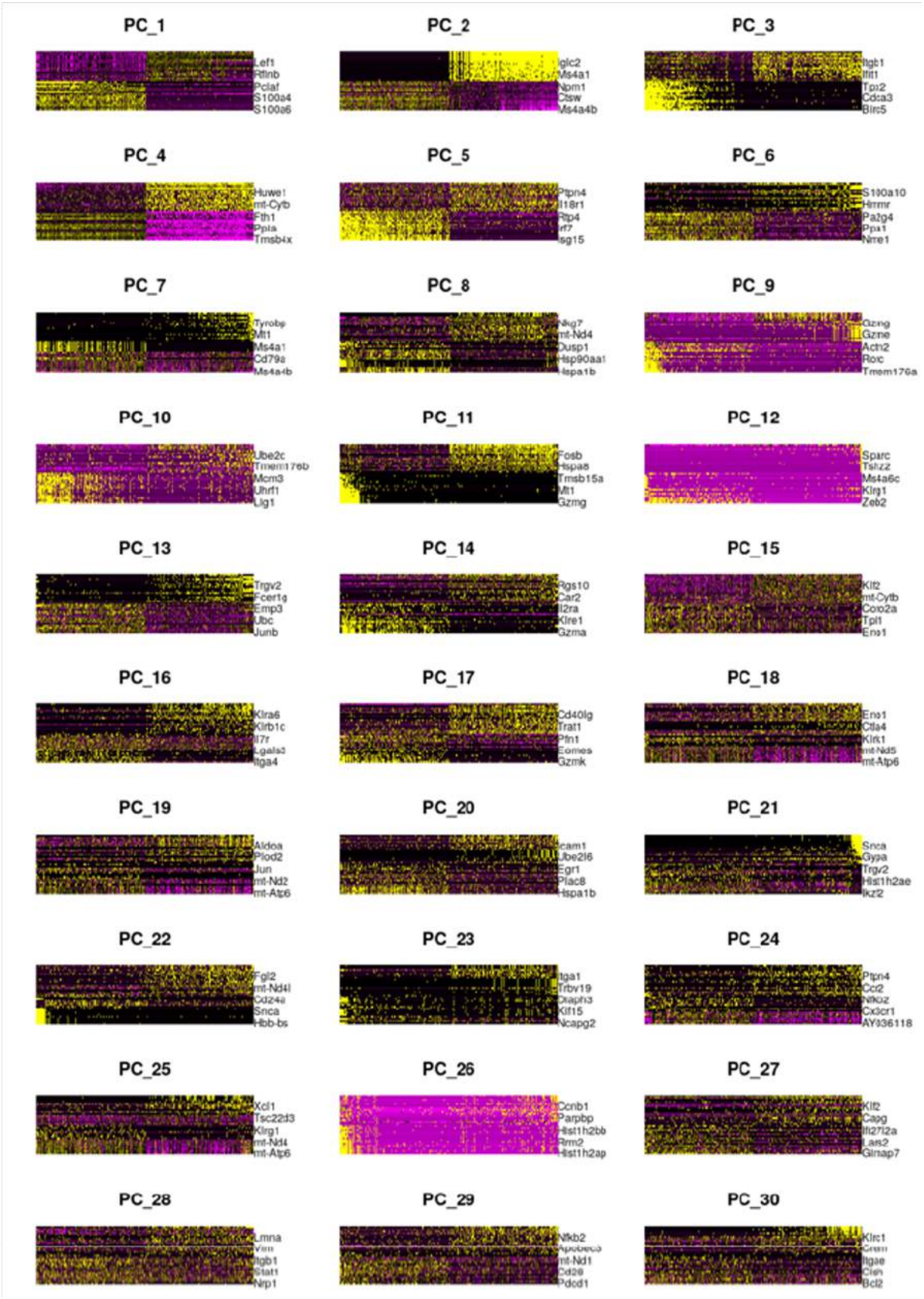
PC_1
Lef1
Rtkn
Pclaf
S100a4
S100a6
PC_2
Iglc2
Ms4a1
Npm1
Ctsw
Ms4a4b
PC_3
Hgb1
Ifit1
Tpx2
Cdca3
Birc5
PC_4
Huwe1
mt-Cyb
Fth1
Ppia
Tmsb4x
PC_5
Ptpn4
Il18r1
Rtp4
Irf7
Isg15
PC_6
S100a10
Hmmr
Pa2g4
Ppa1
Nme1
PC_7
Tyrobp
Mt1
Ms4a1
Cd79a
Ms4a4b
PC_8
Nkg7
mt-Nd4
Dusp1
Hsp90aa1
Hspa1b
PC_9
Gzmg
Gzme
Actn2
Rorc
Tmem176a
PC_10
Ube2c
Tmem176b
Mcm3
Uhrf1
Lig1
PC_11
Fosb
Hspa8
Tmsb15a
Mt1
Gzmg
PC_12
Sparc
Tshz2
Ms4a6c
Klrg1
Zeb2
PC_13
Trgv2
Fcer1g
Emp3
Ubc
Junb
PC_14
Rgs10
Car2
Il2ra
Klre1
Gzma
PC_15
Klf2
mt-Cytb
Coro2a
Tpi1
Eno1
PC_16
Klra6
Klrb1c
Il7r
Lgals3
Itga4
PC_17
Cd40lg
Trat1
Ptn1
Eomes
Gzmk
PC_18
Eno1
Ctla4
Klrk1
mt-Nd5
mt-Atp6
PC_19
Aldoa
Plod2
Jun
mt-Nd2
mt-Atp6
PC_20
Icam1
Ube2l6
Egr1
Plac8
Hspa1b
PC_21
Snca
Gypa
Trgv2
Hist1h2ae
Ikzf2
PC_22
Fgl2
mt-Nd4l
Cd24a
Snca
Hbb-bs
PC_23
Itga1
Trbv19
Diaph3
Klf15
Ncapg2
PC_24
Ptpn4
Ccr2
Zfp36l2
Cx3cr1
AY036118
PC_25
Xcl1
Tsc22d3
Klrg1
mt-Nd4
mt-Atp6
PC_26
Ccnb1
Parpbp
Hist1h2bb
Rrm2
Hist1h2ap
PC_27
Klf2
Capg
Ifi27l2a
Lars2
Glrnap7
PC_28
Lmna
Vim
Itgb1
Stat1
Nrp1
PC_29
Nfkb2
mt-Nd1
Cd28
Pdcd1
PC_30
Klrc1
Itgae
Cish
Bcl2

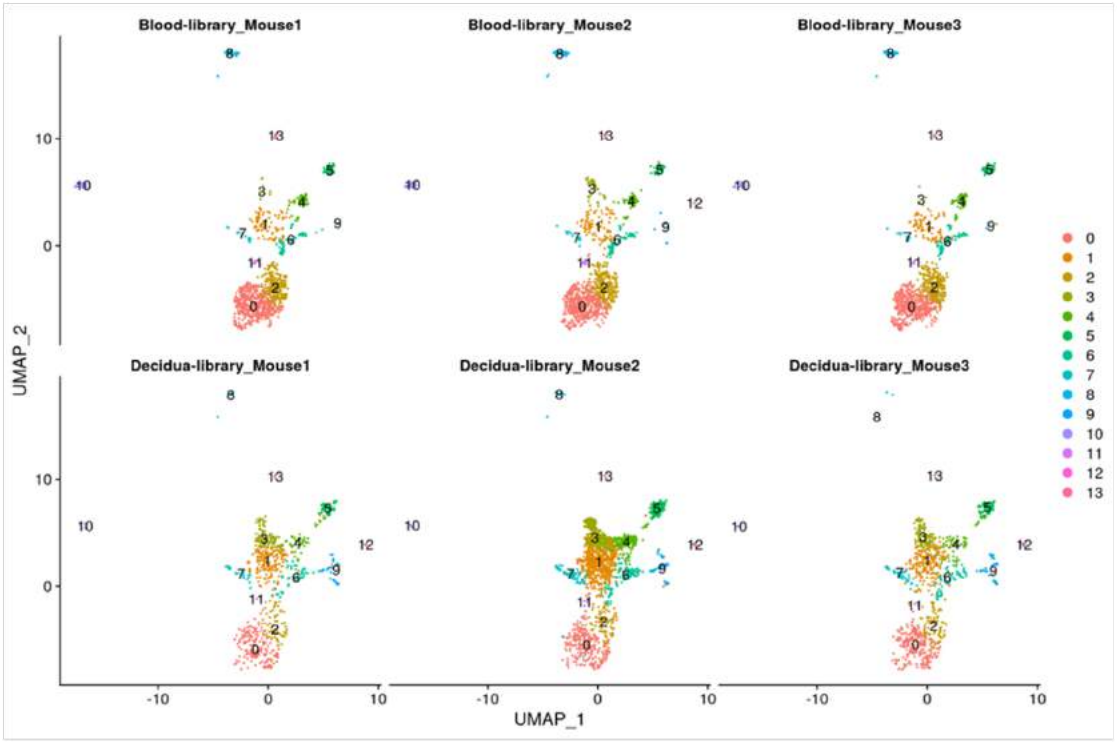

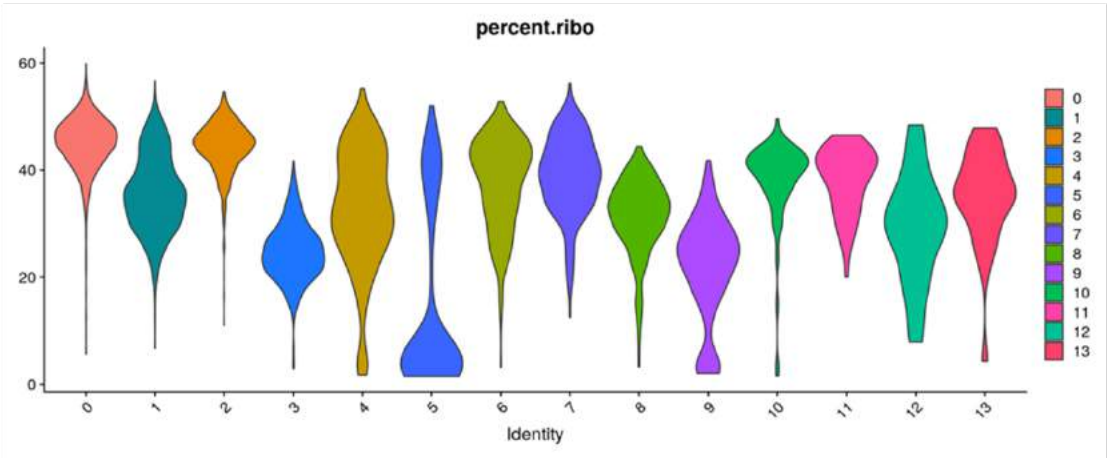

Appendix 3: Comparison of CD8 + T cell subsets in blood and uterus from single -cell RNA sequencing data

After processing and integration of the single-cell RNA sequencing data from blood and uterus, CD8+ T cells were compared between the two organs. Clusters were identified by Seurat (Resolution 0.3) and visualised by the dimensionality reduction UMAP (Uniform manifold approximation and projection) (A) and further visualised separated by the organ (B). All clusters were found in both organs but in different frequencies (C). Most notably, the cluster 0, containg mainly naive cells is enriched in blood while cluster 1, and other more differentiated effector and memory subsets are enriched in the uterus. Heatmap of selected genes involved in relevant pathways further shows different gene signature in uterus compared to blood in terms of for instance higher activation and effector function (D). Identification of the top 10 genes in

each cluster further pinpoints an important difference in gene expression between blood and uterus (E). In this dissertation, this set of data was used for general confirmation and identification of difference in CD8+ T cell subsets between blood and uterus, supporting findings from flow cytometry data. Further analysis will be carried out in the future for an in-depth analysis of each cluster.

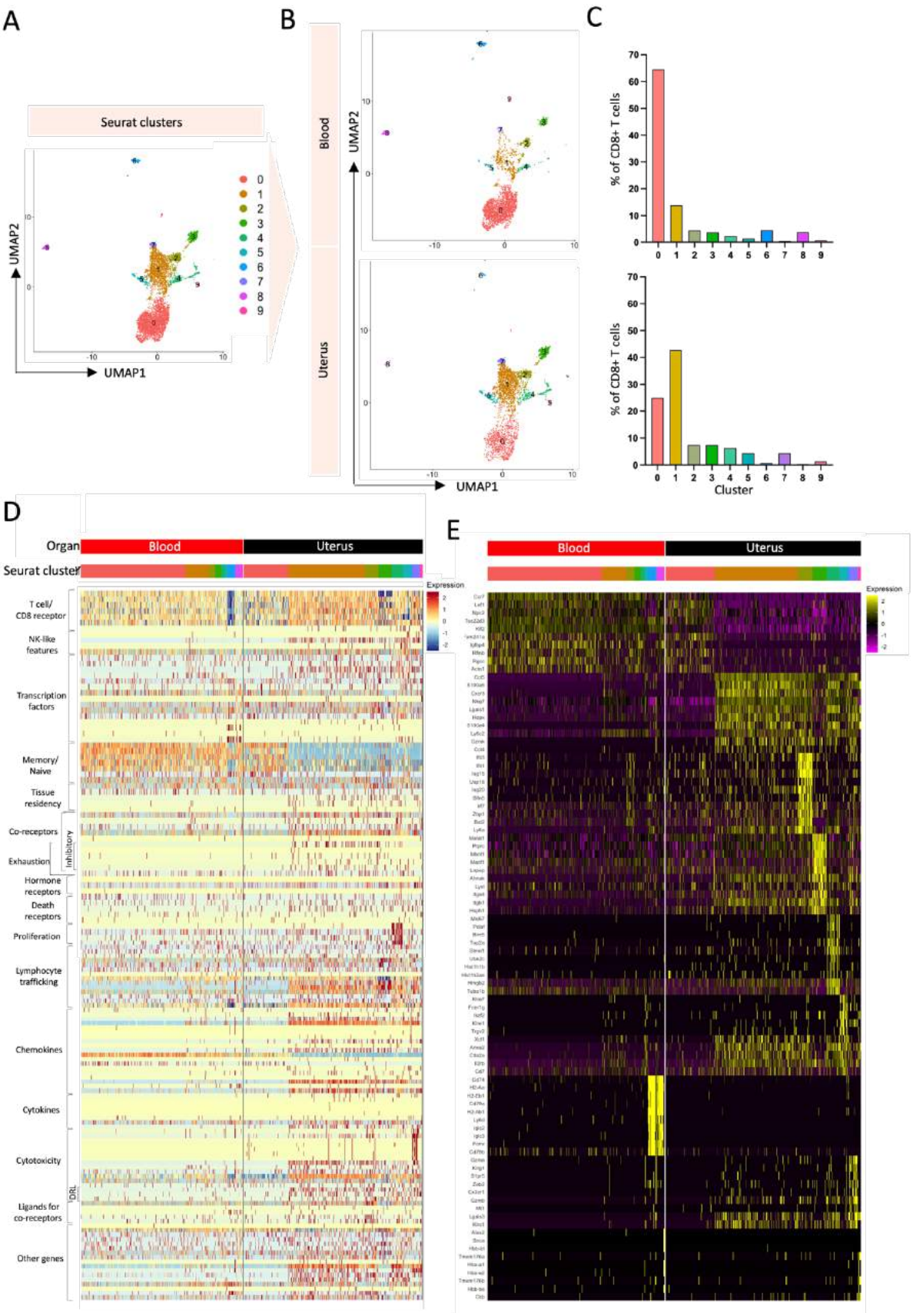
A
Seurat clusters
UMAP2
UMAP1
B
Blood
Uterus
UMAP2
UMAP1
C
% of CD8+ T cells
% of CD8+ T cells
Cluster
D
Organ
Blood
Uterus
Seurat cluster
T cell/ CD8 receptor
NK-like features
Transcription factors
Memory/ Naive
Tissue residency
Co-receptors
Exhaustion
Inhibitory
Hormone receptors
Death receptors
Proliferation
Lymphocyte trafficking
Chemokines
Cytokines
Cytotoxicity
Ligands for co-receptors
Other genes
DRL
Expression
E
Blood
Uterus
Expression

Appendix 4: List of genes of interest and their protein names.

A table showing the full name and protein name for genes presented in gene groups from single-cell RNA sequencing analysis.

Gene group	Gene name	Full name/protein name
T/ CD8 receptors	Cd3d	CD3d CD3 antigen, delta polypeptide
	Cd3e	CD3e CD3 epsilon subunit of T-cell receptor complex
	Cd3g	CD3g CD3 antigen, gamma polypeptide
	Cd8a	CD8a CD8 antigen, alpha chai
	Cd8b1	CD8b CD8 antigen, beta chain 1
	Lck	LCK, Lymphocyte protein tyrosine kinase
	Trgv2	T cell receptor gamma variable 2
NK like features	Klrb1c	NK1.1, Killer cell lectin-like receptor subfamily B member 1C/
	Klrc1	NKG2A: Killer Cell Lectin Like Receptor C1 /NKG2,CD159
	Klrc2	Killer Cell Lectin Like Receptor C2/NKG2/CD159c
	Klrd1	CD95, Natural killer cells antigen
Transcription factors	Batf	BATF, Basic leucine zipper transcriptional factor ATF-like
	Gata3	GATA3, Trans-acting T-cell-specific transcription factor GATA-3
	Tbx21	T-bet/T-box transcription factor TBX21
	Eomes	Eomes, Eomesodermin homolog
	Nfkb1	Nuclear factor NF-kappa-B p105 subunit
	Nfkb2	Nuclear factor NF-kappa-B p100 subunit
	Nfkbia	NF-kappa-B inhibitor alpha
	Maf	Transcription factor Maf/c-Maf
	Irf1	IRF-1, Interferon regulatory factor 1
	Irf2	IRF-2, Interferon regulatory factor 2
	Irf3	IRF-3, Interferon regulatory factor 3
	Irf4	IRF-4, Interferon regulatory factor 4
	Irf5	IRF-5, Interferon regulatory factor 5
	Irf6	IRF-6, Interferon regulatory factor 6
	Irf8	IRF-8, Interferon regulatory factor 8
Memory/Naive	Lef1	LEF-1, Lymphoid enhancer-binding factor 1
	Ccr7	CCR7, C-C chemokine receptor type 7
	Sell	CD62L, L-selectin
	Tcf7	TCF1, T-cell-specific transcription factor 1
	Il7r	CD107, Interleukin-7 receptor subunit alpha
	Bach2	BACH2, Transcription regulator protein
	Cd27	CD27
Tissue residency	Cd69	CD69, Early activation antigen
	Itgae	CD103, Integrin alpha-E,
	Itga1	CD49a, CD49 antigen-like family member A, Integrin alpha-1
	Zfp683	ZNF683, Tissue-resident T-cell transcription regulator protein
	Prdm1	Blimp-1, PR domain zinc finger protein 1
Co-receptors % exhaustion	Cd28	CD28, T-cell-specific surface glycoprotein
	Cd40lg	CD40-L, CD40 ligand, TRAP, CD154
	Icos	Inducible T-cell costimulator, CD278,
	Itgb2	Integrin beta-2, CD18
	Tnfrsf4	OX40 antigen, OX40L receptor, CD137, Tumor necrosis factor receptor superfamily member 4
	Pdcd1	Programmed cell death protein 1 , PD1, CD279

	Havcr2	Tim3, Hepatitis A virus cellular receptor 2 homolog
	Ctla4	Cytotoxic T-lymphocyte protein 4
	Lag3	Lymphocyte activation gene 3 protein
	Tigit	T-cell immunoreceptor with Ig and ITIM domains
	Tox	TOX, Thymocyte selection-associated high mobility group box protein TOX 1
Hormone receptors	Pgr	PR, progesterone receptor
	Nr3c1	GR, Glucocorticoid receptor
	Esr1	ER, Estrogen receptor
Death receptors	Fas	Fas receptor/ APO-1
	Tnfrsf1a	Tumor necrosis factor receptor type 1-associated DEATH domain protein
	Tnfrsf1b	Tumor necrosis factor receptor superfamily member 1B
	Tnfrsf25	Tumor necrosis factor ligand superfamily member 15
	Tnfrsf10b	Tumor necrosis factor receptor superfamily member 10B/Death receptor 5
Proliferation	Mki67	Proliferation marker protein Ki-67
	Pcna	Proliferating cell nuclear antigen
	Mcm2	DNA replication licensing factor MCM2
	Mcm3	DNA replication licensing factor MCM3
Lymphocyte trafficking	Ctnnb1	Catenin beta-1
	Pecam1	Platelet endothelial cell adhesion molecule, PECAM-1, CD31
	Cxcr4	C-X-C chemokine receptor type 4, Fusin
	Itga4	Integrin alpha-4, CD49 antigen-like family member D, CD49d
	Mbp	Myelin basic protein, MBP
	Icam1	Intercellular adhesion molecule 1, ICAM-1, CD54
	Mapk11	Mitogen-activated protein kinase 11, MAPK11
	Arhgdib	Rho GDP-dissociation inhibitor 2, RhoGDI 2
	Itgal	Integrin alpha-L, Cd11A
	Itgb1	Integrin beta-1 , CD29
	Itgb2	Integrin beta-2, CD18
	Mapk14	Mitogen-activated protein kinase 14, MAPK14
	Ncf4	Neutrophil cytosol factor 4, NCF-4
	Thy1	Thy-1 membrane glycoprotein, CD90
Chemokines	Ccl25	C-C motif chemokine 25
	Ccl3	C-C motif chemokine 3
	Ccl4	C-C motif chemokine 4
	Ccl5	C-C motif chemokine 5
	Ccl6	C-C motif chemokine 6
	Ccl9	C-C motif chemokine 9
	Ccr10	C-C chemokine receptor type 10
	Ccr2	C-C chemokine receptor type 2
	Ccr4	C-C chemokine receptor type 4
	Ccr5	C-C chemokine receptor type 5
	Ccr7	C-C chemokine receptor type 7
	Ccr8	C-C chemokine receptor type 8
	Ccr9	C-C chemokine receptor type 9
	Ccrl2	C-C chemokine receptor-like 2
	Cx3cr1	CX3C chemokine receptor 1
	Cxcl10	C-X-C motif chemokine 10
	Cxcr3	C-X-C chemokine receptor type 3
	Cxcr5	C-X-C chemokine receptor type 5
	Cxcr6	C-X-C chemokine receptor type 6
Cytokines	Il2	IL-2, Interleukin-2
	Il15	IL-15, Interleukin-2
	Il18	IL-18, Interleukin-2

	Tnfsf13b	Tumor necrosis factor ligand superfamily member 13B, CD257
	Lif	Leukemia inhibitory factor, /Differentiation-stimulating factor (D factor)
	Osm	Oncostatin-M
	Tgfb1	Transforming growth factor beta-1 proprotein
	Ifng	Interferon gamma
Cytotoxicity	Gzma	Granzyme A, GZMA
	Gzmb	Granzyme B, GZMB
	Gzmc	Granzyme C, GZMC
	Gzmd	Granzyme D, GZMD
	Gzme	Granzyme E, GZME
	Gzmf	Granzyme F, GZMF
	Gzmg	Granzyme G, GZMG
	Gzmk	Granzyme K, GZMK
	Gzmm	Granzyme M, GZMM
	Prf1	Perforin 1, PRFF1
	Nkg7	NKG7, Natural killer cell protein 7
	Lamp1	Lysosome-associated membrane glycoprotein 1, CD107a
	Lamp2	Lysosome-associated membrane glycoprotein 2, CD107b
Death receptor ligands	Fasl	Tumor necrosis factor ligand superfamily member 6, CD95 ligand (CD95-L) /Fas antigen ligand (Fas ligand; FasL)
	Tnf	Tumor necrosis factor, TNF
	Tnfsf10	Tumor necrosis factor ligand superfamily member 10, TNF-related apoptosis-inducing ligand (Protein TRAIL)
Ligands for co-receptors	Lgals9	Galectin-9, GAL-9
	Pvr	poliovirus receptor, CD155
	Icosl	ICOS ligand, CD275
	Cd86	T-lymphocyte activation antigen CD86
	Cd274	Programmed cell death 1 ligand 1, PDL1, CD274
Other genes	Hmox1	Heme oxygenase 1, HMOX-1
	Jak1	Tyrosine-protein kinase JAK1, Janus kinase1, JAK1
	Pik3r1	phosphoinositide-3-kinase regulatory subunit 1, PIK3R1, PI3K
	Socs3	suppressor of cytokine signaling 3
	Jak2	Tyrosine-protein kinase JAK2, Janus kinase2, JAK2
	Jak3	Tyrosine-protein kinase JAK3, Janus kinase3, JAK3
	Mapk1	mitogen-activated protein kinase 1, ERK
	Socs1	suppressor of cytokine signaling 1
	Socs2	suppressor of cytokine signaling 2
	Lgals1	Galectin-1, GAL-1
	Lgals3	Galectin-3, GAL-3
	Jaml	Junctional adhesion molecule-like
	Xcl1	Lymphotactin, C motif chemokine 1
	Ptpn6	protein tyrosine phosphatase, non-receptor type 6
	Bmp7	Bone morphogenetic protein 7
	Il10ra	Interleukin-10 receptor subunit alpha, CD210
	Il10rb	Interleukin-10 receptor subunit beta,

Appendix 5: Verification of MR1 staining for detection of Mucosal-associated invariant (MAIT) cells.

Mucosal MAIT cells were evaluated in pregnancy. MR1 tetramer antibody staining (MR1-5-OP-RU) was verified with an isotype control (6-FP) in liver samples, showing the isotype control was negative for the staining while the MR1 tetramer showed positive cells.

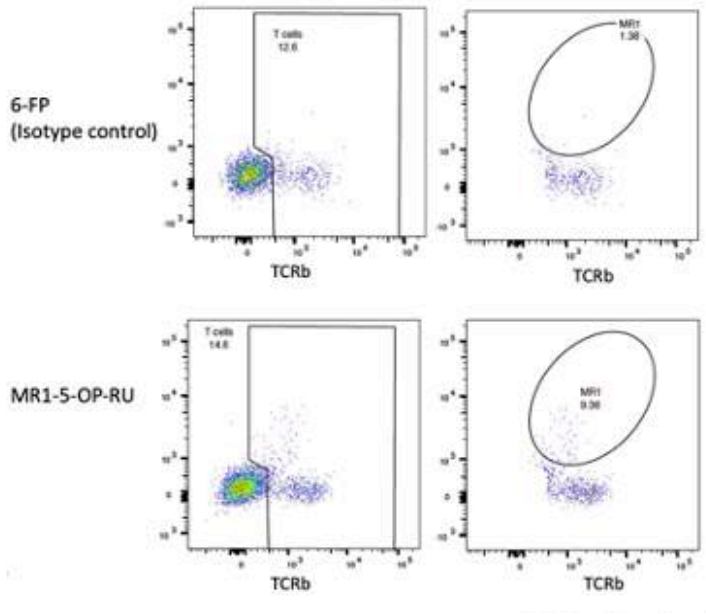

Appendix 6: PD1 expression levels in blood and uterus across pregnancy.

Expression levels of PD1 in CD8+ T cells have been associated with exhaustion, in particular high levels of PD1. Therefore, PD1 high, intermediate, and negative levels were investigated in uterus and blood across pregnancy. Representative histograms of PD1 expression (A) from a concatenated file of multiple samples from uterus (top) and blood (bottom) shows the three subdivided expression levels (X axis), where values are represented as normalised to mode (Y axis). PD1 high cells are enriched in the uterus while barely detectable in blood, with majority of uterine and blood PD1 expression containing intermediate expression levels (B).

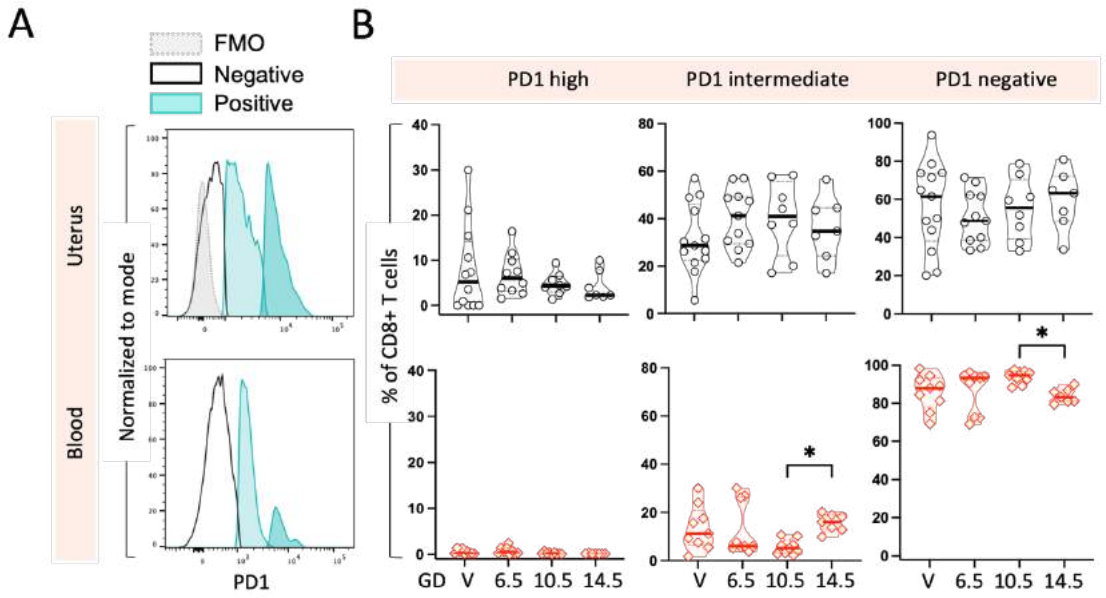

Appendix 7: CD8+ T cell dynamics in second pregnancy.

In addition to investigating CD8+ T cells in PBMC‘s across first pregnancy, the same analysis was applied to first, second and third trimester of the second (subsequent) pregnancy from the same women (A). PD1 expression was significantly higher in second pregnancy and the rise of Tim3 observed in first pregnancy continue to rise. 2B4 and CD39 followed similar trends in both pregnancies, with seemingly higher levels of CD39 in second pregnancy, although not significantly (B). Y axis represent percentages of CD8+ T cells, X axis indicate pregnancy (first pregnancy: white filled bar, second pregnancy: dotted bar), and corresponding trimesters. Overall, dynamics of the CD8+ T cell populations followed a similar trend in second pregnancy as was seen in first pregnancy (C). Mean fluorescence intensity (MFI) was visualised (Y axis) in each CD8+ population (X axis) in first pregnancy showing highest MFI of PD1 and 2B4 in effectors, indicating those contain the exhausted cells (D). tSNE plot of all six time points combined (E) were separated by pregnancy and trimesters to visualise the difference between time points as density tSNE plots (F). Statistical analyses were performed with non-parametric One-way ANOVA and the p values were corrected for multiple comparison, n= 15. *p< 0.05; **p< 0.01; ***p< 0.001.

APPENDIX

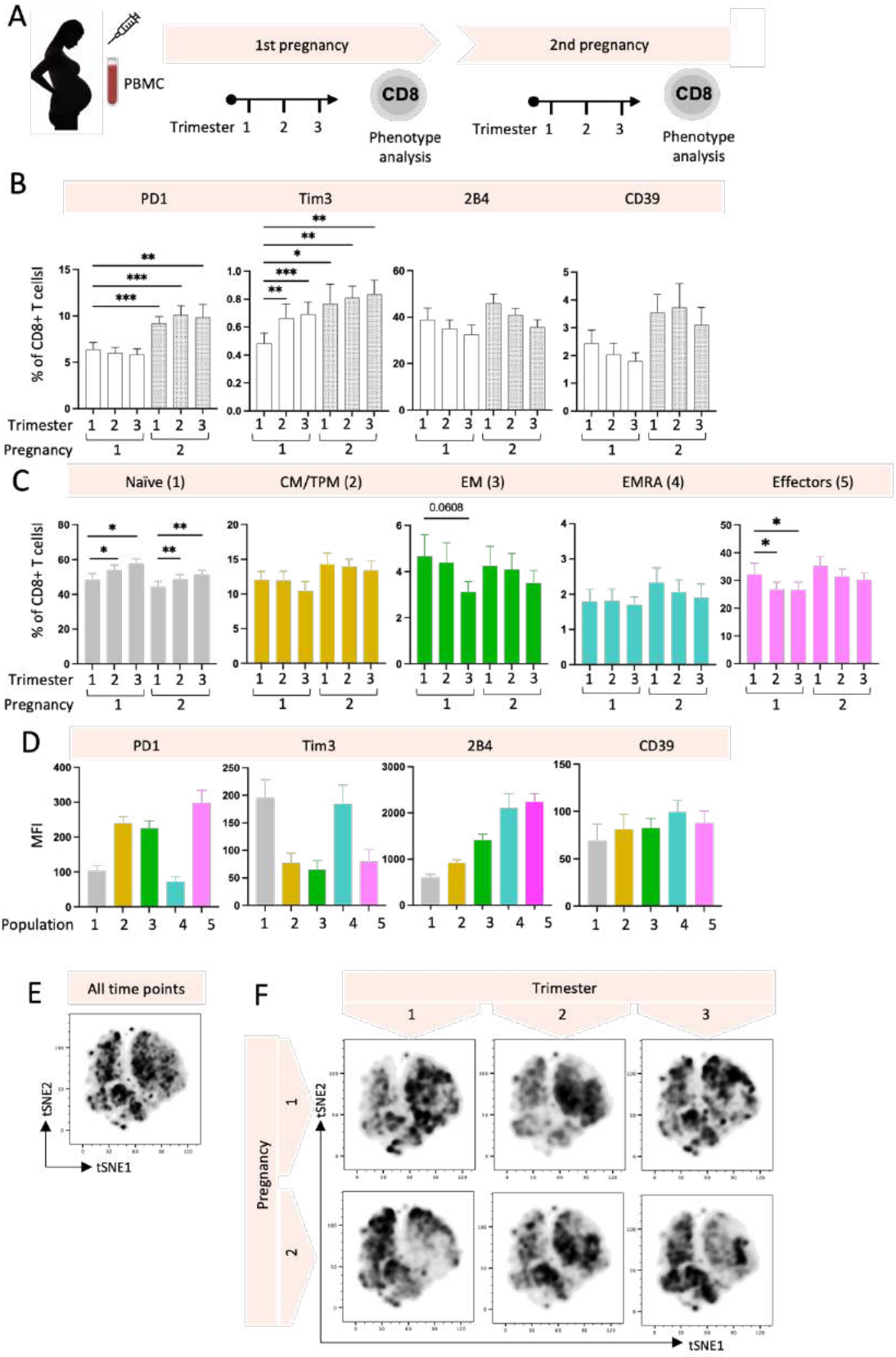
A
PBMC
1st pregnancy
2nd pregnancy
Trimester 1 2 3
CD8
Phenotype analysis
Trimester 1 2 3
CD8
Phenotype analysis
B
PD1
Tim3
2B4
CD39
% of CD8+ T cells
Trimester 1 2 3 1 2 3
Pregnancy 1 2
C
Naïve (1)
CM/TPM (2)
EM (3)
EMRA (4)
Effectors (5)
0.0608
% of CD8+ T cells
Trimester 1 2 3 1 2 3
Pregnancy 1 2
D
PD1
Tim3
2B4
CD39
MFI
Population 1 2 3 4 5
E
All time points
tSNE2
tSNE1
F
Trimester
1
2
3
Pregnancy
1
2
tSNE2
tSNE1

Appendix 8: CD8 alpha and beta chain expression in CD8+ and CD8+CD122+ T cells.

Expression of the alpha and the beta chain of CD8 was assessed by flow cytometry. Representative contour plot shows expression and gating of CD8α+ T cells plotted against CD8β+ T cells (A). The majority of CD8+ T cells and CD8+CD122+ T cells in blood and uterus were CD8αβ cells (green) , with low frequency of CD8αα cells (grey) (B), represented as a stacked bars where Y axis represents percentage out of CD8α+ T cells and X axis indicates the tissue and frequency in CD8α+ T cells or CD8α+CD122+ T cells. Next, CD8α+ T cells expressing high and low levels of CD8α, referred to as $CD8\alpha^{hi}$ and $CD8\alpha^{lo}$ cells, respectively, were evaluated in blood and uterus (C), in both CD8αβ (D-left) and CD8αα (D-right) cells. The majority of CD8αβ T cells had high expression of CD8α in both organs, but CD8αα cells had higher frequency of $CD8\alpha^{lo}$ expression (B).

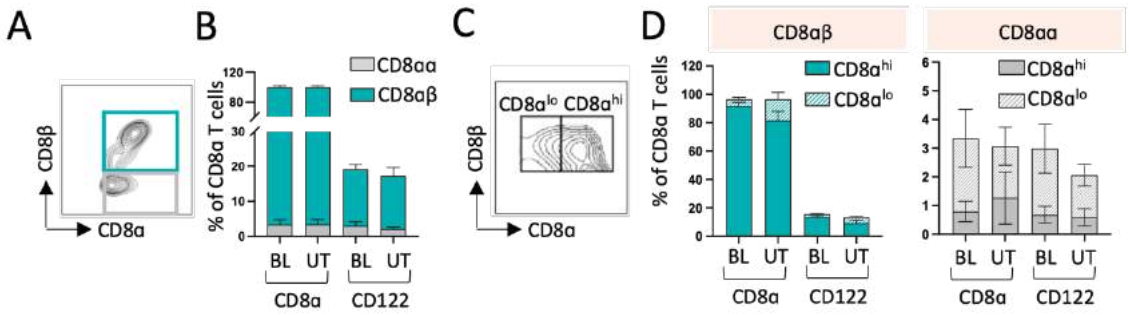

Appendix 9: Comparison of CD8+ subpopulations in CD8+CD122+ and CD8+CD122- T cell and their dynamics in uterus across pregnancy.

Dynamics of CD8+ T cell effector, memory, and naive subsets in CD8+CD122+ T cells (solid line) were compared to dynamics of CD8+CD122- T cells (dotted line) in pregnancy in uterus (A). Y axis represents percentages of CD8+ T cells. X axis indicates gestation day (GD). CD8+CD122+ T cells with a short-lived effector cell (SLEC) phenotype peak before their CD8+CD122- counterparts indicating a quicker response to pregnancy events. Furthermore, CD122+ central memory-like (CM-like) cells are significantly higher in mid-late pregnancy, compared to CD122- central memory-like cells. These observed peaks of central memory-like and short-lived effector cell within CD122+ T cells were accompanied with CD69 expression, suggesting an activation of these cells (B). Statistical analyses were performed with t-test and of each time point, n= 7-14. *p< 0.05; **p< 0.01; ***p< 0.001; ****p<0.0001.

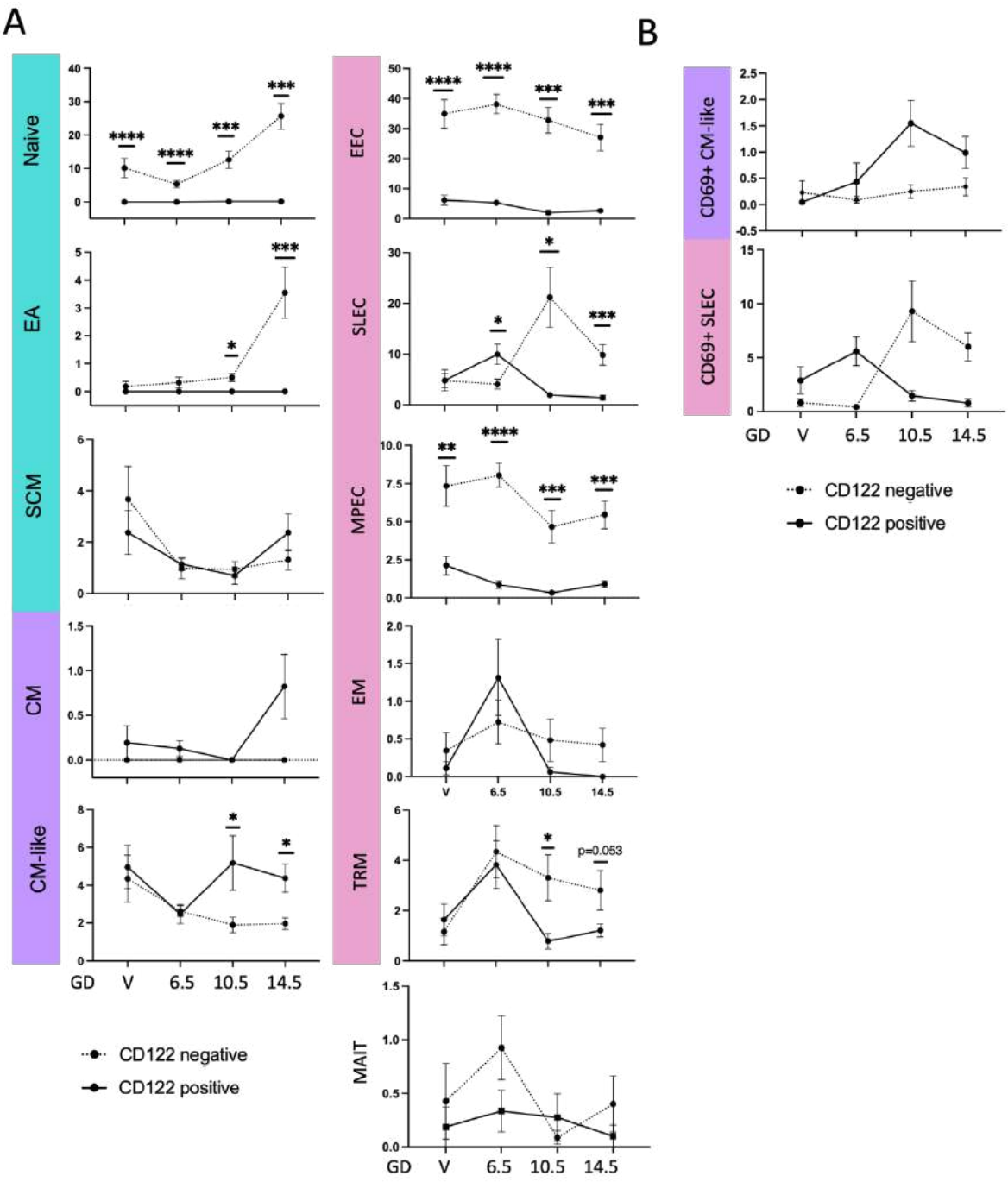
A
B
Naive
EA
SCM
CM
CM-like
EEC
SLEC
MPEC
EM
TRM
MAIT
CD69+ CM-like
CD69+ SLEC
GD
V
6.5
10.5
14.5
CD122 negative
CD122 positive
p=0.053

Appendix 10: Information about donor cells for adoptive transfer.

Isolated cells from pooled blood, spleen and uterus were sorted to acquire purified CD8+CD122- and CD8+CD122+ T cells (A). Sorted cells were adoptively transferred to pregnant females on day zero (D0). Unsorted CD8+ T cells were stained with an antibody panel for detection of CD44 and CD62L, with majority of cells containing CD44-CD62L+ phenotype (including naive cells), followed by CD44+CD62L+ phenotype (including central memory cells) and some belonging to CD44+CD62L- (including effector and memory cells). Thus, donor cells consisted of all three subtypes. On day four, termed D4, cells were isolated from blood, spleen and uterus and adoptively transferred CD8+ T cells were identified by the gating strategy shown in C. Identified adoptively transferred cells in Rag2γcKO females on D4 were mainly activated cells with few naive cells in spleen and uterus, with particularly high CD44+CD62L- (including effector and memory cells) in the uterus (D). Likewise, identified adoptively transferred CD8+ T cells in Bl6 females in the uterus contained activated phenotype, while endogenous CD8+ T cells contained both activated and naive cells in the uterus (E-F). Figure G shows representative contour plots of comparable CD122 expression in Rag2γcKO and Bl6 females in blood, and representative histograms of CD122 expression in blood, spleen, and uterus in Rag2γcKO and Bl6 females. Fluorescence minus one (FMO) negative control for CD122 is coloured grey. Y axis represents values normalised to mode. Figure H contains information from normal Bl6 cells that did not receive adoptive transfer. The figure shows higher levels of proliferation, measured by Ki67, in uterine CD8+ CD122+ T cells compared to CD8+CD122- T cells on GD 10.5 and GD 14.5 in physiological pregnancy.

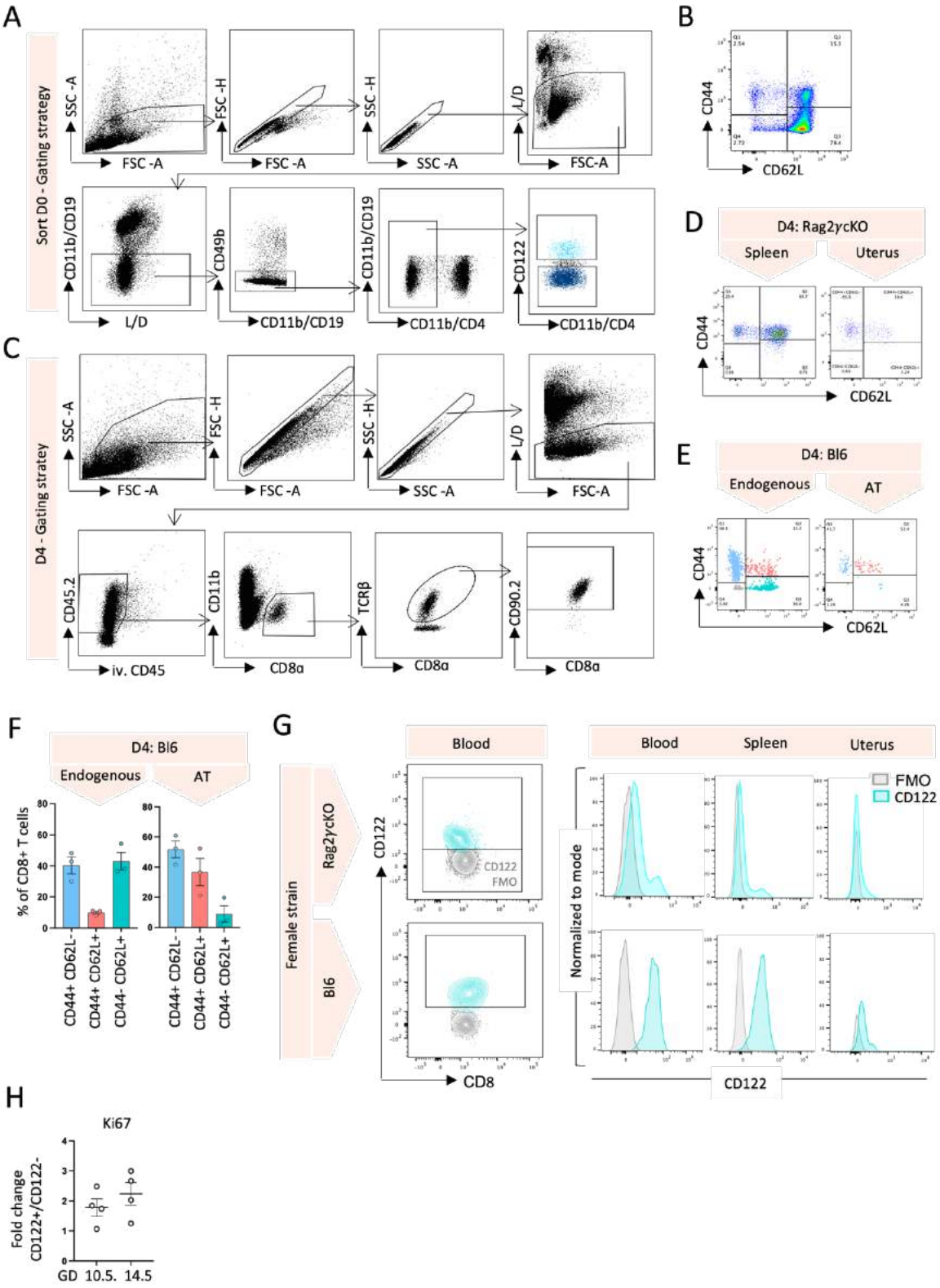
A
Sort D0 - Gating strategy
SSC -A
FSC -A
FSC -H
FSC -A
SSC -H
SSC -A
L/D
FSC-A
CD11b/CD19
L/D
CD49b
CD11b/CD19
CD11b/CD19
CD11b/CD4
CD122
CD11b/CD4
B
CD44
CD62L
C
D4 - Gating strategy
SSC -A
FSC -A
FSC -H
FSC -A
SSC -H
SSC -A
L/D
FSC-A
CD45.2
iv. CD45
CD11b
CD8α
TCRβ
CD8α
CD90.2
CD8α
D
D4: Rag2γcKO
Spleen
Uterus
CD44
CD62L
E
D4: Bl6
Endogenous
AT
CD44
CD62L
F
D4: Bl6
Endogenous
AT
% of CD8+ T cells
CD44+ CD62L-
CD44+ CD62L+
CD44- CD62L+
CD44+ CD62L-
CD44+ CD62L+
CD44- CD62L+
G
Blood
Blood
Spleen
Uterus
Female strain
Rag2γcKO
Bl6
CD122
CD122
FMO
FMO
CD122
Normalized to mode
CD8
CD122
H
Ki67
Fold change
CD122+/CD122-
GD 10.5. 14.5

Appendix 11: mRNA gene expression data compared to CITE-sequencing data

mRNA gene expression levels of selected genes, for validation of findings from flow cytometry data, were visualised in a UMAP plot generated from uterine single-cell RNA sequencing data confirming presence of markers for effector and memory subsets, migration, and proliferation in the pregnant uterus.

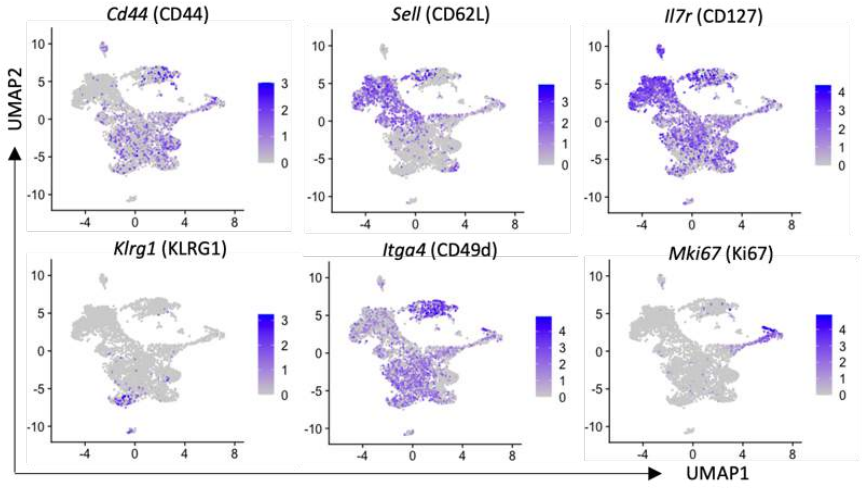

Appendix 12: Comparison of CD8+CD122+ phenotype in adoptively transferred CD8+CD122+ and CD8+CD122- T cells in spleen and uterus.

Remarkably, only CD8+CD122+ T cells that originated from the adoptively transferred CD8+CD122+ T cells expressed Ly49, while originally adoptively transferred CD8+CD122- T cells that had upregulated CD122 did not express Ly49. Although only few mice allowed for discrimination of adoptively transferred CD122+ and CD122- T cells by CD45.1 and CD45.2 (n=3), this comparison can give indication of differences in the originally adoptively transferred CD122+ T cells, of which dams had reduced abortion rate, compared with those receiving only adoptively transferred CD122- and upregulated CD122 (B).

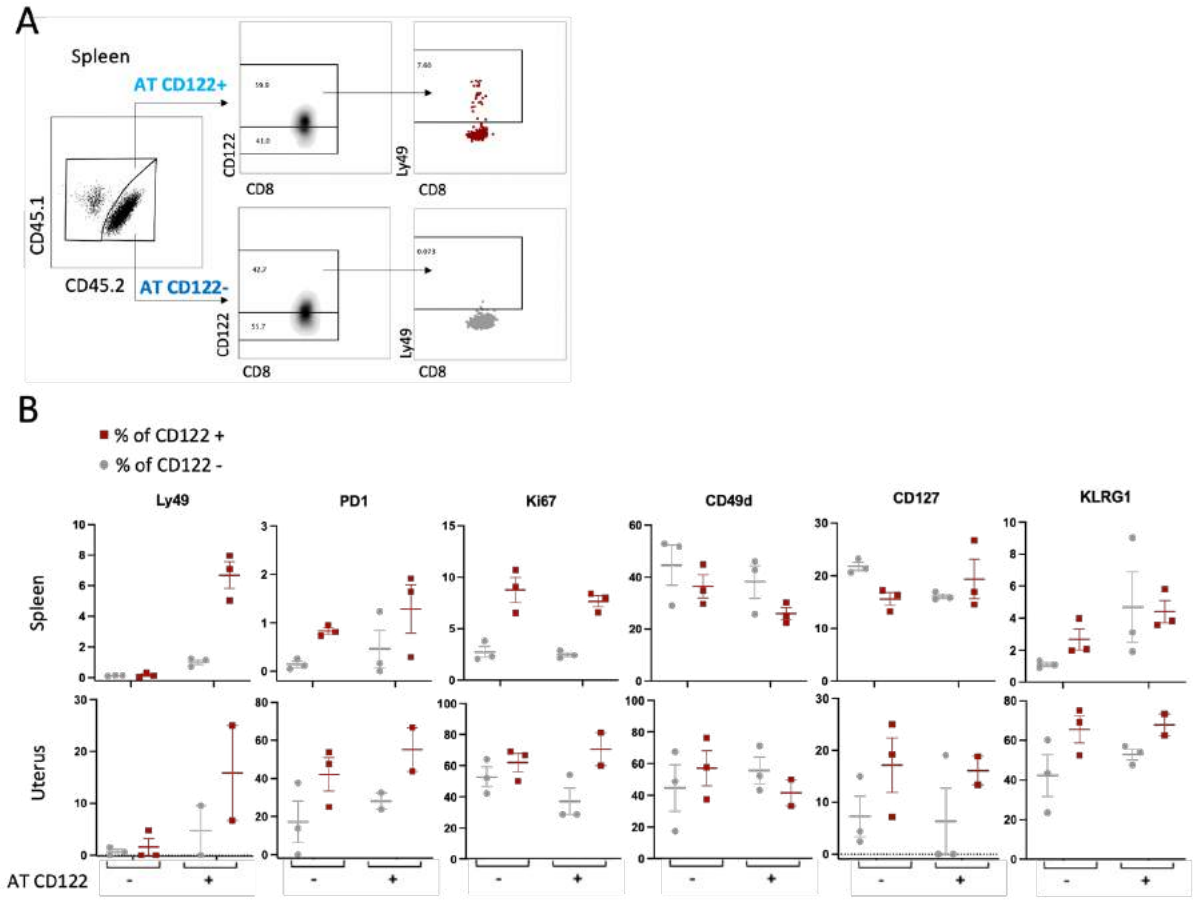

Appendix 13: Criteria for selection of five subgroups in single-cell RNA sequencing data.

Three genes were used for creating five subgroups of CD8+ T cells from uterine data. They were *Il2rb* (CD122), *Klra7* (Ly49G) and *Pdcd1* (PD1). *Klra7* was chosen because it's expression was highly correlated to *Klra6* expression and both have been associated with CD8+ regulatory T cell function (Kim et al., 2011). First gene expression threshold value was based on density plot of each gene (A), then gene expression criteria was set for separating each subset (B), followed by a visual verification of the selected threshold value as a heatmap (C).

A

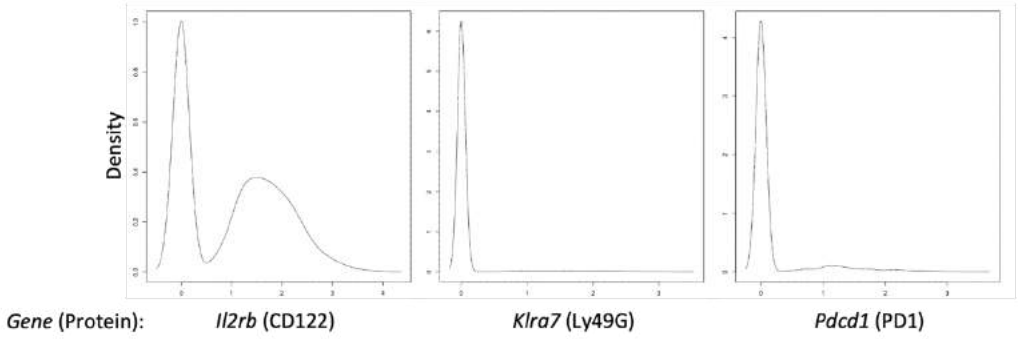

B

Group name	Selection criteria	Count
CD122-PD1-	Il2rb: <= 0.7, Pdcd1: <= 0.4	1659
CD122-PD1+	Il2rb: <= 0.7, Pdcd1: > 0.4	117
CD122+PD1-Ly49-	Il2rb: > 0.7, Pdcd1: <= 0.4, Klra7: <= 0.2	1943
CD122+Ly49-PD1+	Il2rb: > 0.7, Pdcd1: > 0.4, Klra7: <= 0.2	341
CD122+Ly49+	Il2rb: > 0.7, Klra7: <= 0.2	148

C

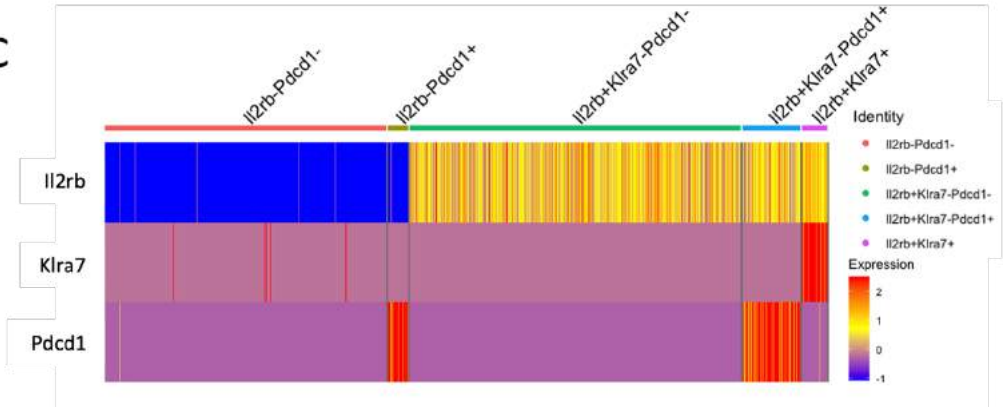

Appendix 14: Processing of uterus from single-cell RNA sequencing data and CITE-sequencing.

The uterine data was processed individually for a more in-depth analysis, including CITE-sequencing (protein expression) analysis. This data processing and analysis was performed by this dissertation's author. The data was processed with similar steps that were explained in Appendix 2.

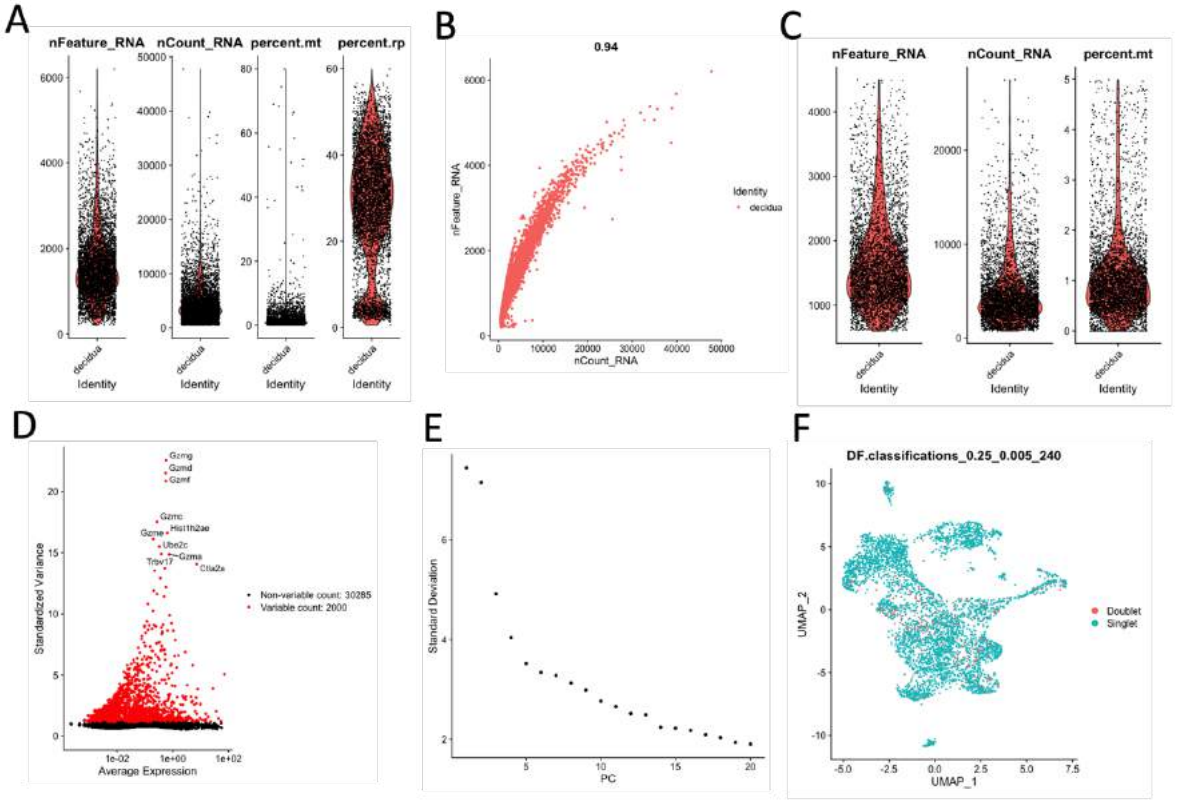
A
nFeature_RNA
nCount_RNA
percent.mt
percent.rp
decidua
Identity
B
0.94
nFeature_RNA
nCount_RNA
Identity
decidua
C
nFeature_RNA
nCount_RNA
percent.mt
decidua
Identity
D
Standardized Variance
Average Expression
Non-variable count: 30285
Variable count: 2000
E
Standard Deviation
PC
F
DF.classifications_0.25_0.005_240
UMAP_2
UMAP_1
Doublet
Singlet

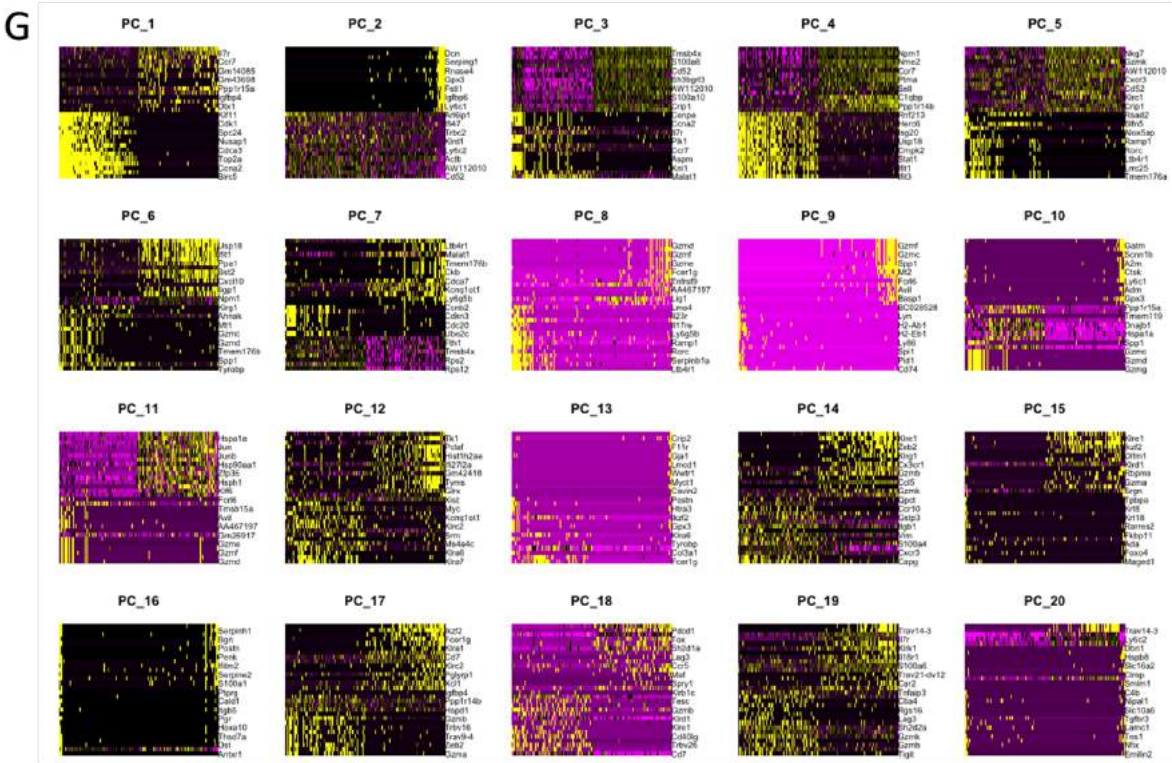
G
PC_1
PC_2
PC_3
PC_4
PC_5
PC_6
PC_7
PC_8
PC_9
PC_10
PC_11
PC_12
PC_13
PC_14
PC_15
PC_16
PC_17
PC_18
PC_19
PC_20

Appendix 15: Comparison of RNA expression and protein expression from single-cell RNA sequencing dataset.

Uterine CD8+ T cell mRNA gene expression levels of selected markers were compared with CITE-sequencing barcoded antibody for protein expression, side by side as heatmap visualisation of an UMAP. Variable correlation was detected among the selected markers.

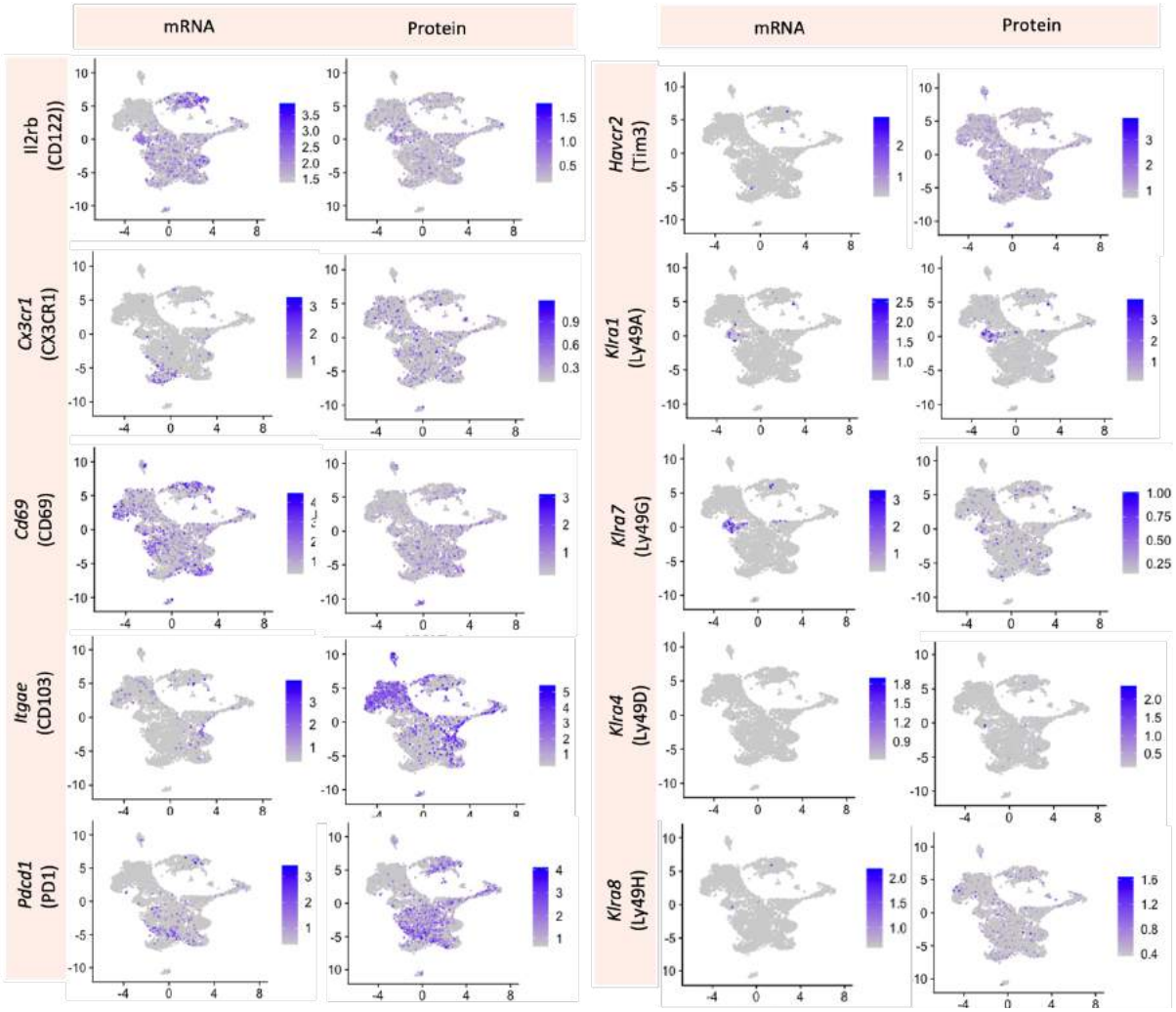

Appendix 16: Raw heatmap of selected genes involved in selected pathways in the uterus.

Raw heatmap of selected genes involved in selected pathways in the uterus. The heatmap shows individual cells, compressed in a heatmap. The data is separated by five pre-selected subgroups as explained in appendix 13, showing the relative size of each subgroup. Of note, not all cells in the dataset are shown due to compression/down-sampling of the heatmap/cells.

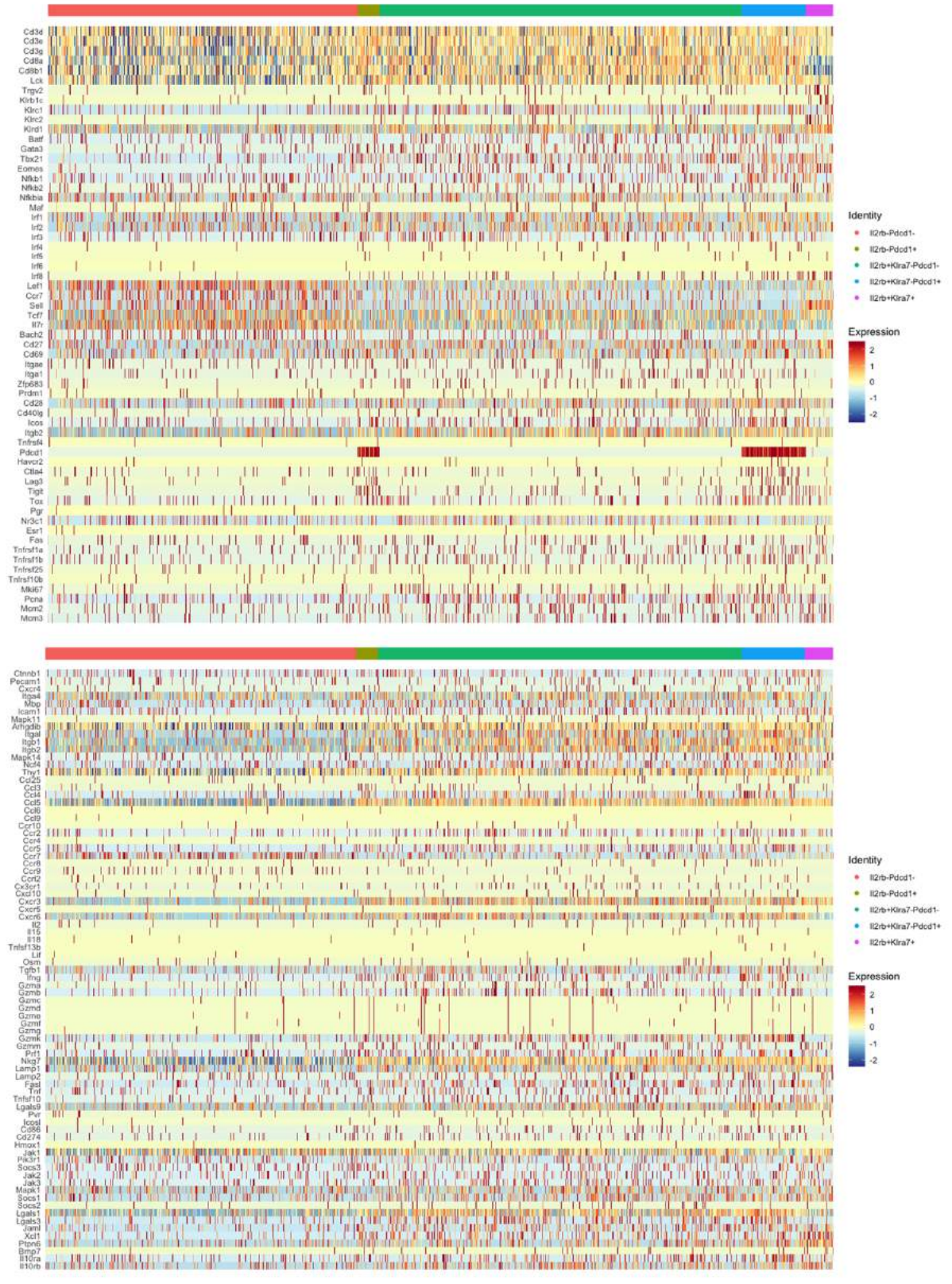
Identity
Il2rb-Pdcd1-
Il2rb-Pdcd1+
Il2rb+Klra7-Pdcd1-
Il2rb+Klra7-Pdcd1+
Il2rb+Klra7+
Expression
2
1
0
-1
-2

Appendix 17: Top genes from uterine single-cell RNA- sequencing dataset.

Top genes (highest expressed) in each of the five subgroups from uterine single-cell RNA-sequencing dataset. Purple indicates low expression, black indicates intermediate expression and yellow indicates high expression.

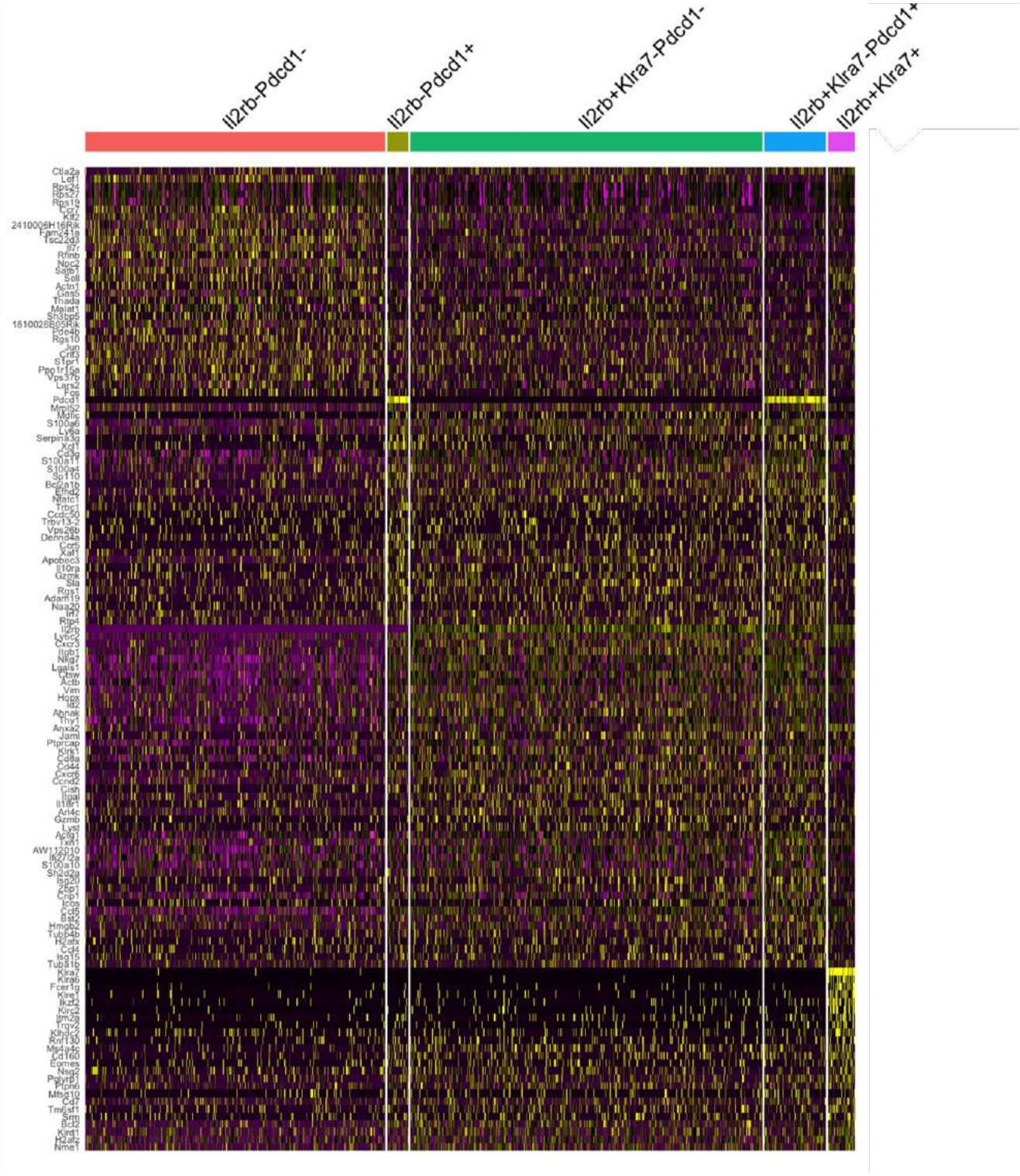

Appendix 18: Glycosylation of CD8+ and CD8+CD122+ T cells in uterus.

Lectin panel recognising specific O – glycan and N-glycan structures and sialyation was used on isolated uterine cells from pregnant Bl6 mice on GD 14.5 (Borowski et al., 2020; Boscher et al., 2011)(A). Glycosylation was evaluated in CD8+ CD122+ and CD8+CD122- T cells by measuring five lectins: MAA, SNA-I, LEA, PNA and PHA-L by flow cytometry, which demonstrates the difference in glycosylation pattern between the two subsets (B-C). X axis indicates the expression combination of the lectins. Y axis represents percentage out of CD8+ T cells (B) and percentage of relative parent population: white bar in C represents percentage out of CD8+CD122- T cells while grey bar represents percentage out of CD8+CD122+ T cells.

A

Lectin	Full name	Recognition
SNA-I	Sambucus nigra agglutinin	α2-6 linked sialic acid (sialyation)
MAA	Maackia amurensis lectin	α2-3 linked sialic acid (sialyation)
PHA-L	Phaseolus vulgaris lectin	MGAT-5 modified N-glycans which are ligands for gal-1 and gal-3 β1,6GlcNAc-branched complex N-glycans
PNA	Arachis hypogaea	Asialo-Core 1 O-Glycans
LEA	Lyopersicon esculentum	Core 2 O-glycans

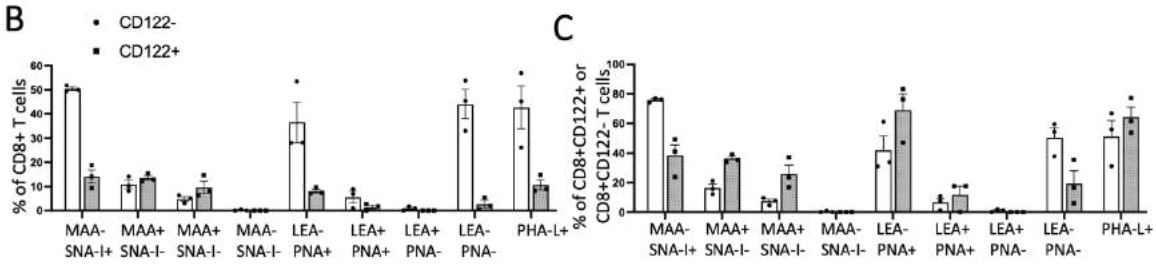

Appendix 19: Further flow cytometry analysis of inhibitory receptors in CD8+CD122+ cells.

MFI values of inhibitory receptors (Y axis) in CD8+ T cells positive for CD122 (dark red) and negative for CD122 (grey), demonstrating enriched protein expression of inhibitory receptors (A). Dynamics of CD122+PD1^{hi}, CD122+PD1^{int,} CD122+PD1^{lo} and CD122- subpopulations across pregnancy, showing a relatively stable expression of CD122+ T cells across pregnancy in the uterus (B). Y axis represents a percentage of CD8+ T cells. Dynamics of inhibitory receptors shown as MFI (Y axis) in each subpopulation across pregnancy, pinpointing a general enrichment of inhibitory receptors in CD122+PD1^{hi} throughout pregnancy (C) X axis in A-C

indicates gestation day. The CD122- population was analysed via same means as CD122+ cells, where CD122-PD1^{hi} did not show enriched expression of inhibitory receptors as was observed in the CD122+PD1^{hi} subset (D).

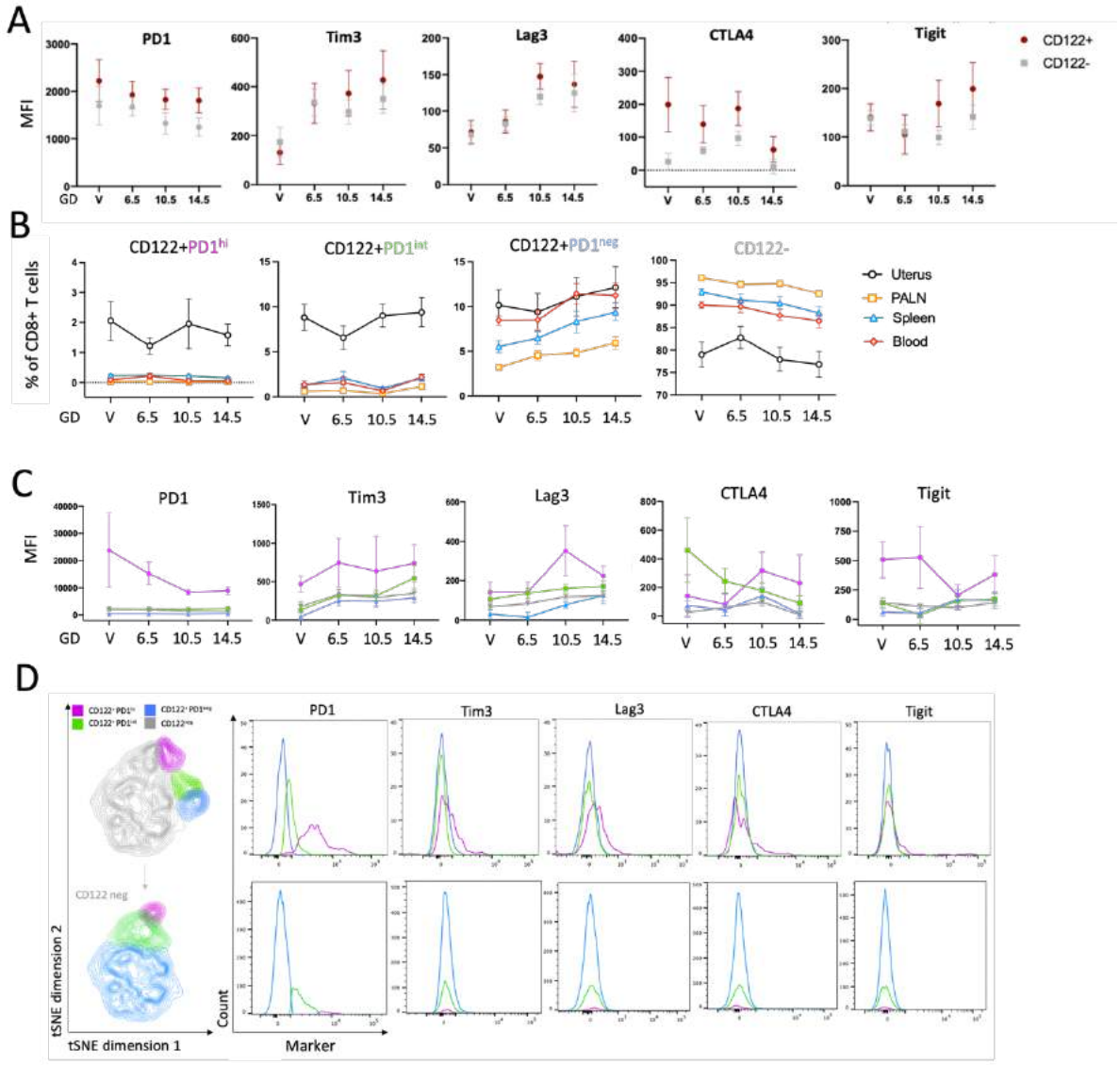

Appendix 20: CD8+ T cell subsets in mesometrial and anti-mesometrial uterus on GD 18.5

Comparison of CD8+ T cell subsets in mesometrial (MUt: black) compared to anti-mesometrial (AMUt: dark red) uterus on gestation day (GD) 18.5, demonstrating similar differences as observed on GD 10.5 and GD 14.5. Y axis represents percentages of CD8+ T cells.

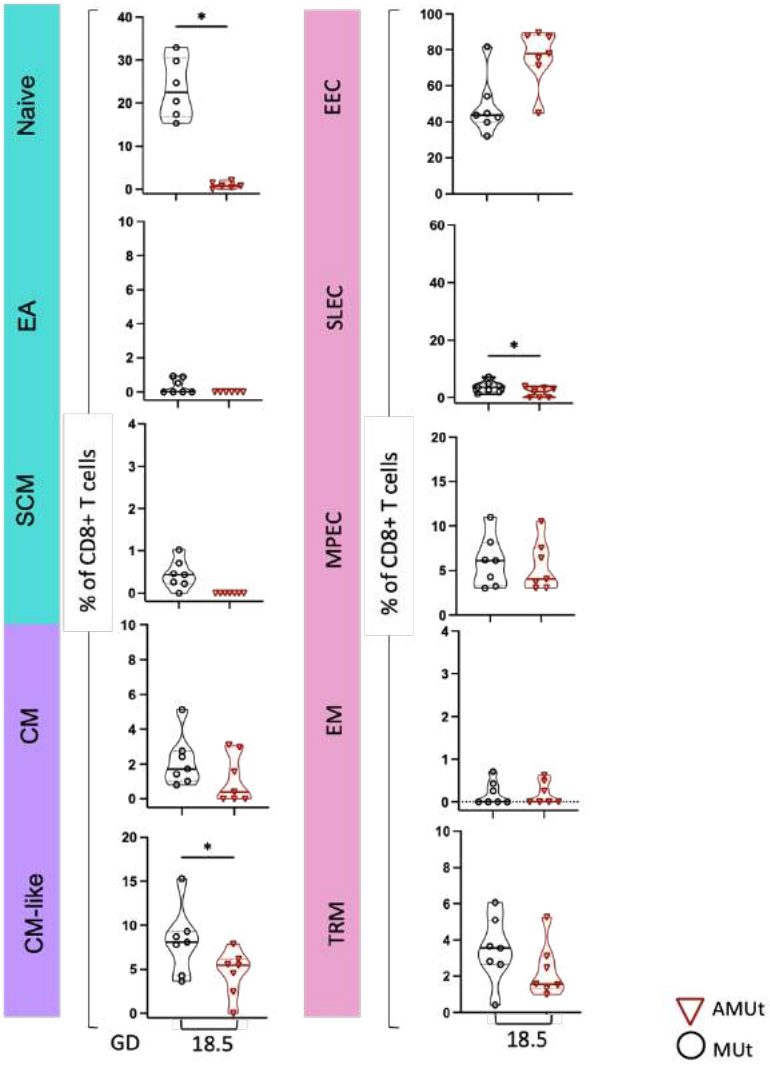
Naive
EA
SCM
CM
CM-like
% of CD8+ T cells
GD
18.5
EEC
SLEC
MPEC
EM
TRM
% of CD8+ T cells
18.5
AMUt
MUt

11 Acknowledgement

First and foremost, I would like to thank my mentor Prof. Dr. Emilia Solano for the opportunity to do my doctorate studies in this fascinating topic within reproductive immunology and for spreading enthusiasm for the topic. I hold her support within and beyond scientific matters deeply in my heart and am thankful for everything she has done for my growth as a scientist and as a person. I would like to thank Petra Arck and her research group for their support and assistance. Special thanks go to Prof. Dr. Hans-Willi Mittrücker, Prof. Dr. Eva Tolosa and PD Dr. Andrea Horst for their valuable contribution to the project and discussions. I also want to thank Prof. Dr. Angela Köninger for providing the exciting opportunity to continue my doctorate research at University Hospital Regensburg for which I am very thankful for. Special thanks go to Dr. Victoria Bazzano, my lab companion and emotional supporter, for all her help with the mice, when I needed more hands and advice. Furthermore, I thank Antonia Waldmann, my medical student, for providing beautiful histology and immunohistology data, as well as Ms. Roberta Acri for her assistance with the OVA genotyping, Ms. Sara Frömmel with her assistance with histology stainings, Dr. Wenqin Shi and Melanie Sponbrucker for their assistance in the lab which I highly appreciate. I thank Dr. Nicholas Striede and Laura Glau for their help with the computational analysis of the single-cell RNA sequencing data. I would also like to thank my former colleagues Veronica Sternemann and Katrin Widmann for immediately taking me under their wing and making sure I have some fun beyond work, they truly made a difference to my stay in Germany.

I would like to thank my parents, Jóna and Hörður, and my brother, Egill, for providing me with the opportunity for my education, for all their support and for understanding my long absence from home. Finally, I would like to thank my life partner, Siggi, for going through this PhD journey together with me, for understanding the weekends with the mice, and late nights at the flow cytometer, and all the encouragement and love.

12 Curriculum Vitae

Omitted for privacy reasons

13 Publications, oral presentations, posters and awards

Hardardottir L, Bazzano MV, Glau L, Gattinoni L, Köninger A, Tolosa E, Solano ME. The new old CD8+ T cells in the immune paradox of pregnancy. Front Immunol. 2021 Nov 16;12:765730. doi:10.3389/fimmu.2021.765730. PMID: 34868016; PMCID:PMC8635142.

Poster presentation at the European Society for Reproductive Immunology (ESRI), France 2022.

Oral presentation at the European Congress of Immunology (ECI) 2021. Title of talk: The critical expansion of uterine CD8+ T cells in pregnancy is under tight homeostatic control.

ISIR Young Investigator Award at the 14th World Congress of the International Society for Immunology of Reproduction, Japan, November 2019. Title of poster: A distinct central memory and regulatory phenotype characterizes decidual CD8+CD122+ T regulatory cells in mice.

14 Affidavit

Ich versichere ausdrücklich, dass ich die Arbeit selbständig und ohne fremde Hilfe verfasst, andere als die von mir angegebenen Quellen und Hilfsmittel nicht benutzt und die aus den benutzten Werken wörtlich oder inhaltlich entnommenen Stellen einzeln nach Ausgabe (Auflage und Jahr des Erscheinens), Band und Seite des benutzten Werkes kenntlich gemacht habe.
Ferner versichere ich, dass ich die Dissertation bisher nicht einem Fachvertreter an einer anderen Hochschule zur Überprüfung vorgelegt oder mich anderweitig um Zulassung zur Promotion beworben habe.
Ich erkläre mich einverstanden, dass meine Dissertation vom Dekanat der Medizinischen Fakultät mit einer gängigen Software zur Erkennung von Plagiaten überprüft werden kann.

Unterschrift: .....